

UNIVERSITE DE STRASBOURG

THESE

pour obtenir le grade de

DOCTEUR DE L'UNIVERSITE DE STRASBOURG

Spécialité : **CHIMIE**

Présentée par

FLIEDEL Christophe

*Synthèse de ligands polyfonctionnels
pour la chimie de coordination et la catalyse*

Soutenue le 19 juin 2010 devant la commission d'examen :

Dr.	BRAUNSTEIN Pierre	Directeur de Recherche CNRS à l'UdS Strasbourg, <i>Directeur de thèse</i>
Pr.	ELSEVIER Cornelis	Professeur à l'Université d'Amsterdam, Pays-Bas Amsterdam, <i>Rapporteur externe</i>
Pr.	POLI Rinaldo	Professeur à l'ENSIACET Toulouse, <i>Rapporteur externe</i>
Pr.	TUREK Philippe	Professeur à l'Université de Strasbourg Strasbourg, <i>Examinateur</i>
Pr.	WELTER Richard	Professeur à l'Université de Strasbourg Strasbourg, <i>Examinateur</i>

Remerciements

Je tiens tout d'abord à remercier Pierre Braunstein, mon directeur de thèse, pour m'avoir accueilli au sein du Laboratoire de Chimie de Coordination de l'Université de Strasbourg pour effectuer ce travail et le valoriser au mieux. Je voulais, par la même occasion, lui exprimer ma reconnaissance pour la confiance, la disponibilité et le soutien dont il a fait preuve à mon égard.

Je souhaite remercier les professeurs Cornelis Elsevier, Rinaldo Poli, Philippe Turek et Richard Welter de me faire l'honneur de juger mon travail.

Je remercie le Ministère de la Recherche et l'Université Franco-Allemande (DFH/UFA - International Research Training Group 532-GRK532) pour leur soutien financier.

Je voudrais remercier le docteur Roberto Pattacini pour ses conseils, la résolution des structures et le temps qu'il m'a consacré. Un grand merci également au docteur Vitor Rosa pour son aide lors de son passage au LCC. Merci à vous deux pour votre amitié et les bons moments passés ensemble, au labo et en-dehors.

Je remercie « mes petits », Nadine, Annanet', Gillou, Cristina et Alessandra, les étudiants de passage au laboratoire avec qui j'ai pris un plaisir énorme à travailler ainsi que toutes les personnes qui m'ont aidé dans mon travail : Marc Mermillon-Fournier, pour les heures passées devant le GC et beaucoup d'aide « technique », Mélanie Boucher et les services communs de l'Université de Strasbourg de RMN, de spectrométrie de masse, d'analyse élémentaire, le magasin et Soumia Hnini pour tous les aspects administratifs lié à la thèse qu'elle a gérés.

Je remercie très chaleureusement tous les membres du laboratoire (et anciens) pour leur accueil, leur soutien pendant ce temps passé ensemble : tout d'abord « mon premier bureau » : Patty et Magno qui m'ont beaucoup aidé à m'intégrer, puis le « crazy bureau » : Shuanming et Hao qui m'ont supporté pendant les derniers moments de la thèse et Sabrina, Thomas (choupinou), Sophie, Matthew, Farba, Suyun, Laure, Jonathan, Riccardo, Anthony, Adel, Abdelatif, Günter, Corinna, Anja, Elisa, Marco, Weiwei, Martin, Paulin, Lisa, Anthony, Shaofeng, Pierre, Jacky, Catherine, Lucie et tout particulièrement Matthieu pour son amitié et tout ce que l'on a partagé ensemble.

Je tiens à adresser quelques mots de remerciements à mes amis chimistes « hors labo » pour les moments partagés, Jean-Thomas, Georges, Cédric, Fred, Anne-Laure, Amandine, Paco, Pape, Nico, Charles, Nasser, Rafa, Stéphane, Aline, Samuel, les membres du GRK532, Pauline, Amadou, Hakima et Markus en particulier et mes amis non-chimistes que j'ai un peu délaissé pendant cette période.

Je finirai par remercier ceux sans qui je n'aurai jamais pu en arriver là, ma famille, en particulier mes parents pour leur soutien inébranlable et la confiance qu'ils m'ont toujours témoigné, et Pauline pour m'avoir accompagné, soutenu et supporté pendant tous ces moments.

TABLE DES MATIERES*

Introduction Générale

Ligands polyfonctionnels : Définition, propriétés et applications.....	2
Hémilabilité et catalyse	
Ancrage et matériaux	
Les ligands carbènes <i>N</i> -hétérocycliques (NHCs)	7
Définition	
Caractéristiques électroniques	
Caractéristiques stériques	
Synthèse	
Les ligands diphosphines.....	12
Définition	
Caractéristiques électroniques	
Caractéristiques stériques	
Synthèse	
Objectifs de la thèse.....	18
Références	20

Chapitre 1 – Versatile Coordination Modes of Novel Hemilabile S-NHC Ligands

Résumé du Chapitre 1.....	2
Abstract of Chapter 1	3
Paper	4
Experimental Section.....	10
References	25

Chapitre 2 – Synthesis of *N,N'*-bis(thioether)-functionalized Imidazolium Salts: Their Reactivity towards Ag and Pd Complexes and First *S,C_{NHC},S* Free Carbene

Résumé du Chapitre 2.....	2
Abstract of Chapter 2	3
Introduction	4
Results and Discussion	5
Conclusion	13
Experimental Section.....	15
References	24

* Chaque section de ce mémoire a une pagination autonome.

Chapitre 3 – Thioether-functionalized N-Heterocyclic Carbenes: Mono-, and Bis-(*S,C_{NHC}*)
Palladium Complexes, Catalytic C-C coupling and Characterization of a
unique Ag₄I₄(*S,C_{NHC}*)₂ Planar Cluster

Résumé du Chapitre 3	2
Abstract of Chapter 3	4
Introduction	6
Results and Discussion	8
Conclusion	22
Experimental Section	23
References	40

Chapitre 4 – Thioether-functionalized Bis(diphenylphosphino)amine Ligands: Synthesis,
Coordination Chemistry and Applications

Résumé du Chapitre 4	2
Abstract of Chapter 4	3
Introduction	4
Results and Discussion	6
Conclusion	28
Experimental Section	29
References	38

Chapitre 5 – Mono- and Dinuclear Complexes and Tetranuclear Clusters with Bromine-
functionalized Bis(diphenylphosphino)amine Ligands

Résumé du Chapitre 5	2
Abstract of Chapter 5	3
Introduction	4
Experimental Section	5
Results and Discussion	11
Conclusion	21
References	23

Conclusion Générale

Plan de la thèse

La thèse est composée d'une introduction générale et d'une conclusion générale.

Les chapitres 1 à 3 et le chapitre 5 sont rédigés sous la forme de leur publication respective, avec leur propre introduction, conclusion et bibliographie. La référence de la publication ainsi que les co-auteurs sont mentionnés en début de chapitre.

Le chapitre 4 est composé d'une unique introduction et d'une conclusion, mais rassemble des travaux qui feront l'objet de plusieurs publications.

Le chapitre 1 a fait l'objet d'une communication parue dans la revue *Dalton Transactions*.

Le chapitre 2 a fait l'objet d'un article paru dans la revue *Dalton Transactions*.

Le chapitre 3 a fait l'objet d'un article paru dans la revue *Organometallics*.

Le chapitre 4 n'a pas encore été soumis pour publication.

Le chapitre 5 a fait l'objet d'un article paru dans la revue *Journal of Cluster Science*.

La police et la mise en page ont été homogénéisées par rapport au format de publication, pour plus de confort de lecture.

Introduction Générale

Le sujet de cette thèse portait sur le design de ligands polyfonctionnels et l'étude de leur réactivité vis-à-vis des métaux de transition. Dans cette introduction, nous proposons de définir les propriétés d'un ligand polyfonctionnel, la diversité des modes de coordination résultante et enfin les applications potentielles en chimie et physique. Nous finirons par présenter les classes de fonctions que nous avions décidé d'assembler.

Ligands polyfonctionnels : Définition, propriétés et applications¹

La chimie organométallique reste à ce jour un domaine d'investigation considérable, que ce soit dans le cadre de recherches fondamentales ou d'applications industrielles. Dans les deux cas, le paramètre que l'on cherche à contrôler et à comprendre est l'interaction entre le ligand et le centre métallique. Cette interaction est contrôlée par plusieurs facteurs, dont les plus importants sont les propriétés électroniques et stériques du ligand. C'est en modulant ces propriétés, en fonction du centre métallique étudié, que les chimistes peuvent espérer contrôler les architectures résultantes à l'état solide de ces composés, et/ou leur comportement en solution mais aussi et surtout leur réactivité.

Une première classe de ligands polyfonctionnels, aussi appelés ligands hybrides ou mixtes, est le résultat de l'association de deux, ou plus, sites donneurs différents portés par la même molécule. Par site donneur, on entend toutes les fonctions classiques utilisées en chimie de coordination pour interagir avec un centre métallique ; phosphine, carbène, imine, alcoolate, *etc.* Dans le cas d'une autre classe de ligands polyfonctionnels, l'un des sites donneurs peut être remplacé par une fonction de greffage ; alkoxysilane, thiol, *etc.* La nature et la longueur de l'espaceur entre les deux sites influencent ou contraignent l'orientation des sites donneurs et sont donc des paramètres non négligeables lors du design des ligands (Schéma 1).

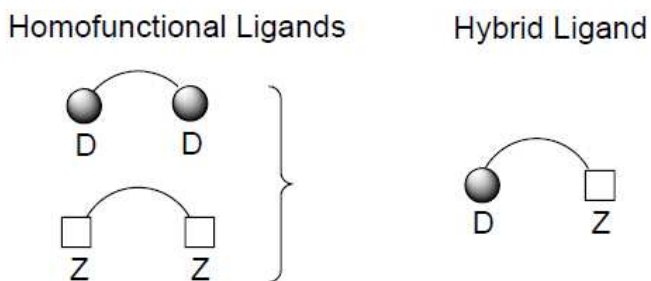


Schéma 1 : représentation schématique d'un ligand hybride composé de deux sites donneurs différents, D et Z.

La somme de ces paramètres entraîne différents modes de coordination possibles. Si D et Z sont des sites donneurs, on peut à priori en observer trois. Dans le cas d'un centre métallique ayant une affinité pour seulement l'une ou l'autre des fonctions donneuses on peut observer un mode de coordination monodente. Lorsque le métal et les deux donneurs sont compatibles, le ligand peut se coordiner de façon bidentée chélatante. Si la rigidité de l'espace ne le permet pas, il peut se former des complexes bimétalliques, dans lesquels le ligand sera lié de manière bidentée pontante (Schéma 2).

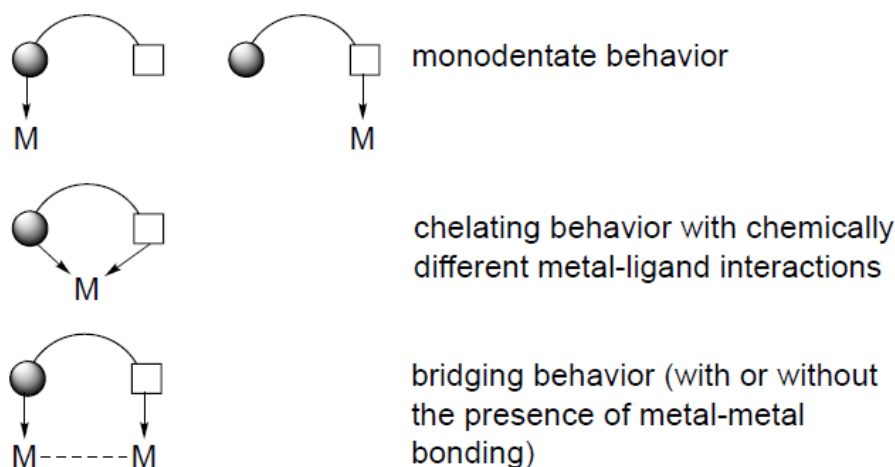


Schéma 2 : modes de coordination possibles d'un ligand bi-fonctionnel

En fonction des propriétés et des applications potentielles recherchées, il ne reste plus aux chimistes qu'à associer les fonctions chimiques à leur disposition, pour créer, après réaction avec un centre métallique, les systèmes recherchés.

Hémilabilité et catalyse

Lorsqu'un ligand mixte est composé de deux sites donneurs à caractères différents, un donneur « mou » et un donneur « dur » par exemple, selon la théorie HSAB (Hard and Soft Acids and Bases), après coordination avec un centre métallique, on peut obtenir des systèmes dits hémidabiles. Le terme « hémidabile » a été introduit à la fin des années 70 par Jeffrey and Rauchfuss,² même si ce phénomène a pu être observé avant par Braunstein *et al.*³ L'hémilabilité est un comportement dynamique en solution. La caractéristique de ce type de ligands est la possible coordination/décoordination réversible de l'un des donneurs, c'est le donneur labile (Z), alors que l'autre (ou les autres) fonction donneuse (D) reste irréversiblement liée au métal. Ce phénomène a été essentiellement étudié sur des systèmes mononucléaires, mais peut être étendu à des systèmes dinucléaires, voir même de plus haute nucléarité ou dans le cas de clusters moléculaires (Schéma 3).

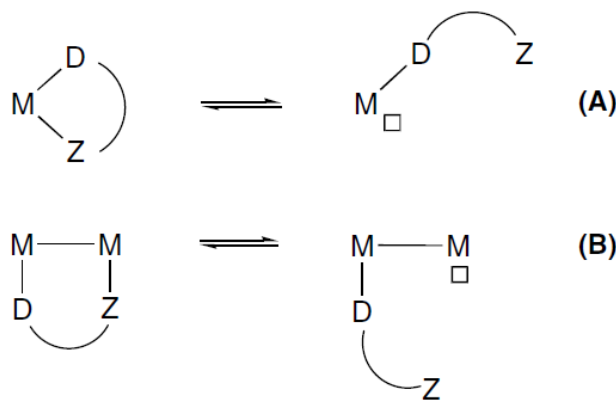


Schéma 3 : comportement hémilabile d'un ligand mixte en interaction avec un (A) ou deux (B) centres métalliques

Ce type de ligand et les complexes résultants ont rapidement trouvé des applications en catalyse homogène. En effet, la décoordination de (**Z**), l'« ouverture » du chélate dans le cas d'une espèce mononucléaire, libère un site de coordination du métal qui devient accessible. Ceci permet à une autre molécule, un réactif ou substrat (**S**) dans le cas d'une réaction catalytique, d'interagir avec le centre métallique. Pendant cette phase, le donneur (**D**) reste lié au centre métallique, ce qui permet de « garder » géographiquement à proximité le donneur (**Z**). Après transformation assistée par le centre métallique, le produit de la réaction (**P**) est libéré et le catalyseur est stabilisé par la re-coordination du donneur (**Z**) (Schéma 4).

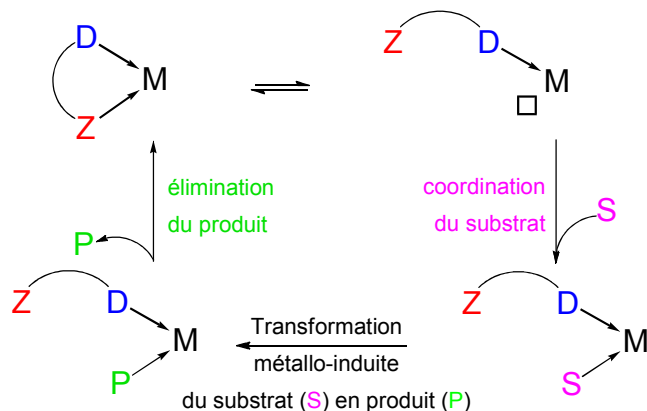


Schéma 4 : dynamique d'un ligand mixte lors d'un cycle catalytique

Des systèmes hémilabiles basés sur des ligands de type phosphine-oxazoline (**P,N**) associés au nickel ou au palladium ont été étudiés au Laboratoire de Chimie de Coordination de Strasbourg ces dernières années (Schéma 5).⁴ Dans ces systèmes, le phosphore joue le rôle du donneur **D**, il est le « meilleur » ligand alors que l'azote joue le rôle du donneur labile **Z**. Ces composés ont montré de très bonnes activités en catalyse homogène d'oligomérisation d'éthylène et/ou de co-polymérisation éthylène/CO.

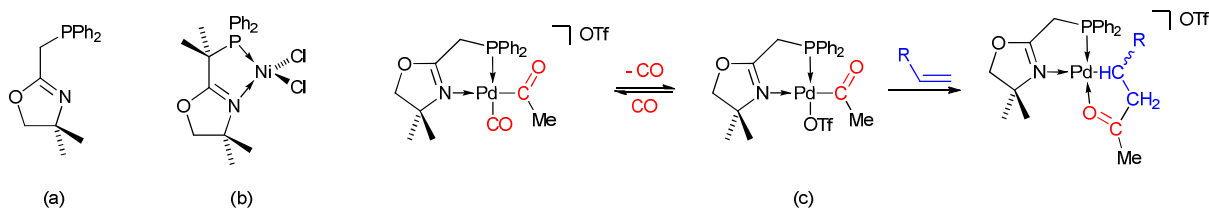


Schéma 5 : (a) ligand P,N ; (b) complexe de Ni utilisé en oligomérisation d'éthylène ; (c) complexe de Pd lors de la catalyse de copolymérisation éthylène/CO

Des ligands tridentes (N,P,N et NOPON) contiennent un squelette oxazoline et ont montré un comportement dynamique en solution, basé sur un mode de coordination bidente dans lequel les deux bras oxazoline s'échangent rapidement (Schéma 6).

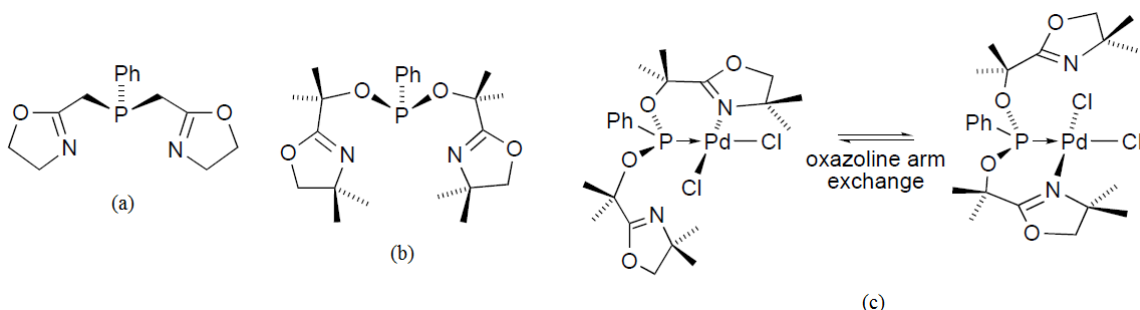


Schéma 6 : (a) ligand N,P,N ; (b) ligand NOPON et (c) illustration de leur comportement dynamique

Avant le début des travaux de cette thèse, les ligands hémilabiles faisant intervenir un ligand NHC n'avaient pas été étudiés au laboratoire.

Ancrage et matériaux

Comme annoncé précédemment, l'autre intérêt à la synthèse de ligands polyfonctionnels est l'association d'un site donneur qui sera engagé dans des réactions de chimie de coordination vis-à-vis de centres métalliques ou clusters moléculaires et d'une fonction dédiée à l'ancrage des molécules sur des supports inorganiques (Schéma 7).

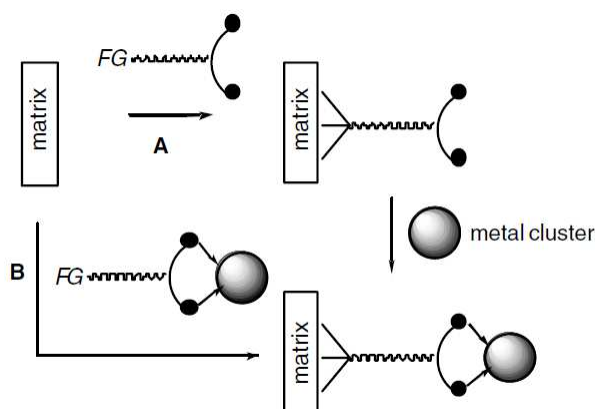


Schéma 7 : vue schématique des applications d'un ligand mixte comportant une fonction de greffage (FG) associé à un cluster moléculaire

Au sein de notre laboratoire, des ligands possédant cette architecture ont été développés et étudiés vis-à-vis de clusters moléculaires de type Co_4 ou RuCo_3 .⁵ Les sites donneurs dédiés à la chimie de coordination étudiés étaient de type phosphine (P) ou diphosphines (P,P), pour leurs affinités connues pour ces molécules. Quant aux fonctions dédiées à l'ancrage, les études se sont orientées vers les alkoxy silanes pour des applications en procédé sol-gel et vers les fonctions soufrées pour les dépôts sur des surfaces métalliques. Ce travail a permis, en collaboration avec des équipes de physiciens de l'IPCMS (Strasbourg) et/ou de l'Université de Haute Alsace (Mulhouse), de greffer des clusters moléculaires dans des matrices mésoporeuses^{1,5} ou sur des surfaces d'or⁶ et d'en analyser les assemblages résultants (Schéma 8).

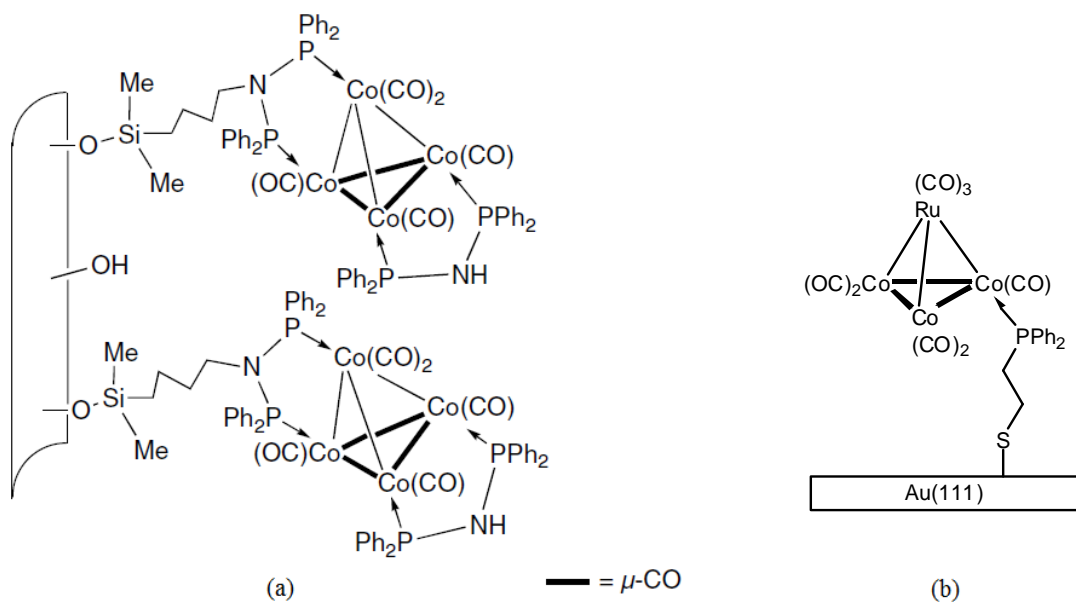


Schéma 8 : assemblages moléculaires (a) greffés dans des matrices mésoporeuses ; (b) déposés sur surface d'or

Les ligands carbènes *N*-hétérocycliques (NHCs)

Historiquement, Öfele et Wanzlick ont été les premiers à synthétiser des complexes carbènes *N*-hétérocycliques en 1968,^{7,8} mais ce n'est que depuis l'isolement du premier carbène libre par Arduengo *et coll.*⁹ en 1991 que l'étude de cette nouvelle classe de ligands prit son essor. Cet engouement s'explique par la capacité de ces ligands à former des liaisons fortes avec la plupart des métaux de transition, ils peuvent constituer une alternative intéressante aux phosphines. En effet, les précurseurs des ligands carbènes, les sels d'imidazoliums, sont stables à l'air au contraire des phosphines, qui peuvent rapidement s'oxyder. Le fort caractère σ -donneur des NHCs leur permet de stabiliser des métaux à bas ou haut degré d'oxydation, ce qui rend les complexes généralement moins enclins à la décomposition et accroît leurs performances catalytiques du métal. L'exemple classique est le gain d'activité obtenu en métathèse des oléfines par substitution d'une phosphine PCy_3 par un carbène de type 1,3-bis(mésityl)imidazolinylidène (SIMes) entre le catalyseur de Grubbs dit de première et celui dit de deuxième génération (Schéma 9).

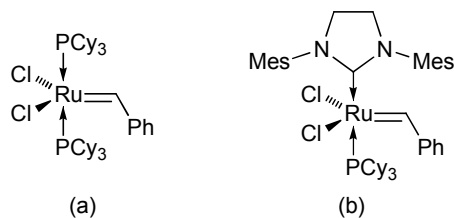
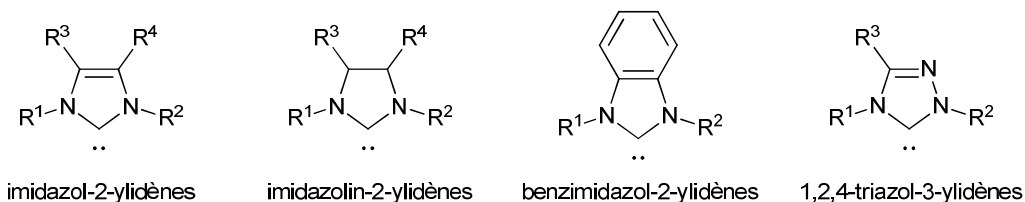


Schéma 9 : catalyseur de Grubbs (a) de première et (b) de deuxième génération pour la métathèse des oléfines

Il ne s'agit pas, dans ce manuscrit, de faire le bilan complet de la chimie de ces composés car ils font l'objet d'un grand nombre de revues.¹⁰

Définition

Les carbènes *N*-hétérocycliques (NHCs) sont des composés neutres cycliques comportant un atome de carbone divalent à six électrons de valence et entouré de deux atomes d'azote, c'est pourquoi on les appelle aussi parfois diaminocarbènes. La figure 10 présente les familles de ligands NHCs les plus courantes. On dénombre également quelques récents exemples de carbènes cycliques à quatre,¹¹ six¹² ou sept¹³ chaînons mais également des diaminocarbènes acycliques¹⁴ présentant à priori les mêmes propriétés. Ces dernières années, des études sur la chimie de coordination de NHCs où l'un des atomes d'azote a été remplacé par un atome de soufre¹⁵ ou d'oxygène¹⁶ ont été publiées.

Schéma 10 : les grandes familles de carbènes *N*-hétérocycliques

Caractéristiques électroniques

Les ligands NHCs ont un caractère σ -donneur typique et peuvent déplacer des ligands donneurs de deux électrons, tels que les nitriles, amines, alcènes ou carbonyles souvent présents sur les précurseurs métalliques employés. Ce caractère σ -donneur s'explique par la présence des deux atomes d'azote en α du carbone carbénique. Les azotes apportent une contribution de type π -donneur σ -accepteur ce qui permet de conserver l'électroneutralité du centre carbénique. De ce fait, l'orbitale π liante du carbène est stabilisée par la contribution des paires d'électrons libres des azotes et l'orbitale σ est stabilisée par leur effet inductif attracteur. Il faut aussi tenir compte des substituants portés par ces mêmes atomes d'azote, qui pourront avoir un effet donneur ou accepteur qui influencera le caractère donneur du carbène. Le schéma 11, présente ces effets électroniques et le mode de coordination typique avec un métal de transition qui en résulte.

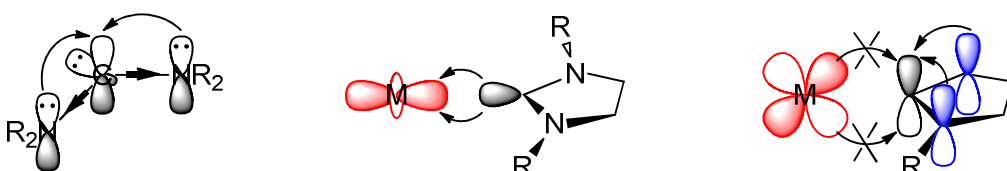


Schéma 11 : effets électroniques des azotes des diaminocarbènes et leur mode de coordination typique

Le meilleur pouvoir σ -donneur de ce type de ligand par rapport aux phosphines a été mis en évidence par comparaison des fréquences de vibration des carbonyles dans des complexes de métaux de transition portant dans un cas un ligand NHC et dans l'autre cas un ligand PR_3 et des CO.¹⁷ Comme représenté sur le schéma 11, les diaminocarbènes étaient considérés comme des ligands faiblement π -donneurs et accepteurs. Par contre, de récentes études mettent en doute cette affirmation, appuyées par des études théoriques qui estiment que l'interaction π , dans des complexes de nickel riches en électrons, peut atteindre 43% de l'énergie totale d'interaction des orbitales.¹⁸

Caractéristiques stériques

D'un point de vue géométrique, lors de la formation de complexes de coordination, le plan de l'imidazole, celui qui contient le fragment NCN est très peu encombré, ou alors, en retrait du métal dans le cas d'imidazoles substitués en positions C4 ou C5. A contrario, les axes contenant les *N*-substituants sont plus encombrants, et orientés en direction du métal. Un modèle permettant de quantifier l'encombrement stérique des ligands NHCs a été développé. Il est basé sur le pourcentage du volume occupé par les atomes du ligand dans une sphère centrée sur le métal, % $V_{\text{occupé}}$ (Schéma 12).¹⁷ Ce modèle permet de comparer les ligands carbéniques avec d'autres ligands, particulièrement les phosphines tertiaires, dont ils ont longtemps été considérés comme les analogues carbonés. Les calculs de % $V_{\text{occupé}}$ des systèmes PR_3 ont permis des comparaisons directes, où les substituants R portés par le phosphore étaient identiques à ceux portés par les azotes du NHC. Ainsi, on a pu montrer que dans le cas du groupement tertiobutyle (*t*-Bu), le ligand NHC était stériquement plus encombré que son analogue phosphine.

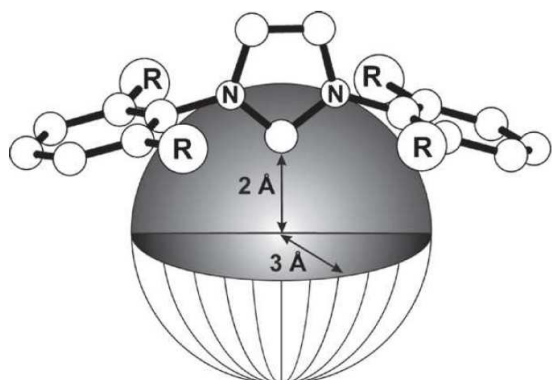


Schéma 12 : Représentation des dimensions de la sphère pour la détermination des paramètres stériques (% $V_{\text{occupé}}$) des ligands NHCs

Synthèse

Il existe différentes voies de synthèse pour la formation des sels d'imidazoliums, précurseurs des ligands carbènes *N*-hétérocycliques (Schéma 13). On privilégiera l'une ou l'autre en fonction de la symétrie du ligand désirée, R¹ et R² identiques ou non, et/ou des réactifs disponibles, les amines correspondantes aux substituants désirés ou leurs halogénures.

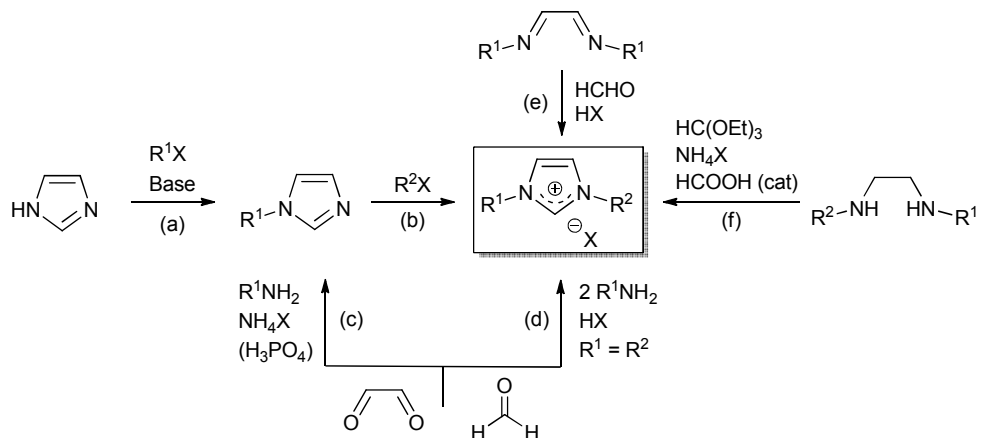


Schéma 13 : voies d'accès aux sels d'imidazoliums

La première voie est une synthèse par alkylations successives. La première étape est la réaction de l'imidazole avec un halogénure d'alkyle en présence d'une base (Schéma 13, (a)). On obtient ainsi les dérivés 1-(alkyl)imidazoles. Ces composés peuvent ensuite être mis à réagir avec un autre halogénure d'alkyle pour obtenir des 1,3-(dialkyl)imidazoles (Schéma 13, (b)). Ce chemin réactionnel permet l'obtention rapide de sels d'imidazoliums dissymétriques si les dérivés halogénés des *N*-substituants sont facilement accessibles.

Les autres voies de synthèse font intervenir les amines correspondantes aux substituants que l'on désire introduire. On peut noter sur le schéma 13, les voies (d) et (e) qui ne permettent l'obtention que d'imidazoliums symétriques. Dans le cas de (d), c'est une réaction en une seule étape, à partir de deux équivalents de l'amine à condenser, de glyoxal et de formaldéhyde en milieu acide. La voie (e) est proche, à la différence que le réactif initial engagé est un 1,2-diimine déjà formé à la place de l'amine et du glyoxal. Pour pouvoir former des imidazoliums dissymétriques à partir d'amines différentes, il faut au préalable synthétiser la 1,2-diamine correspondante puis la formation du cycle imidazole se fait en utilisant du triethylorthoformate en présence d'un sel d'ammonium par catalyse acide, voie (f).¹⁹ Finalement, une synthèse mixte (Schéma 13 (c) et (b), respectivement), où le premier *N*-substituant est introduit par son amine correspondante pour former le 1-(aryl ou alkyl)imidazole par la même réaction que pour (d). Le second substituant est introduit *via* son dérivé halogéné par la voie (b) pour obtenir le précurseur de ligand carbène désiré.

La formation des ligands carbènes nécessite la déprotonation des imidazoliums pour former le carbène libre, qui peut alors se coordiner au métal. C'est cette réaction qui a permis à Arduengo d'isoler le premier carbène libre stable à température ambiante à l'abri de l'air (Schéma 14).

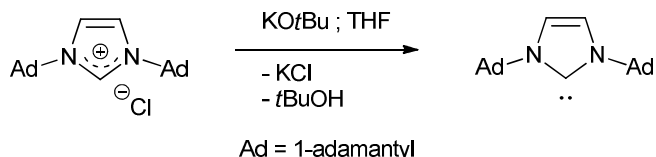


Schéma 14 : synthèse d'un NHC par déprotonation du chlorure d'imidazolium correspondant

Il existe plusieurs méthodes pour la complexation des ligands NHCs.²⁰ Parmi les plus couramment utilisées, on retrouve, la coordination à partir d'un carbène libre isolé, mais cela nécessite que le carbène en question soit stable et puisse être conservé. Le carbène peut être engendré *in situ* en présence d'un métal, avec lequel il réagira. Une autre méthode très utilisée est la réaction de transmétallation à partir des complexes d'argent [AgX(NHC)], qui le plus souvent sont formés *in situ* et directement mis à réagir avec le précurseur métallique désiré.²¹

Nous avons, à ce stade mis en avant les caractéristiques qui ont rendu ces ligands très attractifs en chimie organométallique et en catalyse homogène, mais le lien avec l'intitulé de ce manuscrit : « Ligands polyfonctionnels ... » reste vague. En effet, les stratégies de synthèse décrites dans le schéma 13 ont permis ces dernières années de développer des ligands polyfonctionnels de type *D*-NHC, où *D* représente un second site donneur porté par le substituant de l'atome d'azote du cycle imidazole. Ces nouvelles classes de ligands *D*-NHC associent un excellent donneur, très robuste, très peu dissociant idéal en catalyse (NHC) et un donneur plus labile (*D*), on peut donc facilement imaginer un comportement hémidurable des systèmes résultants. C'est pourquoi les complexes qui découlent de l'association des *D*-NHC avec les métaux de transition ont rapidement trouvé leur place en catalyse homogène. Les fonctions les plus étudiées sont de types *N*-NHC²² (où *N* représente les fonctions amine ou imine), *P*-NHC²³ (*P* = phosphine) pour les donneurs à deux électrons et *O*-NHC²⁴ (*O* = alkoxyde) en tant que ligand anionique. A ce jour, très peu d'exemples de systèmes associant les ligands carbènes à une fonction soufrée (*S*-NHC) ont été décrits.²⁵

Les ligands diphosphines²⁶

Définition

Les ligands à base de phosphore (III) sont probablement à ce jour, les ligands qui ont été les plus étudiés en chimie organométallique. Associés aux métaux de transition, leurs complexes ont montré des applications nombreuses et variées en catalyse homogène. Des composés organophosphorés courants de phosphore (III) sont représentés dans le Schéma 15. La possibilité de modifier les groupements Rⁿ, donc les propriétés électroniques et stériques du ligand influencent la liaison métal-phosphore ainsi que sa réactivité. Ces caractéristiques furent un atout indéniable pour le développement de catalyseurs à base de ces composés. Nous verrons plus loin certains modèles utilisés pour quantifier les contributions électroniques et stériques de ces ligands dans les complexes de métaux de transition.

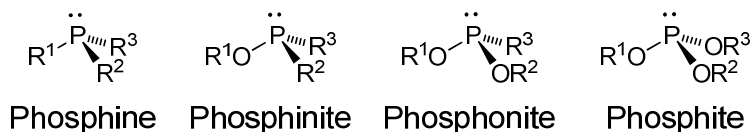


Schéma 15 : composés de phosphores (III) utilisés en chimie de coordination

Dans cette introduction, nous nous limiterons aux ligands bidentes de type diphosphines (P,P) et aux possibilités de les modifier pour les rendre polyfonctionnels (P,P,X).

Notre intérêt pour les diphosphines fut motivé par le fait que les ligands phosphorés sont connus pour former des liaisons très fortes et robustes avec les métaux de transition, ce qui s'explique par la théorie HSAB (Hard and Soft Acids and Bases). Les ligands phosphorés ont l'avantage d'offrir une sonde supplémentaire, claire et facilement accessible, par l'intermédiaire de la RMN ³¹P, pour informer le chimiste sur ce qui se passe en solution. De plus, plusieurs éléments de la structure des diphosphines peuvent être modifiés, comme l'espaceur entre les deux atomes de phosphores et les substituants terminaux, R¹ et R², de ces derniers (Schéma 16).

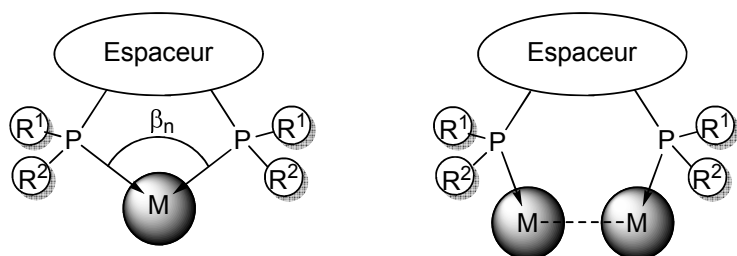
Espaceur, R¹ et R² = variables

Schéma 16 : représentation schématique d'un ligand diphosphine illustrant les parties variables

Ces différents paramètres doivent être pris en compte lors du design du ligand en fonction des applications qu'on lui destine. C'est également l'utilisation des complexes formés qui déterminera le métal employé. Le Schéma 17 représente les diphosphines les plus courantes ou les plus connues. On peut noter la présence de diphosphines possédant un seul atome entre les deux phosphores, tel que la DPPM (bis(diphenylphosphino)methane) et la DPPA (bis(diphenylphosphino)amine). On peut ensuite différencier les diphosphines s'articulant autour d'un espaceur rigide, comme la DPPF (1,1'-bis(diphenylphosphino)ferrocene) ou la *R,R*-DuPhos et celles construites autour d'un espaceur flexible comme le DPPE (1,2-bis(diphenylphosphino)ethane) ou la *R,R*-DIOP. Enfin, on peut noter que certaines diphosphines sont des ligands chiraux, développés pour la catalyse asymétrique. La chiralité peut être « classique » comme dans le cas de la *R,R*-DuPhos, où les phosphores portent des substituants comportant des carbones asymétriques, ou alors imposée par l'espaceur comme dans le cas de la *R*-BINAP ou la *R,R*-DIOP.

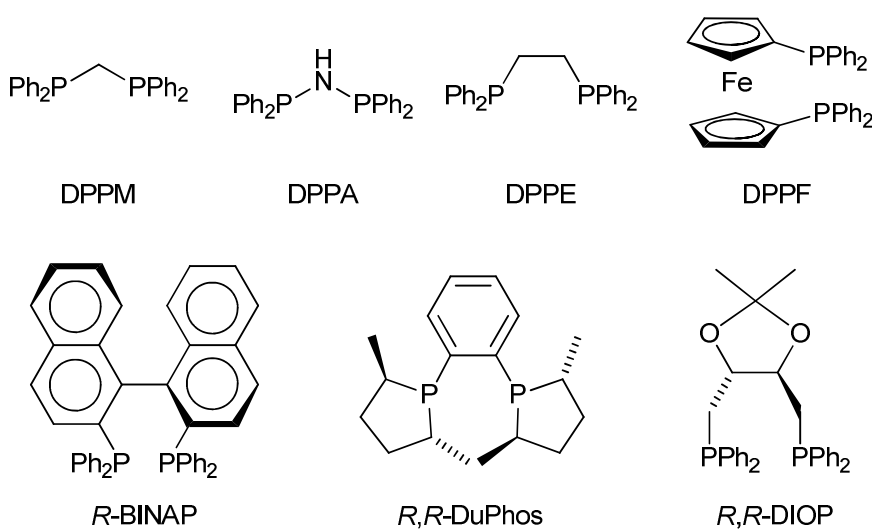


Schéma 17 : sélection de ligands de type diphosphines

Caractéristiques électroniques

A ce jour encore, de nombreuses recherches sont menées pour déterminer les contributions électroniques des phosphines dans leurs complexes organométalliques. Certaines études de la fin des années 60 à la fin des années 70 ont permis de développer des systèmes assez complets pour comprendre, évaluer et mettre à profit les propriétés électroniques des ligands phosphines. Sur la base du système développé par Strohmeier et Müller en 1967,²⁷ Tolman développa un paramètre électronique χ permettant de quantifier les contributions électroniques des ligands phosphines. Ce paramètre est défini par la variation de la fréquence de vibration de l'elongation CO dans le système étudié de type $[\text{Ni}(\text{CO})_3\text{L}]$, où L représente la phosphine étudiée, par rapport au complexe de référence $[\text{Ni}(\text{CO})_3\text{P}(t\text{-Bu})_3]$.²⁸ Cette méthode permet de mesurer le pouvoir donneur du ligand mais pas de quantifier les contributions respectives des caractères σ -donneur et π -accepteur. Ces deux contributions sont fortement dépendantes des substituants portés par le phosphore. On s'accorde à dire que la σ -donation est une donation du doublet libre du phosphore vers une orbitale vide du métal. La π -rétrodonation est le partage de densité électronique d'orbitales pleines basées sur le métal avec des orbitales vides de la phosphine (Schéma 18). Même si les débats concernant la nature de l'orbitale recevant cette densité électronique ne sont pas clos, il est admis que cette donation se fait d'une orbitale d du métal vers les orbitales P-C σ^* du ligand phosphoré.²⁹

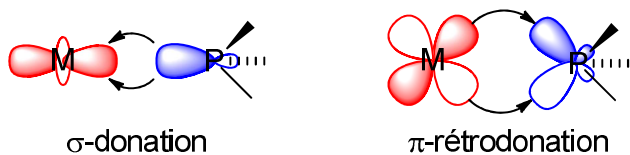


Schéma 18 : illustration des deux composantes de la liaison Phosphore - Métal

Caractéristiques stériques

Même si plusieurs modèles pour décrire l'effet stérique des ligands phosphines ont été développés ces dernières années,³⁰ le concept qui reste le plus largement appliqué est le modèle de Tolman.^{28,31} Il est basé sur l'angle du cône (θ) qui permet de déterminer le volume du cône occupé par une monophosphine, sur la base des modèles CPK en plaçant le métal à une distance invariable de 2.28 Å (Schéma 19, (a)). La limitation de ce modèle est que les phosphines ne forment que très rarement un cône parfait, en particulier si plusieurs ligands différents sont coordinés au métal. White *et al.* au milieu des années 90 introduira le concept d'angle solide sur la base de données cristallographiques et de structures modélisées. Dans ce modèle, les rayons atomiques des composants du ligand sont projetés à la surface du métal, donnant ainsi la mesure de l'encombrement stérique du ligand (Schéma 19, (b)).³² Dans le cas des ligands diphosphines dans un mode de coordination chélatant, la mesure de l'angle de cône pour décrire l'effet stérique des ligands n'est pas suffisante. Casey et Whiteker furent les premiers à décrire l'angle de chélation naturel (β), c'est l'angle (P-M-P') préférentiel adopté dans le complexe (Schéma 19, (c)).³³ Cet angle est influencé par la géométrie de coordination du métal, la nature de l'espaceur et les influences électroniques des substituants des atomes de phosphore. Une étude récente sur plus de 900 structures moléculaires de complexes de platine issues de la Cambridge Database et plus de 280 diphosphines a permis d'établir un nouveau paramètre ($\bar{\theta}_b$) pour traduire les effets stériques de ces ligands.³⁴ Ce nouveau paramètre est basé sur le concept de l'angle de Tolman, mais de plus, par l'intermédiaire du facteur de correction (b), il tient compte de la distance Métal-Phosphore dans le complexe et de l'angle de chélation (β) qui est fonction de la diphosphine étudiée.

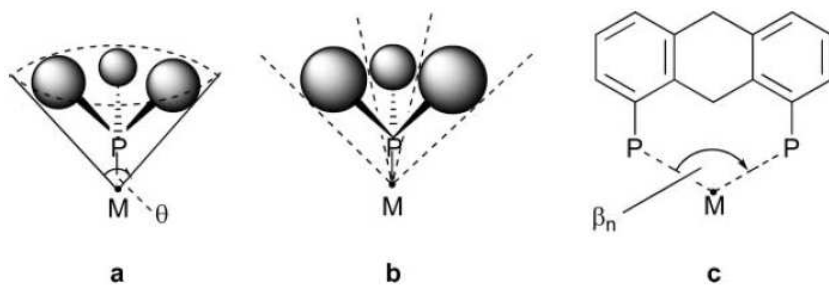


Schéma 19 : (a) angle de cône de Tolman, (b) angle solide de White et (c) angle de chélation de Casey et Whiteker

C'est l'ensemble de ces paramètres qui orienta notre choix vers un ligand de type diphosphine pour le développement de nos ligands polyfonctionnels. Le choix de l'espaceur entre les deux atomes donneurs s'est naturellement orienté vers le fragment NH (DPPA). En

effet, le ligand DPPA est connu pour sa large variabilité de modes de coordination, il peut agir comme ligand bidente chélatant, bidente pontant ou encore comme ligand monodente (Schéma 2). Enfin, l'hydrogène porté par l'atome d'azote est un hydrogène dit : « acide », ce qui devrait faciliter la fonctionnalisation du fragment DPPA.

Synthèse

Dans cette partie, nous limiterons les descriptions de synthèses relatives aux diphosphines de type R-DPPA, où R représente un substituant quelconque. Le ligand bis(diphenylphosphino)amine (DPPA = Ph₂P(NH)PPh₂) est une diphosphine synthétisée à partir de l'hexaméthyldisilazane et de chlorophosphine selon le schéma réactionnel 20.³⁵ Dans la DPPA, l'espaceur entre les deux atomes donneurs, les phosphores, n'est constitué que d'un atome, l'azote. De ce fait, la coordination de ce ligand vis-à-vis des centres métalliques est contrôlée par l'angle PNP et les géométries de coordination préférentielles du métal utilisé.

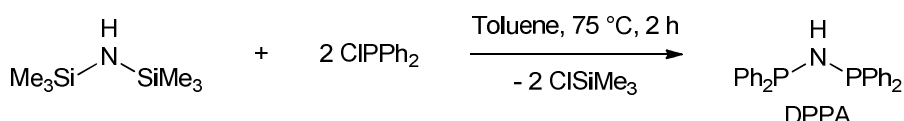


Schéma 20 : synthèse du ligand bis(diphenylphosphino)amine (DPPA)

Au Laboratoire de Chimie de Coordination de Strasbourg, ce ligand a été largement utilisé comme ligand assembleur pour associer plusieurs centres métalliques ou pour stabiliser/fonctionnaliser des clusters moléculaires préformés.³⁶ Au vue de la structure de cette molécule, on peut facilement imaginer introduire un troisième site donneur lié à l'atome d'azote. La fonctionnalisation par déprotonation de la fonction NH suivie d'une réaction avec un électrophile organique paraît triviale (Schéma 21, (a)). Néanmoins, cette stratégie ne fonctionne que dans certains cas très rares et/ou donne de très faibles rendements. Il paraît plus avantageux d'appliquer cette démarche à un complexe organométallique préformé plutôt qu'à la DPPA libre (Schéma 21, (b)).³⁷

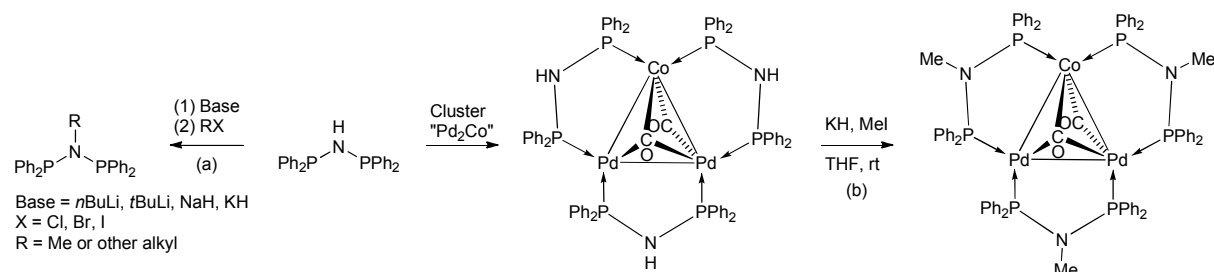


Schéma 21 : (a) fonctionnalisation directe de la DPPA ; (b) fonctionnalisation de la DPPA après coordination à un cluster moléculaire

La meilleure solution pour l'obtention de ligands de type DPPA *N*-fonctionnalisés est de faire réagir l'amine primaire correspondante avec deux équivalents de chlorodiphénylphosphine (Schéma 22).³⁸ De par cette méthode, on peut obtenir un grand choix de *N*-substituants, soit si l'amine primaire correspondante est commerciale, soit par sa formation *via* une synthèse de Gabriel par exemple. Depuis la fin des années 90 et le développement de cette méthode, on a pu observer un regain d'intérêt pour ces diphosphines et leurs complexes organométalliques. Les multiples fonctionnalisations possibles de la DPPA ont permis de modifier les caractéristiques électroniques et stériques du ligand résultant et donc des complexes cibles. On retrouve la démarche classique du développement de catalyseurs homogènes. Un exemple caractéristique est le nombre de publications parues sur le thème de l'oligomérisation catalytique de l'éthylène par des complexes contenant des ligands de type DPPA *N*-fonctionnalisés.³⁹

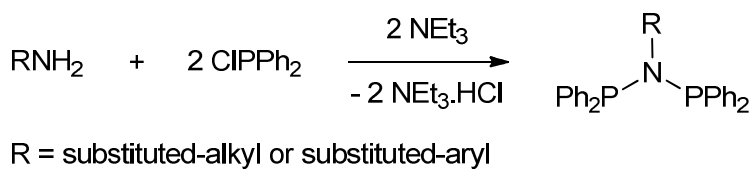


Schéma 22 : synthèse de ligands de type DPPA *N*-fonctionnalisée

En analysant la structure de ces dérivés, on observe que l'orientation du *N*-substituant du ligand est opposée au plan de coordination PNP. On peut difficilement envisager une interaction intramoléculaire du *N*-substituant avec le centre métallique coordonné aux deux phosphores. La présence d'un site donneur peut tout de même conduire à la formation de systèmes hémilabiles en solution par interactions intermoléculaires. Par contre, cette orientation se prête parfaitement à l'ancrage de ces composés dans des matrices inorganiques ou sur des surfaces métalliques par introduction de fonctions adéquates portées par le *N*-substituant. C'est cette stratégie qui, au sein du laboratoire, permet de greffer des clusters métalliques portant des dérivées de la DPPA fonctionnalisées par des groupements alkoxy silanes⁵ dans des matrices mésoporeuses (Schéma 7) et la préparation après traitement thermique, de particules métalliques hautement dispersées.⁴⁰ On a pu noter que comme dans le cas des ligands NHCs, très peu d'exemples de ligands de type DPPA portant une fonction soufrée (*S*-DPPA) ont été décrits.

Objectifs de la thèse

Les objectifs de cette thèse étaient de développer deux familles de ligands polyfonctionnels associant l'une des deux classes de ligands bien connus décrites ci-dessus, les ligands carbènes *N*-hétérocycliques et les ligands diphosphinoamines, à une deuxième fonction encore très peu étudiée. La nature de cette dernière et celle de l'espaceur entre les deux types de sites de coordination furent motivées par le type de complexes que l'on désirait obtenir et leurs applications potentiellement les plus intéressantes.

Dans le cas des ligands NHCs, notre objectif était de synthétiser des ligands potentiellement chélatants lors de leur coordination avec un centre métallique, donc avec un espaceur « souple » composé de un à trois carbones aliphatiques. L'application première qui a été envisagée pour les complexes formés est la catalyse homogène. Etant donné le peu d'études de systèmes de type S-NHC, notre attention s'est focalisée sur la fonction thioéther. Cette fonction soufrée présente l'avantage d'une plus grande inertie que la fonction thiol, par exemple, sujette à l'oxydation et permettant également un contrôle stérique au niveau du substituant R' (Schéma 23). Le choix d'une fonction soufrée reste compatible avec de possibles études d'ancre sur des surfaces métalliques (Au 1,1,1) ou lors de la formation de nanoparticules, qui pourrait conduire à des catalyseurs supportés.

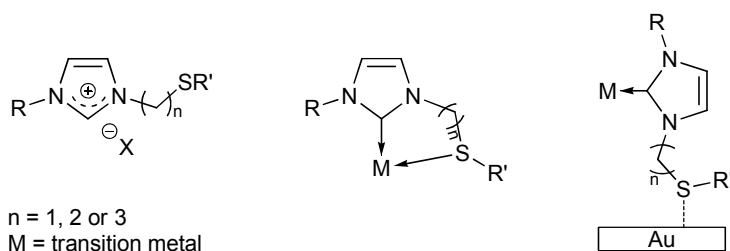


Schéma 23 : ligand de type S-NHC, complexe chélate pour la catalyse et complexe ancré sur une surface d'or par une fonction thioéther

Dans le cas des ligands dérivés de la DPPA, nous ne recherchions pas à former des complexes métalliques pincés par le ligand, nous avons vu précédemment qu'il était presque impossible de coordiner le *N*-substituant au métal. Notre objectif était de développer deux types de ligands DDPA *N*-substitués. Premièrement, nous avons décidé d'étudier des ligands de type DPPA substitués par une fonction thioéther (*S*-DPPA) et leur chimie de coordination. Dans ce cas là, la nature de l'espaceur nous semblait être un paramètre non négligeable, tant électroniquement que stériquement. La nature du métal des complexes formés à partir de ces ligands et leur topologies seront choisis en fonction de l'application désirée (catalyse,

fonctionnalisation de surfaces métalliques...). Le Schéma 24 représente les deux ligands de type S-DPPA que nous nous sommes proposés de synthétiser et d'étudier.

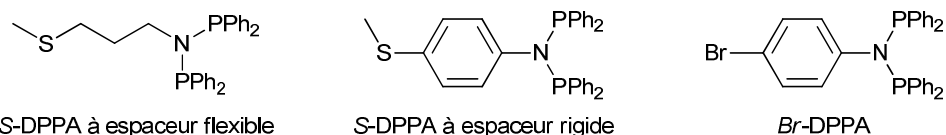


Schéma 24 : ligands de type S-DPPA et *Br*-DPPA étudiés

Enfin, la dernière association qui nous paraissait judicieuse était celle d'un ligand de type DPPA à une fonction bromée (*Br*-DPPA, Schéma 24) qui pourrait nous permettre, par des réactions très simples de former des complexes polynucléaires ou de coupler ces entités à des molécules portant des groupements complémentaires par des réactions de couplage classiques.

Références

- (1) P. Braunstein, *J. Organomet. Chem.*, 2004, **689**, 3953.
- (2) J. C. Jeffrey, T. B. Rauchfuss, *Inorg. Chem.*, 1979, **18**, 2658.
- (3) (a) P. Braunstein, D. Matt, F. Mathey and D. Thavard, *J. Chem. Res.*, 1978, **232**, 3041 (S), (M) ;
 (b) P. Braunstein, D. Matt, Y. Dusausoy, J. Fischer, A. Mitschler and L. Ricard, *J. Am. Chem. Soc.*, 1981, **103**, 5115 ; (c) P. Braunstein, D. Matt and Y. Dusausoy, *Inorg. Chem.*, 1983, **22**, 2043 ; (d) P. Braunstein, J. Fischer, D. Matt and M. Pfeffer, *J. Am. Chem. Soc.*, 1984, **106**, 410.
- (4) (a) P. Braunstein, J. Pietsch, Y. Chauvin, A. DeCian and J. Fischer, *J. Organomet. Chem.*, 1997, **529**, 387 ; (b) P. Braunstein, J. Pietsch, Y. Chauvin, A. DeCian and J. Fischer, *J. Organomet. Chem.*, 1999, **582**, 370 ; (c) P. Braunstein, C. Graiff, F. Naud, A. Pfaltz and A. Tiripicchio, *Inorg. Chem.*, 2000, **39**, 4468 ; (d) P. Braunstein, F. Naud, A. Pfaltz and S. J. Rettig, *Organometallics*, 2000, **19**, 2676 ; (e) P. Braunstein, J. Zhang and R. Welter, *Dalton Trans.*, 2003, 507 ; (f) P. Braunstein, *J. Organomet. Chem.*, 2004, **689**, 3953 ; (g) F. Speiser, P. Braunstein and L. Saussine, *Organometallics*, 2004, **23**, 2625 ; (h) A. Kermagoret and P. Braunstein, *Organometallics*, 2008, **27**, 88.
- (5) (a) A. Choualeb, P. Braunstein, J. Rosé, S.-E. Bouaoud and R. Welter *Organometallics*, 2003, **22**, 4405 ; (b) F. Schweyer-Tihay, P. Braunstein, C. Estournes, J. L. Guille, B. Lebeau, J. L. Paillaud, M. Richard-Plouet, and J. Rosé, *Chem. Mater.*, 2003, **15**, 57.
- (6) A. Naitabdi, O. Toulemonde, J. P. Bucher, J. Rosé, P. Braunstein, R. Welter and M. Drillon, *Chem. Eur. J.*, 2008, **14**, 2355.
- (7) K. Öfele, *J. Organomet. Chem.*, 1968, **12**, P42.
- (8) H.-W. Wanzlick and H.-J. Schonherr, *Angew. Chem. Int. Ed.*, 1968, **7**, 141.
- (9) A. J. Arduengo III, R. L. Harlow and M. J. Kline, *J. Am. Chem. Soc.*, 1991, **113**, 361.
- (10) (a) U. Radius and F. M. Bickelhaupt, *Coord. Chem. Rev.*, 2009, **253**, 678 ; (b) F. E. Hahn and M. C. Jahnke, *Angew. Chem. Int. Ed.*, 2008, **47**, 3122 ; (c) S. Diez-Gonzalez and S. P. Nolan, *Coord. Chem. Rev.*, 2007, **251**, 874 ; (d) F. E. Hahn, *Angew. Chem. Int. Ed.*, 2006, **45**, 1348 ; (e) N. M. Scott and S. P. Nolan, *Eur. J. Inorg. Chem.*, 2005, 1815 ; (f) V. César, S. Bellemin-Laponnaz and L. H. Gade, *Chem. Soc. Rev.*, 2004, 619 ; (g) W. A. Herrmann, *Angew. Chem. Int. Ed.*, 2002, **41**, 1290 ; (h) D. Bourissou, O. Guerret, F. P. Gabbaï and G. Bertrand, *Chem. Rev.*, 2000, **100**, 39.
- (11) E. Despagnet-Ayoub and R. H. Grubbs, *J. Am. Chem. Soc.*, 2004, **126**, 10198.
- (12) P. Bazinet, P. A. Yap Glenn and S. Richeson Darrin, *J. Am. Chem. Soc.*, 2003, **125**, 13314. ; M. Mayr, K. Wurst, K.-H. Ongaria and M. R. Buchmeiser, *Chem. Eur. J.*, 2004, **10**, 1256. ; J. Yun, E. R. Martinez and R. H. Grubbs, *Organometallics*, 2004, **23**, 4172.
- (13) C. C. Scarborough, M. J. W. Grady, I. A. Guzei, B. A. Gandhi, E. E. Bunel and S. S. Stahl,

- Angew. Chem. Int. Ed.*, 2005, **44**, 5269.
- (14) (a) B. Dhudshia and A. N. Thadani, *Chem. Commun.*, 2006, 668 ; (b) M. Otto, S. Conejero, Y. Canac, V. D. Romanenko, V. Rudzhevitch and G. Bertrand, *J. Am. Chem. Soc.*, 2004, **126**, 1016 ; (c) A. M. Magill, K. J. Cavell and B. F. Yates, *J. Am. Chem. Soc.*, 2004, **126**, 8717 ; (d) M.-T. Lee and C.-H. Hu, *Organometallics*, 2004, **23**, 976 ; (e) R. W. Alder, M. E. Blake, L. Chaker and F. P. V. Paolini, *Chem. Commun.*, 2004, 2172 ; (f) R. W. Alder, M. E. Blake, L. Chaker, J. N. Harvey, F. Paolini and J. Schütz, *Angew. Chem. Int. Ed.*, 2004, **43**, 5896 ; (g) W. A. Herrmann, K. Öfele, D. Preysing and E. Herdtweck, *J. Organomet. Chem.*, 2003, **684**, 235 ; (h) M. Tafipolsky, W. Scherer, K. Öfele, G. Artus, B. Pedersen, W. A. Herrmann and G. S. McGrady, *J. Am. Chem. Soc.*, 2002, **124**, 5865 ; (i) K. Denk, P. Sirsch and W. A. Herrmann, *J. Organomet. Chem.*, 2002, **649**, 219 ; (j) R. W. Alder, M. E. Blake and J. M. Olivia, *J. Phys. Chem. A*, 1999, **103**, 11200 ; (k) R. W. Alder and M. E. Blake, *Chem. Commun.*, 1997, 1513 ; (l) R. W. Alder, P. R. Allen, M. Murray and A. G. Orpen, *Angew. Chem. Int. Ed.*, 1996, **35**, 1121.
- (15) par exemple (a) R. Lindner, C. Wagner and D. Steinborn, *J. Am. Chem. Soc.*, 2009, **131**, 8861 ; (b) S. K. Yen, L. L. Koh, H. V. Huynh and T. S. Andy Hor, *J. Organomet. Chem.*, 2009, **694**, 332 ; (c) S. K. Yen, D. J. Young, H. V. Huynh, L. L. Koh and T. S. A. Hor, *Chem. Commun.*, 2009, 6831 ; (d) D. G. Gusev, *Organometallics*, 2009, **28**, 6458 ; (e) G. C. Vougioukalakis and R. H. Grubbs, *J. Am. Chem. Soc.*, 2008, **130**, 2234 ; (f) S. K. Yen, L. L. Koh, H. V. Huynh and T. S. A. Hor, *Chem. Asian J.*, 2008, **3**, 1649 ; (g) S. K. Yen, L. L. Koh, H. V. Huynh and T. S. A. Hor, *Dalton Trans.*, 2008, 699 ; (h) D. C. Graham, K. J. Cavell and B. F. Yates, *Dalton Trans.*, 2007, 4650 ; (i) S. K. Yen, L. L. Koh, H. V. Huynh and T. S. A. Hor, *Dalton Trans.*, 2007, 3952 ; (j) S. K. Yen, L. L. Koh, F. E. Hahn, H. V. Huynh and T. S. A. Hor, *Organometallics*, 2006, **25**, 5105.
- (16) (a) S. Bellemin-Laponnaz, *Polyhedron*, 2010, **29**, 30 ; (b) R. Bertani, M. Mozzon and R. A. Michelin, *Inorg. Chem.*, 1988, **27**, 2809 ; (c) D. C. Graham, K. J. Cavell and B. F. Yates, *Dalton Trans.*, 2007, 4650 ; (d) J. A. Cabeza, I. del Rio, D. Miguel, E. Perez-Carreno and M. G. Sanchez-Vega, *Dalton Trans.*, 2008, 1937 ; (e) J. A. Cabeza, I. del Rio, D. Miguel, E. Perez-Carreno and M. G. Sanchez-Vega, *Organometallics*, 2008, **27**, 211 ; (f) R. Lindner, C. Wagner and D. Steinborn, *J. Am. Chem. Soc.*, 2009, **131**, 8861.
- (17) S. Díez-González and S. P. Nolan, *Coord. Chem. Rev.*, 2007, **251**, 874.
- (18) U. Radius and F. M. Bickelhaupt, *Coord. Chem. Rev.*, 2009, **253**, 678.
- (19) A. W. Waltman and R. H. Grubbs, *Organometallics*, 2004, **23**, 3105.
- (20) E. Peris, *Top. Organomet. Chem.*, 2007, **21**, 83.
- (21) H. M. J. Wang and I. J. B. Lin, *Organometallics*, 1998, **17**, 972.
- (22) par exemple : (a) M. V. Jiménez, J. J. Pérez-Torrente, M. I. Bartolomé, V. Gierz, F. J. Lahoz and

- L. A. Oro, *Organometallics*, 2008, **27**, 224 ; (b) N. Stylianides, A. A. Danopoulos and N. Tsoureas, *J. Organomet. Chem.*, 2005, **690**, 5948 ; (c) L. H. Gade, V. César and S. Bellemín-Lapponnaz, *Angew. Chem. Int. Ed.*, 2004, **43**, 1014 ; (d) D. S. McGuinness and K. J. Cavell, *Organometallics*, 2000, **19**, 741.
- (23) par exemple : (a) C. C. Lee, W. C. Ke, K. T. Chan, C. L. Lai, C. H. Hu and H. M. Lee, *Chem. Eur. J.*, 2007, **13**, 582 ; (b) J. Wolf, A. Labande, J. C. Daran and R. Poli, *J. Organomet. Chem.*, 2006, **691**, 433 ; (c) L. D. Field, B. A. Messerle, K. Q. Vuong and P. Turner, *Organometallics*, 2005, **24**, 4241 ; (d) C. Yang, H. M. Lee and S. P. Nolan, *Org. Lett.*, 2001, **3**, 1511.
- (24) par exemple : (a) P. L. Arnold, M. Rodden and C. Wilson, *Chem. Commun.*, 2005, 1743 ; (b) H. Clavier, L. Coutable, L. Toupet, J. C. Guillemin and M. Mauduit, *J. Organomet. Chem.*, 2005, **690**, 5237 ; (c) A. W. Waltman and R. H. Grubbs, *Organometallics*, 2004, **23**, 3105.
- (25) (a) S. T. Liu, C.-I. Lee, C.-F. Fu, C.-H. Chen, Y.-H. Liu, C. J. Elsevier, S.-M. Peng and J.-T. Chen, *Organometallics*, 2009, **28**, 6957 ; (b) J. Iglesias-Sigüenza, A. Ros, E. Diez, A. Magriz, A. Vazquez, E. Alvarez, R. Fernandez and J. M. Lassaletta, *Dalton Trans.*, 2009, 8485 ; (c) H. V. Huynh, D. Yuan and Y. Han, *Dalton Trans.*, 2009, 7262 ; (d) C. Gandolfi, M. Heckenroth, A. Neels, G. Laurenczy and M. Albrecht, *Organometallics*, 2009, **28**, 5112 ; (e) C. Fliedel, G. Schnee and P. Braunstein, *Dalton Trans.*, 2009, 2474 ; (f) D. S. McGuinness, J. A. Suttil, M. G. Gardiner and N. W. Davies, *Organometallics*, 2008, **27**, 4238 ; (g) S. J. Roseblade, A. Ros, D. Monge, M. Alcarazo, E. Alvarez, J. M. Lassaletta and R. Fernandez, *Organometallics*, 2007, **26**, 2570 ; (h) J. Wolf, A. Labande, J. C. Daran and R. Poli, *Eur. J. Inorg. Chem.*, 2007, 5069 ; (i) H. V. Huynh, C. H. Yeo and G. K. Tan, *Chem. Commun.*, 2006, 3833 ; (j) A. Ros, D. Monge, M. Alcarazo, E. Alvarez, J. M. Lassaletta and R. Fernandez, *Organometallics*, 2006, **25**, 6039 ; (k) J. A. Cabeza, I. da Silva, I. del Rio and M. G. Sanchez-Vega, *Dalton Trans.*, 2006, 3966 ; (l) J. A. Cabeza, I. del Rio, M. G. Sanchez-Vega and M. Suarez, *Organometallics*, 2006, **25**, 1831 ; (m) H. Seo, H. J. Park, B. Y. Kim, J. H. Lee, S. U. Son and Y. K. Chung, *Organometallics*, 2003, **22**, 618 ; (n) D. Sellmann, W. Prechtel, F. Knoch and M. Moll, *Organometallics*, 1992, **11**, 2346.
- (26) J. A. Gillespie, D. L. Dodds and P. C. J. Kamer, *Dalton Trans.*, 2010, **39**, 2751.
- (27) W. Strohmeier and F. J. Müller, *Chem. Ber.*, 1967, **100**, 1812.
- (28) C. A. Tolman, *Chem. Rev.*, 1977, **77**, 313.
- (29) S. Xiao, W. C. Trogler, D. E. Ellis and Z. Berkovitch-Yellin, *J. Am. Chem. Soc.*, 1983, **105**, 7033.
- (30) par exemple : (a) E. Burello, G. Rothenberg, *Int. J. Mol. Sci.* **2006**, **7**, 375 ; (b) K. A. Bunten, L. Chen, A. L. Fernandez, A. J. Poë, *Coord. Chem. Rev.* **2002**, 233–234, 41 ; (c) T. L. Brown, K. J. Lee, *Coord. Chem. Rev.* **1993**, **128**, 89.
- (31) (a) C. A. Tolman, *J. Am. Chem. Soc.*, 1970, **92**, 2956 ; (b) C. A. Tolman, *J. Am. Chem. Soc.*, 1970, **92**, 2953.

- (32) D. White, B. C. Tavener, P. G. L. Leach and N. J. Coville, *J. Organomet. Chem.*, 1994, **478**, 205.
- (33) C. P. Casey and G. T. Whiteker, *Isr. J. Chem.*, 1990, **30**, 299.
- (34) T. Niksch, H. Görls and W. Weigand, *Eur. J. Inorg. Chem.*, 2010, 95.
- (35) H. Nöth and L. Meinl, *Z. Anorg. Allg. Chem.*, 1967, **349**, 223.
- (36) I. Bachert, I. Bartusseck, P. Braunstein, E. Guillon, J. Rosé and G. Kickelbick, *J. Organomet. Chem.*, 1999, **588**, 144.
- (37) I. Bachert, P. Braunstein, M. K. McCart, F. Fabrizi de Biani, F. Laschi, P. Zanello, G. Kickelbick and U. Schubert, *J. Organomet. Chem.*, 1999, **573**, 47.
- (38) Par exemple : I. Bachert, P. Braunstein, and R. Hasselbring, *New J. Chem.*, 1996, **20**, 993.
- (39) Par exemple : (a) A. Dulai, H. de Bod, M. J. Hanton, D. M. Smith, S. Downing, S. M. Mansell, and D. F. Wass, *Organometallics*, 2009, **28**, 4613; (b) L. Lavanant, A.-S. Rodrigues, E. Kirillov, J.-F. Carpentier, and R. F. Jordan, *Organometallics*, 2008, **27**, 2107; (c) Z. Weng, S. Teo, and T. S. A. Hor, *Dalton Trans.*, 2007, 3493; (d) K. Blann *et al.*, *J. Catal.*, 2007, **249**, 244; (e) A. J. Rucklidge *et al.*, *Organometallics* (2007), **26**, 2782; (f) D. S. McGuinness, M. Overett, R. P. Tooze, K. Blann, J. T. Dixon, and A. M. Z. Slawin, *Organometallics*, 2007, **26**, 1108; (g) P. R. Elowe, C. McCann, P. G. Pringle, S. K. Spitzmesser, and J. E. Bercaw, *Organometallics*, 2006, **25**, 5255; (h) S. J. Schofer, M. W. Day, L. M. Henling, J. A. Labinger, and J. E. Bercaw, *Organometallics*, 2006, **25**, 2743; (i) T. Agapie, M. W. Day, L. M. Henling, J. A. Labinger, and J. E. Bercaw, *Organometallics*, 2006, **25**, 2733; (j) A. Jabri, P. Crewdson, S. Gambarotta, I. Korobkov, and R. Duchateau, *Organometallics*, 2006, **25**, 715; (k) A. Bollmann *et al.*, *J. Am. Chem. Soc.*, 2004, **126**, 14712; (l) T. Agapie, S. J. Schofer, J. A. Labinger, and J. E. Bercaw, *J. Am. Chem. Soc.*, 2004, **126**, 1304; (m) N. A. Cooley, S. M. Green, D. F. Wass, K. Heslop, A. G. Orpen, and P. G. Pringle, *Organometallics*, 2001, **20**, 4769.
- (40) P. Braunstein, H.-P. Kormann, W. Meyer-Zaika, R. Pugin, and G. Schmid, *Chem. Eur. J.*, 2000, **6**, 4637.

Chapitre 1

Versatile Coordination Modes of Novel
Hemilabile *S*-NHC Ligands

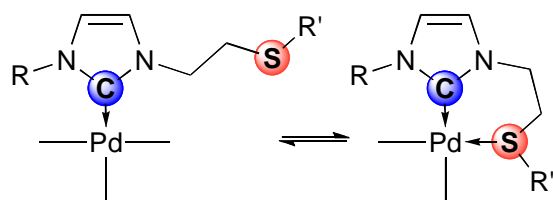
Résumé du chapitre 1

Les complexes carbéniques d'Ag(I) et les complexes hémilabiles de Pd(II) obtenus en une étape à partir de nouveaux sels d'imidazoliums fonctionnalisés par un groupement thioéther illustrent la diversité des modes de coordination de ces nouveaux ligands S,C_{NHC} .

Référence et synopsis du chapitre 1

Christophe Fliedel, Gilles Schnee and Pierre Braunstein,

Dalton Transactions, 2009, 2474-2476.



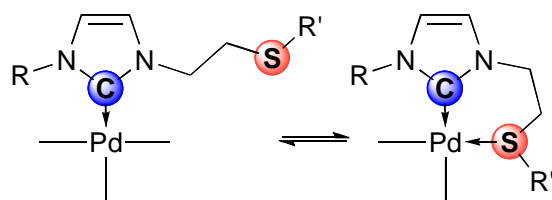
Abstract of Chapter 1

The Ag(I) and hemilabile Pd(II) carbene complexes obtained in one-step from novel thioether-functionalized imidazolium salts synthesised illustrate the diversity of coordination modes of these new S,C_{NHC} ligands.

Reference and Synopsis of Chapter 1

Christophe Fliedel, Gilles Schnee and Pierre Braunstein,

Dalton Transactions, 2009, 2474-2476.

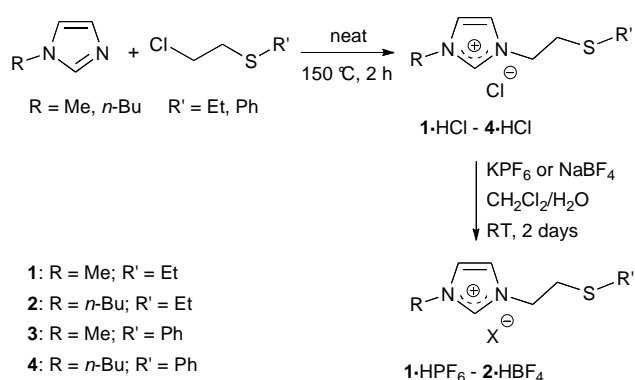


Introduction

The unique properties of *N*-Heterocyclic carbenes (NHCs) as strong donor and robust ligands make them very attractive in organometallic chemistry and homogenous catalysis.¹ Recently, the functionalization of NHCs by introduction of a donor function on the nitrogen atoms has resulted in interesting catalytic properties of their *N*,² *O*,³ and *P*-NHCs⁴ complexes owing to their hemilabile character.⁵ Although the presence of a sulfur atom appears favorable in catalytic reactions, there are only a few examples of *S*-NHCs complexes. They have been prepared either from the corresponding imidazolium salt⁶ or by oxidative addition of a C-S bond across a zero valent metal.⁷ Furthermore, sulfur-containing molecules are of interest in materials sciences because the affinity of thiol or thioether functions for gold surfaces allows their selective anchoring.⁸ Here we report an efficient, one step and solvent-free synthesis of new NHCs precursors bearing a thioether function on a nitrogen atom. Their silver complexes have been fully characterised and used for the synthesis of mono- and bis-NHC palladium complexes with tunable coordination modes of the *S*-NHCs.

Results and Discussion

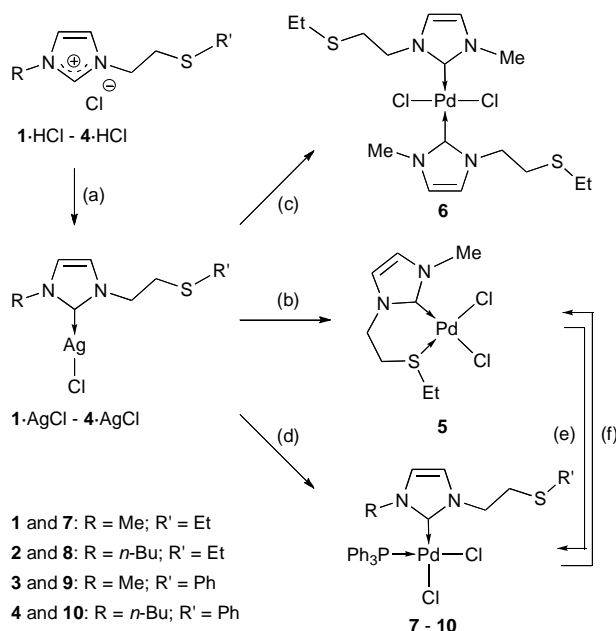
The imidazolium chlorides **1·HCl** - **4·HCl** were obtained in nearly quantitative yield by reaction between the commercially available 2-chloroethyl ethylsulfide or 2-chloroethyl phenylsulfide and 1-methylimidazole or 1-*n*-butylimidazole (Scheme 1). Their ¹H NMR spectra show typical resonances for 2-H between 10.36 and 10.51 ppm and the ¹³C{¹H} NMR resonance of their NCN carbon is found between 137.7 and 138.3 ppm. The most intense peak in the ESI mass spectra corresponds to [M-Cl]⁺.†



Scheme 1 Synthesis of the carbene precursors.

(†: see Experimental Section)

A direct route was then investigated to prepare palladium(II) complexes using $[\text{Pd}(\text{OAc})_2]$. The latter was reacted with one or two equivalents of **1**·HCl in the presence of excess NaI, but these attempts led to mixtures of complexes. However, reaction of the imidazolium salt with excess Ag_2O at room temperature in dichloromethane yielded the corresponding silver NHC complexes.⁹ Their formation was established by the shift of the C2-carbon signals between 179.4 and 180.4 ppm in the $^{13}\text{C}\{\text{H}\}$ NMR spectra and the absence of the resonance for the 2H-imidazolium proton in ^1H NMR, which also showed a significant upfield shift of the 4,5H-imidazolium protons. The ESI mass spectrum of **3**·AgCl showed as major product in solution the cationic species $[\text{Ag}(\mathbf{3})_2]^+$. Unfortunately, all crystallization attempts of the $[\text{AgCl}(\text{NHC})]$ complexes were unsuccessful. Ion exchange of the imidazolium salts to modify their solubility and perhaps favor crystallization was performed: **1**·HCl was reacted with an excess KPF_6 at room temperature in a $\text{CH}_2\text{Cl}_2/\text{H}_2\text{O}$ mixture for 2 days and similarly, **2**·HCl with NaBF_4 . This resulted in their quantitative conversion to the salts **1**· HPF_6 and **2**· HBF_4 , respectively. Their ^1H NMR spectra showed an upfield shift of the 2-H resonances at 8.49 ppm and 8.78 ppm, respectively, consistent with the anion exchange. The $^{13}\text{C}\{\text{H}\}$ NMR resonance of the NCN carbon at 136.0 and 135.1 ppm, respectively, was also affected by the ion exchange. After these silver complexes were fully characterised, they were subsequently prepared in situ and used to prepare palladium complexes by transmetallation, after filtration through Celite to remove unreacted silver oxide (Scheme 2).



Scheme 2 Synthetic pathway for the preparation of the Ag(I) complexes and the transmetallation reaction with the different Pd(II) precursors.

(a) 1 eq. Ag_2O ; (b) 1 eq. $[\text{PdCl}_2(\text{NCPh})_2]$; (c) $\frac{1}{2}$ eq. $[\text{PdCl}_2(\text{NCPh})_2]$; (d) 1 eq. $[\text{Pd}(\mu-\text{Cl})\text{Cl}(\text{PPh}_3)_2]$; (e) 1 eq. PPh_3 ; (f) 1 eq. $[\text{AuCl}(\text{THT})]$.

In order to evaluate the donor ability of the thioether function by coordination to a Pd(II) centre, one equivalent of the silver complex **1**·AgCl was reacted with one equivalent [PdCl₂(NCPH)₂] in dichloromethane. The ¹H NMR spectrum at room temperature in CD₂Cl₂ showed very broad signals (see below) for the aliphatic protons of the thioether function, which are all chemically and/or magnetically inequivalent owing to the presence, after formation of the S,C_{NHC} chelate in **5**, of a stereogenic sulfur atom. The molecular structure of **5** is depicted in Fig. 1.[†] The complex adopts a distorted square planar geometry in which the ligand forms a C,S chelate, with a bite angle of 90.7(2)[°]. The stronger *trans* influence of the carbene compared to the sulfur donor is illustrated by a Pd(1)-Cl(1) bond longer than Pd(1)-Cl(2). Owing to S coordination, the NHC ring makes an angle of 50.0(2)[°] with the Pd coordination mean plane, instead of the electronically preferred 90[°] angle. The broad ¹H NMR resonances at room temperature and the different sets of signals observed at lower temperature could be due to exchange between boat-like and chair-like conformations of the six-membered palladacycle or to the reversible decoordination of the dative S→Pd bond. The lability of this bond, resulting in the formation of a neutral, chloride-bridged dinuclear species with uncoordinated sulfur, is supported by the presence of a peak corresponding to [2M-Cl]⁺ in the mass spectrum (ESI-MS : *m/z* = 660.9). A related claim for S→Pd bond lability has previously been based on a ligand displacement reaction rather than on genuine hemilabile behaviour.^{6d} The low solubility of this compound prevented recording of a ¹³C{¹H} NMR spectrum.

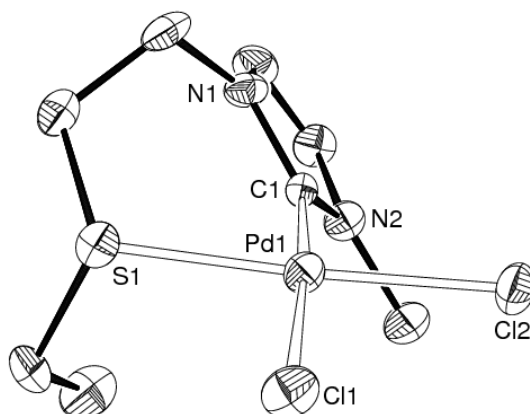


Fig. 1 ORTEP plot of the molecular structure of **5** emphasizing the boat-like conformation of the palladacycle. H atoms are omitted for clarity. Ellipsoids are represented at 50% probability level. Selected bond distances (Å) and angles (°): Pd(1)-C(1) 1.984(7), Pd(1)-S(1) 2.279(2), Pd(1)-Cl(1) 2.374(2), Pd(1)-Cl(2) 2.3239(19), C(1)-N(1) 1.353(9), C(1)-N(2) 1.339(10), C(1)-Pd(1)-S(1) 90.7(2), C(1)-Pd(1)-Cl(2) 90.6(2), S(1)-Pd(1)-Cl(1) 85.41(7), N(2)-C(1)-N(1) 106.2(6).

With the objective to synthesize palladium complexes where *S* coordination would be prevented in order to keep this function available for further anchoring experiments, **1·AgCl** and $[\text{PdCl}_2(\text{NCPh})_2]$ were reacted in a Ag/Pd ratio of 2:1. This afforded complex **6** in 65% yield after crystallization. Its ^1H NMR spectrum reveals a high molecular symmetry that could be confirmed in the solid-state by single crystal X-ray diffraction. In this centrosymmetric structure, the palladium centre has a distorted square planar coordination geometry (Fig. 2).† The sulfur atom is not coordinated to the metal centre and is pointing away from the C(1)-Pd(1)-Cl(1) plane, a situation a priori favorable for further deposition experiments.

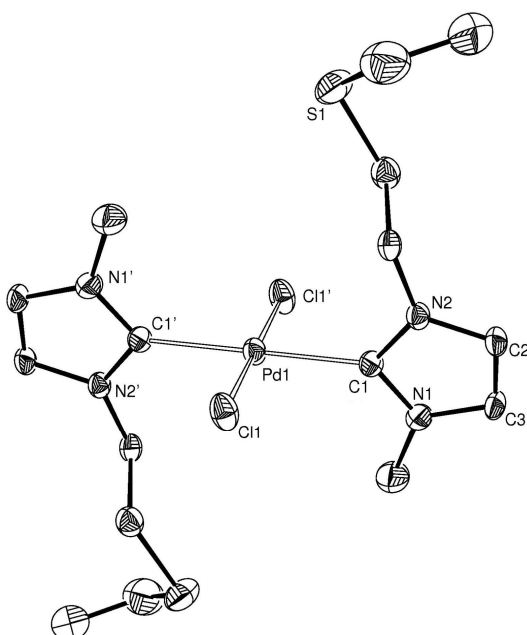


Fig. 2 ORTEP plot of the molecular structure of **6**. H atoms are omitted for clarity. Ellipsoids are represented at 50% probability level. Selected bond distances (\AA) and angles ($^\circ$): Pd(1)-C(1) 2.031(6), Pd(1)-Cl(1) 2.3081(16), C(1)-N(1) 1.341(7), C(1)-N(2) 1.344(7), C(1)-Pd(1)-Cl(1) 90.21(16), N(1)-C(1)-N(2) 105.1(5).

Furthermore, we reacted **1·AgCl** and $[\text{Pd}(\mu\text{-Cl})\text{Cl}(\text{PPh}_3)]_2$ in a 1:1 ratio to synthesize the complex **7**. This complex could also be obtained by addition of 1 eq. of PPh_3 to **5**, resulting in displacement of the thioether function. The reverse reaction, namely recoordination of the $-\text{SR}'$ group, occurs by using $[\text{AuCl}(\text{THT})]$ as a phosphine abstractor. The success of this reaction was monitored by ^{31}P NMR.† The reactions of **2·AgCl**, **3·AgCl** or **4·AgCl** with $[\text{Pd}(\mu\text{-Cl})\text{Cl}(\text{PPh}_3)]_2$ similarly afforded the fully characterised complexes **8-10**, respectively.† The molecular structure of **8** is depicted in Fig. 3 and those of **9·0.75CH₂Cl₂** and **10** are reported in the ESI.†

The phosphane and NHC ligands are in mutual *cis* position and the geometry around the palladium centre is distorted square planar. Like in **6**, the S(1)-C(19)-Pd(1) plane is almost orthogonal to the metal coordination plane.

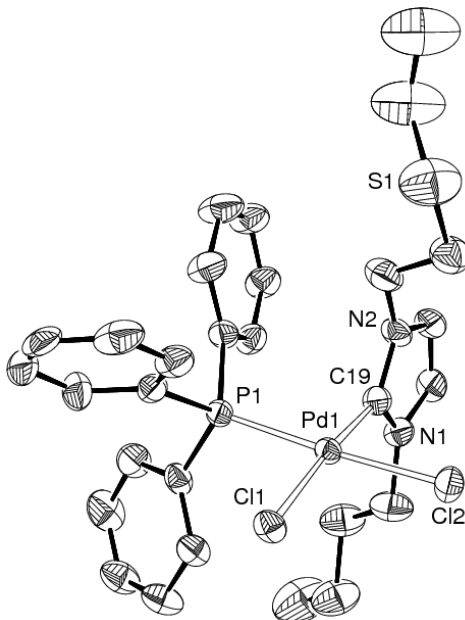


Fig. 3 ORTEP plot of the molecular structure of **8**. H atoms are omitted for clarity. Ellipsoids are represented at 50% probability level. Selected bond distances (\AA) and angle ($^{\circ}$): Pd(1)-C(19) 1.978(6), Pd(1)-P(1) 2.2549(15), Pd(1)-Cl(1) 2.3554(15), Pd(1)-Cl(2) 2.3596(15), N(1)-C(19) 1.350(7), N(2)-C(19) 1.350(8), C(19)-Pd(1)-P(1) 91.62(17), P(1)-Pd(1)-Cl(1) 90.78(5), C(19)-Pd(1)-Cl(2) 85.35(17), Cl(1)-Pd(1)-Cl(2) 92.43(5), N(1)-C(19)-N(2) 105.5(5).

Conclusion

These experiments confirm that the “on-off” coordination of potentially chelating *S,N*HC ligands to a palladium centre can be readily fine-tuned, which is important for subsequent applications.

Preliminary catalytic studies were performed in Suzuki-Miyaura cross coupling reaction using the *S*-NHC chelate complex **5** and the NHC-PPh₃ complex **7**. Under standard conditions,¹⁰ using 2 mol% catalyst and Cs₂CO₃ as a base, 80% conversion of 4-bromotoluene was observed in dioxane after 2 h reaction at 100 °C. Under these conditions, complex **7** gave a conversion of 78%. Using DMSO as solvent with complex **5** the conversion rate increased to 90% due to a higher solubility. Further catalytic experiments are in progress to optimize the system.

Acknowledgment

We are grateful to Drs Roberto Pattacini and Lydia Breloz for the resolution of the X-ray structures and to the CNRS, the Ministère de la Recherche (Paris) and the DFH/UFA (International Research Training Group 532-GRK532) for funding.

Supplementary Materials

† Electronic supplementary information (ESI) available: Experimental details, characterisation and X-ray crystal structures of compounds **5**, **6**, **8**, **9**·0.75CH₂Cl₂ and **10**. CCDC reference numbers 710767–710771. For ESI and crystallographic data in CIF or other electronic format see DOI: 10.1039/b902314n

Experimental Section

Supporting Information for *Dalton Trans.* B902314N

Versatile coordination modes of novel hemilabile S-NHC ligands.

Christophe Fliedel, Gilles Schnee and Pierre Braunstein*

Contents

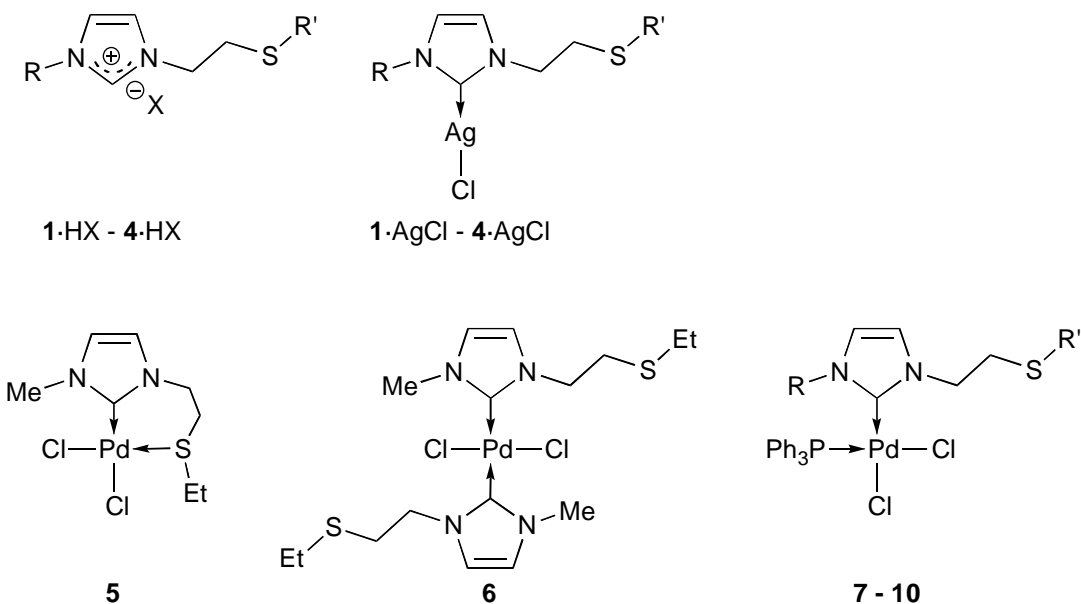
S1. Synthesis and characterisation of the compounds

S2. Crystallographic data

Laboratoire de Chimie de Coordination, Institut de Chimie, UMR 7177 CNRS,
Université de Strasbourg, 4 rue Blaise Pascal, F-67070 Strasbourg Cedex, France.
E-mail: braunstein@chimie.u-strasbg.fr ; Fax: +33 390 241 322.

S1. Synthesis and characterisation of the compounds

General procedures. All operations were carried out using standard Schlenk techniques under inert atmosphere. Solvents were purified and dried under nitrogen by conventional methods. d_6 -DMSO was degassed and stored over 4 Å molecular sieves. CD_2Cl_2 was dried over 4 Å molecular sieves, degassed by freeze-pump-thaw cycles and stored under argon. NMR spectra were recorded at room temperature on a Bruker AVANCE 300 spectrometer (1H , 300 MHz; ^{13}C , 75.47 MHz; ^{31}P , 121.49 MHz and ^{19}F , 282.38 MHz) and referenced using the residual proton solvent (1H) or solvent (^{13}C) resonance. Assignments are based on 1H , 1H -COSY, 1H , ^{13}C -HMQC and 1H , ^{13}C -HMBC experiments. IR spectra were recorded in the region 4000-100 cm^{-1} on a Nicolet 6700 FT-IR spectrometer (ATR mode, diamond crystal). Elemental analyses were performed by the “Service de microanalyses”, Université de Strasbourg and by the “Service Central d’Analyse”, USR-59/CNRS, Solaize. Electrospray mass spectra (ESI-MS) were recorded on a microTOF (Bruker Daltonics, Bremen, Germany) instrument using nitrogen as drying agent and nebulising gas and Maldi-TOF analyses were carried out on a Bruker AutiflexII TOF/TOF (Bruker Daltonics, Bremen, Germany), using dithranol (1.8.9 trihydroxyanthracene) as a matrix. Gas chromatographic analyses were performed on a Thermoquest GC8000 Top series gas chromatograph using a HP Pona column (50 m, 0.2 mm diameter, 0.5 μm film thickness). The complexes $[PdCl_2(NCPPh)_2]^{S1}$ and $[PdCl(\mu-Cl)(PPh_3)]_2^{S2}$ were prepared according to literature methods. All other reagents were used as received from commercial suppliers.



Formula of imidazolium salts and complexes described in this paper.

^{S1} F. R. Hartley, *The Chemistry of Platinum and Palladium*, Applied Science Publishers, London, 1973.

^{S2} M. Noskowska, E. Sliwinska and W. Duczmal, *Trans. Met. Chem.*, 2003, **28**, 756-759.

Synthesis of N-(R)-N'-ethyl-(R')-sulfide imidazolium chlorides:

1·HCl: R = methyl ; R' = ethyl:

Pure 1-methylimidazole (4.85 ml, 5.00 g, 60.90 mmol) and 2-chloroethyl ethylsulfide (7.09 ml, 7.59 g, 60.90 mmol) were placed in a Schlenk tube equipped with a magnetic stirrer. The mixture was heated for 2 h at 150 °C and then allowed to cool to room temperature. During heating, the colourless mixture turned brown and became more viscous. After cooling, the brown oil was washed 2 times with 40 ml of dry THF and dried in vacuo. These compounds are known to be very hygroscopic and the elemental analyses performed always afforded carbon and nitrogen percentages lower than theoretical values. Yield: 96%. Anal. Calc. for C₈H₁₅ClN₂S (206.74): C, 46.48; H, 7.31; N, 13.55. Found: C, 45.5; H, 7.2; N, 12.2. FTIR: ν_{max} (pure, diamond orbit)/cm⁻¹: 3373br, 3137sh, 3038s, 2958s, 2866m, 1563s, 1450m, 1426m, 1375w, 1334w, 1266w, 1162vs, 869w, 759s, 716w. ¹H NMR (CD₂Cl₂, 300 MHz) δ: 1.20 (3H, t, ³J = 7.4 Hz, SCH₂CH₃), 2.60 (2H, q, ³J = 7.4 Hz, SCH₂CH₃), 3.04 (2H, t, ³J = 6.6 Hz, NCH₂CH₂S), 4.03 (3H, s, NCH₃), 4.57 (2H, t, ³J = 6.6 Hz, NCH₂CH₂S), 7.41 (1H, pseudo t, ³J = ⁴J = 1.8 Hz, CH=CH), 7.56 (1H, pseudo t, ³J = ⁴J = 1.8 Hz, CH=CH), 10.41 (1H, br s, NCHN). ¹³C{¹H} NMR (CD₂Cl₂, 75.5 MHz) δ: 14.53 (SCH₂CH₃), 25.85 (SCH₂CH₃), 31.73 (NCH₂CH₂S), 36.50 (NCH₃), 49.11 (NCH₂CH₂S), 122.38, 122.93 (CH=CH), 138.33 (NCN). MS (ESI): *m/z* 171.1 [M-Cl]⁺.

2·HCl: R = *n*-butyl ; R' = ethyl:

The same procedure was used with 1-*n*-butylimidazole (5.29 ml, 5.00 g, 40.26 mmol) and 2-chloroethyl ethylsulfide (4.69 ml, 5.018 g, 40.26 mmol). Yield: 98%. Anal. Calc. for C₁₁H₂₁ClN₂S (248.82): C, 53.10; H, 8.51; N, 11.26. Found: C, 51.9; H, 8.6; N, 9.5. FTIR: ν_{max} (pure, diamond orbit)/cm⁻¹: 3378br, 3040m, 2956vs, 2929s, 2869m, 1561s, 1452m, 1374w, 1332w, 1266w, 1159vs, 1062w, 1022w, 972w, 949w, 869w, 752m. ¹H NMR (CD₂Cl₂, 300 MHz) δ: 0.91 (3H, t, ³J = 7.5 Hz, CH₃ butyl), 1.18 (3H, t, ³J = 7.4 Hz, SCH₂CH₃), 1.33 (2H, m, NCH₂CH₂CH₂CH₃), 1.85 (2H, m, NCH₂CH₂CH₂CH₃), 2.58 (2H, q, ³J = 7.4 Hz, SCH₂CH₃), 3.04 (2H, t, ³J = 6.6 Hz, NCH₂CH₂S), 4.27 (2H, t, ³J = 7.2 Hz, NCH₂CH₂CH₂CH₃), 4.57 (2H, t, ³J = 6.6 Hz, NCH₂CH₂S), 7.46 (1H, pseudo t, ³J = ⁴J = 1.8 Hz, CH=CH), 7.73 (1H, pseudo t, ³J = ⁴J = 1.8 Hz, CH=CH), 10.45 (1H, br s, NCHN). ¹³C{¹H} NMR (CD₂Cl₂, 75.5 MHz) δ: 13.21 (CH₃ butyl), 14.54 (SCH₂CH₃), 19.35 (NCH₂CH₂CH₂CH₃), 25.75 (SCH₂CH₃), 31.75 (NCH₂CH₂S), 32.00 (NCH₂CH₂CH₂CH₃), 48.97 (NCH₂CH₂CH₂CH₃), 49.64 (NCH₂CH₂S), 121.67, 122.71 (CH=CH), 137.71 (NCN). MS (ESI): *m/z* 213.1 [M-Cl]⁺.

3·HCl: R = methyl ; R' = phenyl:

The same procedure was used with 1-methylimidazole (4.85 ml, 5.00 g, 60.90 mmol) and 2-chloroethyl phenylsulfide (8.96 ml, 10.52 g, 60.90 mmol). Yield: 95%. Anal. Calc. for C₁₂H₁₅ClN₂S (254.78): C, 56.57; H, 5.93; N, 11.00. Found: C, 55.3; H, 6.3; N, 9.4. FTIR: ν_{max} (pure, diamond

orbit)/cm⁻¹: 3367br, 3045m, 2958s, 2849w, 1571s, 1473m, 1437s, 1334w, 1301w, 1170vs, 1086m, 1023m, 999w, 872m, 741vs, 691vs. ¹H NMR (CD₂Cl₂, 300 MHz) δ: 3.52 (2H, t, ³J = 6.3 Hz, NCH₂CH₂S), 3.93 (3H, s, NCH₃), 4.53 (2H, pseudo t, ³J = 6.3 Hz, NCH₂CH₂S), 7.20-7.41 (6H, m, H arom + CH=CH), 7.55 (1H, t, ³J = ⁴J = 2.1 Hz, CH=CH), 10.36 (1H, br s, NCHN). ¹³C{¹H} NMR (CD₂Cl₂, 75.5 MHz) δ: 34.10 (NCH₂CH₂S), 36.38 (NCH₃), 49.17 (NCH₂CH₂S), 122.79, 122.97 (CH=CH), 126.96 (C_{para}), 129.26 (C_{meta}), 130.10 (C_{ortho}), 133.80 (C_{ipso}), 138.12 (NCN). MS (ESI): *m/z* 219.1 [M-Cl]⁺.

4·HCl: R = *n*-butyl ; R' = phenyl:

The same procedure was used with 1-*n*-butylimidazole (5.29 ml, 5.00 g, 40.26 mmol) and 2-chloroethyl phenylsulfide (5.92 ml, 6.95 g, 40.26 mmol). Yield: 96%. Anal. Calc. for C₁₅H₂₁ClN₂S (296.86): C, 60.69; H, 7.13; N, 9.44. Found: C, 59.7; H, 7.4; N, 8.6. FTIR: ν_{max}(pure, diamond orbit)/cm⁻¹: 3374br, 3137w, 3056w, 2958m, 2871w, 1627m, 1561s, 1438s, 1333w, 1304w, 1157s, 1087w, 1023m, 871w, 741vs, 692vs. ¹H NMR (CD₂Cl₂, 300 MHz) δ: 0.93 (3H, t, ³J = 7.5 Hz, CH₃ butyl), 1.33 (2H, m, CH₂CH₃), 1.82 (2H, m, CH₂CH₂CH₃), 3.54 (2H, t, ³J = 6.3 Hz, NCH₂CH₂S), 4.21 (2H, t, ³J = 7.2 Hz, NCH₂CH₂CH₂), 4.56 (2H, t, ³J = 6.3 Hz, NCH₂CH₂S), 7.18-7.40 (6H, m, H arom + CH=CH), 7.50 (1H, pseudo t, ³J = ⁴J = 1.8 Hz, CH=CH), 10.51 (1H, br s, NCHN). ¹³C{¹H} NMR (CD₂Cl₂, 75.5 MHz) δ: 13.22 (CH₃), 19.41 (CH₂CH₃), 31.92 (NCH₂CH₂S), 34.14 (NCH₂CH₂CH₂), 49.12 (NCH₂CH₂CH₂), 49.73 (NCH₂CH₂S), 121.29, 122.93 (CH=CH), 126.98 (C_{para}), 129.30 (C_{meta}), 130.02 (C_{ortho}), 133.79 (C_{ipso}), 137.78 (NCN). MS (ESI): *m/z* 261.1 [M-Cl]⁺.

General procedure for the anion exchange:

1·HPF₆: R = methyl ; R' = ethyl:

The imidazolium chloride **1**·HCl (1.96 g, 9.53 mmol) and solid KPF₆ (8.77 g, 47.64 mmol) were dissolved in a CH₂Cl₂/H₂O (1:2) mixture and stirred for 2 days at room temperature. Then the suspension was filtered through a Celite pad and the solvent was evaporated under reduced pressure to give a brown oil. Yield: 98%. Anal. Calc. for C₈H₁₅F₆N₂PS (316.25): C, 30.38; H, 4.78; N, 8.86. Found: C, 28.9; H, 5.2; N, 7.7. FTIR: ν_{max}(pure, diamond orbit)/cm⁻¹: 3169w, 3123w, 2964w, 2931w, 2872w, 1564m, 1536m, 1507m, 1456w, 1380w, 1360w, 1207m, 1162s, 1025m, 824vs, 740s, 703m. ¹H NMR (CD₂Cl₂, 300 MHz) δ: 1.23 (3H, t, ³J = 7.5 Hz, SCH₂CH₃), 2.56 (2H, q, ³J = 7.5 Hz, SCH₂CH₃), 2.96 (2H, t, ³J = 6.6 Hz, NCH₂CH₂S), 3.91 (3H, s, NCH₃), 4.33 (2H, t, ³J = 6.6 Hz, NCH₂CH₂S), 7.34 (1H, pseudo t, ³J = ⁴J = 1.8 Hz, CH=CH), 7.42 (1H, pseudo t, ³J = ⁴J = 1.8 Hz, CH=CH), 8.49 (1H, br s, NCHN). ¹³C{¹H} NMR (CD₂Cl₂, 75.5 MHz) δ: 14.40 (SCH₂CH₃), 25.70 (SCH₂CH₃), 31.26 (NCH₂CH₂S), 36.22 (NCH₃), 49.26 (NCH₂CH₂S), 122.56, 123.56 (CH=CH), 136.00 (NCN). ³¹P{¹H} NMR (CD₂Cl₂, 121.5 MHz) δ: - 143.1 (sept., ¹J_{P,F} = 711 Hz, PF₆). ¹⁹F{¹H} NMR (CD₂Cl₂, 282.4 MHz) δ: - 72.4 (d, ¹J_{P,F} = 711 Hz, PF₆). MS (ESI): *m/z* 171.1 [M-PF₆]⁺.

2·HBF₄: R = *n*-butyl ; R' = ethyl:

The same procedure was used with **2**·HCl (1.93 g, 7.83 mmol) and NaBF₄ (4.77 g, 43.48 mmol). Yield: 98%. Anal. Calc. for C₁₁H₂₁BF₄CIN₂S (300.17): C, 44.01; H, 7.05; N, 9.33. Found: C, 42.7; H, 7.2; N, 8.3. FTIR: ν_{max} (pure, diamond orbit)/cm⁻¹: 3152w, 3115w, 2962w, 2931w, 2874w, 1564m, 1507m, 1456m, 1378w, 1359w, 1209m, 1159s, 1033vs, 825m, 751s, 704m. ¹H NMR (CD₂Cl₂, 300 MHz) δ: 0.91 (3H, t, ³J = 7.5 Hz, CH₃ butyl), 1.19 (3H, t, ³J = 7.4 Hz, SCH₂CH₃), 1.30 (2H, m, NCH₂CH₂CH₂CH₃), 1.85 (2H, m, NCH₂CH₂CH₂CH₃), 2.53 (2H, q, ³J = 7.4 Hz, SCH₂CH₃), 2.97 (2H, t, ³J = 6.6 Hz, NCH₂CH₂S), 4.20 (2H, t, ³J = 7.2 Hz, NCH₂CH₂CH₂CH₃), 4.38 (2H, t, ³J = 6.6 Hz, NCH₂CH₂S), 7.46 (1H, pseudo t, ³J = ⁴J = 1.8 Hz, CH=CH), 7.53 (1H, pseudo t, ³J = ⁴J = 1.8 Hz, CH=CH), 8.78 (1H, br s, NCHN). ¹³C{¹H} NMR (CD₂Cl₂, 75.5 MHz) δ: 12.38 (CH₃ butyl), 13.72 (SCH₂CH₃), 18.55 (NCH₂CH₂CH₂CH₃), 24.87 (SCH₂CH₃), 30.72 (NCH₂CH₂S), 31.11 (NCH₂CH₂CH₂CH₃), 48.38 (NCH₂CH₂CH₂CH₃), 49.08 (NCH₂CH₂S), 121.60, 122.01 (CH=CH), 135.14 (NCN). ¹⁹F{¹H} NMR (CD₂Cl₂, 282.4 MHz) δ: -150.7 (BF₄). MS (ESI): *m/z* 213.1 [M-BF₄]⁺.

General procedure for the synthesis of the silver (I**) carbene complexes:****1·AgCl: R = methyl ; R' = ethyl:**

The imidazolium **1**·HCl (0.300 g, 1.47 mmol) was dissolved in dry CH₂Cl₂ and solid Ag₂O (0.340 g, 1.47 mmol) was added under nitrogen. The reaction mixture was stirred for 2 h in the dark at room temperature. Then the suspension was filtered through a Celite pad and the solvent was evaporated under reduced pressure to give a light sensitive white solid. Yield: 82%. Anal. Calc. for C₈H₁₄AgClN₂S (313.60): C, 30.64; H, 4.50; N, 8.93. Found: C, 29.9; H, 4.7; N, 8.5. FTIR: ν_{max} (pure, diamond orbit)/cm⁻¹ 3421br, 3094w, 2959w, 2922m, 2868w, 1652w, 1565w, 1457s, 1441s, 1404s, 1375w, 1351w, 1263m, 1222s, 1158w, 1117w, 1097w, 972w, 874w, 729vs, 698sh, 663w. ¹H NMR (CD₂Cl₂, 300 MHz) δ: 1.28 (3H, t, ³J = 7.4 Hz, SCH₂CH₃), 2.57 (2H, q, ³J = 7.4 Hz, SCH₂CH₃), 2.96 (2H, t, ³J = 6.7 Hz, NCH₂CH₂S), 3.86 (3H, s, NCH₃), 4.31 (2H, t, ³J = 6.7 Hz, NCH₂CH₂S), 7.03 and 7.11 (2H, AB spin system, ³J = 1.8 Hz, CH=CH). ¹³C{¹H} NMR (CD₂Cl₂, 75.5 MHz) δ: 14.60 (SCH₂CH₃), 26.34 (SCH₂CH₃), 33.09 (NCH₂CH₂S), 38.85 (NCH₃), 51.50 (NCH₂CH₂S), 121.49, 122.19 (CH=CH), 180.19 (NCN). MS (ESI): *m/z* 277.0 [M-Cl]⁺.

2·AgCl: R = *n*-butyl ; R' = ethyl:

The same procedure was used with **2**·HCl (0.300 g, 1.21 mmol) and Ag₂O (0.280 g, 1.21 mmol). Yield: 78%. Anal. Calc. for C₁₁H₂₀AgClN₂S (355.68): C, 37.15; H, 5.67; N, 7.88. Found: C, 36.5; H, 5.7; N, 7.1. FTIR: ν_{max} (pure, diamond orbit)/cm⁻¹ 3438br, 3090w, 2956s, 2926s, 2869m, 1635w, 1563w, 1454s, 1417s, 1375w, 1261m, 1229s, 1202w, 1156w, 1105w, 1060w, 973w, 874w, 750s, 666w. ¹H NMR (CD₂Cl₂, 300 MHz) δ: 0.97 (3H, t, ³J = 7.5 Hz, CH₃ butyl), 1.25 (3H, t, ³J = 7.4 Hz, SCH₂CH₃), 1.37 (2H, m, NCH₂CH₂CH₂CH₃), 1.82 (2H, m, NCH₂CH₂CH₂CH₃), 2.54 (2H, q, ³J = 7.4 Hz, SCH₂CH₃), 2.96 (2H, t, ³J = 6.6 Hz, NCH₂CH₂S), 4.13 (2H, t, ³J = 7.2 Hz, NCH₂CH₂CH₂CH₃), 4.32 (2H, t, ³J = 6.6 Hz, NCH₂CH₂S), 7.07 and 7.15 (2H, AB spin system, ³J = 1.8 Hz, CH=CH).

$^{13}\text{C}\{\text{H}\}$ NMR (CD_2Cl_2 , 75.5 MHz) δ : 13.44 (CH_3 butyl), 14.59 (SCH_2CH_3), 19.69 ($\text{NCH}_2\text{CH}_2\text{CH}_2\text{CH}_3$), 26.34 (SCH_2CH_3), 33.08 ($\text{NCH}_2\text{CH}_2\text{S}$), 33.44 ($\text{NCH}_2\text{CH}_2\text{CH}_2\text{CH}_3$), 51.66 ($\text{NCH}_2\text{CH}_2\text{CH}_2\text{CH}_3$), 51.90 ($\text{NCH}_2\text{CH}_2\text{S}$), 120.86, 121.45 ($\text{CH}=\text{CH}$), 179.44 (NCN). MS (ESI): m/z 319.0 [$\text{M}-\text{Cl}]^+$.

3·AgCl: R = methyl ; R' = phenyl:

The same procedure was used with **3**·HCl (0.300 g, 1.01 mmol) and Ag_2O (0.230 g, 1.01 mmol). Yield: 81%. Anal. Calc. for $\text{C}_{12}\text{H}_{14}\text{AgClN}_2\text{S}$ (361.64): C, 39.85; H, 3.90; N, 7.75. Found: C, 39.0; H, 3.9; N, 6.9. FTIR: ν_{max} (pure, diamond orbit)/cm⁻¹ 3444br, 3095w, 2942w, 1580m, 1478m, 1458m, 1437m, 1404m, 1350w, 1273w, 1221m, 1155w, 1112w, 1086w, 1023w, 735vs, 690s, 659w. ^1H NMR (CD_2Cl_2 , 300 MHz) δ : 3.36 (2H, t, $^3J = 6.6$ Hz, $\text{NCH}_2\text{CH}_2\text{S}$), 3.74 (3H, s, NCH_3), 4.31 (2H, t, $^3J = 6.6$ Hz, $\text{NCH}_2\text{CH}_2\text{S}$), 7.01 (1H, br s, $\text{CH}=\text{CH}$), 7.13 (1H, br s, $\text{CH}=\text{CH}$), 7.16-7.35 (5H, m, H arom). $^{13}\text{C}\{\text{H}\}$ NMR (CD_2Cl_2 , 75.5 MHz) δ : 35.05 ($\text{NCH}_2\text{CH}_2\text{S}$), 38.81 (NCH_3), 51.03 ($\text{NCH}_2\text{CH}_2\text{S}$), 121.72, 122.38 ($\text{CH}=\text{CH}$), 126.59 (C_{para}), 129.28 (C_{meta}), 128.50 (C_{ortho}), 134.54 (C_{ipso}), 180.41 (NCN). MS (ESI): m/z 545.1 [$\text{Ag}(\mathbf{3})_2]^+$.

4·AgCl: R = *n*-butyl ; R' = phenyl:

The same procedure was used with **4**·HCl (0.320 g, 1.07 mmol) and Ag_2O (0.250 g, 1.07 mmol). Yield: 80%. Anal. Calc. for $\text{C}_{15}\text{H}_{20}\text{AgClN}_2\text{S}$ (403.72): C, 44.63; H, 4.99; N, 6.94. Found: C, 43.8; H, 5.7; N, 6.2. FTIR: ν_{max} (pure, diamond orbit)/cm⁻¹ 3456br, 3089w, 2955m, 2928m, 2869w, 1580w, 1478m, 1457m, 1437s, 1416s, 1344w, 1271w, 1227s, 1198m, 1086m, 1023m, 875w, 731vs, 689vs, 667sh. ^1H NMR (CD_2Cl_2 , 300 MHz) δ : 0.94 (3H, t, $^3J = 7.5$ Hz, CH_3 butyl), 1.32 (2H, m, CH_2CH_3), 1.75 (2H, m, $\text{CH}_2\text{CH}_2\text{CH}_3$), 3.37 (2H, t, $^3J = 6.7$ Hz, $\text{NCH}_2\text{CH}_2\text{S}$), 4.05 (2H, t, $^3J = 7.2$ Hz, $\text{NCH}_2\text{CH}_2\text{CH}_2$), 4.32 (2H, t, $^3J = 6.7$ Hz, $\text{NCH}_2\text{CH}_2\text{S}$), 7.03 (1H, d, $^3J = 1.8$ Hz, $\text{CH}=\text{CH}$), 7.15 (1H, br s, $\text{CH}=\text{CH}$), 7.18-7.38 (5H, m, H arom). $^{13}\text{C}\{\text{H}\}$ NMR (CD_2Cl_2 , 75.5 MHz) δ : 13.56 (CH_3 butyl), 19.72 (CH_2CH_3), 33.43 ($\text{NCH}_2\text{CH}_2\text{S}$), 35.05 ($\text{CH}_2\text{CH}_2\text{CH}_3$), 51.12 ($\text{NCH}_2\text{CH}_2\text{CH}_2$), 51.84 ($\text{NCH}_2\text{CH}_2\text{S}$), 121.04, 121.69 ($\text{CH}=\text{CH}$), 126.62 (C_{para}), 129.32 (C_{meta}), 129.46 (C_{ortho}), 134.55 (C_{ipso}), 179.44 (NCN). MS (ESI): m/z 369.0 [$\text{M}-\text{Cl}]^+$.

General procedure for the transmetallation reaction:

The imidazolium chloride was dissolved in dry CH_2Cl_2 and solid Ag_2O was added under nitrogen. The reaction mixture was stirred for 2 h in the dark at room temperature. Then the suspension was filtered through a Celite pad under nitrogen and the resulting clear solution was slowly added to a suspension of the desired palladium precursor. A white solid precipitated rapidly. The suspension was then filtered through Celite and the solvent was evaporated under reduced pressure. The resulting solid was then washed with pentane (2 x 25 mL) and crystallized from a dichloromethane/pentane solution.

Formation of **5** (R = methyl; R' = ethyl): **1**·HCl (0.190 g, 0.92 mmol), Ag₂O (0.213 g, 0.92 mmol) and [PdCl₂(NCPh)₂] (0.352 g, 0.92 mmol). Yield: 72%. This complex is poorly soluble in CH₂Cl₂ and in DMSO. Anal. Calc. for C₈H₁₄Cl₂N₂PdS (347.60): C, 27.64; H, 4.06; N, 8.06. Found: C, 27.8; H, 4.2; N, 7.6. FTIR: ν_{max} (pure, diamond orbit)/cm⁻¹ 3472br, 3154w, 3100w, 2954w, 2929w, 2225w, 2160w, 2034w, 1978w, 1566w, 1471s, 1446m, 1407s, 1373w, 1342w, 1284w, 1263w, 1238s, 1206m, 1166w, 1127w, 1089w, 1066w, 1051w, 969w, 883w, 847w, 739vs, 680vs, 310vs ($\nu_{\text{Pd-Cl}}$), 298vs ($\nu_{\text{Pd-Cl}}$). ¹H NMR (CD₂Cl₂, 300 MHz) δ : 1.40 (3H, t, ³J = 7.5 Hz, SCH₂CH₃), 2.61 (2H, m br, SCH₂CH₃), 3.03 (2H, m br, NCH₂CH₂S), 4.09 (3H, s, NCH₃), 4.45 (2H, t br, NCH₂CH₂S), 6.95 and 7.02 (2H, AB spin system, ³J = 1.8 Hz, CH=CH). MS (ESI): *m/z* 313.0 [M-Cl]⁺, 660.9 [2M-Cl]⁺.

Formation of **6** (R = methyl; R' = ethyl): **1**·HCl (0.188 g, 0.91 mmol), Ag₂O (0.211 g, 0.91 mmol) and [PdCl₂(NCPh)₂] (0.175 g, 0.46 mmol). Yield: 65%. This complex is poorly soluble in CH₂Cl₂ or CHCl₃. Anal. Calc. for C₁₆H₂₈Cl₂N₄PdS₂ (517.88): C, 37.11; H, 5.45; N, 10.82. Found: C, 37.0; H, 5.7; N, 10.2. FTIR: ν_{max} (pure, diamond orbit)/cm⁻¹ 3499br, 3125w, 3055w, 2991w, 2947w, 1576w, 1540w, 1473s, 1441s, 1407m, 1360w, 1334w, 1284w, 1237m, 1205w, 1106m, 1071sh, 1022w, 999w, 834w, 744vs, 684vs. ¹H NMR (CD₂Cl₂, 300 MHz) δ : 1.26 (3H, t, ³J = 7.5 Hz, SCH₂CH₃), 2.59 (2H, q, ³J = 7.5 Hz, SCH₂CH₃), 3.21 (2H, m br, NCH₂CH₂S), 4.07 (3H, s, NCH₃), 4.63 (2H, t, ³J = 6.6 Hz, NCH₂CH₂S), 6.96 (1H, br, CH=CH), 7.12 (1H, br, CH=CH). ¹³C{¹H} NMR (CD₂Cl₂, 75.5 MHz) δ : 14.64 (SCH₂CH₃), 22.32 (SCH₂CH₃), 32.54 (NCH₂CH₂S), 37.74 (NCH₃), 50.72 (NCH₂CH₂S), 121.68, 123.96 (CH=CH), (NCN) not observed. MS (ESI): *m/z* 483.0 [M-Cl]⁺.

Formation of **7** (R = methyl; R' = ethyl): **1**·HCl (0.400 g, 1.93 mmol), Ag₂O (0.452 g, 1.93 mmol) and [PdCl(μ -Cl)(PPh₃)₂] (0.851 g, 0.97 mmol). Yield: 69%. This complex is soluble in CH₂Cl₂, CHCl₃ or THF, but insoluble in toluene or pentane. Anal. Calc. for C₂₆H₂₉Cl₂N₂PPdS (609.89): C, 51.20; H, 4.79; N, 4.59. Found: C, 50.6; H, 4.8; N, 4.3. FTIR: ν_{max} (pure, diamond orbit)/cm⁻¹ 3380br, 3147w, 3087w, 3048w, 2960w, 2925w, 1568w, 1480m, 1468m, 1434s, 1404m, 1371w, 1337w, 1268m, 1230m, 1185w, 1169w, 1129w, 1098s, 1092s, 1026w, 997w, 853w, 762m, 750s, 741vs, 706s, 696vs, 685vs. ¹H NMR (CD₂Cl₂, 300 MHz) δ : 1.24 (3H, t, ³J = 7.5 Hz, SCH₂CH₃), 2.49 (2H, q, ³J = 7.5 Hz, SCH₂CH₃), 2.86 (1H, m, NCH₂CHHS), 3.08 (1H, m, NCHHCH₂S), 3.59 (3H, s, NCH₃), 3.72 (1H, m, NCH₂CHHS), 4.42 (1H, m, NCHHCH₂S), 6.64 and 6.77 (2H, AB spin system, ³J = 2.1 Hz, CH=CH), 7.35-7.60 (15H, m, H arom). ¹³C{¹H} NMR (CD₂Cl₂, 75.5 MHz) δ : 14.81 (SCH₂CH₃), 26.24 (SCH₂CH₃), 31.21 (NCH₂CH₂S), 37.53 (NCH₃), 50.62 (NCH₂CH₂S), 122.16, 122.84 (CH=CH), 128.55 (d, $J_{\text{P-C}} = 11.0$ Hz, CH arom), 129.83 (d, $J_{\text{P-C}} = 54.1$ Hz, C_{ipso}), 131.23 (d, $J_{\text{P-C}} = 2.4$ Hz, CH arom), 134.03 (d, $J_{\text{P-C}} = 11.1$ Hz, CH arom), 161.01 (NCN). ³¹P{¹H} NMR (CD₂Cl₂, 121.5 MHz) δ : 28.6. MS (ESI): *m/z* 575.0 [M-Cl]⁺.

Formation of **8** ($R = n\text{-butyl}$; $R' = \text{ethyl}$): **2** $\cdot\text{HCl}$ (0.300 g, 1.21 mmol), Ag_2O (0.279 g, 1.21 mmol) and $[\text{PdCl}(\mu\text{-Cl})(\text{PPh}_3)]_2$ (0.530 g, 0.60 mmol). Yield: 73%. This complex is soluble in CH_2Cl_2 , CHCl_3 or THF, but insoluble in toluene or pentane. Anal. Calc. for $\text{C}_{29}\text{H}_{35}\text{Cl}_2\text{N}_2\text{PPdS}$ (651.97): C, 53.42; H, 5.41; N, 4.30. Found: C, 53.1; H, 5.8; N, 4.3. FTIR: $\nu_{\text{max}}(\text{pure, diamond orbit})/\text{cm}^{-1}$ 3394br, 3151w, 3115w, 3096w, 3073w, 3052w, 2957m, 2928m, 2871m, 1566w, 1480w, 1463m, 1432s, 1374w, 1353w, 1331w, 1311w, 1267m, 1242m, 1228s, 1202w, 1183w, 1157m, 1131w, 1096vs, 1028w, 998w, 973w, 874w, 844w, 798w, 754s, 749s, 741s, 707s, 692vs, 684vs, 533vs, 513vs, 494vs, 453m, 441m, 429m, 305vs ($\nu_{\text{Pd-Cl}}$), 284vs ($\nu_{\text{Pd-Cl}}$). ^1H NMR (CD_2Cl_2 , 300 MHz) δ : 0.88 (3H, t, $^3J = 7.5$ Hz, CH_3 butyl), 1.23 (3H, t, $^3J = 7.2$ Hz, SCH_2CH_3), 1.30 (2H, m, $\text{NCH}_2\text{CH}_2\text{CH}_2\text{CH}_3$), 1.48 (1H, m, $\text{NCH}_2\text{CHHCH}_2\text{CH}_3$), 1.81 (1H, m, $\text{NCH}_2\text{CHHCH}_2\text{CH}_3$), 2.49 (2H, q, $^3J = 7.2$ Hz, SCH_2CH_3), 2.85 (1H, m, NCH_2CHHS), 3.08 (1H, m, NCHHCH_2S), 3.71 (2H, m, $\text{NCHHCH}_2\text{CH}_2\text{CH}_3$ and NCH_2CHHS), 4.17 (1H, m, $\text{NCHHCH}_2\text{CH}_2\text{CH}_3$), 4.44 (1H, m, NCHHCH_2S), 6.67 and 6.81 (2H, AB spin system, $^3J = 1.8$ Hz, CH=CH), 7.34-7.58 (15H, m, H arom). $^{13}\text{C}\{\text{H}\}$ NMR (CD_2Cl_2 , 75.5 MHz) δ : 13.38 (CH_3 butyl), 14.81 (SCH_2CH_3), 19.92 ($\text{NCH}_2\text{CH}_2\text{CH}_2\text{CH}_3$), 26.25 (SCH_2CH_3), 31.10 ($\text{NCH}_2\text{CH}_2\text{S}$), 31.69 ($\text{NCH}_2\text{CH}_2\text{CH}_2\text{CH}_3$), 50.72 ($\text{NCH}_2\text{CH}_2\text{CH}_2\text{CH}_3$), 50.81 ($\text{NCH}_2\text{CH}_2\text{S}$), 121.04, 122.18 (CH=CH), 128.51 (d, $J_{\text{P-C}} = 11.0$ Hz, CH arom), 129.87 (d, $J_{\text{P-C}} = 53.8$ Hz, C_{ipso}), 131.18 (d, $J_{\text{P-C}} = 2.4$ Hz, CH arom), 134.10 (d, $J_{\text{P-C}} = 11.0$ Hz, CH arom), 160.32 (NCN). $^{31}\text{P}\{\text{H}\}$ NMR (CD_2Cl_2 , 121.5 MHz) δ : 28.5. MS (ESI): m/z 617.1 [$\text{M-Cl}]^+$.

Formation of **9** ($R = \text{methyl}$; $R' = \text{phenyl}$): **3** $\cdot\text{HCl}$ (0.283 g, 1.11 mmol), Ag_2O (0.257.4 g, 1.11 mmol) and $[\text{PdCl}(\mu\text{-Cl})(\text{PPh}_3)]_2$ (0.488 g, 0.56 mmol). Yield: 72%. This complex is soluble in CH_2Cl_2 , CHCl_3 or THF, but insoluble in toluene or pentane. Anal. Calc. for $\text{C}_{30}\text{H}_{29}\text{Cl}_2\text{N}_2\text{PPdS}$ (657.93): (9 \cdot 0.75 CH_2Cl_2) C, 51.17; H, 4.27; N, 3.88. Found: C, 51.1; H, 4.4; N, 3.7. ^1H NMR (CD_2Cl_2 , 300 MHz) δ : 3.07 (1H, m, NCH_2CHHS), 3.58 (1H, m, NCH_2CHHS), 3.63 (3H, s, NCH_3), 3.78 (1H, m, NCHHCH_2S), 4.51 (1H, m, NCHHCH_2S), 6.63 and 6.67 (2H, AB spin system, $^3J = 1.8$ Hz, CH=CH) 7.26-7.59 (20H, m, H arom). $^{13}\text{C}\{\text{H}\}$ NMR (CD_2Cl_2 , 75.5 MHz) δ : 31.63 ($\text{NCH}_2\text{CH}_2\text{S}$), 37.56 (NCH_3), 49.72 ($\text{NCH}_2\text{CH}_2\text{S}$), 121.87, 123.10 (CH=CH), 126.14 (C_{para} SPh), 128.23 (C_{meta} SPh), 128.49 (d, $J_{\text{P-C}} = 11.1$ Hz, CH arom PPh₃), 129.71 (C_{ortho} SPh), 129.73 (d, $J_{\text{P-C}} = 54.2$ Hz, C_{ipso} PPh₃), 131.12 (d, $J_{\text{P-C}} = 2.4$ Hz, CH arom PPh₃), 133.95 (d, $J_{\text{P-C}} = 11.2$ Hz, CH arom PPh₃), 134.27 (C_{ipso} SPh), (NCN) not observed. $^{31}\text{P}\{\text{H}\}$ NMR (CD_2Cl_2 , 121.5 MHz) δ : 28.6. MS (ESI): m/z 623.0 [$\text{M-Cl}]^+$.

Formation of **10** ($R = n\text{-butyl}$; $R' = \text{phenyl}$): **4** $\cdot\text{HCl}$ (0.288 g, 0.97 mmol), Ag_2O (0.225 g, 0.97 mmol) and $[\text{PdCl}(\mu\text{-Cl})(\text{PPh}_3)]_2$ (0.427 g, 0.49 mmol). Yield: 55%. This complex is soluble in CH_2Cl_2 , CHCl_3 or THF, but insoluble in toluene or pentane. Anal. Calc. for $\text{C}_{33}\text{H}_{35}\text{Cl}_2\text{N}_2\text{PPdS}$ (700.01): C, 56.62; H, 5.04; N, 4.00. Found: C, 56.3; H, 5.6; N, 3.4. FTIR: $\nu_{\text{max}}(\text{pure, diamond orbit})/\text{cm}^{-1}$ 3386br, 3156w, 3122w, 3095w, 3050w, 2957m, 2929m, 2870m, 1582m, 1571w, 1479m, 1462m, 1437s, 1421s, 1379w, 1356w, 1277w, 1260m, 1231s, 1203w, 1158m, 1088s, 1073sh, 1022s, 949w, 895w, 873w,

799s, 736vs, 728vs, 704s, 689vs, 533vs, 512s, 494s, 475vs, 350vs, 307s (Pd-Cl), 287s ($\nu_{\text{Pd-Cl}}$). ^1H NMR (CD_2Cl_2 , 300 MHz) δ : 0.88 (3H, t, $^3J = 7.2$ Hz, CH_3 butyl), 1.30 (2H, m, $\text{NCH}_2\text{CH}_2\text{CH}_2\text{CH}_3$), 1.46 (1H, m, $\text{NCH}_2\text{CHHCH}_2\text{CH}_3$), 1.81 (1H, m, $\text{NCH}_2\text{CHHCH}_2\text{CH}_3$), 3.07 (1H, m, NCH_2CHHS), 3.57 (1H, m, NCH_2CHHS), 3.76 (2H, m, $\text{NCHHCH}_2\text{CH}_2\text{CH}_3$ and NCHHCH_2S), 4.20 (1H, m, $\text{NCHHCH}_2\text{CH}_2\text{CH}_3$), 4.54 (1H, m, NCHHCH_2S), 6.67 and 6.71 (2H, AB spin system, $^3J = 2.1$ Hz, $\text{CH}=\text{CH}$), 7.26-7.58 (20H, m, H arom). $^{13}\text{C}\{\text{H}\}$ NMR (CD_2Cl_2 , 75.5 MHz) δ : 13.39 (CH_3), 19.93 ($\text{NCH}_2\text{CH}_2\text{CH}_2\text{CH}_3$), 31.50 ($\text{NCH}_2\text{CH}_2\text{S}$), 31.63 ($\text{NCH}_2\text{CH}_2\text{CH}_2\text{CH}_3$), 49.88 ($\text{NCH}_2\text{CH}_2\text{CH}_2\text{CH}_3$), 50.85 ($\text{NCH}_2\text{CH}_2\text{S}$), 121.36, 121.98 ($\text{CH}=\text{CH}$), 126.06 (C_{para} SPh), 128.16 (C_{meta} SPh), 128.46 (d, $J_{\text{P-C}} = 11.0$ Hz, CH arom PPh₃), 129.67 (C_{ortho} SPh), 129.72 (d, $J_{\text{P-C}} = 54.1$ Hz, C_{ipso} PPh₃), 131.09 (d, $J_{\text{P-C}} = 2.5$ Hz, CH arom PPh₃), 134.00 (d, $J_{\text{P-C}} = 11.0$ Hz, CH arom PPh₃), 134.36 (C_{ipso} SPh), 160.84 (NCN). $^{31}\text{P}\{\text{H}\}$ NMR (CD_2Cl_2 , 121.5 MHz) δ : 28.6. MS (ESI): *m/z* 665.1 [M-Cl]⁺.

Procedure for the ligand displacement reactions:

Formation of **7** starting from **5**: Complex **5** (0.070 g, 0.201 mmol) and solid PPh₃ (0.053 g, 0.201 mmol) were placed in a Schlenk tube and dry CH_2Cl_2 was added under nitrogen. The reaction mixture was stirred for 12 h at room temperature. The volume of the yellow solution was reduced to 1/3 under reduced pressure and the product was precipitated by addition of pentane. Yield: 89%.

Formation of **5** starting from **7**: Complex **7** (0.070 g, 0.115 mmol) was dissolved in dry CH_2Cl_2 and solid [AuCl(THT)] (0.037 g, 0.115 mmol) was added under nitrogen. The reaction mixture was stirred for 12 h at room temperature. The solvent of the resulting yellow solution was evaporated under reduced pressure. Then the [AuCl(PPh₃)] formed was extracted with THF and the product was crystallized from a dichloromethane/pentane solution. Yield: 84%.

Procedure for the Suzuki–Miyaura cross-coupling reaction with complex **5:**

Complex **5** (6.95 mg, 0.02 mmol), phenyl boronic acid (146.3 mg, 1.20 mmol) and Cs₂CO₃ (651.6 mg, 2.00 mmol) were placed in a Schlenk tube and DMSO (3 ml) was added under nitrogen. Then 4-bromotoluene (123.1 μl , 171.0 mg, 1.00 mmol) was added and the reaction mixture was heated for 2 h at 100 °C. The reaction was then quenched by rapid cooling down to room temperature and the suspension was filtered through a Celite pad. The resulting solution was then analysed by gas chromatography and showed 90% conversion.

Following the same procedure in dioxane (3 ml) as solvent gave only 80% conversion.

Procedure for the Suzuki–Miyaura cross-coupling reaction with complex **7:**

Complex **7** (12.2 mg, 0.02 mmol), phenyl boronic acid (146.3 mg, 1.20 mmol) and Cs₂CO₃ (651.6 mg, 2.00 mmol) were placed in a Schlenk tube and dioxane (3 ml) was added under nitrogen. Then 4-bromotoluene (123.1 μl , 171.0 mg, 1.00 mmol) was added and the reaction mixture was heated for 2 h at 100 °C. The reaction was then quenched by rapid cooling down to room temp. and the suspension filtered through Celite. The resulting solution was then analysed by GC and showed 78% conversion.

S2. Crystallographic data

The intensity data was collected at 173(2) K on a Kappa CCD diffractometer^{S3} (graphite monochromated MoK α radiation, $\lambda = 0.71073 \text{ \AA}$). The structures were solved by direct methods (SHELXS-97) and refined by full-matrix least-squares procedures (based on F^2 , SHELXL-97)^{S4} with anisotropic thermal parameters for all the non-hydrogen atoms. The hydrogen atoms were introduced into the geometrically calculated positions (SHELXS-97 procedures) and refined *riding* on the corresponding parent atoms. In view of the relatively low absorption coefficient and the small size of the crystals, we have chosen not to apply any absorption correction. The molecular structure of **6** is centrosymmetric, the centre being located on the Pd atom. In **8**, the butyl and the ethyl moieties were severely disordered. Attempts to refine a satisfactory model for this disorder failed and the atoms were refined with restrained C-C distances (1.54 \AA) and anisotropic thermal parameters restrained to isotropic ones. The asymmetric unit of **9**·0.75CH₂Cl₂ consisted in two crystallographically independent molecules of **9** and two dichloromethane molecules, one of which was found disordered in two positions close to the symmetry centre, with an occupancy factor of 0.5. The latter was refined with restrained anisotropic thermal parameters and C-Cl distances (1.74 \AA).

^{S3} Bruker-Nonius, *Kappa CCD Reference Manual*, Nonius BV, The Netherlands, **1998**.

^{S4} M. Sheldrick, *SHELXL-97*, Program for crystal structure refinement; University of Göttingen: Germany, **1997**.

S2.1 Crystallographic data of compound 5:

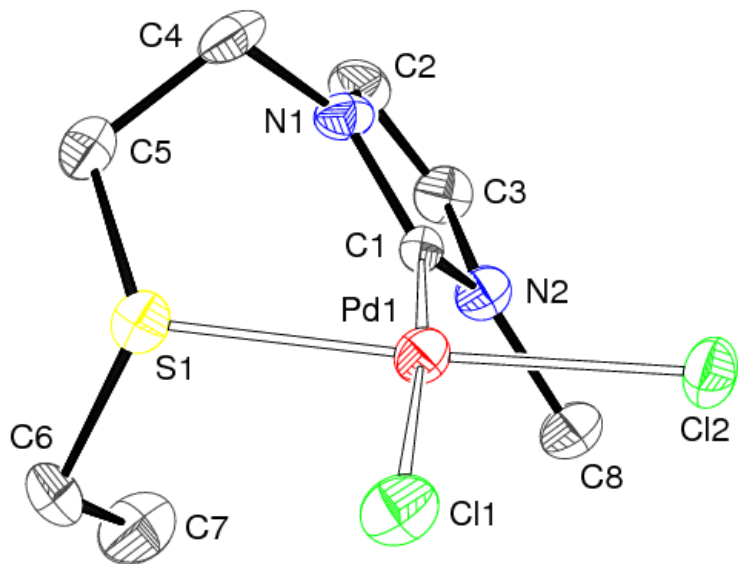


Figure S-1. Suitable crystals for X-ray diffraction were obtained by slow diffusion of pentane into a saturated solution of **5** in dichloromethane. ORTEP plot of the molecular structure of **5** (50% probability level chosen for the ellipsoids, hydrogen atoms omitted for clarity). Selected bond distances (\AA) and angles ($^\circ$): Pd(1)-C(1) 1.984(7), Pd(1)-S(1) 2.279(2), Pd(1)-Cl(1) 2.374(2), Pd(1)-Cl(2) 2.3239(19), C(1)-N(1) 1.353(9), C(1)-N(2) 1.339(10); C(1)-Pd(1)-S(1) 90.7(2), C(1)-Pd(1)-Cl(2) 90.6(2), S(1)-Pd(1)-Cl(1) 85.41(7), N(2)-C(1)-N(1) 106.2(6).

Data collection and refinement parameters: formula $\text{C}_8\text{H}_{14}\text{Cl}_2\text{N}_2\text{PdS}$, $M = 347.57$, monoclinic, space group $P2_1/c$, $a = 10.9199(6)$, $b = 8.3242(4)$, $c = 14.8290(9) \text{\AA}$, $\beta = 118.849(4)$, $V = 1180.66(11) \text{\AA}^3$, $Z = 4$, crystal size = $0.05 \times 0.05 \times 0.03 \text{ mm}^3$, $D_c = 1.955 \text{ g}\cdot\text{cm}^{-3}$, $\mu = 2.164 \text{ mm}^{-1}$ (Mo-K α), $T = 173(2)$, $R(I > 2\sigma(I)) = 0.050$, $wR(I > 2\sigma(I)) = 0.1379$, $S = 1.087$ for all 2443 unique data (4371 meas., $R_{\text{int}} = 0.0442$, max $2\theta = 53$) and 129 refined parameters, ρ_{max} and $\rho_{\text{min}} = 1.844$ and $-1.012 \text{ e}/\text{\AA}^3$.

S2.2 Crystallographic data of compound 6:

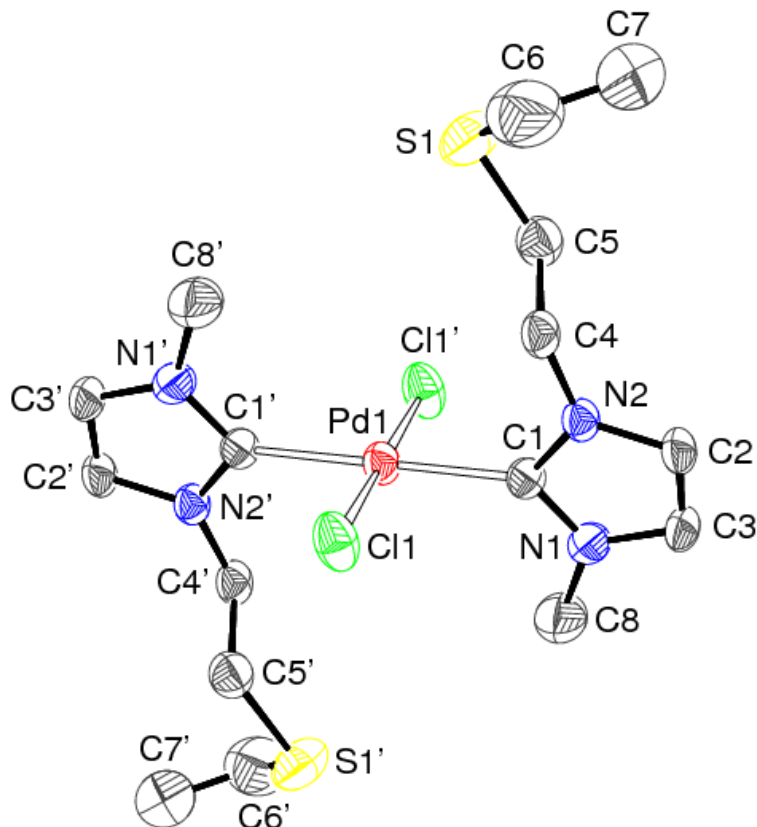


Figure S-2. Suitable crystals for X-ray diffraction were obtained by slow diffusion of pentane into a saturated solution of **6** in dichloromethane. ORTEP plot of the molecular structure of **6** (50% probability level chosen for the ellipsoids, hydrogen atoms omitted for clarity). Selected bond distances (\AA) and angles ($^\circ$): Pd(1)-C(1) 2.031(6), Pd(1)-Cl(1) 2.3081(16), C(1)-N(1) 1.341(7), C(1)-N(2) 1.344(7); C(1)-Pd(1)-Cl(1) 90.21(16), N(1)-C(1)-N(2) 105.1(5). Symmetry operations generating equivalent atoms (''): -x, -y, -z.

Data collection and refinement parameters: formula $\text{C}_{16}\text{H}_{28}\text{Cl}_2\text{N}_4\text{PdS}_2$, $M = 517.84$, triclinic, space group $P-1$, $a = 7.8872(8)$, $b = 7.9205(9)$, $c = 9.8308(7)$ \AA , $\alpha = 96.521(6)$, $\beta = 91.623(6)$, $\gamma = 114.409(4)$, $V = 553.7(1)$ \AA^3 , $Z = 1$, crystal size = $0.06 \times 0.06 \times 0.01$ mm^3 , $D_c = 1.553$ $\text{g}\cdot\text{cm}^{-3}$, $\mu = 1.275$ mm^{-1} (Mo-K α), $T = 173(2)$, $R(I > 2\sigma(I)) = 0.0529$, $wR(I > 2\sigma(I)) = 0.1156$, $S = 1.024$ for all 2172 unique data (4911 meas., $R_{\text{int}} = 0.0729$, max $2\theta = 52$) and 115 refined parameters, ρ_{max} and $\rho_{\text{min}} = 0.933$ and -1.122 $\text{e}/\text{\AA}^3$.

S2.3 Crystallographic data of compound 8:

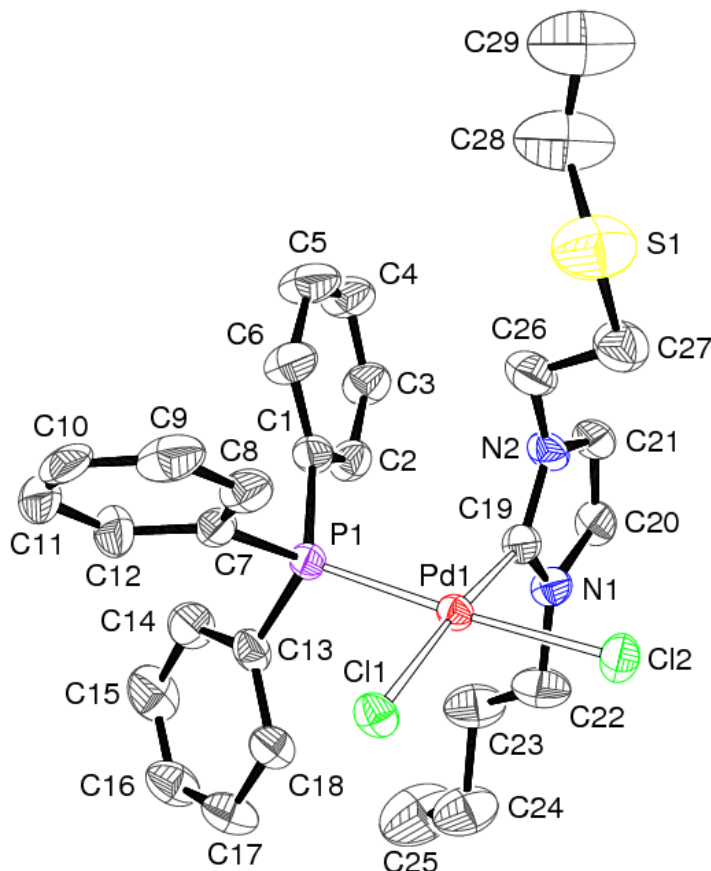


Figure S-3. Suitable crystals for X-ray diffraction were obtained by slow diffusion of pentane into a saturated solution of **8** in dichloromethane. ORTEP plot of the molecular structure of **8** (50% probability level chosen for the ellipsoids, hydrogen atoms omitted for clarity). Selected bond distances (\AA) and angles ($^{\circ}$): Pd(1)-C(19) 1.977(5), Pd(1)-P(1) 2.2547(13), Pd(1)-Cl(1) 2.3549(13), Pd(1)-Cl(2) 2.3585(13), C(19)-N(1) 1.346(6), C(19)-N(2) 1.346(7); P(1)-Pd(1)-C(19) 91.68(15), P(1)-Pd(1)-Cl(1) 90.74(5), C(19)-Pd(1)-Cl(2) 85.33(15), Cl(1)-Pd(1)-Cl(2) 92.44(5), N(1)-C(19)-N(2) 105.2(4).

Data collection and refinement parameters: formula $\text{C}_{29}\text{H}_{35}\text{Cl}_2\text{N}_2\text{PPdS}$, $M = 651.92$, monoclinic, space group $P2_1/c$, $a = 12.8722(6)$, $b = 17.6615(5)$, $c = 18.3472(6) \text{\AA}$, $\beta = 133.128(2)$, $V = 3044.18(22) \text{\AA}^3$, $Z = 4$, crystal size = 0.07 x 0.06 x 0.06 mm³, $D_c = 1.422 \text{ g}\cdot\text{cm}^{-3}$, $\mu = 0.927 \text{ mm}^{-1}$ (Mo-K α), $T = 173(2)$, $R(I > 2\sigma(I)) = 0.0595$, $wR(I > 2\sigma(I)) = 0.1665$, $S = 1.129$ for all 5669 unique data (16443 meas., $R_{\text{int}} = 0.0575$, max $2\theta = 51$) and 329 refined parameters, ρ_{max} and $\rho_{\text{min}} = 2.245$ and $-1.11 \text{ e}/\text{\AA}^3$.

S2.4 Crystallographic data of compound 9·0.75CH₂Cl₂:

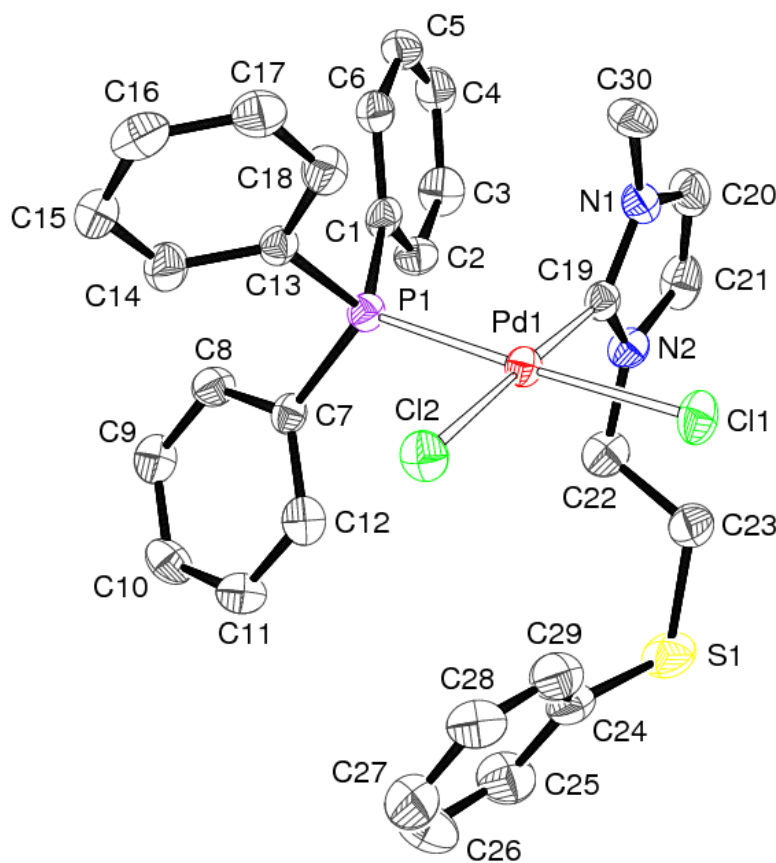


Figure S-4. Suitable crystals for X-ray diffraction were obtained by slow diffusion of pentane into a saturated solution of **9** in dichloromethane. ORTEP plot of the molecular structure of **9**·0.75CH₂Cl₂ (independent molecule A (molecule B is very similar), 50% probability level chosen for the ellipsoids, molecules of solvent and hydrogen atoms omitted for clarity). Selected bond distances (Å) and angles (°): Pd(1)-C(19) 1.987(5) [A] 1.973(5) [B], Pd(1)-P(1) 2.2528(12) [A] 2.2559(14) [B], Pd(1)-Cl(1) 2.3583(12) [A] 2.3437(13) [B], Pd(1)-Cl(2) 2.3417(13) [A] 2.3698(13) [B], C(19)-N(1) 1.346(6) [A] 1.345(6) [B], C(19)-N(2) 1.350(6) [A] 1.368(6) [B]; P(1)-Pd(1)-C(19) 92.01(13) [A] 90.77(14) [B], P(1)-Pd(1)-Cl(2) 88.56(5) [A] 176.93(5) [B], P(1)-Pd(1)-Cl(1) 177.17(5) [A] 89.26(5) [B], C(19)-Pd(1)-Cl(1) 87.24(13) [A] 177.66(13) [B], C(19)-Pd(1)-Cl(2) 178.32(15) [A] 87.46(14) [B], Cl(1)-Pd(1)-Cl(2) 92.26(5) [A] 92.41(5) [B], N(1)-C(19)-N(2) 105.3(4) [A] 104.6(4) [B].

Data collection and refinement parameters: formula C_{30.75}H_{30.50}Cl_{3.50}N₂PPdS, $M = 721.58$, triclinic, space group *P*-1, $a = 10.1476(2)$, $b = 14.9042(5)$, $c = 20.9556(6)$ Å, $\alpha = 97.881(1)$, $\beta = 90.739(2)$, $\gamma = 97.207(2)$, $V = 3113.2(1)$ Å³, $Z = 4$, crystal size = 0.07 x 0.06 x 0.06 mm³, $D_c = 1.540$ g·cm⁻³, $\mu = 1.039$ mm⁻¹ (Mo-Kα), $T = 173(2)$, $R(I > 2\sigma(I)) = 0.0539$, $wR(I > 2\sigma(I)) = 0.1388$, $S = 1.036$ for all 12890 unique data (31306 meas., $R_{\text{int}} = 0.0557$, max 2θ = 53) and 711 refined parameters, ρ_{max} and $\rho_{\text{min}} = 2.079$ and -1.653 e/Å³.

S2.5 Crystallographic data of compound 10:

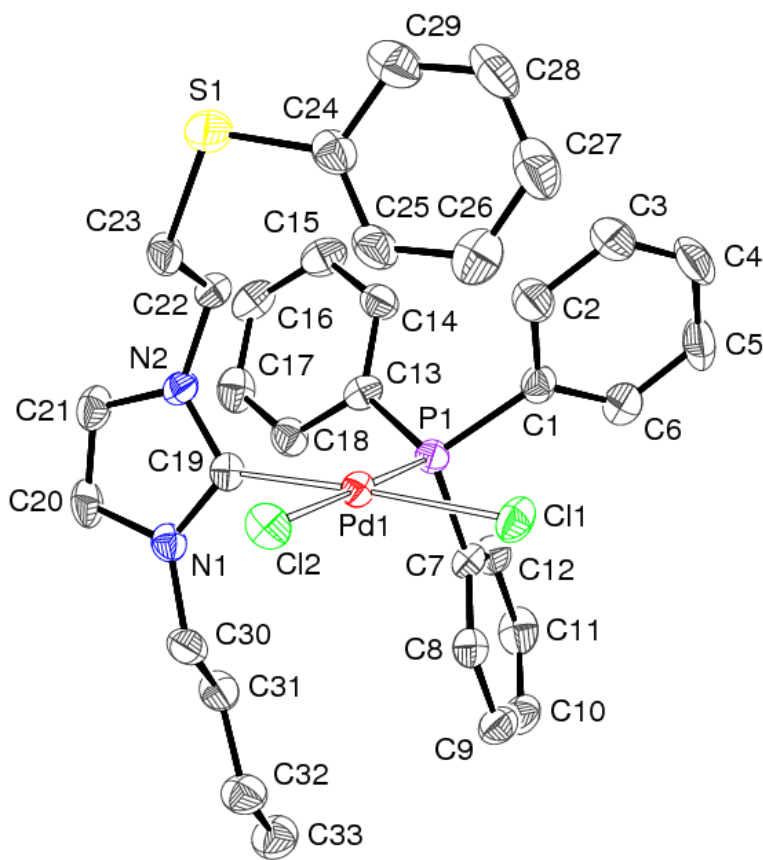


Figure S-5. Suitable crystals for X-ray diffraction were obtained by slow diffusion of pentane into a saturated solution of **10** in dichloromethane. ORTEP plot of the molecular structure of **10** (50% probability level chosen for the ellipsoids, hydrogen atoms omitted for clarity). Selected bond distances (\AA) and angles ($^{\circ}$): Pd(1)-C(19) 1.982(6), Pd(1)-P(1) 2.2601(15), Pd(1)-Cl(1) 2.3463(16), Pd(1)-Cl(2) 2.3580(15), C(19)-N(1) 1.340(7), C(19)-N(2) 1.356(7); P(1)-Pd(1)-C(19) 92.48(16), P(1)-Pd(1)-Cl(1) 89.44(6), C(19)-Pd(1)-Cl(2) 85.82(16), Cl(1)-Pd(1)-Cl(2) 92.26(6), N(1)-C(19)-N(2) 106.2(5).

Data collection and refinement parameters: formula $\text{C}_{33}\text{H}_{35}\text{Cl}_2\text{N}_2\text{PPdS}$, $M = 699.96$, monoclinic, space group $P2_1/c$, $a = 19.5332(10)$, $b = 9.1372(5)$, $c = 20.1256(8)$ \AA , $\beta = 117.700(2)$, $V = 3180.3(3)$ \AA^3 , $Z = 4$, crystal size = $0.05 \times 0.05 \times 0.04$ mm^3 , $D_c = 1.462$ $\text{g}\cdot\text{cm}^{-3}$, $\mu = 0.893$ mm^{-1} (Mo-K α), $T = 173(2)$, $R(I > 2\sigma(I)) = 0.0487$, $wR(I > 2\sigma(I)) = 0.1027$, $S = 0.992$ for all 6256 unique data (20288 meas., $R_{\text{int}} = 0.0927$, max $2\theta = 52$) and 362 refined parameters, ρ_{max} and $\rho_{\text{min}} = 1.244$ and -1.481 $\text{e}/\text{\AA}^3$.

References

- (1) (a) F. E. Hahn and M. C. Jahnke, *Angew. Chem. Int. Ed.*, 2008, **47**, 3122-3172; (b) D. Bourissou, O. Guerret, F. P. Gabbaï and G. Bertrand, *Chem. Rev.*, 2000, **100**, 39-91; (c) W. A. Herrmann, *Angew. Chem. Int. Ed.*, 2002, **41**, 1290-1309; (d) N. M. Scott and S. P. Nolan, *Eur. J. Inorg. Chem.*, 2005, 1815-1828; (e) F. E. Hahn, *Angew. Chem. Int. Ed.*, 2006, **45**, 1348-1352; (f) V. César, S. Bellemín-Lapponnaz and L. H. Gade, *Chem. Soc. Rev.*, 2004, 619-636.
- (2) (a) M. V. Jiménez, J. J. Pérez-Torrente, M. I. Bartolomé, V. Gierz, F. J. Lahoz and L. A. Oro, *Organometallics*, 2008, **27**, 224-234; (b) N. Stylianides, A. A. Danopoulos and N. Tsoureas, *J. Organomet. Chem.*, 2005, **690**, 5948-5958; (c) D. S. McGuinness and K. J. Cavell, *Organometallics*, 2000, **19**, 741-748; (d) L. H. Gade, V. César and S. Bellemín-Lapponnaz, *Angew. Chem. Int. Ed.*, 2004, **43**, 1014-1017.
- (3) (a) H. Clavier, L. Coutable, L. Toupet, J. C. Guillemin and M. Mauduit, *J. Organomet. Chem.*, 2005, **690**, 5237-5254; (b) A. W. Waltman and R. H. Grubbs, *Organometallics*, 2004, **23**, 3105-3107; (c) P. L. Arnold, M. Rodden and C. Wilson, *Chem. Commun.*, 2005, 1743-1745.
- (4) (a) A. C. Yang, H. M. Lee and S. P. Nolan, *Org. Lett.*, 2001, **3**, 1511-1514; (b) C. C. Lee, W. C. Ke, K. T. Chan, C. L. Lai, C. H. Hu and H. M. Lee, *Chem. Eur. J.*, 2007, **13**, 582-591; (c) L. D. Field, B. A. Messerle, K. Q. Vuong and P. Turner, *Organometallics*, 2005, **24**, 4241-4250.
- (5) (a) P. Braunstein and F. Naud, *Angew. Chem. Int. Ed.*, 2001, **40**, 680-699; (b) P. Braunstein, *J. Organomet. Chem.*, 2004, **689**, 3953-3967.
- (6) (a) H. Seo, H. J. Park, B. Y. Kim, J. H. Lee, S. U. Son and Y. K. Chung, *Organometallics*, 2003, **22**, 618-620; (b) J. Wolf, A. Labande, J. C. Daran and R. Poli, *Eur. J. Inorg. Chem.*, 2007, 5069-5079; (c) S. J. Roseblade, A. Ros, D. Monge, M. Alcarazo, E. Alvarez, J. M. Lassaletta and R. Fernandez, *Organometallics*, 2007, **26**, 2570-2578; (d) H. V. Huynh, C. H. Yeo and G. K. Tan, *Chem. Commun.*, 2006, 3833-3835; (e) A. Ros, D. Monge, M. Alcarazo, E. Alvarez, J. M. Lassaletta and R. Fernandez, *Organometallics*, 2006, **25**, 6039-6046.
- (7) (a) J. A. Cabeza, I. da Silva, I. del Río and M. G. Sánchez-Vega, *Dalton Trans.*, 2006, 3966-3971; (b) J. A. Cabeza, I. del Río, M. G. Sánchez-Vega, M. Suárez, *Organometallics*, 2006, **25**, 1831-1834.
- (8) (a) K. Hara, R. Akiyama, S. Takakusagi, K. Uosaki, T. Yoshino, H. Kagi and M. Sawamura, *Angew. Chem. Int. Ed.*, 2008, **47**, 5627-5630; (b) T. Belser, M. Stöhr and A. Pfaltz, *J. Am. Chem. Soc.*, 2005, **127**, 8720-8731.
- (9) H. M. J. Wang and I. J. B. Lin, *Organometallics*, 1998, **17**, 972-975.
- (10) G. A. Grasa, M. S. Viciu, J. Huang, C. Zhang, M. L. Trudell, S. P. Nolan, *Organometallics*, 2002, **21**, 2866-2873.

Chapitre 2

Synthesis of *N,N'*-bis(thioether)-functionalized
Imidazolium Salts: Their Reactivity Towards
Ag and Pd Complexes and First S,C_{NHC},S Free
Carbene

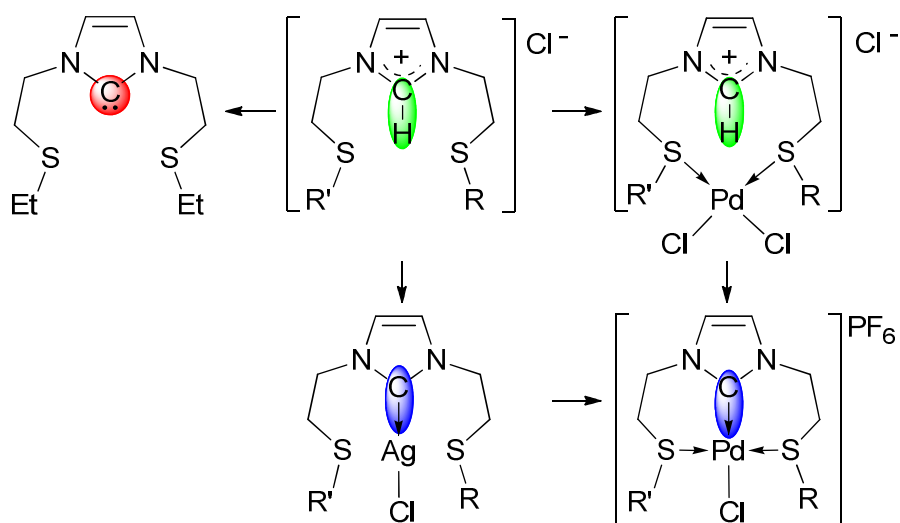
Résumé du chapitre 2

La synthèse de sels d'imidazoliums bi-fonctionnalisés par des groupements thioéthers, la caractérisation du premier carbène libre de type S,C_{NHC},S et les complexes carbéniques d'Ag(I) et de Pd(II) correspondants sont présentés dans ce chapitre. Ces derniers ont été préparés à partir des complexes carbéniques d'Ag(I) isolés en utilisant la procédure de transmétallation ou par réaction des sels d'imidazoliums avec $[PdCl_2(COD)]$, suivie de la déprotonation de cet intermédiaire dans lequel les deux fonctions thioéthers sont coordinées au Pd(II).

Référence et synopsis du chapitre 2

Christophe Fliedel, Alessandra Sabbatini and Pierre Braunstein,

Dalton Transactions, 2010, **39**, 8820–8828.



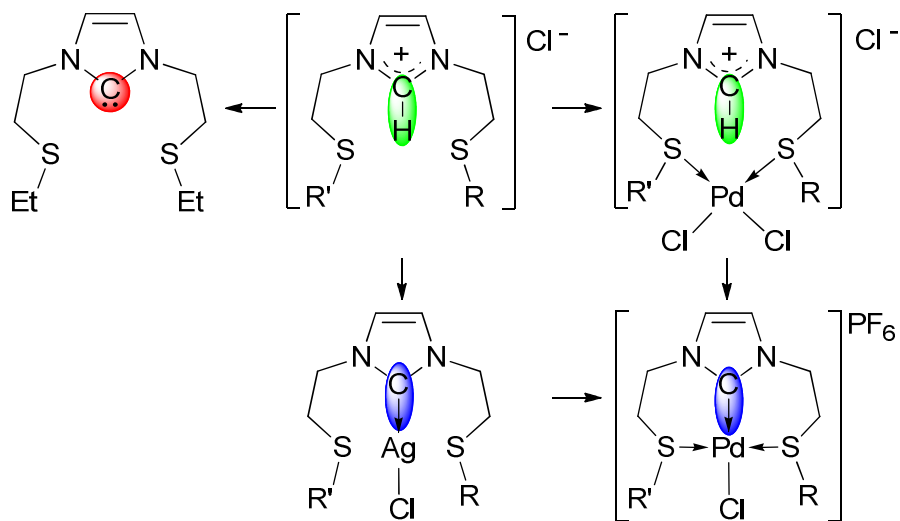
Abstract of Chapter 2

The synthesis of bis(thioether)-functionalized imidazolium salts, the characterisation of the first S,C_{NHC},S free carbene ligand and the corresponding Ag(I) and Pd(II) functional carbene complexes are reported. The latter have been prepared from the isolated Ag(I) carbene complexes using the transmetallation procedure or by reaction of the imidazolium salts with $[\text{PdCl}_2(\text{COD})]$, followed by deprotonation of the intermediate in which both thioether functions are coordinated to Pd(II).

Reference and Synopsis of Chapter 2

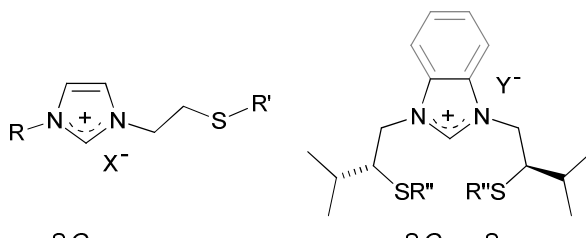
Christophe Fliedel, Alessandra Sabbatini and Pierre Braunstein,

Dalton Transactions, 2010, **39**, 8820–8828.



Introduction

N-Heterocyclic carbenes (NHCs) are known to be strong donors and robust ligands¹ and therefore have been extensively studied in organometallic chemistry and homogeneous catalysis.² They have been used as phosphine mimics and their palladium complexes have been successfully used in many cross-coupling reactions.³ The possibility of attaching donor groups to the nitrogen atoms opens new possibilities for creating heterofunctional donor ligands. Different combinations have emerged, which have allowed the formation of *N*-,⁴ *O*-,⁵ and *P*-C_{NHC}⁶ complexes. Owing to their hemilabile character,⁷ these compounds rapidly attracted attention for applications in homogeneous catalysis. Few examples of *S*-C_{NHC} metal complexes have been recently described and the presence of the *S*-containing function appears beneficial in catalytic reactions (Scheme 1). These complexes have been obtained by conventional methods^{8,16} or by oxidative-addition of a C–S bond across a zero valent metal centre,⁹ and generally showed in solution fast exchange on the ¹H NMR time-scale, consistent with the lability of the coordinated thioether.



R = Me, *n*-Bu; R' = Et, Ph; R'' = Cy, *t*-Bu, Ph, Bn;
X = Cl, BF₄, PF₆; Y = Cl, Br

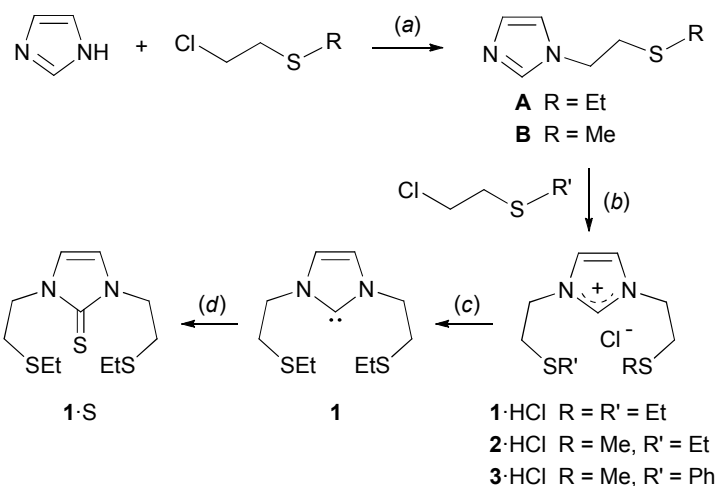
Scheme 1 Examples of *S*,C_{NHC} and *S*,C_{NHC},S precursors.

Here we report the stepwise synthesis of new NHC precursors bearing a thioether function on each nitrogen atom of the imidazolium salt. The methodology used allows for the introduction of identical or different thioether groups. The silver NHC complexes prepared from the corresponding imidazolium salts have been fully characterised and, in one case, used for the synthesis by transmetalation of a *S*,C_{NHC},S Pd(II) pincer complex. An alternative pathway to *S*,C_{NHC},S complexes was used, which involved first, coordination of the thioether functions to Pd(II), followed by deprotonation of the imidazolium group. The first examples of cationic, imidazolium-containing bis(thioether) *S,S*-PdCl₂ complexes were thus isolated and characterized. Neutral bis(thioether) complexes have recently been studied for allylic oxidation and displayed better performances than previous systems.¹⁰

Results and Discussion

Synthesis of the Ligands

The *N*-functionalized imidazoles **A** and **B** were obtained by a reaction between imidazole and commercially available 2-chloroethyl ethylsulfide or 2-chloroethyl methylsulfide, respectively, in the presence of sodium *tert*-butoxide in refluxing toluene (Scheme 2). The NMR spectra show typical resonances for aliphatic-substituted imidazoles at 7.56 and 7.41 ppm for the 2-H protons, respectively, and at 137.1 ppm for the NCN carbon of both **A** and **B**. The analogous products obtained from 2-chloroethyl phenylsulfide could be observed by NMR spectroscopy but were not isolated in pure form.



Scheme 2 Ligand synthesis.

(a) 1.2 equiv. KO*t*-Bu, toluene, reflux, overnight; (b) neat, 150 °C, 2 h; (c) 1 equiv. KHMDS, THF, room temperature, 2 h; (d) 1 equiv. S₈, THF, room temperature, 2 h.

An atom efficient reaction applied to **A** and **B** afforded homo- and hetero-bis(thioether) imidazolium salts, respectively (Scheme 2). The *C*₂-symmetric cation in **1·HCl** was obtained in nearly quantitative yield by neat reaction between **A** and 2-chloroethyl ethylsulfide, following a method described for the synthesis of mono(thioether) imidazoliums.^{8e,16} When the same procedure was applied to the reaction of **B** with 2-chloroethyl ethylsulfide or 2-chloroethyl phenylsulfide, it afforded the unsymmetrical derivatives **2·HCl** and **3·HCl**, respectively (Scheme 2). To the best of our knowledge, the latter are the only reported examples of hetero-bis(thioether) imidazolium salts, while *C*₂-symmetric homo-bis(thioether) imidazolium salts were published during the course of our work.^{8b} The ¹H NMR spectra of **1·HCl**–**3·HCl** show typical resonances between 10.40 and 10.68 ppm for the 2-H proton and

the $^{13}\text{C}\{^1\text{H}\}$ NMR peak of their NCN carbon is found between 137.7 and 138.2 ppm. The ^1H NMR spectrum of **1**·HCl contains only one signal for the equivalent 4,5-H imidazolium protons, consistent with a C_2 -symmetry of the ligand, while two pseudo-triplets are observed for **2**·HCl and **3**·HCl ($^3J \approx ^4J \approx 1.5\text{--}1.8$ Hz). The most intense peaks in the ESI mass spectra correspond to $[\text{M}-\text{Cl}]^+$.

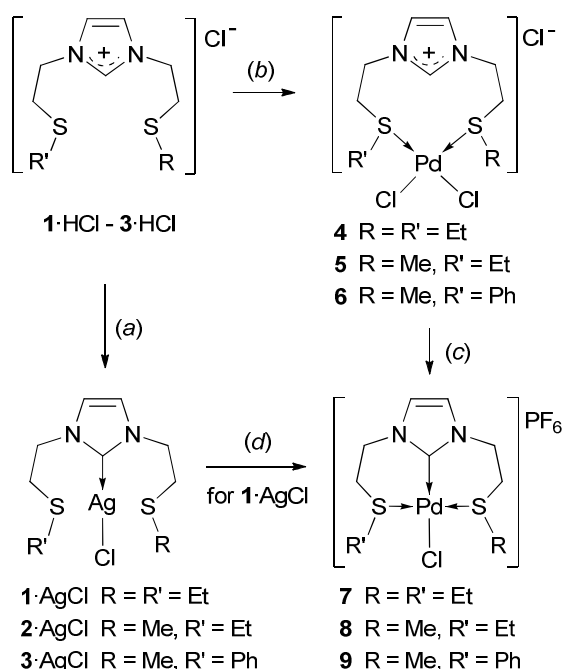
The free carbene **1** was readily generated in quantitative yield by deprotonation of **1**·HCl with potassium hexamethyldisilazane (KHMDS) in THF at room temperature. It was characterized by multinuclear NMR spectroscopy, but degraded slowly in solution after several hours.

The ^1H NMR spectrum of **1** confirms the absence of the 2H-imidazolium proton and shows a significant upfield shift of the 4,5-H imidazolium protons from 7.58 (in CDCl_3) to 6.96 ppm (in $\text{THF}-d_8$). A strong downfield shift was observed for the broad and weak $^{13}\text{C}\{^1\text{H}\}$ NMR signal of the NCN carbon at 195.9 ppm. For comparison, the carbene carbon of free *N,N*'-(dimethyl)imidazol-2-ylidene resonates at 215.2 ppm.¹¹ This could be consistent with the significant influence of *N*-substitution on the electronic properties of the carbene centre¹² and/or with the formation in solution of a potassium adduct favored by the presence of stabilizing donor functions on the imidazole ring. Unfortunately, all attempts to crystallize **1** were unsuccessful owing to its low stability and since no similar ligand is available for comparison, we could not confirm the latter hypothesis. Ligand **1** is the first characterized bis(thioether)-functionalized carbene and despite the recent report of bis(thioether) imidazolium salts, the authors did not characterize the corresponding free carbenes.^{8b}

Since **1** was not stable enough to be structurally characterized, we attempted to isolate its thione derivative **1**·S. Stepwise formation of **1**·S involved first the deprotonation of **1**·HCl by one equivalent KHMDS in THF at room temperature, followed by the addition of one equivalent S_8 to the reaction mixture. After filtration, **1**·S was obtained in good yield and was fully characterized. As in the case of **1**, disappearance of the 2H-imidazolium ^1H NMR signal was noted. A typical $^{13}\text{C}\{^1\text{H}\}$ NMR signal at 161.8 ppm is assigned to the NCN carbon. In contrast to the free carbene **1**, its thione derivative **1**·S is air-stable in solution and in the solid state, but unfortunately, no crystal suitable for X-ray diffraction could be obtained. The free carbenes **2** and **3** were prepared similarly from **2**·HCl and **3**·HCl, respectively.

Synthesis of the Silver(I) Complexes

Reaction of the imidazolium salts with excess Ag_2O at room temperature in dichloromethane afforded, after filtration through Celite to remove unreacted Ag_2O , the corresponding silver (I) NHC complexes $\mathbf{1}\cdot\text{AgCl}-\mathbf{3}\cdot\text{AgCl}$ in good yields (Scheme 3a). Formation of the latter was established by the absence of the 2H-imidazolium proton resonance in the ^1H NMR spectrum, which also showed a significant upfield shift of the 4,5H-imidazolium protons. The $^{13}\text{C}\{^1\text{H}\}$ NMR spectra showed typical downfield shifts, compared to the corresponding imidazolium salts, of the C2-carbon signals between 179.8 and 179.9 ppm, characteristic of the formation of $\text{Ag}(\text{I})$ NHC complexes.



Scheme 3 Synthesis of the $\text{Ag}(\text{I})$ complexes and the S,S and $S,\text{C}_{\text{NHC}},S$ $\text{Pd}(\text{II})$ complexes.

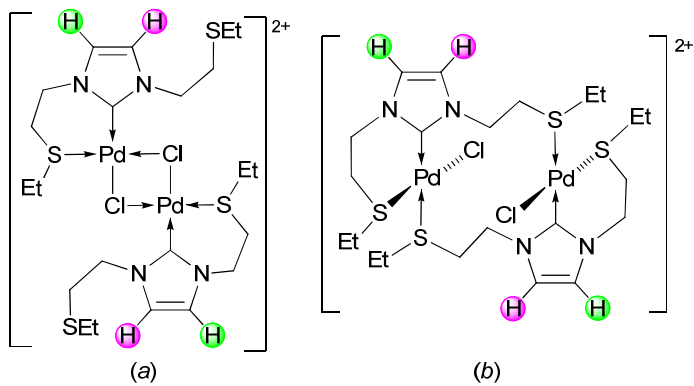
(a) 1 equiv. Ag_2O , CH_2Cl_2 , room temperature, 2 h; (b) 1 equiv. $[\text{PdCl}_2(\text{COD})]$, CH_2Cl_2 , room temperature, 4 h; (c) 1.1 equiv. Cs_2CO_3 , 5 equiv. KPF_6 , MeCN , reflux, 6 h; (d) 1 equiv. $[\text{PdCl}_2(\text{COD})]$, 5 equiv. KPF_6 , CH_2Cl_2 , room temperature, 4 h.

Synthesis of the Palladium(II) Complexes

The coordination chemistry of bis(thioether) NHC-type ligands was then investigated using $\text{Pd}(\text{II})$. The *in situ* reaction of carbene **1** with $[\text{PdCl}_2(\text{COD})]$ ($\text{COD} = 1,5\text{-cyclooctadiene}$) afforded a mixture of complexes (NMR evidence). Different routes were thus investigated to obtain the desired complexes in pure form. The carbene complex $\mathbf{1}\cdot\text{AgCl}$ was reacted *in situ* with $[\text{PdCl}_2(\text{COD})]$ and excess KPF_6 to form the $\text{Pd}(\text{II})$ carbene complex **7** by transmetallation (Scheme 3a and d).¹³

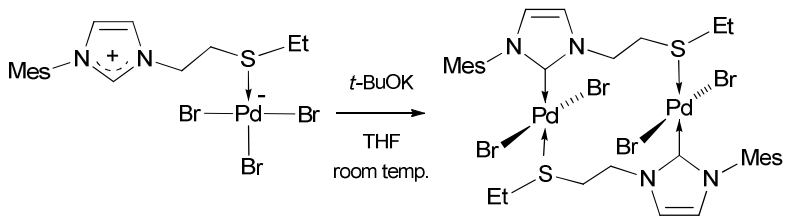
An alternative, stepwise synthesis consisted first of the formation of the non-NHC, cationic complexes **4–6** by reaction of [PdCl₂(COD)] with **1·HCl–3·HCl**, respectively (Scheme 3b). Their ¹H NMR spectra confirmed the presence of the 2-H proton, between 9.23 and 9.26 ppm. For complex **4**, this spectrum also revealed the equivalence of the two side chains because the 4,5H-imidazolium protons gave rise to only one doublet (⁴J = 1.5 Hz) owing to coupling with 2-H. The presence of a *cis*-PdCl₂ unit is proposed on the basis of the values of the ν(Pd–Cl) stretching vibrations (e.g. obtained for **4**: 304 and 289 cm⁻¹) in the far infrared spectrum.¹⁴ These complexes are very stable and easy to handle, which offers a significant advantage over the silver derivatives used for the preparation of the pincer complexes **7–9** (Scheme 3). The coordination of both sulfur atoms provides a spatial pre-organisation, favoring the formation of the pincer complex. Reaction of **4** with a weak base, such as Cs₂CO₃, in the presence of excess KPF₆ in refluxing acetonitrile afforded the desired complex [PdCl(S,C_{NHC},S)]PF₆ (**7**). The pincer complexes **8** and **9** were prepared following the same method (Scheme 3b and c).

The pincer structure of complexes **7–9** was confirmed using their ¹H NMR spectra, which contain broad signals at room temperature for the aliphatic protons of the side chains, which all become chemically and/or magnetically inequivalent owing to the presence of stereogenic sulfur centres, after formation of the S,C_{NHC},S pincer. The pincer bonding mode is also consistent with the broad signal for the 4,5H-imidazolium protons, which reveals a symmetrical structure, maintaining the equivalence of these two protons. Two other structural arrangements corresponding to the same formula could be envisaged for these products. The first one is a chloride bridged-dinuclear structure, in which only one thioether function from each ligand is coordinated to palladium, while the other remains dangling (Scheme 4a). Another conceivable non-pincer structure would be that of a dinuclear complex, in which the ligand acts as a S,C_{NHC} bridge between two PdCl moieties, chelation of the other thioether would complete the Pd(II) coordination sphere (Scheme 4b). In both cases, two chemically inequivalent thioether arms would result but none of these structures are supported by our spectroscopic data.



Scheme 4 Hypothetical (a) chloride-bridged dinuclear and (b) S,C_{NHC} -bridged dinuclear structures for **7**, ruled out by VT NMR studies (see text).

A similar approach to that described in Scheme 3c has been used in only three other cases, to the best of our knowledge. Mono(thioether) imidazolium salts have been first S-coordinated to a Pd(II) centre before deprotonation, resulting in the formation of a dinuclear complex where two PdBr_2 centres were bridged by two S,C_{NHC} ligands in a *trans*, head-to-tail arrangement (Scheme 5).^{8g} However, when this approach was applied to Ni(II)/phosphine-functionalized imidazolium systems, formation of *cis*- P,C_{NHC} Ni(II) chelate complexes was suggested.^{6f} Although not isolated, a phosphine imidazolium Ru(II) complex was suggested to be an intermediate in the synthesis of a *cis*- P , “abnormal carbene” complex.^{6a}



Scheme 5 Synthesis of the dinuclear *trans*-[$\text{PdBr}_2(\mu-\text{S},\text{C}_{\text{NHC}})$]₂ complex reported by Labande *et al.*^{8g}

Variable Temperature ¹H NMR Studies

Variable temperature ¹H NMR studies were performed to identify the different isomers in solution and to confirm that no dinuclear structures are present in our case. Upon cooling a solution of complex **7** from 298 K to 223 K, a splitting of the signals was observed. The broad singlet observed at room temperature for the 4,5H-imidazolium protons was progressively split into two well separated and sharp singlets at 223 K (Fig. 1), confirming that the pincer form is retained in solution. The signals of all the CH₂ protons also sharpen at this

temperature. The presence of a chloride-bridged or C_{NHC},S -bridged dinuclear species (Scheme 4) was ruled out since this should give rise to two doublets for the non-equivalent 4- and 5H-imidazolium protons. We are therefore confident that the only isomers present in solution are mononuclear structures in equilibrium through in-place inversion of the stereogenic sulfur atoms, giving rise to two singlets for the two equivalent 4,5H-imidazolium protons (Scheme 6).¹⁵

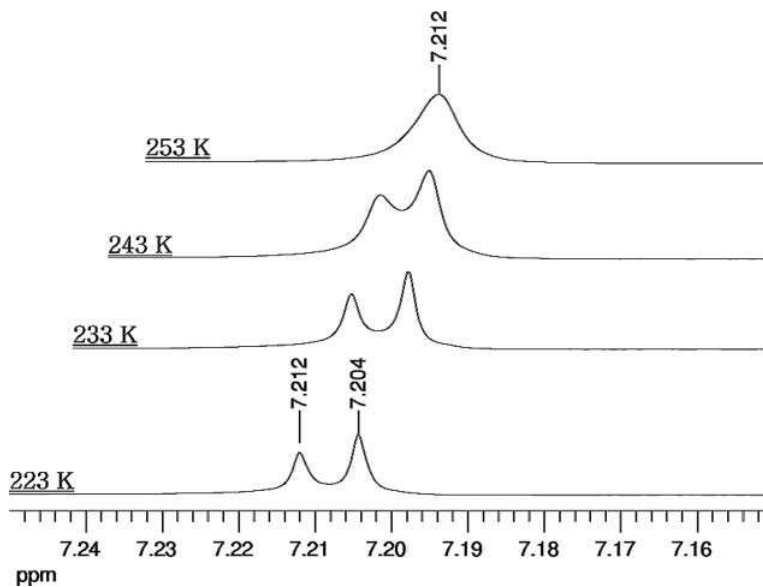
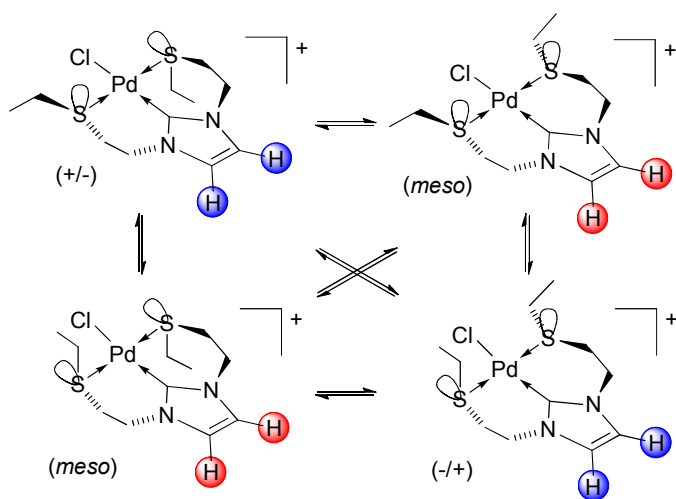
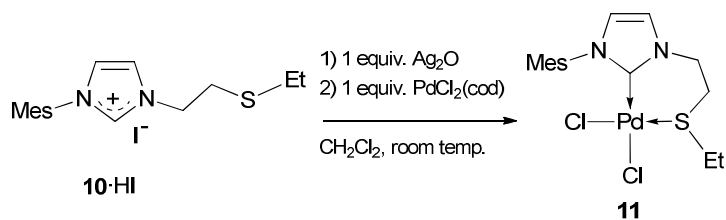


Fig. 1 Variable temperature ^1H NMR spectra in the 4,5H-imidazolium protons region of complex **7**.

For comparison, we also prepared the mono-thioether palladium dichloride complex **11** (Scheme 7) to compare its catalytic properties in Suzuki–Miyaura cross-coupling reactions with those of the bis(thioether) complex **7** (see below). We applied the transmetallation procedure, using the *N*-(2,4,6-trimethylphenyl)-*N'*-ethyl-ethyl-sulfide imidazolium iodide recently described,¹⁶ 1 equiv. Ag_2O in dichloromethane and 1 equiv. of $[\text{PdCl}_2(\text{COD})]$ (Scheme 7). This reaction afforded the S,C_{NHC} complex **11** in good yield. Its chelate structure was suggested by the broad ^1H NMR signals for the aliphatic protons of the thioether function, as always reported after formation upon coordination of stereogenic sulfur centres.⁸ The far-infrared spectrum of this complex contained absorptions for the $\nu(\text{Pd–Cl})$ stretching modes at 319 and 300 cm^{-1} , typical for a *cis*- PdCl_2 unit.¹⁴



Scheme 6 Proposed equilibria for complex **7** in solution with in-place S inversion.



Scheme 7 Synthesis of complex **11**.

The chelate arrangement could finally be unambiguously confirmed from the solid state structure of **11·CH₂Cl₂** determined by single crystal X-ray diffraction analysis (Fig. 2). The structure reveals a distorted square planar coordination geometry around the palladium centre, in which the sulfur and the carbene ligands are in a mutual *cis* arrangement. The stronger *trans* influence of the carbene donor explains the longer $\text{Pd}1-\text{Cl}1$ [2.3645(10) Å] bond compared to $\text{Pd}1-\text{Cl}2$ [2.3066(10) Å]. The angle between the imidazole ring ($\text{C}1-\text{N}1-\text{C}4-\text{C}5-\text{N}2$) and the coordination mean plane ($\text{C}1-\text{Pd}1-\text{S}1-\text{Cl}1-\text{Cl}2$) is 49.04° and not 90°, which would be the most electronically/sterically preferred orientation.

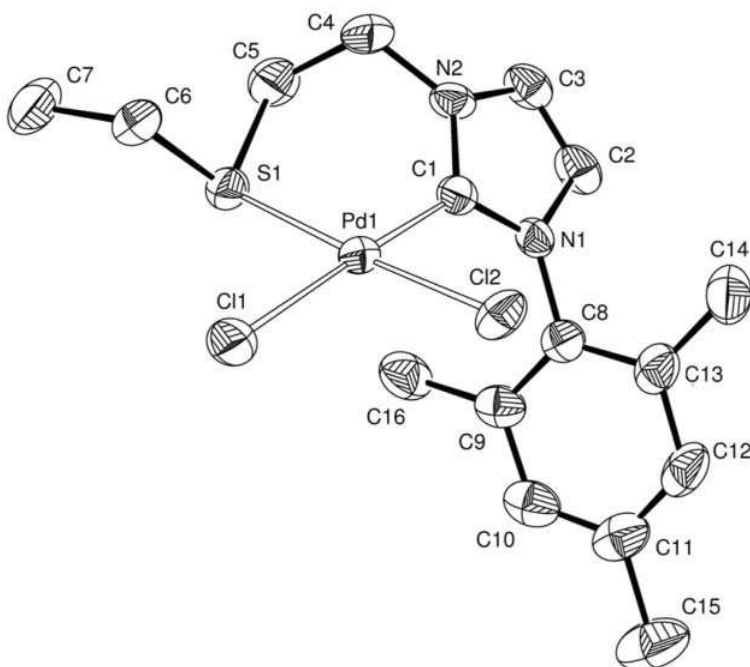


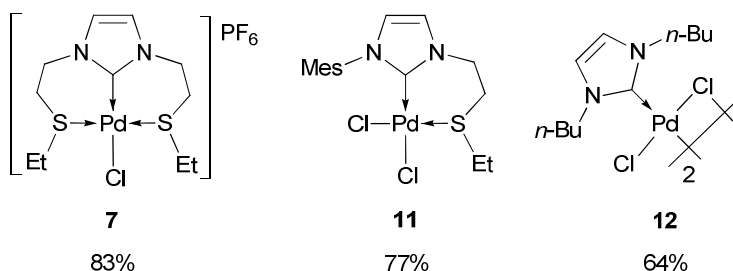
Fig. 2 View of the molecular structure of **11**·CH₂Cl₂. Hydrogen atoms and solvent molecule have been omitted for clarity. Ellipsoids represented at 50% probability level. Selected bond lengths (Å) and angles (°): Pd1–C1 1.976(4); Pd1–S1 2.2823(11); Pd1–Cl2 2.3066(10); Pd1–C11 2.3645(10); C1–Pd1–S1 90.39(11); C1–Pd1–Cl2 89.48(11); N1–C1–N2 106.2(3).

This *cis*-S,C_{NHC} chelate structure observed in all metal complexes involving thioether- or thiophene-functionalized NHCs^{8a–f,8h–l,9} contrasts with the dinuclear structure of the *trans*-dibromo palladium complex obtained by Labande *et al.*^{8g} from *N*-(2,4,6-trimethylphenyl)-*N'*-ethyl-ethyl-sulfide imidazolium bromide (Scheme 5). In view of the structure of complex **11**·CH₂Cl₂, which contains the same ligand, we can conclude that S,C_{NHC} chelation or μ -S,C_{NHC} bridge formation, *i.e.* a *cis* or *trans* arrangement of the donor groups, is not controlled here by the steric properties on the *N*- or *S*-substituents, the only differences between the reactions of Schemes 6 and 7 being the nature of the halides and the reaction/crystallization conditions. We obtained **11** *via* the transmetalation reaction, whereas the dinuclear complex of Scheme 5 was formed by deprotonation of the imidazolium salt.^{8g}

Evaluation of the NHC Complexes in Suzuki–Miyaura Cross-Coupling Reaction

Preliminary catalytic studies were performed in Suzuki–Miyaura cross-coupling reactions of 4-bromotoluene with phenyl boronic acid to evaluate the potential of complex **7**. We compared the conversions to 4-methylbiphenyl obtained with complexes **7**, **11** and **12** (prepared *in situ*)¹⁷ under the same conditions (see experimental section) to identify a potential beneficial effect of one and/or two thioether functions. The results are reported in

Scheme 8. An increase in activity was observed upon introduction of one thioether function from 64% (**12**) to 77% (**11**), but no significant improvement was noticed upon introduction of a second thioether function, 83% (**7**). The conversions are limited by the life-time of the catalyst, as shown by addition of fresh substrates after the reaction was performed for 2 h which did not lead to further conversion.



Scheme 8 NHC–Pd(II) complexes were compared in Suzuki–Miyaura cross-coupling reactions and the corresponding conversions were observed under the conditions detailed in the experimental section.

Conclusion

We have reported an efficient stepwise synthesis of bis(thioether) functionalized imidazolium salts, with the first examples of heterobis(thioether) carbene precursors. We also reported a unique S,C_{NHC},S free carbene and chelated $[\text{PdCl}_2(S,S)]$ complexes containing an imidazolium group well positioned to readily afford S,C_{NHC},S pincer carbene complexes upon deprotonation.

These studies have shown that thioether functions are strong enough donors to displace the COD ligand from the palladium precursor for the preparation of **4–6** and exert favorable anchimeric assistance for the formation of the pincer complexes **7–9**, even in the presence of MeCN.

The synthesis and variable temperature studies performed on complex **7** allow us to conclude that no decoordination of the sulfur atom occurs in solution and that the broad signals observed are due only to in-place inversion of the sulfur centres, giving rise to different stereoisomers in solution. The structural characterization of the *cis*, mononuclear complex **11** provides an interesting contrast with the *trans*, dinuclear structure reported previously for a dibromo complex bearing the same S,C_{NHC} ligand.^{8g}

We plan to use the new pincer complexes **7–9** described here in other catalytic reactions to examine further the influence of two thioether functions on the imidazolium ring.

Acknowledgments

We are grateful to the CNRS, the Ministère de l'Enseignement Supérieur et de la Recherche (Paris), the DFH/UFA (International Research Training Group 532-GRK532 of the Deutsche Forschungsgemeinschaft) and the Erasmus Program for support. A. S. is grateful for the support from the University of Camerino (Italy). We thank Dr Roberto Pattacini for the determination of the crystal structure of **11**·CH₂Cl₂ and Marc Mermillon-Fournier for technical assistance.

Experimental Section

General procedures

All operations were carried out using standard Schlenk techniques under inert atmosphere. Solvents were purified and dried under nitrogen by conventional methods. d₆-DMSO was degassed and stored over 4 Å molecular sieves. CDCl₃ and CD₃CN were dried over 4 Å molecular sieves, degassed by freeze-pump-thaw cycles and stored under argon. NMR spectra were recorded at room temperature on a Bruker AVANCE 300 spectrometer (¹H, 300 MHz; ¹³C{¹H}, 75.47 MHz; and ³¹P{¹H} 121.49 MHz) and referenced using the residual proton solvent (¹H) or solvent (¹³C) resonance or 85% H₃PO₄ for ³¹P{¹H}. Chemical shifts are given in ppm. Assignments are based on ¹H, ¹H-COSY, ¹H, ¹³C-HMQC and ¹H, ¹³C-HMBC experiments. IR spectra were recorded in the region 4000–100 cm⁻¹ on a Nicolet 6700 FT-IR spectrometer (ATRmode, SMART ORBIT accessory, diamond crystal). Elemental analyses were performed by the “Service de microanalyses”, Université de Strasbourg and by the “Service Central d’Analyse”, USR-59/CNRS, Solaize. Electrospray mass spectra (ESI-MS) were recorded on a microTOF (Bruker Daltonics, Bremen, Germany) instrument using nitrogen as a drying agent and nebulising gas and Maldi-TOF analyses were carried out on a Bruker AutiflexII TOF/TOF (Bruker Daltonics, Bremen, Germany), using dithranol (1.8.9 trihydroxyanthracene) as a matrix. Gas chromatographic analyses were performed on a Thermoquest GC8000 Top series gas chromatograph using a HP Pona column (50 m, 0.2 mm diameter, 0.5 µm film thickness). The complex [PdCl₂(COD)]¹⁸ was prepared according to the literature. All other reagents were used as received from commercial suppliers.

Synthesis of *N*-ethyl-(R)-sulfide imidazole

A, R = ethyl. Pure imidazole (5.00 g, 73.44 mmol), sodium *tert*-butoxide (10.59 g, 96.10 mmol) and toluene (100 ml) were placed in a Schlenk tube equipped with a magnetic stirrer. After 2-chloroethyl ethylsulfide (8.55 ml, 9.15 g, 73.44 mmol) was added to the suspension, the mixture was refluxed for 12 h. During heating, the colourless mixture turned light brown. After cooling, the mixture was filtered and the precipitate washed with dry toluene (2 x 20 ml). The volatiles were evaporated under reduced pressure and the brown oil was washed with dry diethyl ether (2 x 40 ml) and dried in vacuo. The product was purified by column chromatography (100% EtOAc). Yield: 25%. Anal. Calc. for C₇H₁₂N₂S (156.25): C, 53.81; H, 7.74; N, 17.93. Found: C, 53.69; H, 7.486; N, 17.34. FTIR: ν_{max} (oil) cm⁻¹: 3106br, 3033br, 2965br, 2925br, 2869br, 2690br, 2606br, 2361w, 2343w, 2324w, 1675w, 1650w, 1589w, 1505 s, 1447 m, 1393w, 1375w, 1357w, 1324w, 1287 m, 1263 m, 1228 s, 1155w, 1107 m,

1077 s, 1063 m, 1033 m, 971w, 926sh, 906 m, 871w, 817 m, 739 s, 698 m, 663 vs. ^1H NMR (CDCl_3 , 300 MHz) δ : 1.23 (3H, t, $^3J = 7.5$ Hz, SCH_2CH_3), 2.44 (2H, q, $^3J = 7.5$ Hz, SCH_2CH_3), 2.86 (2H, t, $^3J = 7.2$ Hz, $\text{NCH}_2\text{CH}_2\text{S}$), 4.14 (2H, t, $^3J = 7.2$ Hz, NCH_2CH_2), 6.97 (1H, br s, $\text{CH}=\text{CH}$), 7.08 (1H, br s, $\text{CH}=\text{CH}$), 7.56 (1H, br s, NCHN). $^{13}\text{C}\{\text{H}\}$ NMR (CDCl_3 , 75.5 MHz) δ : 14.72 (SCH_2CH_3), 26.34 (SCH_2CH_3), 32.84 ($\text{NCH}_2\text{CH}_2\text{S}$), 47.26 ($\text{NCH}_2\text{CH}_2\text{S}$), 118.86 (HCNCH_2), 129.58 (C=NCH), 137.14 (NCN). MS (ESI): m/z 157.1 [M+H] $^+$.

B, R = methyl. The same procedure was used with imidazole (3.08 g, 45.21 mmol), sodium *tert*-butoxide (6.59 g, 58.77 mmol) and 2-chloroethyl methylsulfide (4.50 ml, 5.00 g, 45.21 mmol). Yield: 36%. Anal. Calc. for $\text{C}_6\text{H}_{10}\text{N}_2\text{S}$ (142.22): C, 50.67; H, 7.09; N, 19.70. Found: C, 50.02; H, 7.274; N, 19.51. FTIR: $\nu_{\text{max}}(\text{oil}) \text{ cm}^{-1}$: 3108br, 2916br, 2835br, 2361w, 2343w, 1650w, 1506 s, 1441 m, 1357w, 1324w, 1288 m, 1228 s, 1158w, 1107 m, 1078 s, 1064 m, 1033w, 961w, 915 m, 907 m, 819 m, 741 s, 683 m, 662 vs. ^1H NMR (CDCl_3 , 300 MHz) δ : 1.88 (3H, s, SCH_3), 2.69 (2H, t, $^3J = 6.6$ Hz, $\text{NCH}_2\text{CH}_2\text{S}$), 4.01 (2H, t, $^3J = 6.9$ Hz, NCH_2CH_2), 6.85 (1H, br s, $\text{CH}=\text{CH}$), 6.92 (1H, br s, $\text{CH}=\text{CH}$), 7.41 (1H, br s, NCHN). $^{13}\text{C}\{\text{H}\}$ NMR (CDCl_3 , 75.5 MHz) δ : 15.66 (SCH_3), 35.24 ($\text{NCH}_2\text{CH}_2\text{S}$), 46.75 ($\text{NCH}_2\text{CH}_2\text{S}$), 118.91 (HCNCH_2), 129.39 (C=NCH), 137.12 (NCN). MS (ESI): m/z 143.1 [M+H] $^+$.

Synthesis of *N*-ethyl-(R)-sulfide-*N'*-ethyl-(R')-sulfide imidazolium chloride:

These compounds are known to be very hygroscopic and the elemental analyses performed always afforded carbon and nitrogen percentages lower than the calculated values.

1·HCl: R= R' = ethyl [*N,N'*-bis(ethyl-ethyl-sulfide) imidazolium chloride]. **A** (1.10 g, 7.04 mmol) was placed in a Schlenk tube equipped with a magnetic stirrer and then 2-chloroethyl ethylsulfide (0.820 ml, 0.877 g, 7.04 mmol) was added. The mixture was heated for 2 h at 120 °C and then allowed to cool to room temperature. The pale yellow oil obtained was washed with dry THF (2 x 40 ml) and dried in vacuo. Yield: 93%. Anal. Calc. for $\text{C}_{11}\text{H}_{21}\text{ClN}_2\text{S}_2$ (280.88): C, 47.04; H, 7.54; N, 9.97. Found: C, 45.34; H, 6.970; N, 8.161. FTIR: $\nu_{\text{max}}(\text{oil}) \text{ cm}^{-1}$: 3364br, 3130sh, 3043br, 2962 s, 2925 s, 2868 m, 1561 s, 1448 s, 1415 m, 1375w, 1354w, 1332w, 1264 m, 1155vs, 1105w, 1062w, 1026w, 971w, 835 m, 757 s, 690m. ^1H NMR (CDCl_3 , 300 MHz) δ : 1.21 (6H, t, $^3J = 7.4$ Hz, SCH_2CH_3), 2.58 (4H, q, $^3J = 7.4$ Hz, SCH_2CH_3), 3.04 (4H, t, $^3J = 6.3$ Hz, $\text{NCH}_2\text{CH}_2\text{S}$), 4.57 (4H, t, $^3J = 6.4$ Hz, NCH_2CH_2), 7.58 (2H, d, $^4J = 1.6$ Hz, $\text{CH}=\text{CH}$), 10.68 (1H, s, NCHN). $^{13}\text{C}\{\text{H}\}$ NMR (CDCl_3 , 75.5 MHz) δ : 14.71 (SCH_2CH_3), 26.14 (SCH_2CH_3), 31.92 ($\text{NCH}_2\text{CH}_2\text{S}$), 49.36 ($\text{NCH}_2\text{CH}_2\text{S}$), 122.24, ($\text{CH}=\text{CH}$), 138.27 (NCN). MS (ESI): m/z 245.1 [M-Cl] $^+$.

2·HCl: R = methyl; R' = ethyl. The same procedure was used with **B** (0.810 g, 5.70 mmol) and 2-chloroethyl ethylsulfide (0.663 ml, 0.710 g, 5.70 mmol). Yield: 95%. Anal. Calc. for C₁₀H₁₉ClN₂S₂ (266.85): C, 45.01; H, 7.18; N, 10.50. Found: C, 43.42; H, 6.685; N, 8.868. FTIR: $\nu_{\text{max}}(\text{oil})/\text{cm}^{-1}$: 3375br, 3132w, 3052br, 2962 m, 2918 m, 2868w, 2720br, 1630w, 1561 m, 1449 m, 1375w, 1355w, 1331w, 1261 m, 1215sh, 1154vs, 1086vs, 1062 s, 1028 s, 970sh, 862m, 797s, 760m, 729s, 697m. ¹H NMR (CDCl₃, 300 MHz) δ : 1.21 (3H, t, ³J = 7.2 Hz, SCH₂CH₃), 2.05 (3H, s, NCH₃), 2.47 (2H, q, ³J = 7.5 Hz, SCH₂CH₃), 2.94 (4H, t, ³J = 6.6 Hz, NCH₂CH₂S), 4.48 (4H, m, NCH₂CH₂), 7.66 (1H, pseudo t, ³J = ⁴J = 1.5 Hz, CH=CH), 7.72 (1H, pseudo t, ³J = ⁴J = 1.5 Hz, CH=CH), 10.40 (1H, br s, NCHN). ¹³C{¹H} NMR (CDCl₃, 75.5 MHz) δ : 14.68 (SCH₂CH₃), 15.46 (SCH₃), 25.97 (SCH₂CH₃), 31.77 (NCH₂CH₂SEt), 34.22 (NCH₂CH₂SMe), 48.51 and 49.18 (2 NCH₂CH₂S), 122.50 and 122.55 (CH=CH), 137.72 (NCN). MS (ESI): *m/z* 231.1 [M-Cl]⁺.

3·HCl: R = methyl; R' = phenyl. The same procedure was used with **B** (0.760 g, 5.34 mmol) and 2-chloroethyl phenylsulfide (0.789 ml, 0.923 g, 5.34 mmol). Yield: 88%. Anal. Calc. For C₁₄H₁₉ClN₂S₂ (314.90): C, 53.40; H, 6.08; N, 8.90. Found: C, 53.11; H, 6.243; N, 8.241. FTIR: $\nu_{\text{max}}(\text{oil})/\text{cm}^{-1}$: 3370br, 3132sh, 3051br, 2980br, 2916 m, 2832w, 2722br, 2603br, 1629w, 1561 s, 1508w, 1480 m, 1438 s, 1354w, 1331w, 1289w, 1274w, 1229w, 1155 s, 1106sh, 1087 m, 1024 m, 963w, 865w, 744vs, 693vs. ¹H NMR (CDCl₃, 300 MHz) δ : 2.14 (3H, s, NCH₃), 2.96 (2H, t, ³J = 6.6 Hz, NCH₂CH₂S), 3.49 (2H, t, ³J = 6.3 Hz, NCH₂CH₂S), 4.52 (4H, m, NCH₂CH₂), 7.19–7.36 (5H, m, H arom), 7.48 (1H, pseudo t, ³J = ⁴J = 1.8 Hz, CH=CH), 7.59 (1H, pseudo t, ³J = ⁴J = 1.8 Hz, CH=CH), 10.50 (1H, br s, NCHN). ¹³C{¹H} NMR (CDCl₃, 75.5 MHz) δ : 15.55 (SCH₃), 34.25 and 34.37 (2 NCH₂CH₂S), 48.67 and 49.17 (2 NCH₂CH₂S), 122.26 and 122.64 (CH=CH), 127.38 (*C_{para}*), 129.48 (*C_{meta}*), 130.40 (*C_{ortho}*), 133.30 (*C_{ipso}*), 137.94 (NCN). MS (ESI): *m/z* 279.1 [M-Cl]⁺.

Synthesis of *N,N'*-bis(ethyl-ethyl-sulfide)imidazol-2-ylidene: 1

In the glovebox, solid potassium bis(trimethylsilyl)amide (KHMDS) (0.071 g, 0.36 mmol) was added to a suspension of **1·HCl** (0.100 g, 0.36 mmol) in dry d₈-THF at room temperature. The suspension was stirred at room temperature for 2 h, until **1·HCl** was totally dissolved, and then filtered through a Celite pad. The remaining light orange solution was analysed by multinuclear NMR spectroscopy. ¹H NMR (d₈-THF, 300 MHz) δ : 1.24 (6H, t, ³J = 7.5 Hz, SCH₂CH₃), 2.54 (4H, q, ³J = 7.5 Hz, SCH₂CH₃), 2.91 (4H, t, ³J = 7.5 Hz, NCH₂CH₂), 4.13 (4H, t, ³J = 7.5 Hz, NCH₂CH₂), 6.96 (2H, s, CH=CH).

$^{13}\text{C}\{\text{H}\}$ NMR ($\text{d}_8\text{-THF}$, 75.5 MHz) δ : 14.31 (SCH_2CH_3), 25.45 (SCH_2CH_3), 32.76 (NCH_2CH_2), 50.87 (NCH_2CH_2), 118.62 ($\text{CH}=\text{CH}$), 195.87 (NCN).

Synthesis of *N,N'*-bis(ethyl-ethyl-sulfide)imidazol-2-thione: **1·S**

1·HCl (0.100 g, 0.36 mmol) and sulfur (0.091 g, 0.36 mmol) were placed in a Schlenk tube and dry THF was added. The suspension was stirred at room temperature and then solid potassium bis(trimethylsilyl)amide (KHMDS) (0.071 g, 0.36 mmol) was added under nitrogen. The reaction mixture was stirred for 2 h and then filtered through a Celite pad. The volatiles were removed under reduced pressure and the residue washed with pentane (2 x 25ml). **1·S** was obtained as an orange solid. Yield: 78%. Anal. Calc. for $\text{C}_{11}\text{H}_{20}\text{N}_2\text{S}_3$ (276.48): C, 47.78; H, 7.29; N, 10.13. Found: C, 47.57; H, 7.201; N, 10.24. FTIR: ν_{max} (solid) cm^{-1} 3372s, 3139m, 2967m, 2927m, 2870w, 1630m, 1562s, 1451m, 1415w, 1375w, 1354w, 1333w, 1264m, 1176m (tentatively assigned to the $\text{C}=\text{S}$ stretching vibration), 1153s, 1107w, 1061w, 971w, 869w, 752s. ^1H NMR (CDCl_3 , 300 MHz) δ : 1.24 (6H, t, $^3J = 7.4$ Hz, SCH_2CH_3), 2.54 (4H, q, $^3J = 7.4$ Hz, SCH_2CH_3), 2.90 (4H, t, $^3J = 7.1$ Hz, NCH_2CH_2), 4.19 (4H, t, $^3J = 6.7$ Hz, NCH_2CH_2), 6.74 (2H, s, $\text{CH}=\text{CH}$). $^{13}\text{C}\{\text{H}\}$ NMR (CDCl_3 , 75.5 MHz) δ : 14.82 (SCH_2CH_3), 26.19 (SCH_2CH_3), 29.94 (NCH_2CH_2), 47.23 (NCH_2CH_2), 117.26 ($\text{CH}=\text{CH}$), 161.75 (NCN). MS (ESI): m/z 277.1 [$\text{M}+\text{H}]^+$.

Synthesis of the silver(I) carbene complexes:

1·AgCl: R = R' = ethyl.

The imidazolium **1·HCl** (0.100 g, 0.356 mmol) was dissolved in dry CH_2Cl_2 and solid Ag_2O (0.083 g, 0.356 mmol) was added under nitrogen. The reaction mixture was stirred overnight in the dark at room temperature. Then the suspension was filtered through a Celite pad and the solvent was evaporated under reduced pressure to give a light sensitive white solid. Yield: 0.116 g, 84%. Anal. Calc. for $\text{C}_{11}\text{H}_{20}\text{AgClN}_2\text{S}_2$ (387.74): C, 34.07; H, 5.20; N, 7.22. Found: C, 34.19; H, 5.013; N, 6.904. ^1H NMR (CDCl_3 , 300 MHz) δ : 1.23 (6H, t, $^3J = 7.4$ Hz, SCH_2CH_3), 2.52 (4H, q, $^3J = 7.4$ Hz, SCH_2CH_3), 2.91 (4H, t, $^3J = 6.5$ Hz, $\text{NCH}_2\text{CH}_2\text{S}$), 4.28 (4H, t, $^3J = 6.6$ Hz, $\text{NCH}_2\text{CH}_2\text{S}$), 7.08 (2H, s, $\text{CH}=\text{CH}$). $^{13}\text{C}\{\text{H}\}$ NMR (CDCl_3 , 75.5MHz) δ : 14.70 (SCH_2CH_3), 26.49 (SCH_2CH_3), 33.16 ($\text{NCH}_2\text{CH}_2\text{S}$), 51.68 ($\text{NCH}_2\text{CH}_2\text{S}$), 121.46 ($\text{CH}=\text{CH}$), 179.80 (NCN). MS (ESI): m/z 353.0 [$\text{M}-\text{Cl}]^+$.

2·AgCl: R = methyl; R' = ethyl.

The same procedure was used with **2·HCl** (0.042 g, 0.157 mmol) and Ag_2O (0.036 g, 0.157 mmol). Yield: 88%. Anal. Calc. For $\text{C}_{10}\text{H}_{18}\text{AgClN}_2\text{S}_2$ (373.71): C, 32.14; H, 4.85; N, 7.50.

Found: C, 31.88; H, 4.799; N, 7.316. ^1H NMR (CDCl_3 , 300 MHz) δ : 1.21 (3H, t, $^3J = 7.5$ Hz, CH_2CH_3), 2.08 (3H, s, SCH_3), 2.50 (2H, q, $^3J = 7.5$ Hz, SCH_2CH_3), 2.89 (4H, m, 2 $\text{NCH}_2\text{CH}_2\text{S}$), 4.28 (4H, m, 2 NCH_2CH_2), 7.09 (2H, s, 2 $\text{CH}=\text{CH}$). $^{13}\text{C}\{\text{H}\}$ NMR (CDCl_3 , 75.5 MHz) δ : 14.74 (CH_2CH_3), 16.01 (SCH_3), 26.52 (CH_2CH_3), 33.18 (SCH_2CH_2), 35.72 (SCH_2CH_2), 51.14 ($\text{NCH}_2\text{CH}_2\text{SEt}$), 51.69 ($\text{NCH}_2\text{CH}_2\text{SMe}$), 121.47 and 121.58 ($\text{CH}=\text{CH}$), 179.90 (NCN). MS (ESI): m/z 339.0 [M-Cl] $^+$.

3·AgCl: R = methyl; R' = phenyl.

The same procedure was used with **3·HCl** (0.036 g, 0.114 mmol) and Ag_2O (0.027 g, 0.114 mmol). Yield: 79%. Anal. Calc. For $\text{C}_{14}\text{H}_{18}\text{AgClN}_2\text{S}_2$ (421.76): C, 39.87; H, 4.30; N, 6.64. Found: C, 40.11; H, 4.306; N, 6.891. ^1H NMR (CDCl_3 , 300 MHz) δ : 2.09 (3H, s, SCH_3), 2.84 (2H, t, $^3J = 6.6$ Hz, $\text{NCH}_2\text{CH}_2\text{S}$), 3.32 (2H, t, $^3J = 6.6$ Hz, $\text{NCH}_2\text{CH}_2\text{S}$), 4.27 (4H, m, 2 NCH_2CH_2), 7.01 and 7.02 (2H, AB spin system, $^3J = 1.8$ Hz, $\text{CH}=\text{CH}$), 7.32 (5H, m, H arom). $^{13}\text{C}\{\text{H}\}$ NMR (CDCl_3 , 75.5 MHz) δ : 16.01 (SCH_3), 35.41 ($\text{NCH}_2\text{CH}_2\text{S}$), 35.66 ($\text{NCH}_2\text{CH}_2\text{S}$), 51.17 (2 NCH_2CH_2), 121.30 and 121.77 ($\text{CH}=\text{CH}$), 127.09 (C_{para}), 129.45 (C_{meta}), 129.96 (C_{ortho}), 137.24 (C_{ipso}), 179.91 (NCN). MS (ESI): m/z 387.0 [M-Cl] $^+$.

Synthesis of complexes 4–6.

No $^{13}\text{C}\{\text{H}\}$ NMR spectra could be recorded because of the low solubility of these compounds.

1·HCl (0.050 g, 0.178 mmol) was dissolved in dry CH_2Cl_2 and solid $[\text{PdCl}_2(\text{COD})]$ (0.050 g, 0.178 mmol) was added under inert atmosphere. The reaction mixture was stirred for 4 h until formation of a yellow precipitate was observed. The volatiles were removed *via* cannula and the solid washed with pentane (3 x 25 ml) and dried in vacuo. Complex **4** was isolated as an orange solid, it is poorly soluble in organic solvents. Yield: 76%. Anal. Calc. for $\text{C}_{11}\text{H}_{21}\text{Cl}_3\text{N}_2\text{PdS}_2$ (458.21): C, 28.83; H, 4.62; N, 6.11. Found: C, 28.58; H, 4.607; N, 5.994. FTIR: $\nu_{\text{max}}(\text{solid})/\text{cm}^{-1}$: 3131sh, 3095m, 3046m, 2966m, 2926m, 2869sh, 1616w, 1558s, 1446m, 1411m, 1375w, 1357w, 1334w, 1265m, 1154s, 1103w, 1063w, 1044w, 1018sh, 972w, 881w, 829br, 727vs, 698s, 304vs ($\nu_{\text{Pd-Cl}}$), 289s ($\nu_{\text{Pd-Cl}}$). ^1H NMR ($d_6\text{-DMSO}$, 300 MHz) δ : 1.17 (6H, t, $^3J = 7.2$ Hz, SCH_2CH_3), 2.54 (4H, q, $^3J = 7.5$ Hz, SCH_2CH_3), 2.98 (4H, t, $^3J = 6.6$ Hz, $\text{NCH}_2\text{CH}_2\text{S}$), 4.38 (4H, t, $^3J = 6.6$ Hz, NCH_2CH_2), 7.82 (2H, d, $^4J = 1.5$ Hz, $\text{CH}=\text{CH}$), 9.24 (1H, s, NCHN). MS (ESI): m/z 423.0 [M-Cl] $^+$.

The same procedure was followed for the formation of complex **5** with **2·HCl** (0.100 g, 0.375 mmol) and $[\text{PdCl}_2(\text{COD})]$ (0.107 g, 0.375 mmol) and afforded complex **5** as an orange

solid. Yield: 81%. Anal. Calc. for $C_{10}H_{19}Cl_3N_2PdS_2$ (444.18): C, 27.04; H, 4.31; N, 6.31. Found: C, 26.71; H, 4.024; N, 6.607. FTIR: $\nu_{\text{max}}(\text{solid})/\text{cm}^{-1}$: 305vs ($\nu_{\text{Pd}-\text{Cl}}$), 287s ($\nu_{\text{Pd}-\text{Cl}}$). ^1H NMR (d_6 -DMSO, 300 MHz) δ : 1.17 (3H, t, $^3J = 7.3$ Hz, SCH_2CH_3), 2.08 (3H, s, SCH_3), 2.51 (overlapped with solvent peak, SCH_2CH_3), 2.97 (4H, br m, 2 $\text{NCH}_2\text{CH}_2\text{S}$), 4.40 (4H, q, $^3J = 6.5$ Hz, 2 NCH_2CH_2), 7.82 (2H, br s, $\text{CH}=\text{CH}$), 9.26 (1H, s, NCHN). MS (ESI): m/z 408.9 [M-Cl]⁺.

The same procedure was followed for the formation of complex **6** with **3**·HCl (0.100 g, 0.318 mmol) and [PdCl₂(COD)] (0.091 g, 0.318 mmol) and afforded complex **6** as an orange solid. Yield: 84%. Anal. Calc. for $C_{14}H_{19}Cl_3N_2PdS_2$ (492.22): C, 34.16; H, 3.89; N, 5.69. Found: C, 33.86; H, 4.019; N, 5.771. FTIR: $\nu_{\text{max}}(\text{solid}) \text{ cm}^{-1}$: 306vs ($\nu_{\text{Pd}-\text{Cl}}$), 291s ($\nu_{\text{Pd}-\text{Cl}}$). ^1H NMR (d_6 -DMSO, 300 MHz) δ : 2.09 (3H, s, SCH_3), 2.93 (2H, t, $^3J = 6.6$ Hz, $\text{NCH}_2\text{CH}_2\text{SCH}_3$), 3.50 (2H, t, $^3J = 6.4$ Hz, $\text{NCH}_2\text{CH}_2\text{SPh}$), 4.33–4.43 (4H, m, 2 NCH_2CH_2), 7.25–7.40 (5H, m, Ph), 7.77 (1H, br s, $\text{CH}=\text{CH}$), 7.80 (1H, br s, $\text{CH}=\text{CH}$), 9.23 (1H, s, NCHN). MS (ESI): m/z 456.9 [M-Cl]⁺.

Synthesis of complex **7**.

Method A: Transmetallation reaction. **1**·HCl (0.140 g, 0.498 mmol) was dissolved in dry CH₂Cl₂ and solid Ag₂O (0.116 g, 0.498 mmol) was added under nitrogen. The reaction mixture was stirred for 2 h in the dark at room temperature. Then the suspension was filtered through a Celite pad under nitrogen and the resulting clear solution was slowly added to a suspension of [PdCl₂(COD)] (0.139 g, 0.498 mmol) in CH₂Cl₂. A white solid precipitated rapidly. The suspension was then filtered through Celite and the solvent was evaporated under reduced pressure. The resulting orange solid was then washed with pentane (2 x 25 mL). Yield: 61%.

Method B: Deprotonation of complex **4.** Solid Cs₂CO₃ (0.255 g, 0.783 mmol) was added to a suspension of complex **4** (0.326 g, 0.712 mmol) and KPF₆ (0.655 g, 3.56 mmol) in acetonitrile and the reaction mixture was refluxed for 6 h. During the heating, the colourless liquid phase became orange. The suspension was then filtered through Celite and the solvent was evaporated under reduced pressure. The resulting orange solid was then washed with pentane (2 x 25 mL). Yield: 79%. Anal. Calc. For $C_{11}H_{20}\text{ClF}_6\text{N}_2\text{PPdS}_2$ (531.94): C, 24.87; H, 3.79; N, 5.27. Found: C, 24.63; H, 3.826; N, 5.066. FTIR: $\nu_{\text{max}}(\text{solid})/\text{cm}^{-1}$: 2970br, 2934w, 1566m, 1474s, 1440s, 1415s, 1380m, 1341m, 1333m, 1265m, 1256m, 1195w, 1160m, 1115w, 1069m, 1057m, 971w, 952w, 818vs, 754sh, 747sh, 670s.

¹H NMR (CD₃CN, 300 MHz) δ: 1.45 (6H, t, ³J = 7.5 Hz, SCH₂CH₃), 2.89 (4H, br, SCH₂CH₃), 3.04 (4H, br, NCH₂CH₂S), 4.57 (4H, br, NCH₂CH₂), 7.23 (2H, s, CH=CH). ¹³C{¹H} NMR (CD₃CN, 75.5 MHz) δ: 13.77 (SCH₂CH₃), 28.97 (SCH₂CH₃), 32.48 (NCH₂CH₂S), 49.31 (NCH₂CH₂S), 123.08 (CH=CH), 148.94 (NCN). ³¹P{¹H} NMR (CD₂Cl₂, 121.5 MHz) δ: -143.4 (sept., ¹J_{P,F} = 707 Hz, PF₆). MS (ESI): *m/z* 387.0 [M-PF₆]⁺.

Low temperature ¹H NMR spectrum: ¹H NMR (CD₃CN, 223 K, 400 MHz) δ: 1.36 (3.3H, t, ³J = 7.6 Hz, SCH₂CH₃, isomer A), 1.40 (2.7H, t, ³J = 7.2 Hz, SCH₂CH₃, isomer B), 2.66 (1H, br m, SCHHCH₃, isomer A), 2.76 (1H, br m, SCHHCH₃, isomer A), 2.94 (2H, br m, SCHHCH₃, and SCHHCH₃, isomer B), 3.06–3.25 (2.3H, br m, NCH₂CH₂S, isomer A), 3.33–3.42 (1.7H, br m, NCH₂CH₂S, isomer B), 4.24 (2.2H, br m, NCHHCH₂S and NCHHCH₂S, isomer A), 4.41 (0.8H, br m, NCHHCH₂S, isomer B), 4.48 (1.0H, br m, NCHHCH₂S, isomer B), 7.20 (1.1H, s, CH=CH, isomer A) 7.21 (0.9H, s, CH=CH, isomer B).

Synthesis of complexes **8** and **9** via Method B

The same procedure was used with Cs₂CO₃ (0.122 g, 0.375 mmol), complex **5** (0.166 g, 0.375 mmol) and KPF₆ (0.345 g, 1.87 mmol) and afforded complex **8** as a yellow solid. Yield: 68%. Anal. Calc. for C₁₀H₁₈ClF₆N₂PPdS₂ (517.23): C, 23.22; H, 3.51; N, 5.42. Found: C, 22.82; H, 3.681; N, 5.406. FTIR: $\nu_{\text{max}}(\text{solid})/\text{cm}^{-1}$: 3143w, 2924w, 1563m, 1441m, 1413m, 1157m, 1107w, 1025m, 814vs, 693sh. ¹H NMR (CD₃CN, 300 MHz) δ: 1.35 (3H, t, ³J = 7.4 Hz, SCH₂CH₃), 2.33 (3H, s, SCH₃), 2.76 (4H, br, SCH₂CH₃), 3.25 (4H, br, 2 NCH₂CH₂S), 4.61 (4H, br, 2 NCH₂CH₂), 7.50 (2H, br s, CH=CH). ³¹P{¹H} NMR (CD₂Cl₂, 121.5 MHz) δ: -143.4 (sept., ¹J_{P,F} = 707 Hz, PF₆). MS (ESI): *m/z* 373.0 [M-PF₆]⁺.

The same procedure was used with Cs₂CO₃ (0.103 g, 0.318 mmol), complex **6** (0.156 g, 0.318 mmol) and KPF₆ (0.292 g, 1.59 mmol) and afforded complex **9** as a yellow solid. Yield: 74%. Anal. Calc. for C₁₄H₁₈ClF₆N₂PPdS₂ (565.27): C, 29.75; H, 3.21; N, 4.96. Found: C, 29.47; H, 3.009; N, 5.243. FTIR: $\nu_{\text{max}}(\text{solid})/\text{cm}^{-1}$: 1564w, 1448w, 1413m, 1292w, 1157w, 1034w, 817vs. ¹H NMR (CD₃CN, 300 MHz) δ: 2.33 (3H, s, SCH₃), 3.28 (2H, br, NCH₂CH₂SCH₃), 3.41 (2H, br, NCH₂CH₂SPh), 4.35 (2H, br, NCH₂CH₂), 4.58 (2H, br, NCH₂CH₂), 7.28–7.56 (7H, m, Ph and CH=CH). ¹³C{¹H} NMR (CD₃CN, 75.5 MHz) δ: 19.38 (SCH₃), 33.14 and 36.93 (2 NCH₂CH₂S), 46.81 and 49.08 (2 NCH₂CH₂S), 122.78 and 123.03 (CH=CH), 127.14 (*C_{para}*), 129.46 (*C_{meta}*), 129.96 (*C_{ortho}*), 136.44 (*C_{ipso}*), (NCN) not observed. ³¹P{¹H} NMR (CD₂Cl₂, 121.5 MHz) δ: -143.4 (sept., ¹J_{P,F} = 707 Hz, PF₆). MS (ESI): *m/z* 421.0 [M-PF₆]⁺.

Synthesis of complex 11

Following Method A: Transmetallation reaction, with imidazolium **10**·HI (0.120 g, 0.298 mmol), Ag₂O (0.069 g, 0.298 mmol) and [PdCl₂(COD)] (0.085 g, 0.298 mmol) afforded complex **11** as an orange powder. Yield: 87%. Anal. Calc. for C₁₆H₂₂Cl₂N₂PdS (451.75): C, 42.54; H, 4.91; N, 6.20. Found: C, 42.84; H, 4.87; N, 6.07. FTIR: $\nu_{\text{max}}(\text{solid})/\text{cm}^{-1}$: 3113w, 3087w, 2966m, 2919m, 2858m, 1609w, 1564w, 1485m, 1449m, 1404s, 1375m, 1347m, 1300m, 1262m, 1238m, 1203m, 1156m, 1110w, 1088w, 1034m, 969m, 935w, 883w, 852m, 731vs, 694vs, 319s ($\nu_{\text{Pd-Cl}}$), 300s ($\nu_{\text{Pd-Cl}}$). ¹H NMR (CDCl₃, 300 MHz) δ : 1.50 (3H, t, ³J = 7.2Hz, SCH₂CH₃), 2.18 (6H, s, 2 CH₃ *ortho*-Mes), 2.31 (3H, s, CH₃ *para*-Mes), 2.78 (2H, br, SCH₂CH₃), 3.28 (2H, br, NCH₂CH₂), 4.67 (2H, br, NCH₂CH₂), 6.80 (1H, br s, CH=CH), 6.95 (2H, s, CH *meta*-Mes), 7.38 (1H, br s, CH=CH). MS (ESI): *m/z* 417.0 [M-Cl]⁺.

Procedure for the Suzuki–Miyaura cross-coupling reaction

Complex **7** (10.63 mg, 0.02 mmol), phenyl boronic acid (146.3 mg, 1.20 mmol) and Cs₂CO₃ (651.6 mg, 2.00 mmol) were placed in a Schlenk tube and dioxane (3 ml) was added under nitrogen. Then 4-bromotoluene (123.1 μ l, 171.0 mg, 1.00 mmol) was added and the reaction mixture was heated for 2 h at 100 °C. The reaction was then quenched by rapid cooling down to room temperature and the suspension was filtered through a Celite pad. The resulting solution was then analysed by gas chromatography and showed 83% conversion in 4-methylbiphenyl.

The same procedure was used with complexes **11** (9.04 mg, 0.02 mmol) and **12** (7.15 mg, 0.02 mmol), showing 77% and 64% conversion, respectively.

X-Ray data collection, structure solution and refinement

Suitable crystals for the X-ray analysis of **11**·CH₂Cl₂ were obtained by slow diffusion of pentane into a saturated dichloromethane solution of complex **11**. The intensity data were collected on a Kappa CCD diffractometer¹⁹ (graphite monochromated Mo-K α radiation, $\lambda = 0.71073 \text{ \AA}$) at 173(2) K. Crystallographic and experimental details for the structures are summarized in Table 1. The structures were solved by direct methods (SHELXS-97) and refined by full-matrix least-squares procedures (based on F^2 , SHELXL-97)²⁰ with anisotropic thermal parameters for all the non-hydrogen atoms. The hydrogen atoms were introduced into the geometrically calculated positions (SHELXS-97 procedures) and refined riding on the corresponding parent atoms. A MULTISCAN correction was applied.²¹ CCDC 781531.†

Table 1 Crystallographic data for complex **11**·CH₂Cl₂

Compound reference	11 ·CH ₂ Cl ₂
Chemical formula	C ₁₆ H ₂₂ Cl ₂ N ₂ PdS·CH ₂ Cl ₂
Formula Mass	536.64
Crystal system	Monoclinic
<i>a</i> /Å	12.778(1)
<i>b</i> /Å	11.845(1)
<i>c</i> /Å	14.879(2)
$\beta/^\circ$	103.886(4)
Unit cell volume/Å ³	2186.0(3)
Temperature/K	173(2)
Space group	<i>P</i> 2 ₁ / <i>c</i>
<i>Z</i>	4
Absorption coefficient, μ/mm^{-1}	1.437
No. of reflections measured	12428
No. of independent reflections	5857
R_{int}	0.0413
R_I values ($I > 2\sigma(I)$)	0.0490
$wR(F^2)$ values ($I > 2\sigma(I)$)	0.1138
R_I values (all data)	0.0964
$wR(F^2)$ values (all data)	0.1348
S on F^2	1.045

References

- (1) H. Jacobsen, A. Correa, A. Poater, C. Costabile and L. Cavallo, *Coord. Chem. Rev.*, 2009, **253**, 687.
- (2) (a) P. de Frémont, N. Marion and S. P. Nolan, *Coord. Chem. Rev.*, 2009, **253**, 862; (b) F. E. Hahn and M. C. Jahnke, *Angew. Chem. Int. Ed.*, 2008, **47**, 3122; (c) F. E. Hahn, *Angew. Chem., Int. Ed.*, 2006, **45**, 1348; (d) N.M. Scott and S. P. Nolan, *Eur. J. Inorg. Chem.*, 2005, 1815; (e) W. A. Herrmann, *Angew. Chem. Int. Ed.*, 2002, **41**, 1290; (f) D. Bourissou, O. Guerret, F. P. Gabbaï and G. Bertrand, *Chem. Rev.*, 2000, **100**, 39.
- (3) (a) N. Marion and S. P. Nolan, *Acc. Chem. Res.*, 2008, **41**, 1440; (b) E. A. B. Kantchev, C. J. O'Brien and M. G. Organ, *Angew. Chem. Int. Ed.*, 2007, **46**, 2768; (c) C. Fliedel, A. Maisse-François and S. Bellemin-Laponnaz, *Inorg. Chim. Acta*, 2007, **360**, 143.
- (4) (a) M. C. Jahnke, T. Pape and F. E. Hahn, *Eur. J. Inorg. Chem.*, 2009, 1960; (a) M. V. Jiménez, J. J. Pérez-Torrente, M. I. Bartolomé, V. Gierz, F. J. Lahoz and L. A. Oro, *Organometallics*, 2008, **27**, 224; (c) A. A. Danopoulos, N. Tsoureas, S. A. Macgregor and C. Smith, *Organometallics*, 2007, **26**, 253; (d) N. Stylianides, A. A. Danopoulos and N. Tsoureas, *J. Organomet. Chem.*, 2005, **690**, 5948; (e) L. H. Gade, V. César and S. Bellemin-Laponnaz, *Angew. Chem., Int. Ed.*, 2004, **43**, 1014; (f) V. Cesar, S. Bellemin-Laponnaz and L. H. Gade, *Organometallics*, 2002, **21**, 5204; (g) D. S. McGuinness and K. J. Cavell, *Organometallics*, 2000, **19**, 741.
- (5) (a) N. A. Jones, S. T. Liddle, C. Wilson and P. L. Arnold, *Organometallics*, 2007, **26**, 755; (b) H. Clavier, L. Coutable, L. Toupet, J. C. Guillemin and M. Mauduit, *J. Organomet. Chem.*, 2005, **690**, 5237; (c) P. L. Arnold, M. Rodden and C. Wilson, *Chem. Commun.*, 2005, 1743; (d) P. L. Arnold, A. J. Blake and C. Wilson, *Chem.–Eur. J.*, 2005, **11**, 6095; (e) A. W. Waltman and R. H. Grubbs, *Organometallics*, 2004, **23**, 3105; (f) P. L. Arnold, M. Rodden, K. M. Davis, A. C. Scarisbrick and A. J. Blake, *Chem. Commun.*, 2004, 1612; (g) P. L. Arnold, A. C. Scarisbrick, A. J. Blake and C. Wilson, *Chem. Commun.*, 2001, 2340.
- (6) (a) L. Benhamou, J. Wolf, V. Cesar, A. Labande, R. Poli, N. Lugan and G. Lavigne, *Organometallics*, 2009, **28**, 6981; (b) M. Raynal, X. Liu, R. Pattacini, C. Vallée, H. Olivier-Bourbigou and P. Braunstein, *Dalton Trans.*, 2009, 7288; (c) J. Wolf, A. Labande, J.-C. Daran and R. Poli, *Eur. J. Inorg. Chem.*, 2008, 3024; (d) C. C. Lee, W. C. Ke, K. T. Chan, C. L. Lai, C. H. Hu and H. M. Lee, *Chem.–Eur. J.*, 2007, **13**, 582; (e) A. A. Danopoulos, N. Tsoureas, S. A. Macgregor and C. Smith, *Organometallics*, 2007, **26**, 253; (f) J. Wolf, A. Labande, J. C. Daran and R. Poli, *J. Organomet. Chem.*, 2006, **691**, 433; (g) F. E. Hahn, M. C. Jahnke and T. Pape, *Organometallics*, 2006, **25**, 5927; (h) J. Y. Zeng, M.-H. Hsieh and H. M. Lee, *J. Organomet. Chem.*, 2005, **690**, 5662; (i) L. D. Field, B. A. Messerle, K. Q. Vuong and P. Turner, *Organometallics*, 2005, **24**, 4241; (j) P. L. Chiu and H. M. Lee, *Organometallics*, 2005, **24**, 1692; (k) H. M. Lee, J. Y. Zeng, C.-H. Hu and M.-T. Lee, *Inorg. Chem.*, 2004, **43**, 6822; (l) N.

- Tsoureas, A. A. Danopoulos, A. A. D. Tulloch and M. E. Light, *Organometallics*, 2003, **22**, 4750; (m) C. Yang, H. M. Lee and S. P. Nolan, *Org. Lett.*, 2001, **3**, 1511.
- (7) (a) P. Braunstein, *J. Organomet. Chem.*, 2004, **689**, 3953; (b) P. Braunstein and F. Naud, *Angew. Chem. Int. Ed.*, 2001, **40**, 680.
- (8) (a) S. T. Liu, C.-I. Lee, C.-F. Fu, C.-H. Chen, Y.-H. Liu, C. J. Elsevier, S.-M. Peng and J.-T. Chen, *Organometallics*, 2009, **28**, 6957; (b) J. Iglesias-Sigüenza, A. Ros, E. Diez, A. Magriz, A. Vazquez, E. Alvarez, R. Fernandez and J. M. Lassaletta, *Dalton Trans.*, 2009, 8485; (c) H. V. Huynh, D. Yuan and Y. Han, *Dalton Trans.*, 2009, 7262; (d) C. Gandolfi, M. Heckenroth, A. Neels, G. Laurenczy and M. Albrecht, *Organometallics*, 2009, **28**, 5112; (e) C. Fliedel, G. Schnee and P. Braunstein, *Dalton Trans.*, 2009, 2474; (f) D. S. McGuinness, J. A. Suttil, M. G. Gardiner and N. W. Davies, *Organometallics*, 2008, **27**, 4238; (g) J. Wolf, A. Labande, J. C. Daran and R. Poli, *Eur. J. Inorg. Chem.*, 2007, 5069; (h) S. J. Roseblade, A. Ros, D. Monge, M. Alcarazo, E. Alvarez, J. M. Lassaletta and R. Fernandez, *Organometallics*, 2007, **26**, 2570; (i) A. Ros, D. Monge, M. Alcarazo, E. Alvarez, J. M. Lassaletta and R. Fernandez, *Organometallics*, 2006, **25**, 6039; (j) H. V. Huynh, C. H. Yeo and G. K. Tan, *Chem. Commun.*, 2006, 3833; (k) H. Seo, H. J. Park, B. Y. Kim, J. H. Lee, S. U. Son and Y. K. Chung, *Organometallics*, 2003, **22**, 618; (l) D. Sellmann, W. Prechtel, F. Knoch and M. Moll, *Organometallics*, 1992, **11**, 2346.
- (9) (a) J. A. Cabeza, I. da Silva, I. del Río and M. G. Sánchez-Vega, *Dalton Trans.*, 2006, 3966; (b) J. A. Cabeza, I. del Río, M. G. Sánchez-Vega, M. Suarez, *Organometallics*, 2006, **25**, 1831.
- (10) W. H. Henderson, C. T. Check, N. Proust and J. P. Stambuli, *Org. Lett.*, 2010, **12**, 824.
- (11) A. J. Arduengo III, H. V. R. Dias, R. L. Harlow and M. Kline, *J. Am. Chem. Soc.*, 1992, **114**, 5530.
- (12) J. W. Ogle and S. A. Miller, *Chem. Commun.*, 2009, 5728.
- (13) H. M. J. Wang and I. J. B. Lin, *Organometallics*, 1998, **17**, 972.
- (14) M. Pfeffer, P. Braunstein and J. Dehand, *Spectrochim. Acta*, 1974, **30A**, 341.
- (15) (a) E. W. Abel, A. K. S. Ahmed, G. W. Farrow, K. G. Orrell and V. Sik, *J. Chem. Soc., Dalton Trans.*, 1977, 42; (b) E. W. Abel, G. W. Farrow, K. G. Orrell and V. Sik, *J. Chem. Soc., Dalton Trans.*, 1977, 47.
- (16) C. Fliedel and P. Braunstein, *Organometallics*, 2010, **29**, 5614.
- (17) G. A. Grasa, M. S. Viciu, J. Huang, C. Zhang, M. L. Trudell and S. P. Nolan, *Organometallics*, 2002, **21**, 2866.
- (18) D. Drew and J. R. Doyle, *Inorg. Synth.*, 1972, **13**, 47.
- (19) Bruker-Nonius, *Kappa CCD Reference Manual*, Nonius BV, The Netherlands, 1998.
- (20) G. M. Sheldrick, *Acta Crystallogr., Sect. A: Found. Crystallogr.*, 2008, **64**, 112.
- (21) (a) L. Spek, *J. Appl. Crystallogr.*, 2003, **36**, 7; (b) B. Blessing, *Acta Crystallogr.*, 1995, **51**, 33.

Chapitre 3

Thioether-functionalized N-Heterocyclic Carbenes:
Mono-, and Bis-(S,C_{NHC}) Palladium Complexes,
Catalytic C-C coupling and Characterization of a
unique $\text{Ag}_4\text{I}_4(S,C_{\text{NHC}})_2$ Planar Cluster

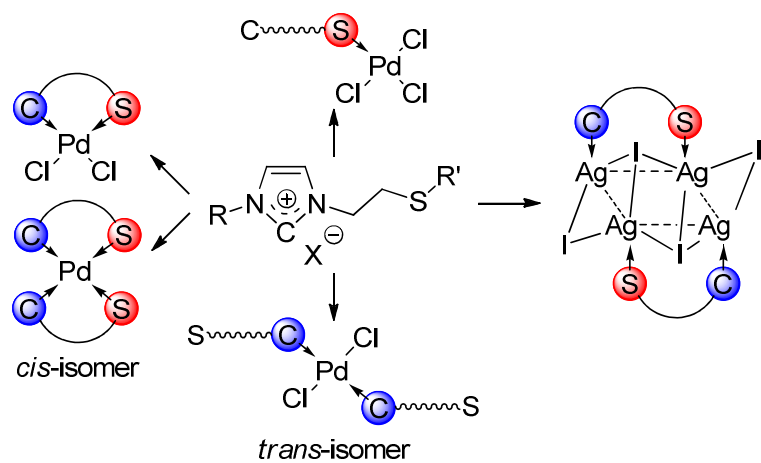
Résumé du chapitre 3

Nous présentons une synthèse “one-step” de nouveaux sels d’imidazolium *N*-aryl-*N*'-thioether qui sont précurseurs de ligands de type (*S,C_{NHC}*) dans des complexes carbéniques. La structure cristalline de l’imidazolium hexafluorophosphate *N*-(2,6-diisopropylphenyl)-*N*'-ethyl-(ethyl)-sulfide **8·HPF₆** a été déterminée par diffraction des rayons X et a montré des interactions de type liaison H entre l’anion PF₆ anion et en particulier le proton imidazolium 2-H. Les complexes NHC d’Ag(I) **1·AgX – 8·AgX** ont été synthétisé et entièrement caractérisés. Un cluster plan, centrosymétrique, sans précédent de formule [Ag₄(μ₃-I)₂(μ₂-I)₂(μ₂-S,C_{NHC})₂] [**5·(AgI)₂**]₂, a été obtenu, dans lequel deux ligands carbènes fonctionnels pontent deux côtés du rectangle d’argent. Avec les ligands *N*-alkyl-*N*'-thioether, des complexes [PdCl₂(*S,C_{NHC}*)₂] ont été préparés par deux différentes voies de synthèse: la réaction classique de transmétallation impliquant le réactif de type Ag(I) NHC ou par une séquence “pas à pas” impliquant la déprotonation de la fonction imidazolium dans un intermédiaire zwitterionique où la fonction thioéther est liée au centre Pd(II). Les structures cristallines de deux complexes représentatifs, **10** et **12**, avec une fonction éthyle- ou phényle-thioéther, respectivement, coordinée au centre Pd(II), ont été déterminées par diffraction des rayons X et confirment leur structure mononucléaire. Dans les complexes neutres *trans*-[PdCl₂(C_{NHC})₂] (**17-20**) le groupement thioéther n'est pas coordonné au centre métallique, ce qui a également été confirmé par la structure obtenue par diffraction des rayons X du complexe dichlorure bis-NHC Pd(II) **18**, qui a également mis en évidence l’arrangement *trans-anti* des ligands. Les premiers exemples de complexes di-cationiques bis-chélatés de palladium(II) complexes avec des ligands NHCs fonctionnalisés par des thioéthers, [Pd(*S,C_{NHC}*)₂][BF₄]₂ (**21-24**), sont présentés, ils ont été obtenus sélectivement avec un arrangement *cis* des ligands. Les complexes de Pd(II) **9-24** ont été testés en réaction de couplage croisé de type Suzuki-Miyaura sous différentes conditions, et une meilleure activité catalytique a été observés pour les complexes dans lesquels l’atome de soufre était coordonné au centre métallique.

Référence et synopsis du chapitre 3

Christophe Fliedel and Pierre Braunstein,

Organometallics, 2010, **29**, 5614–5626.



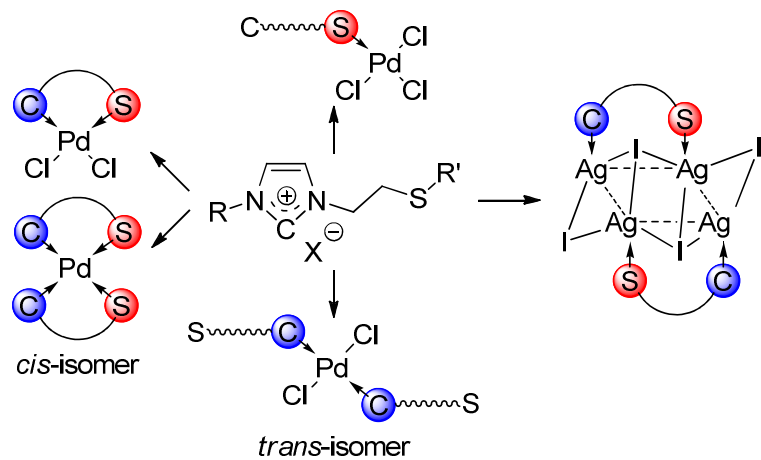
Abstract of Chapter 3

We report a one-step synthesis for new *N*-aryl-*N'*-thioether imidazolium salts that are precursors to (*S,C*_{NHC}) ligands in N-heterocyclic carbene (NHC) complexes. The crystal structure of the *N*-(2,6-diisopropylphenyl)-*N'*-ethyl-(ethyl)-sulfide imidazolium hexafluorophosphate **8·HPF**₆ was determined by X-ray diffraction and revealed H-bonding interactions between the PF₆ anion and, in particular, the imidazolium 2-H proton. The corresponding Ag(I) NHC complexes **1·AgX – 8·AgX** were synthesized and fully characterized. An unprecedented planar, centrosymmetric cluster, [Ag₄(μ₃-I)₂(μ₂-I)2(μ₂-S,C_{NHC})₂] [**5·(AgI)**₂]₂, was obtained in which two functional carbene ligands bridge two edges of a silver rectangle. With the *N*-alkyl-*N'*-thioether ligands, [PdCl₂(*S,C*_{NHC})₂] complexes were prepared by two different routes: the usual transmetalation reaction involving the Ag(I) NHC reagent or a stepwise sequence involving deprotonation of the imidazolium function in zwitterionic intermediates where the thioether function is bound to the Pd(II) center. The crystal structures of two representative complexes, **10** and **12**, with an ethyl- or a phenyl-thioether function, respectively, coordinated to the Pd(II) center, have been determined by X-ray diffraction and confirmed their mononuclear structure. In the neutral complexes trans-[PdCl₂(C_{NHC})₂] (**17-20**) the thioether group is not coordinated to the metal center, as also confirmed by the crystal structure determination by X-ray diffraction of the bis-NHC Pd(II) dichloro complex **18**, which also established the trans-anti arrangement of the ligands. The first examples of bischelated dicationic palladium(II) complexes with thioether-functionalized NHCs, [Pd(*S,C*_{NHC})₂][BF₄]₂ (**21-24**), are reported, which were selectively obtained with a cis arrangement of the ligands. The Pd(II) complexes **9-24** were evaluated in Suzuki-Miyaura cross-coupling reactions under various conditions, and a higher catalytic activity was observed for the complexes in which the sulfur atom is coordinated to the metal center.

Reference and Synopsis of Chapter 3

Christophe Fliedel and Pierre Braunstein,

Organometallics, 2010, **29**, 5614–5626.

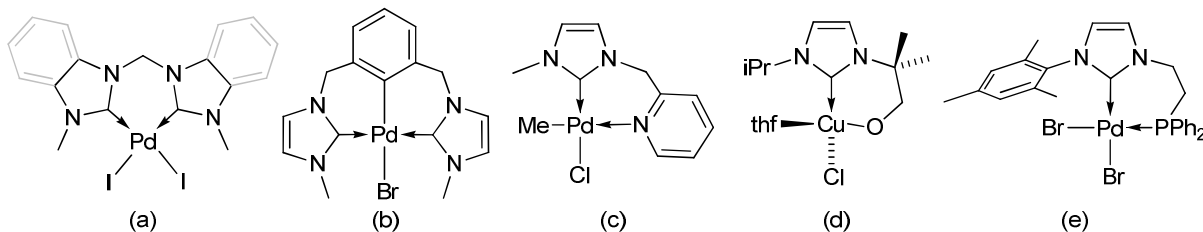


Introduction

N-Heterocyclic carbenes (NHCs) have attracted increasing attention in organometallic chemistry since the pioneering work of Lappert,¹ the report of the first stable free carbene,² the synthesis of various silver-NHC complexes³ and the report of their use as carbene transfer reagents.⁴ Metal-NHC complexes have already found many applications in homogenous catalysis.⁵ NHCs are often used as phosphine alternatives owing to their better stability towards oxidation and the formation of more stable metal complexes.⁶ For cross-coupling reactions, strong σ -donor ligands are necessary and the NHCs are the only class of ligands able to challenge the long used tertiary phosphines.⁷ Although the association of NHCs with palladium(II) precursors has been extensively studied in catalysis⁸ and NHC-Pd complexes compared to phosphine-Pd catalysts,⁹ the use of well-defined NHC-Pd(II) complexes as precatalysts for cross-coupling reactions remains underdeveloped.¹⁰

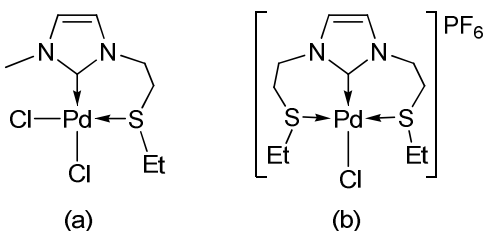
The number of bis- and more generally, polydentate NHC-containing ligands has grown very rapidly.¹¹ Varying the nature of the linker between the donor functions and/or the nature of the latter allows the creation of diversified families of ligands. Examples of complexes containing two carbene donors linked through a single atom, a pyridine or a phenylene backbone have been described [Chart 1, (a) and (b)].¹² The synthesis of functional NHCs associating a carbene ligand with a chemically different donor function has given rise to the formation *N*-,¹³ *O*-¹⁴ and *P,C*_{NHC}¹⁵ metal complexes [Chart 1, (c)-(e)]. These complexes rapidly showed great potential in homogenous catalysis.^{5f,8a,16} The chelating ability of these ligands resulted in the formation of highly stable complexes with a strong σ -donor function (NHC) and a more labile one, which could result in a hemilabile behavior of the resulting systems in solution.¹⁷ In turn, this could lead to the temporary dissociation of the heteroatom donor from the metal during a catalytic cycle, allowing the coordination of a substrate, its metal-assisted transformation and after product elimination, stabilizing recoordination of this function.

Chart 1. Examples of (a) Single-Atom-Bridged Bis(*C*_{NHC}),^{12o,q} (b) Phenylene-Bridged Bis(*C*_{NHC}),¹²ⁿ (c) *N*-,^{13g} (d) *O*-^{14e} and (e) *P,C*_{NHC}^{15j} Metal Complexes.



Although the presence of a sulfur atom in the side chain attached to nitrogen has revealed beneficial for some catalytic reactions, e.g., catalytic Mizoroki-Heck coupling, ketone hydrosilylation, or allylic substitution reactions,^{18,19} only a few S,C_{NHC} metal complexes have been described until now. Examples of mono(thioether) imidazolium¹⁸ and bis(thioether) imidazolium salts¹⁹ and S,C_{NHC} complexes obtained by oxidative addition of a carbon sulfur bond across zero valent metal precursor have been reported (**Chart 2**).²⁰

Chart 2. Examples of (a) Chelate S,C_{NHC}^{18e} and (b) pincer S,C_{NHC},S^{19a} Palladium(II) Complexes.

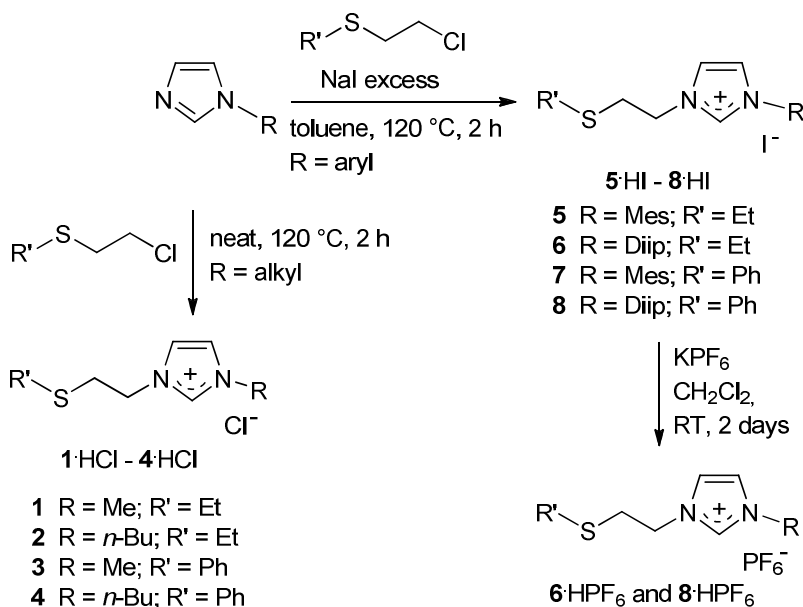


We recently reported an atom efficient, one step and solvent-free synthesis of new S,C_{NHC} precursors bearing a thioether function on a nitrogen atom, together with their Ag(I) and Pd(II) complexes.^{18e} In the light of preliminary catalytic results, we decided to extend our investigations to this ligand class. Here, we report the synthesis of mono-carbene chelate complexes $[\text{PdCl}_2(S,C_{\text{NHC}})]$ by transmetalation reaction or by an alternative pathway involving zwitterionic intermediates where the functional imidazolium ligand is first coordinated to the metal through its thioether function and then deprotonated at the imidazolium site by a weak base. We also prepared bis-carbene complexes $[\text{PdCl}_2(S,C_{\text{NHC}})_2]$ in which the sulfur atom remains uncoordinated and C,S bis-chelated dicationic species $[\text{Pd}(S,C_{\text{NHC}})_2][\text{BF}_4]_2$ attractive for catalysis owing to a potentially easily accessible vacant coordination site produced by displacement of the sulfur donors. Since we could not isolate the corresponding free carbenes, their thione derivatives were prepared in order to show that the imidazolium salts can be deprotonated by an external base. We then extended this family of ligands to aryl thioether imidazolium salts to modify the physical properties, solubility, and steric and electronic characteristics of the resulting complexes. The corresponding silver(I) complexes were synthesized and the structure of a unique $[\text{Ag}_4\text{I}_4(S,C_{\text{NHC}})_2]$ planar cluster is reported.

Results and Discussion

Preparation of the Carbene Precursors. The *N*-alkyl-*N'*-thioether imidazolium chlorides **1·HCl – 4·HCl** were prepared as described previously.^{18d} This procedure was slightly modified for the preparation of the *N*-aryl-*N'*-thioether imidazolium salts. The solid reagents, *N*-(2,4,6-trimethylphenyl) and *N*-(2,6-diisopropylphenyl) imidazole, were dissolved in toluene, and addition of an excess NaI favored the reaction with 2-chloroethyl ethylsulfide or 2-chloroethyl phenylsulfide. This reaction resulted at the same time in a counter anion exchange, which afforded the *N*-aryl-*N'*-thioether imidazolium iodides, **5·HI – 8·HI** (Scheme 1). This anion exchange and the electronic effect of the aryl substituents resulted in an upfield shift for the 2-H protons for **5·HI – 8·HI** between 9.26 and 9.78 ppm compared to **1·HCl – 4·HCl** for which the 2-H proton signal appears between 10.36 and 10.51 ppm. The $^{13}\text{C}\{\text{H}\}$ NMR resonances of the NCN carbons between 137.2 and 137.8 ppm, were also affected. Whereas the corresponding bromide salt **5·HBr** has been previously described,^{18g} its synthesis involved first that of the *N*-(2-bromoethyl)-*N'*-(2,4,6-trimethylphenyl) imidazolium bromide, in two steps, with an overall yield of 60%.²¹

Scheme 1. Synthesis of the Carbene Precursors.



Reaction of the *N*-(2,6-diisopropylphenyl) substituted imidazolium iodides with excess KPF₆ at room temperature in CH₂Cl₂ for 2 days resulted in their quantitative conversion to the hexafluorophosphate salts **6·HPF₆** and **8·HPF₆**. Consistent with the anion exchange, an upfield shift was observed in their ¹H NMR spectra for the 2-H resonances at 9.04 ppm and 8.68 ppm and in the ¹³C{¹H} NMR spectra for the NCN carbons at 136.0 and 135.1 ppm, respectively. Single crystals of **8·HPF₆** suitable for X-ray diffraction studies were obtained by slow diffusion of pentane into a saturated dichloromethane solution of **8·HPF₆**. Its molecular structure is depicted in Figure 1. The aromatic substituent at N2 is almost orthogonal to the NCN ring, the angle between the 2,6-diisopropylphenyl and the imidazole rings being 84.2 °. The steric constrains are also minimized on the N1 side with a torsion angle C1-N1-C4-C5 of 105.9 ° and an angle between the N1-C4-C5 and the imidazole ring of 70.0 °. In the solid state, non-classical hydrogen bonds exist between the imidazolium and the PF₆ counteranion. The strongest one is between the acidic hydrogen H1 and the fluorine atom F4 (2.20 Å). The orientation of the phenyl ring from the thioether moiety is probably also influenced by the three non-classical H bonds between their hydrogen atoms H11 and H12 and the fluorine F2, F3 and F4 (see values below).

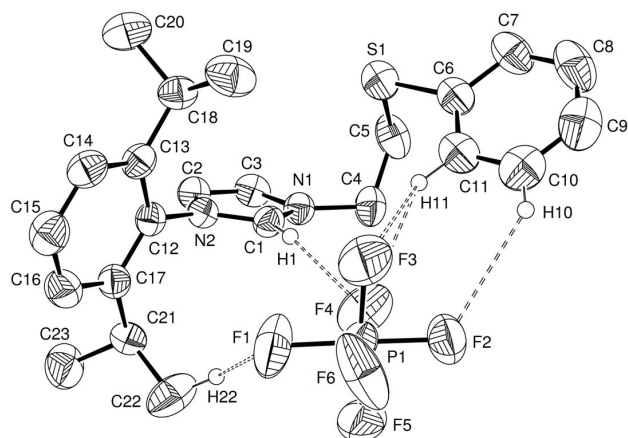
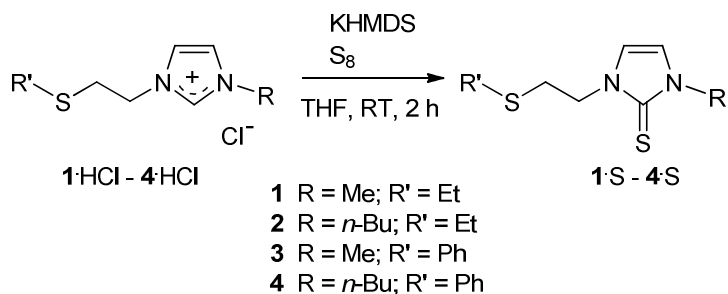


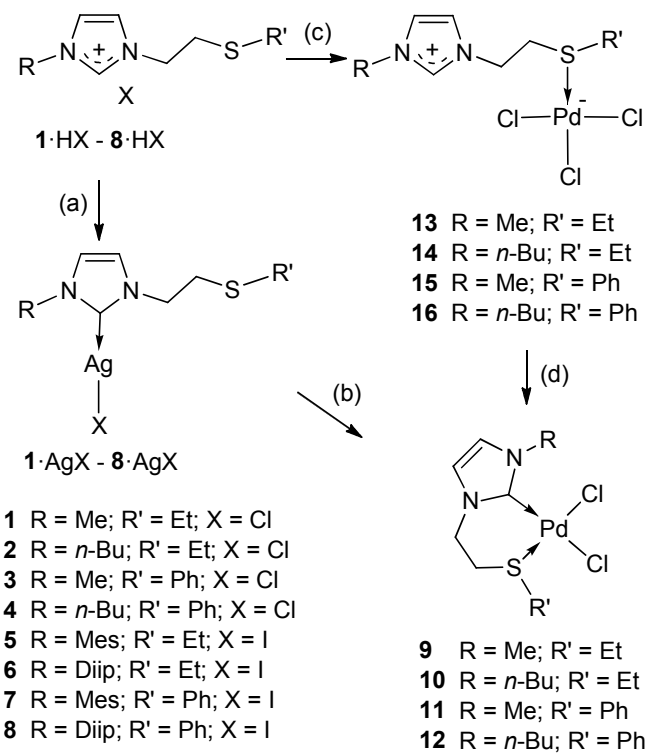
Figure 1. View of the molecular structure of **8·HPF₆**. Only the hydrogen atoms involved in H-bonding are shown for clarity. Ellipsoids are represented at 50% probability level. Selected bond lengths (Å), bond angles (deg) and torsion angles (deg): C1-N1 1.319(3), C1-N2 1.328(3), C1-H1 0.95(2), H1-F4 2.200(2), C10-F2 3.527(5), C11-F3 3.340(1), C11-F4 3.460(1), C22-F1 3.421(3), N1-C1-N2 109.24(19), N1-C4-C5 110.4(2), C14-C13-N2 117.5(2), C1-N1-C4-C5 105.9(3), C1-N2-C12-C13 81.4(3).

Synthesis of the Thione Derivatives. The free carbenes **1 – 4** could not be isolated, owing to their low stability in solution, but addition of sulfur to the reaction mixture yielded the corresponding thiones **1·S – 4·S**, respectively, which could be isolated and characterized (Scheme 2). Deprotonation of the imidazolium salts was established by the disappearance of the 2-H imidazolium ^1H NMR resonance. The $^{13}\text{C}\{\text{H}\}$ NMR spectra of these thiones showed a typical downfield shift for the NCN carbon signal between 161.6 and 162.1 ppm. The ESI-MS spectra and the elemental analysis confirmed the C=S bond formation. By comparison with the IR spectra of the corresponding imidazolium salts, the C=S stretching vibration of the thiones **1·S-4·S** is tentatively assigned to an intense absorption in the region 1225–1230 cm^{-1} .

Scheme 2. Synthesis of the Thione Derivatives of the NHC, **1·S – 4·S**.



Synthesis of the Silver(I) Complexes. Formation of NHC metal complexes by transmetallation from the corresponding silver carbene complexes is a well known procedure.⁴ Before using these complexes *in situ* as transmetalation reagents, we attempted to isolate and fully characterize them. Reaction of the imidazolium salts, in CH_2Cl_2 at room temperature, with excess Ag_2O as a base resulted in the formation of the corresponding Ag(I) NHC complexes formulated as **1·AgCl – 4·AgCl** on the basis of mass spectrometry data (Scheme 3).^{18e} The same procedure was followed for the formation of **5·AgI – 8·AgI**. The success of the reaction is shown by the disappearance of the 2-H proton resonance in the ^1H NMR spectra of the complexes. Their formation was also established by a characteristic downfield shift of the NCN $^{13}\text{C}\{\text{H}\}$ NMR resonance between 181.5 and 183.3 ppm. The reaction of Ag_2O with the hexafluorophosphate imidazolium salts did not lead to complete conversion. This could be due to strong interactions between the 2-H imidazolium proton and the counteranion (Figure 1), which may partially prevent deprotonation for steric reasons. In the following experiments involving the $[\text{AgX(NHC)}]$ complexes, these will be prepared *in situ* and used as transmetalation agents, after filtration of their solution through a Celite pad to remove the unreacted silver oxide.

Scheme 3. Two Pathways for the Synthesis of $[PdCl_2(S,C_{NHC})]$ Complexes^a

^a Conditions: (a): 1 equiv. Ag_2O , CH_2Cl_2 , RT; (b): 1 equiv. $[PdCl_2(\text{cod})]$, CH_2Cl_2 , RT; (c): 1 equiv. $[PdCl_2(\text{cod})]$, CH_2Cl_2 , RT; (d): 1 equiv. Cs_2CO_3 , $MeCN$, 60 °C.

Slow diffusion of pentane into a saturated dichloromethane solution obtained by reaction of **5·HI** and Ag_2O afforded colorless single crystals suitable for X-ray diffraction and a brownish oil. The crystals were found to correspond to the formulation $[Ag_2(\mu_3\text{-I})(\mu_2\text{-I})(\mu_2\text{-}S,C_{NHC})]_2$. Its solid-state molecular structure is depicted in Figure 2 and exhibits an unexpected arrangement (Scheme 4).

Although the coordination chemistry of NHCs toward silver salts is very diversified,^{3a,22} the centrosymmetric structure of this polynuclear complex shows an unprecedented planar Ag_4 core with two bridging S,C_{NHC} ligands. The two chemically different Ag atoms have different coordination geometries: $Ag1$ has a slightly distorted trigonal-planar geometry formed by $C1$, $I1$ and $I2$ whereas $Ag2$ has a slightly distorted tetrahedral coordination geometry formed by $S1$, $I1$, $I1'$ and $I2'$. The angles involving the capping iodides deviate significantly from those in a regular coordination environment [see e.g. $C1\text{-}Ag1\text{-}I1 = 128.7(2)^\circ$ and $S1\text{-}Ag2\text{-}I1 = 121.42(6)^\circ$]. The distances between the silver atoms supported by the bridging S,C_{NHC} ligand are significantly longer than that between the silver atoms doubly bridged by iodide ligands; $Ag1\text{-}Ag2 = 3.219(2)$ Å and $Ag1\text{-}Ag2' = 2.9657(18)$ Å, respectively. The two iodide ligands have different coordination modes, since $I2$ acts as a

μ_2 -bridging ligand, supporting the Ag1…Ag2' interaction, whereas I1 is μ_3 -capping three metal centers (Ag1, Ag2 and Ag2'). The Ag…Ag distances [2.9657(18) and 3.219(2) Å] are notably shorter than those in the only other structurally characterized related Ag₄I₄ cluster (to the best to our knowledge), which contains phosphine ligands [Ag…Ag 3.0953(13) and 3.4378(21) Å].²³ The carbene-silver bond length of 2.128(7) Å is in agreement with literature values and the S-Ag distance is slightly longer than those observed for other donor groups (such as N- or P- donors), in functional NHC complexes.²⁴ The far-infrared spectrum of crystalline [5·(AgI)₂]₂ exhibits strong absorptions at 236 and 154 cm⁻¹, which are tentatively assigned to the stretching vibrations of the μ_2 -bridging and μ_3 -capping iodides, respectively.

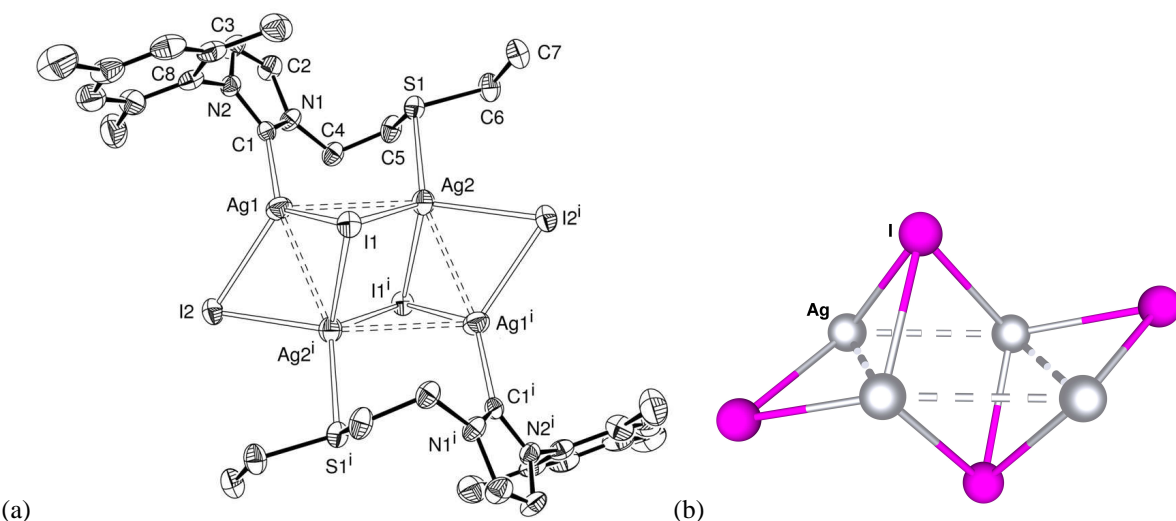
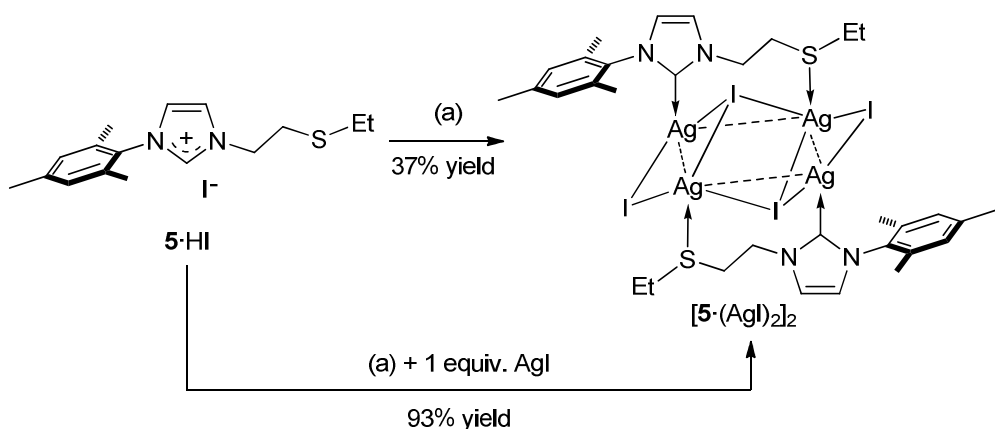


Figure 2. (a) View of the molecular structure of [5·(AgI)₂]₂. Hydrogen atoms are omitted for clarity. Ellipsoids are represented at 30% probability level. Selected bond lengths (Å) and bond angles (deg). Ag1-C1 2.128(1), Ag2-S1 2.552(3), Ag1-Ag2 3.219(2), Ag1-Ag2i 2.9657(18), Ag1-I1 2.8259(17), Ag1-I2 2.790(2), Ag2-I1 2.8826(19), Ag2-I2i 2.8423(18), Ag1-I1i 2.953(2), C1-Ag1-I1 128.7(2), C1-Ag1-I2 122.4(2), I1-Ag1-I2 108.07(5), S1-Ag2-I1 121.42(6), S1-Ag2-I1i 110.92(6), S1-Ag2-I2i 109.74(7), Ag1-Ag2-Ag1i 110.43(5). (b) Simplified view of the Ag₄I₄ core. Color code: grey: silver; pink, iodine.

The Ag/I/NHC stoichiometry of 2:2:1 in [5·(AgI)₂]₂ differs from that of the reagents (1:1:1). This observation explains why the yield of the formation of this cluster was less than 50%. When the reaction was carried out with an additional equivalent of AgI, the cluster [5·(AgI)₂]₂ was formed in 93% yield (Scheme 4).

Scheme 4. Preparation of the Planar Cluster $[5\cdot(\text{AgI})_2]_2^a$ 

^a Conditions: (a): 1 equiv. Ag_2O , CH_2Cl_2 , RT.

Synthesis of the Mono-NHC Palladium(II) Complexes. Two routes were investigated for the formation of $[\text{PdCl}_2(S,C_{\text{NHC}})]$ complexes.

Route A: Transmetalation Reaction (Scheme 3, (a) and (b)). This classical method involves the *in situ* synthesis of the corresponding silver complexes, $1\cdot\text{AgCl} - 4\cdot\text{AgCl}$ and their reaction with the palladium precursor, $[\text{PdCl}_2(\text{cod})]$ ($\text{cod} = 1,5\text{-cyclooctadiene}$), in a 1:1 ratio, to give the desired chelate complexes $[\text{PdCl}_2(S,C_{\text{NHC}})]$ (**9 – 12**), as reported recently for **9**.^{18e}

Route B: In Situ Deprotonation of a Zwitterionic Intermediate (Scheme 3, (c) and (d)). Our motivation to explore an alternative route was to establish the possible beneficial effect of the presence of the sulfur atom on complex formation under mild conditions and to avoid the use of Ag(I) intermediates, which may interfere in subsequent catalytic reactions. Addition of $[\text{PdCl}_2(\text{cod})]$ to a stirred dichloromethane solution of the imidazolium salts $1\cdot\text{HCl} - 4\cdot\text{HCl}$ led to the displacement of the cod ligand and coordination of the thioether function. The pure product precipitated rapidly, affording complexes **13 – 16** in good yields after washing the solids with pentane to eliminate the traces of cod. The coordination sphere of the palladium atom comprised three Cl and one thioether ligand, and the resulting zwitterionic structure was confirmed spectroscopically. The characteristic signal for the 2H-imidazolium proton is present in the ^1H NMR spectra of all complexes between 9.10 and 9.23 ppm. The ESI-MS spectra reveal as most intense peaks are $[\text{M}+\text{Na}]^+$ and $[\text{M}-\text{Cl}]^+$ ions, with the expected isotopic distributions, which rules out a hypothetical ion-pair structure of general formula $[(\text{L}\cdot\text{H})_2(\text{PdCl}_4)]$ ($\text{L} = \text{carbene } 1 - 4$). The far-infrared spectra of the complexes **13 – 16** showed a typical pattern for the $\nu(\text{Pd-Cl})$ vibrations of a LPdCl_3 fragment.²⁵ The elemental analyses of these complexes were also in good agreement with the calculated values. Owing

to the low solubility of these compounds in organic solvents, characteristic for highly polar compounds, no $^{13}\text{C}\{\text{H}\}$ NMR spectra could be recorded for complexes **13 – 15** and the NCN signal was not observed in the spectrum of **16**. These Pd(II) complexes are not air-, light- or moisture-sensitive and can be stored for weeks without any trace of degradation, in contrast to most silver NHC complexes. This pathway thus allows a stepwise and easy access to catalyst precursors, which could be immediately engaged in catalysis. We thus examined the formation of chelate species by deprotonation of the zwitterionic complexes **13 – 16** for 3 h with one equivalent of the weak base Cs_2CO_3 in refluxing acetonitrile. This afforded the desired complexes of general formula, $[\text{PdCl}_2(\text{S},\text{C}_{\text{NHC}})]$ (**9 – 12**), respectively. All the spectroscopic data confirm their mononuclear structure and the *cis* arrangement of the ligands. Broad signals were observed in the ^1H NMR spectra, owing to the formation of a stereogenic sulfur atom after its coordination to palladium.^{18e} The values of the $\nu(\text{Pd}-\text{Cl})$ stretching vibration in the far-infrared spectrum (ca. 312 and 295 cm^{-1}) are also consistent with a *cis* arrangement of the chlorides.^{19a,26} Using a stronger base, such as $\text{KO}t\text{-Bu}$, on a similar system, Wolf *et al.* observed the formation of a dinuclear species, in which the ligand acted as a *C,S*-bridge between two metal centers.^{18h} The solid-state molecular structures of complexes **10** and **12** are depicted in Figure 3 and Figure 4, respectively. They are very similar, and in each case, the complexes adopt a distorted square-planar geometry around the palladium centers. The ligands form a *C,S* chelate with a bite angle of $83.19(11)^\circ$ and $88.99(13)^\circ$ for **10** and **12**, respectively. The higher *trans* influence of the carbene ligands compared to the sulfur is illustrated by longer Pd(1)-Cl(1) bonds compared to Pd(1)-Cl(2). The six-membered palladacycle formed by the metal and the chelate ligand adopts a boat-like conformation, in which C(4) and Pd(1) are on the same side of the C1-N2(1)-C5-S1 plane. Due to the short side chain (two methylene groups) and coordination of the sulfur atom, the angles between the imidazole rings and the palladium coordination plane deviate from the electronically preferred 90° , with values of $56.8(3)$ and $53.1(9)^\circ$ for **10** and **12**, respectively.

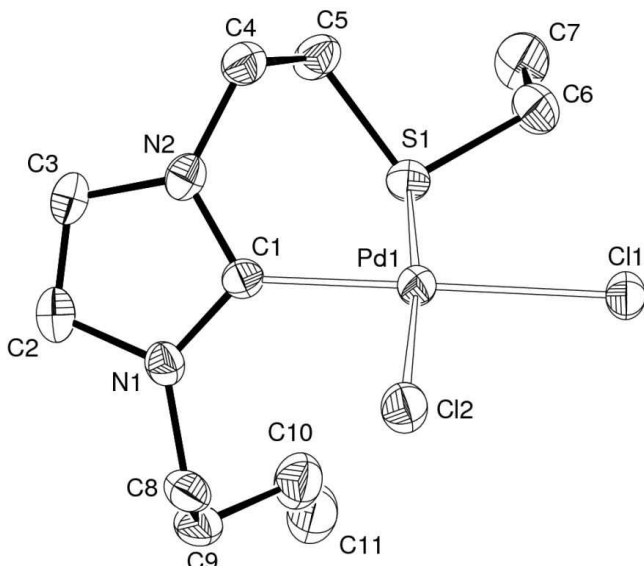


Figure 3. View of the molecular structure of **10**. Hydrogen atoms are omitted for clarity. Ellipsoids are represented at 50% probability level. Selected bond lengths (\AA) and bond angles (deg): Pd1-C1 1.989(4), Pd1-S1 2.2955(11), Pd1-Cl1 2.3631(10), Pd1-Cl2 2.3317(10), C1-N1 1.333(5), C1-N2 1.342(5), C1-Pd1-S1 83.19(11), C1-Pd1-Cl2 90.99(11), S1-Pd1-Cl1 93.30(4), N1-C1-N2 106.8(3).

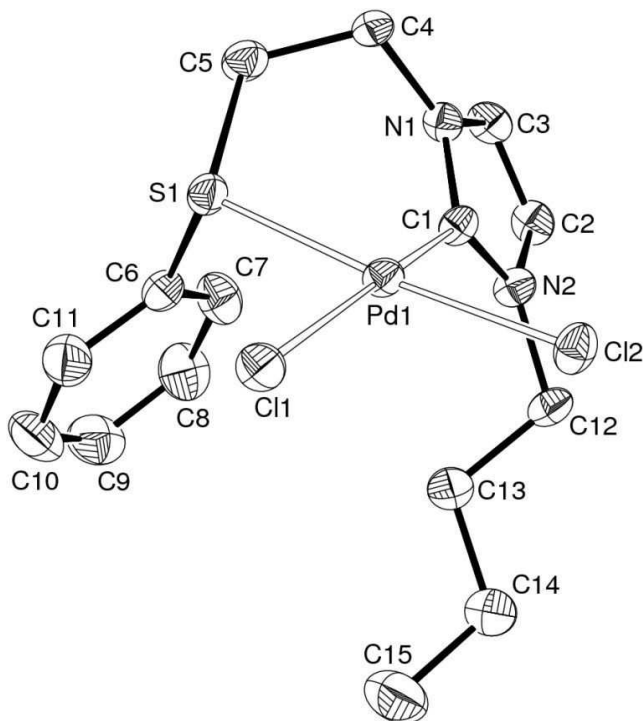
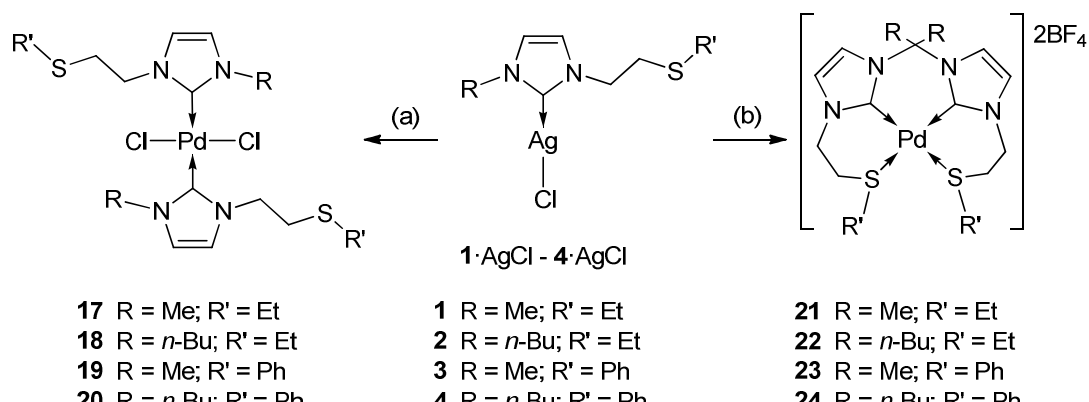


Figure 4. View of the molecular structure of **12**. Hydrogen atoms are omitted for clarity. Ellipsoids are represented at 50% probability level. Selected bond lengths (\AA) and bond angles (deg): Pd1-C1 1.978(4), Pd1-S1 2.2858(12), Pd1-Cl1 2.3709(12), Pd1-Cl2 2.3301(12), C1-N1 1.340(5), C1-N2 1.346(5), C1-Pd1-S1 88.99(13), C1-Pd1-Cl2 91.89(13), S1-Pd1-Cl1 86.55(4), N1-C1-N2 106.0(4).

By using the procedure of route B (Scheme 3, (c) and (d)), which has only limited precedents,^{18h,19a} we found that the presence of a thioether moiety exerts a favorable anchimeric assistance for the selective formation of $[\text{PdCl}_2(S,C_{\text{NHC}})]$ chelate complexes without the constraints of a transmetalation reaction. Another beneficial aspect of this method compared to transmetalation is that the catalyst precursor can be formed directly *in situ* and immediately engaged in a catalytic process with no silver contamination. This has been tested with **1**·HCl to form *in situ* complex **9** in the catalytic studies described below.

Synthesis of the Bis-NHC Palladium(II) Complexes. Since NHC ligands are known to be strong donor ligands that rarely dissociate from the metal, the presence of two NHC ligands on the palladium center could lead to attractive species for catalytic applications. Two types of bis-carbene palladium complexes were synthesized in the course of this work.

Scheme 5. Synthetic Pathways for the Synthesis of Bis-NHC Palladium(II) Complexes^a



^a (a) 1/2 equiv. [PdCl₂(cod)], CH₂Cl₂, RT ; (b) 1/2 equiv. [Pd(NCMe)₄][BF₄]₂, CH₂Cl₂, RT.

Starting from the corresponding silver complexes synthesized *in situ*, reaction with [PdCl₂(cod)] in a 2:1 ratio afforded the bis-carbene palladium dichloride complexes of general formula [PdCl₂(L)₂], **17 – 20** (Scheme 5, (a)). Only one isomer formed during the reaction, and the NMR spectra of these complexes only showed one set of signals for the ligands. The sharp ¹H NMR signals are consistent with dangling lateral side chains bonded to the nitrogen atoms. At this stage, it is reasonable to suggest that the *trans* isomer is formed, and the value of the v(Pd-Cl) stretching vibration around 340 cm⁻¹ is in accordance with this hypothesis.²⁶ The *trans-anti* arrangement was confirmed by the solid state X-ray structures of **17**^{18e} and **18** (Figure 5). The palladium atom occupies a center of symmetry for the molecule, and the square-planar coordination geometry around the palladium center is only slightly distorted (C1-Pd1-Cl1 90.3(1) $^\circ$).

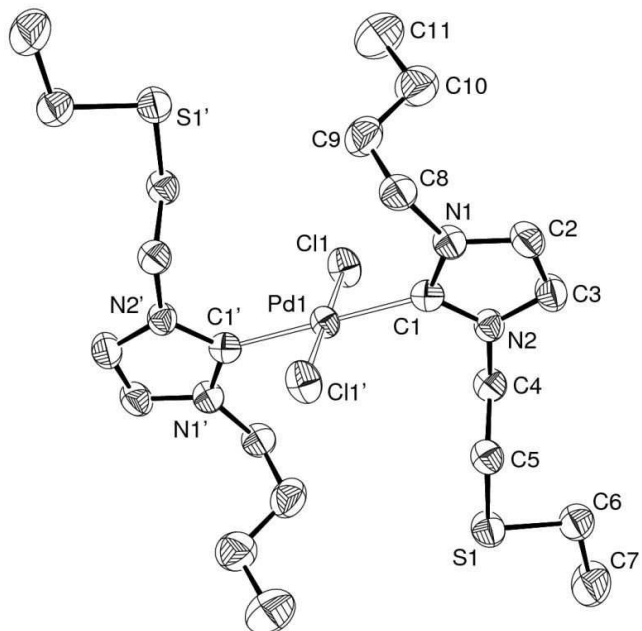


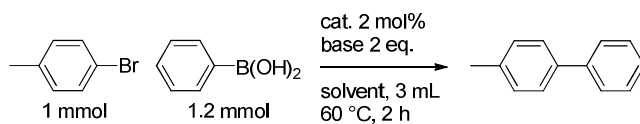
Figure 5. View of the molecular structure of **18**. Only one of the two analogous crystallographically independent molecules is depicted. Hydrogen atoms are omitted for clarity. Ellipsoids are represented at 50% probability level. Selected bond lengths (\AA) and bond angles (deg): Pd1-C1 2.025(4), Pd1-Cl1 2.3094(10), C1-N1 1.351(5), C1-N2 1.349(5), C1-Pd1-Cl1 90.29(11), N1-C1-N2 105.3(3).

A second type of bis-NHC palladium complexes was synthesized, starting from the silver complexes **1·AgCl** – **4·AgCl**. Reaction of 0.5 equiv of $[\text{Pd}(\text{NCMe})_4]\text{[BF}_4\text{]}_2$ with the corresponding silver complex generated *in situ*, at room temperature in dichloromethane, afforded the dicationic, bis-chelated palladium(II) complexes **21** – **24**, of general formula $[\text{Pd}(S,C_{\text{NHC}})_2]\text{[BF}_4\text{]}_2$. Their formation results from the easy displacement of the palladium-bound acetonitrile ligands, which was confirmed by ^1H NMR spectroscopy. Only a few examples of bis-chelated dicationic Pd complexes, with donor-functionalized NHC ligands, have been described and they showed interesting catalytic activities in coupling reactions.^{13a,27} Bis-chelated dicationic $[\text{Pd}(N,C_{\text{NHC}})_2]X_2$ with N representing a picoline donor moiety were recently reported and have been studied in Heck-type coupling reactions.^{13a,g} To the best of our knowledge, no example with thioether side chains was reported. Such complexes could offer advantages for catalytic applications: they bear two strong ligands known to be efficient in homogenous catalysis and have two coordination sites readily accessible by displacement of the soft sulfur ligands. These properties could lead to catalysts active for Suzuki-Miyaura couplings under very mild, room temperature conditions.²⁸ Like in the case of the mono-chelate palladium dichloride complexes, the sulfur atom becomes a stereogenic center upon

coordination to the metal center, and this gives rise to a broadening of the ^1H NMR resonances. This is in accordance with the bis-chelation of the ligands in the dicationic complexes, whereas sharp signals were observed for the dichloro-bis-NHC complexes. The broadening is due to a more rigid structure of the side chain, in contrast to the situation in the dichloro complexes. The carbenic carbons of **21 – 24** resonate, in $^{13}\text{C}\{^1\text{H}\}$ NMR, between 155.1 and 157.8 ppm, strongly upfield shifted compared to the neutral *trans* complexes, e.g. 170.1 ppm for **20**, and to reported $[\text{Pd}(N,\text{C}_{\text{NHC}})_2][\text{BF}_4]_2$ complexes (*N*-donor from a picoline moiety in a *cis* arrangement) between 167.3 and 166.1 ppm,^{13a,g} but more downfield than a $[\text{Pd}(N,\text{C}_{\text{NHC}})_2][\text{PF}_6]_2$ complex (150.9 ppm).^{27d} This very large upfield shift results from the *cis* arrangement of the carbene donors, the coordination of the thioether function and the formally dicationic charge on the Pd center. The latter will increase the donation from the carbenic carbon, which is illustrated by their chemical shift. We could thus show that selective formation of *trans*- $[\text{PdCl}_2(\text{C}_{\text{NHC}})_2]$ and *cis*- $[\text{Pd}(\text{S},\text{C}_{\text{NHC}})_2][\text{BF}_4]_2$ complexes is possible starting from readily accessible $\text{Ag}(\text{NHC})$ complexes.

Catalytic studies. The palladium complexes **9 – 24** were evaluated in Suzuki-Miyaura cross-coupling reaction. The complexes were first tested using the procedure described in Scheme 6, and then for the most interesting complexes, the conditions were varied. The results obtained with the mono-NHC complexes, **9 – 16**, are reported in Table 1.

Scheme 6. Typical Procedure for the Catalytic Reactions



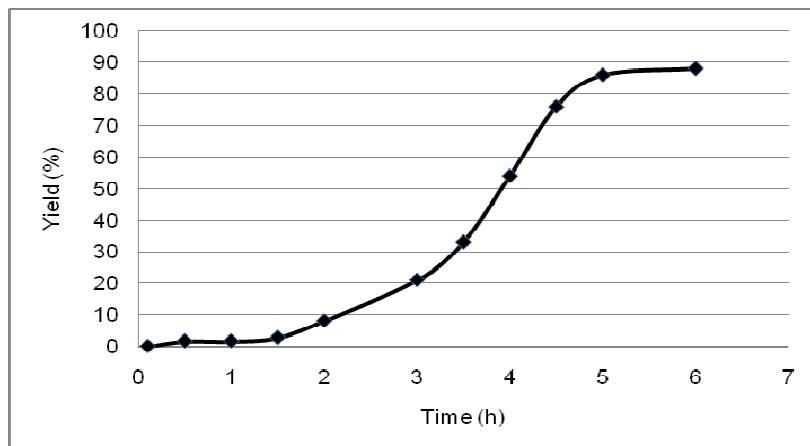
The choice of DMSO as a solvent resulted from the low solubility of these complexes in dioxane, which is the common solvent for this reaction. The conversions to 4-methyl-biphenyl observed with the chelate complexes **9 – 12** are nearly quantitative. The best yields, 94% and 91%, were obtained for the complexes bearing an *N*-*n*-Bu substituent, **10** and **12**, respectively. The presence of this side chain probably induces a higher solubility of the precursors. The conversions observed with the zwitterionic compounds **13 – 16** were lower than those obtained with the corresponding chelate species.

Table 1. Catalytic Activities for Mono-NHC Palladium Complexes^a

complex	yield (%)	complex	yield (%)
9	88	13	62 ^a , 86 ^b
10	94	14	71 ^a , 95 ^b
11	86	15	51 ^a , 87 ^b
12	91	16	47 ^a , 91 ^b

^a Yields determined by GC. Reaction conditions: cat. 2 mol %, base Cs₂CO₃, solvent DMSO, temp. 60 °C, reaction time 2 h. ^b Reaction time 5 h.

The reaction mixtures did not turn dark with formation of potentially active Pd(0) species, in contrast to the case of the NHC complexes **9** – **12**. Runs performed with **13** – **16** for 5 h reaction time led to similar yields to those in the case of the chelated pre-catalysts (+/- 2%). Assuming that the zwitterionic compounds **13** – **16** are not the direct catalyst precursors, but are first transformed during the induction period to the corresponding neutral chelate species **9** – **12**, a catalytic reaction starting from complex **13** was run for 6 h and a plot of the conversion as a function of time is shown in Figure 6.

**Figure 6.** Evolution of the conversion to 4-methyl-biphenyl as a function of time in the Suzuki-Miyaura cross-coupling reaction starting from zwitterionic complex **13**.

During the first 2 h, almost no conversion was observed, this time being necessary for the formation of the carbene complex **9** by deprotonation of **13** by the slight excess of base present in the reaction mixture. During the next 3 h, the conversion was similar to that observed when starting from complex **9** (Figure 6). This experiment indicates the stepwise formation of the precatalyst in the reactor by reaction of the imidazolium salt, the palladium

precursor and the base used for the catalytic reaction. It could be interesting to extend this procedure to other metal complexes such as Ni(II) or Rh(I) and to donor functions like amines or phosphines, which are involved in diverse catalytic reactions. With the most efficient catalyst, complex **10**, different solvents and bases were used to optimize the reaction conditions (Table 2). As expected, the highly polar solvent DMSO was the best for these complexes (94%), but we also observed a good activity with toluene as solvent (71%). DMF, another polar solvent, was also tested but no better activity than in the case of DMSO was observed. Four inorganic bases were tested with this complex and carbonates were the most efficient, Cs_2CO_3 being the best (91%). The organic base NEt_3 gave rise to less than 30% conversion (Table 2).

Table 2. Solvent and Base Effects on the Catalysis Reaction with Complex **10**^a

solvent	yield ^b (%)	base	yield ^c (%)
Dioxane	80	NaOAc	36
DMSO	94	NaCO_3	74
DMF	57	K_2CO_3	70
Toluene	71	NEt_3	29
Water	0	Cs_2CO_3	91

^a Yields determined by GC. Reaction conditions: cat. 2 mol%, base, solvent, temp. 60 °C, time 2 h. ^b Base Cs_2CO_3 . ^c Solvent DMSO.

The bis-NHC palladium complexes **17 – 24** were also evaluated in Suzuki-Miyaura cross-coupling reactions, and the results obtained are reported in Table 3. The catalytic tests were performed under the conditions optimized for the mono-NHC palladium complexes (see above). The dichloride compounds led to relatively good yields, between 68% (**18**) and 79% (**20**). Finally, with the dicationic, bis-chelated species **21 – 24**, the best activities of all the palladium complexes synthesized in this work were observed, especially with complex **22** which gave 98% conversion.

Table 3. Catalytic Activities for Bis-NHC Palladium Complexes^a

complex	yield (%)	complex	yield (%)
17	74	21	90
18	68	22	98
19	72	23	91
20	79	24	96

^a Yields determined by GC. Reaction conditions: cat. 2 mol%, base Cs₂CO₃, solvent DMSO, temp. 60 °C, reaction time 2 h.

In view of these results, further experiments were performed with the best catalysts. These were tested first with a lower catalyst loading and then with *p*-chlorotoluene as substrate. The results of these catalytic runs are reported in Table 4.

Table 4. Catalytic Activities for Complexes **10** and **22** under Modified Reaction Conditions^a

		catalyst base 2 eq. solvent, 3 mL 60 °C, 2 h	
Complex	Conversion ^b	Complex	Conversion ^c
	(%)		(%)
10	54	10	30
22	58	22	38

^a Yields determined by GC. Reaction conditions: base Cs₂CO₃, solvent DMSO, temp. 60 °C, reaction time 2 h. ^b Catalyst 1 mol%, X = Br. ^c Catalyst 2 mol%, X = Cl.

With complexes **10** and **22**, a decrease of conversion when 1 mol% precatalyst was used instead of 2 mol%, as in the previous experiments; however, the conversion was not divided by two. It is more difficult to achieve the cross-coupling reaction with chlorinated than with brominated substrates,²⁹ which explains the drop of the conversion from 94% (**10**) and 98% (**22**) to 30 and 38% for **10** and **22**, respectively.

Conclusion

The scope of a procedure recently described for the synthesis of new functionalized N-heterocyclic carbene precursors, bearing as side arms a bulky aromatic group and a thioether function able to coordinate to a metal center, has been extended and could gain wider applicability.^{18e,19a} Thus, linking an imidazolium cation to a metal center via its functional side chain tends to favor its subsequent deprotonation and formation of the carbene-metal bond. Four different types of palladium(II) complexes bearing thioether-NHC ligands were obtained, and the ligand was acting as a *S,C_{NHC}* chelate in complexes **9 – 12** and **21 – 24**. However, an unprecedented planar Ag₄I₄ cluster has been structurally characterized in which the *S,C_{NHC}* ligand bridges two Ag centers with different coordination geometries. Among the Pd(II) complexes that were evaluated in Suzuki-Miyaura cross-coupling reactions, a higher catalytic activity was observed for those in which the sulfur atom is coordinated to the metal center. It will be interesting to see whether similar observations apply to other catalytic reactions.

Acknowledgment

We thank Gilles Schnee (University of Strasbourg) and Alessandra Sabbatini (University of Camerino, Italy) for their contribution to this work and Marc Mermillon-Fournier and Mélanie Boucher for technical assistance. We are most grateful to Dr. Roberto Pattacini for the resolution of the X-ray structures and to the CNRS, the Ministère de la Recherche (Paris) and the DFH/UFA (International Research Training Group 532-GRK532) for funding.

Experimental Section

General Procedures. All operations were carried out using standard Schlenk techniques under inert atmosphere. Solvents were purified and dried under nitrogen by conventional methods. d_6 -DMSO was degassed and stored over 4 Å molecular sieves. CD_2Cl_2 , CDCl_3 and CD_3CN were dried over 4 Å molecular sieves, degassed by freeze-pump-thaw cycles and stored under argon. NMR spectra were recorded at room temperature on a Bruker AVANCE 300 spectrometer (^1H , 300 MHz; ^{13}C , 75.47 MHz; ^{31}P , 121.49 MHz and ^{19}F , 282.38 MHz) and referenced using the residual proton solvent (^1H) or solvent (^{13}C) resonance. Assignments are based on ^1H , ^1H -COSY, ^1H , ^{13}C -HMQC and ^1H , ^{13}C -HMBC experiments. Chemical shifts (δ) are given in ppm. IR spectra were recorded in the region 4000-100 cm^{-1} on a Nicolet 6700 FT-IR spectrometer (ATR mode, SMART ORBIT accessory, Diamond crystal). Elemental analyses were performed by the “Service de microanalyses”, Université de Strasbourg and by the “Service Central d’Analyse”, USR-59/CNRS, Solaize. Electrospray mass spectra (ESI-MS) were recorded on a microTOF (Bruker Daltonics, Bremen, Germany) instrument using nitrogen as drying agent and nebulising gas and Maldi-TOF analyses were carried out on a Bruker AutiflexII TOF/TOF (Bruker Daltonics, Bremen, Germany), using dithranol (1,8,9-trihydroxyanthracene) as a matrix. Gas chromatographic analyses were performed on a Thermoquest GC8000 Top series gas chromatograph using a HP Pona column (50 m, 0.2 mm diameter, 0.5 μm film thickness). The imidazolium salts **1**·HCl to **4**·HCl^{18e} and the complexes [PdCl₂(cod)],³⁰ [Pd(NCMe)₄][BF₄]₂,³¹ **1**·AgCl - **4**·AgCl,^{18e} **9**^{18e} and **17**^{18e} were prepared according to literature methods. All other reagents were used as received from commercial suppliers.

Abbreviations: Mes = 2,4,6-trimethylphenyl ; Diip = 2,6-diisopropylphenyl ; KHMDS = potassium hexamethyldisilazane.

Synthesis of *N*-(R)-*N'*-ethyl-(R')-sulfide Imidazolium Iodides 5·HI - 8·HI:

These compounds are known to be very hygroscopic and the elemental analyses always afforded carbon and nitrogen percentages lower than calculated values.

5·HI: R = 2,4,6-trimethylphenyl ; R' = ethyl.

Pure *N*-(2,4,6-trimethylphenyl)imidazole (2.00 g, 10.74 mmol), 2-chloroethyl ethylsulfide (1.25 mL, 1.34 g, 10.74 mmol) and sodium iodide (3.22 g, 21.48 mmol) were placed in a Schlenk tube equipped with a magnetic stirrer and toluene added. The mixture was refluxed for 2 h and then allowed to cool to room temperature. During heating, the colorless mixture turned light brown. After cooling, the mixture was filtered to eliminate the excess of salts formed and/or remaining. The volatiles were evaporated under reduced pressure and the brown oil was washed with dry diethyl ether (2 x 40 mL) and dried under vacuum. The residue was purified by precipitation from a saturated MeOH solution in cold Et₂O. The product was isolated as a yellow oil. Yield: 84%. Anal. Calc. for C₁₆H₂₃IN₂S (402.34): C, 47.76; H, 5.76; N, 6.96 Found: C, 45.51; H, 6.13; N, 5.76. FTIR: $\nu_{\text{max}}(\text{oil})/\text{cm}^{-1}$: 3118sh, 3057br, 2968br, 2920br, 2866sh, 1606w, 1561m, 1545s, 1484m, 1446s, 1376w, 1329w, 1263w, 1199vs, 1157s, 1104w, 1067s, 1034m, 968w, 934w, 854s, 750m, 730sh, 698w, 666s. ¹H NMR (CDCl₃, 300 MHz) δ: 1.24 (3H, t, ³J = 7.2 Hz, SCH₂CH₃), 2.10 (6H, s, 2 CH₃ *ortho*-Mes), 2.34 (3H, s, CH₃ *para*-Mes), 2.68 (2H, q, ³J = 7.2 Hz, SCH₂CH₃), 3.13 (2H, t, ³J = 6.0 Hz, NCH₂CH₂S), 4.95 (2H, t, ³J = 6.0 Hz, NCH₂CH₂S), 7.01 (2H, s, 2H *meta*-Mes), 7.18 (1H, pseudo t, ³J = ⁴J = 1.8 Hz, CH=CHNCH₂), 7.98 (1H, pseudo t, ³J = ⁴J = 1.8 Hz, MesNCH=CH), 9.78 (1H, t, ⁴J = 1.5 Hz, NCHN). ¹³C{¹H} NMR (CDCl₃, 75.5 MHz) δ: 14.74 (SCH₂CH₃), 17.89 (2 CH₃ *ortho*-Mes), 21.16 (CH₃ *para*-Mes), 26.14 (SCH₂CH₃), 32.29 (NCH₂CH₂S), 49.71 (NCH₂CH₂S), 123.00, 123.65 (CH=CH), 129.92 (2 CH *meta*-Mes), 130.48 (C *ipso*-Mes), 134.40 (2 C *ortho*-Mes), 137.69 (NCN), 141.51 (C *para*-Mes). MS (ESI): *m/z* 275.2 [M - I]⁺.

6·HI: R = 2,6-diisopropylphenyl ; R' = ethyl.

The same procedure was used with *N*-(2,6-diisopropylphenyl)imidazole (5.07 g, 27.20 mmol), 2-chloroethyl ethylsulfide (4.00 mL, 4.70 g, 27.20 mmol) and sodium iodide (8.15 g, 54.39 mmol). The product was isolated as a yellow oil. Yield: 81%. Anal. Calc. for C₁₉H₂₉IN₂S (444.42): C, 51.35; H, 6.58; N, 6.30 Found: C, 48.96; H, 6.62; N, 5.30. FTIR: $\nu_{\text{max}}(\text{oil})/\text{cm}^{-1}$: 3152br, 3071br, 2964br, 2929br, 2871br, 1592w, 1564m, 1547m, 1458m, 1414sh, 1387w, 1367m, 1315w, 1264w, 1245sh, 1190m, 1130sh, 1105m, 1071m, 1060m, 959w, 938w, 874sh, 829vs, 759s, 739s, 693m, 670s. ¹H NMR (CDCl₃, 300 MHz) δ: 0.82-0.99 (15H, 2d ³J = 6.9

Hz, 2 CH(CH₃)₂, and t, ³J = 7.2 Hz, SCH₂CH₃), 2.10 (2H, sept, ³J = 6.6 Hz, 2 CH(CH₃)₂), 2.44 (2H, q, ³J = 7.4 Hz, SCH₂CH₃), 2.89 (2H, t, ³J = 6.0 Hz, NCH₂CH₂S), 4.72 (2H, t, ³J = 6.0 Hz, NCH₂CH₂S), 7.02 (1H, pseudo t, ³J = ⁴J = 1.8 Hz, CH=CHNCH₂), 7.16 (2H, d, ³J = 8.1 Hz, 2H *meta*-Diip), 7.27 (1H, t, ³J = 8.1 Hz, H *para*-Diip), 8.28 (1H, pseudo t, ³J = ⁴J = 1.8 Hz, DiipNCH=CH), 9.76 (1H, t, ⁴J = 1.5 Hz, NCHN). ¹³C{¹H} NMR (CDCl₃, 75.5 MHz) δ: 14.41 (SCH₂CH₃), 24.00, 24.42 (2 CHCH₃), 25.60 (SCH₂CH₃), 28.29 (2 CHCH₃), 32.30 (NCH₂CH₂S), 48.56 (NCH₂CH₂S), 123.58, 124.02 (CH=CH), 124.42 (CH *meta*-Diip), 128.67 (C *ipso*-Diip), 131.68 (CH *para*-Diip), 137.75 (NCN), 145.28 (C *ortho*-Diip). MS (ESI): *m/z* 317.2 [M - I]⁺.

7·HI: R = 2,4,6-trimethylphenyl ; R' = phenyl.

The same procedure was used with *N*-(2,4,6-trimethylphenyl)imidazole (5.07 g, 27.20 mmol), 2-chloroethyl phenylsulfide (4.00 mL, 4.70 g, 27.20 mmol) and sodium iodide (8.15 g, 54.39 mmol). The product was isolated as a yellow solid. Yield: 85%. Anal. Calc. for C₂₀H₂₃IN₂S (450.38): C, 53.34; H, 5.15; N, 6.22 Found: C, 51.73; H, 5.27; N, 4.82. FTIR: ν_{max}(solid)/cm⁻¹: 3145br, 3096w, 3050br, 2947w, 1627w, 1604w, 1581w, 1561m, 1547s, 1479m, 1446s, 1436s, 1380w, 1364w, 1346w, 1324w, 1280w, 1247w, 1200vs, 1154s, 1109w, 1087w, 1067s, 1035m, 1023m, 967w, 935w, 865s, 821m, 782m, 743vs, 703m, 692vs, 663vs. ¹H NMR (CDCl₃, 300 MHz) δ: 2.05 (6H, s, 2 CH₃ *ortho*-Mes), 2.32 (3H, s, CH₃ *para*-Mes), 3.62 (2H, t, ³J = 6.0 Hz, NCH₂CH₂S), 4.90 (2H, t, ³J = 6.0 Hz, NCH₂CH₂S), 6.98 (2H, s, 2H *meta*-Mes), 7.17 (1H, pseudo t, ³J = ⁴J = 1.8 Hz, CH=CHNCH₂), 7.20 – 7.37 (5H, m, H aromatics), 8.01 (1H, pseudo t, ³J = ⁴J = 1.8 Hz, MesNCH=CH), 9.69 (1H, t, ⁴J = 1.5 Hz, NCHN). ¹³C{¹H} NMR (CDCl₃, 75.5 MHz) δ: 17.88 (2 CH₃ *ortho*-Mes), 21.15 (CH₃ *para*-Mes), 34.85 (NCH₂CH₂S), 49.25 (NCH₂CH₂S), 122.98, 123.34 (CH=CH), 127.32 (CH *para*-phenyl), 129.64 (2 CH *meta*-phenyl), 129.90 (2 CH *meta*-Mes), 130.01 (2 CH *ortho*-phenyl), 130.44 (C *ipso*-Mes), 133.28 (C *ipso*-phenyl), 134.32 (2 C *ortho*-Mes), 137.26 (NCN), 141.50 (C *para*-Mes). MS (ESI): *m/z* 323.2 [M - I]⁺.

8·HI: R = 2,6-diisopropylphenyl ; R' = phenyl.

The same procedure was used with *N*-(2,6-diisopropylphenyl)imidazole (5.07 g, 27.20 mmol), 2-chloroethyl phenylsulfide (4.00 mL, 4.70 g, 27.20 mmol) and sodium iodide (8.15 g, 54.39 mmol). The product was isolated as a yellow solid. Yield: 92%. Anal. Calc. for C₂₃H₂₉IN₂S (492.46): C, 56.10; H, 5.94; N, 5.69 Found: C, 55.01; H, 5.80; N, 4.46. FTIR: ν_{max}(solid)/cm⁻¹: 3148br, 3053br, 2967br, 2929br, 2871br, 1584w, 1562w, 1546w, 1459m, 1440w, 1420w, 1388w, 1367w, 1354sh, 1313w, 1264s, 1187m, 1103w, 1088sh, 1070w,

1059w, 1025w, 895w, 844s, 806m, 730vs, 700vs, 671s. ^1H NMR (CDCl_3 , 300 MHz) δ : 1.19 (12H, 2 d, $^3J = 6.9$ Hz, 2 $\text{CH}(\text{CH}_3)_2$), 2.34 (2H, sept, $^3J = 6.9$ Hz, 2 $\text{CH}(\text{CH}_3)_2$), 3.62 (2H, t, $^3J = 5.7$ Hz, $\text{NCH}_2\text{CH}_2\text{S}$), 4.90 (2H, t, $^3J = 5.7$ Hz, $\text{NCH}_2\text{CH}_2\text{S}$), 7.21 (1H, pseudo t, $^3J = ^4J = 1.8$ Hz, $\text{CH}=\text{CHNCH}_2$), 7.25 – 7.33 (7H, m, 5H phenyl and 2H *meta*-Diip), 7.55 (1H, t, $^3J = 7.8$ Hz, H *para*-Diip), 8.03 (1H, pseudo t, $^3J = ^4J = 1.7$ Hz, DiipNCH=CH), 9.26 (1H, t, $^4J = 1.5$ Hz, NCHN). $^{13}\text{C}\{\text{H}\}$ NMR (CDCl_3 , 75.5 MHz) δ : 24.41 (2 CHCH_3), 28.69 (2 CHCH_3), 34.96 ($\text{NCH}_2\text{CH}_2\text{S}$), 49.24 ($\text{NCH}_2\text{CH}_2\text{S}$), 124.17, 124.21 ($\text{CH}=\text{CH}$), 124.82 (2 CH *meta*-Diip), 127.46 (CH *para*-phenyl), 129.72 (2 CH *meta*-phenyl), 129.81 (C *ipso*-Diip), 129.91 (2 CH *ortho*-phenyl), 132.16 (CH *para*-Diip), 133.00 (C *ipso*-phenyl), 137.19 (NCN), 145.52 (C *ortho*-Diip). MS (ESI): m/z 365.2 [M - I] $^+$.

General Procedure for the Anion Exchange.

6·HPF₆: R = 2,6-diisopropylphenyl ; R' = ethyl.

The imidazolium iodide **6·HI** (0.200 g, 0.45 mmol) and solid KPF₆ (0.414 g, 2.25 mmol) were mixed in a CH_2Cl_2 and stirred for 2 days at room temperature. Then the suspension was filtered through a Celite pad and the solvent was evaporated under reduced pressure to give a yellow solid. Yield: 97%. Anal. Calc. for C₁₉H₂₉F₆N₂PS (462.48): C, 49.34; H, 6.32; N, 6.06 Found: C, 48.96; H, 6.47; N, 6.24. FTIR: $\nu_{\text{max}}(\text{solid})/\text{cm}^{-1}$: 3151br, 2966br, 2930br, 2872br, 2360br, 1626br, 1564m, 1548m, 1459m, 1388w, 1367w, 1315w, 1261w, 1216w, 1190m, 1104w, 1071w, 1060w, 911s, 837vs, 806sh, 757sh, 729vs, 669s. ^1H NMR (CDCl_3 , 300 MHz) δ : 1.17 (12H, 2 d, $^3J = 6.9$ Hz, 2 $\text{CH}(\text{CH}_3)_2$), 1.22 (3H, t, $^3J = 7.2$ Hz, SCH_2CH_3), 2.35 (2H, sept, $^3J = 6.9$ Hz, 2 $\text{CH}(\text{CH}_3)_2$), 2.62 (2H, q, $^3J = 7.2$ Hz, SCH_2CH_3), 3.06 (2H, t, $^3J = 6.0$ Hz, $\text{NCH}_2\text{CH}_2\text{S}$), 4.74 (2H, t, $^3J = 6.0$ Hz, $\text{NCH}_2\text{CH}_2\text{S}$), 7.21 (1H, pseudo t, $^3J = ^4J = 1.8$ Hz, $\text{CH}=\text{CHNCH}_2$), 7.30 (2H, d, $^3J = 8.1$ Hz, 2H *meta*-Diip), 7.53 (1H, t, $^3J = 8.1$ Hz, H *para*-Diip), 7.91 (1H, pseudo t, $^3J = ^4J = 1.8$ Hz, DiipNCH=CH), 9.04 (1H, t, $^4J = 1.5$ Hz, NCHN). $^{13}\text{C}\{\text{H}\}$ NMR (CDCl_3 , 75.5 MHz) δ : 14.55 (SCH_2CH_3), 24.22, 24.29 (2 CHCH_3), 25.59 (SCH_2CH_3), 28.56 (2 CHCH_3), 32.18 ($\text{NCH}_2\text{CH}_2\text{S}$), 49.23 ($\text{NCH}_2\text{CH}_2\text{S}$), 123.43, 124.53 (CH=CH), 124.69 (CH *meta*-Diip), 129.89 (C *ipso*-Diip), 132.00 (CH *para*-Diip), 137.39 (NCN), 145.59 (C *ortho*-Diip). $^{31}\text{P}\{\text{H}\}$ NMR (CDCl_3 , 121.5 MHz) δ : - 142.9 (sept., $^1J_{\text{P}, \text{F}} = 711$ Hz, PF₆). $^{19}\text{F}\{\text{H}\}$ NMR (CDCl_3 , 282.4 MHz) δ : - 72.5 (d, $^1J_{\text{P}, \text{F}} = 711$ Hz, PF₆). MS (ESI): m/z 317.2 [M - PF₆] $^+$.

8·HPF₆: R = 2,6-diisopropylphenyl ; R' = phenyl.

The same procedure was used with **8·HI** (0.200 g, 0.41 mmol) and solid KPF₆ (0.374 g, 2.03 mmol). The product was isolated as a yellow solid. Yield: 98%. Anal. Calc. for C₂₃H₂₉F₆N₂PS

(510.17): C, 54.11; H, 5.73; N, 5.49 Found: C, 54.34; H, 5.40; N, 5.09. FTIR: $\nu_{\text{max}}(\text{solid})/\text{cm}^{-1}$: 3155br, 3103w, 2968br, 2929w, 2872br, 1634br, 1565w, 1553m, 1474m, 1455m, 1442w, 1408w, 1389w, 1366w, 1350w, 1306w, 1288w, 1278w, 1265w, 1245w, 1217w, 1191s, 1153w, 1106w, 1089w, 1073w, 1059w, 1037w, 1024w, 1005w, 961w, 940w, 927w, 915w, 875s, 841vs, 820vs, 758vs, 698s, 671v, 652m. ^1H NMR (CDCl_3 , 300 MHz) δ : 1.16 (12H, 2 d, $^3J = 6.9$ Hz, 2 $\text{CH}(\text{CH}_3)_2$), 2.31 (2H, sept, $^3J = 6.8$ Hz, 2 $\text{CH}(\text{CH}_3)_2$), 3.50 (2H, t, $^3J = 5.9$ Hz, $\text{NCH}_2\text{CH}_2\text{S}$), 4.66 (2H, t, $^3J = 5.8$ Hz, $\text{NCH}_2\text{CH}_2\text{S}$), 7.22 – 7.33 (8H, m, $\text{CH}=\text{CHNCH}_2$, 5H phenyl and 2H *meta*-Diip), 7.54 (1H, t, $^3J = 7.8$ Hz, H *para*-Diip), 7.79 (1H, pseudo t, $^3J = 4J = 1.5$ Hz, Diip $\text{NCH}=\text{CH}$), 8.68 (1H, br s, NCHN). $^{13}\text{C}\{\text{H}\}$ NMR (CDCl_3 , 75.5 MHz) δ : 24.10, 24.36 (2 CHCH_3), 28.59 (2 CHCH_3), 34.56 ($\text{NCH}_2\text{CH}_2\text{S}$), 49.09 ($\text{NCH}_2\text{CH}_2\text{S}$), 123.88 ($\text{CH}=\text{CH}$), 124.73 (br, 2 CH *meta*-Diip and $\text{CH}=\text{CH}$), 127.42 (CH *para*-phenyl), 129.68 (2 CH *meta*-phenyl), 129.84 (*C ipso*-Diip), 129.93 (2 CH *ortho*-phenyl), 132.07 (CH *para*-Diip), 133.03 (*C ipso*-phenyl), 136.87 (NCN), 145.57 (*C ortho*-Diip). $^{31}\text{P}\{\text{H}\}$ NMR (CDCl_3 , 121.5 MHz) δ : - 143.1 (sept., $^1J_{\text{P}, \text{F}} = 711$ Hz, PF_6^-). $^{19}\text{F}\{\text{H}\}$ NMR (CDCl_3 , 282.4 MHz) δ : - 72.4 (d, $^1J_{\text{P}, \text{F}} = 711$ Hz, PF_6^-). MS (ESI): *m/z* 365.2 [M - PF_6^-]⁺.

Synthesis of the Thiones 1·S - 4·S.

1·S: R = methyl ; R' = ethyl.

Solid KHMDS (0.289 g, 1.45 mmol) was added to a stirred suspension of **1·HCl** (0.300 g, 1.45 mmol) and S₈ (0.186 g, 0.73 mmol) in THF at room temperature. After 2 h, the reaction mixture was filtered through a Celite pad and the THF evaporated under reduced pressure. The residue was washed with pentane (2 x 20 mL) and dried under vacuum. The product was obtained as an orange solid. Yield: 72%. Anal. Calc. for C₈H₁₄N₂S₂ (202.34): C, 47.49; H, 6.97; N, 13.84. Found: C, 47.09; H, 7.26; N, 13.73. FTIR: $\nu_{\text{max}}(\text{solid})/\text{cm}^{-1}$: 3159br, 3125br, 3093br, 2956br, 2926br, 2869br, 1666w, 1582w, 1567w, 1457s, 1438s, 1400vs, 1358m, 1332m, 1265w, 1227s, 1205sh, 1182s, 1133w, 1086w, 1061w, 1023w, 971w, 936w, 872w, 797sh, 739m, 708s, 691sh, 669vs. ^1H NMR (CDCl_3 , 300 MHz) δ : 1.26 (3H, t, $^3J = 7.5$ Hz, SCH_2CH_3), 2.57 (2H, q, $^3J = 7.5$ Hz, SCH_2CH_3), 2.92 (2H, t, $^3J = 6.9$ Hz, $\text{NCH}_2\text{CH}_2\text{S}$), 3.60 (3H, s, NCH₃), 4.20 (2H, t, $^3J = 6.9$ Hz, $\text{NCH}_2\text{CH}_2\text{S}$), 6.67 and 6.75 (2H, AB spin system, $^3J = 2.4$ Hz, $\text{CH}=\text{CH}$). $^{13}\text{C}\{\text{H}\}$ NMR (CDCl_3 , 75.5 MHz) δ : 14.85 (SCH_2CH_3), 26.19 (SCH_2CH_3), 30.06 ($\text{NCH}_2\text{CH}_2\text{S}$), 35.10 (NCH₃), 48.01 ($\text{NCH}_2\text{CH}_2\text{S}$), 117.30, 117.49 (CH=CH), 162.09 (NCN). MS (ESI): *m/z* 225.1 [M + OLi]⁺.

2·S: R = *n*-butyl ; R' = ethyl.

The same procedure was used with KHMDS (0.241 g, 1.21 mmol), **2·HCl** (0.300 g, 1.21 mmol) and S₈ (0.155 g, 0.60 mmol). The product was isolated as an orange solid. Yield: 69%. Anal. Calc. for C₁₁H₂₀N₂S₂ (244.42): C, 54.05; H, 8.25; N, 11.46. Found: C, 53.68; H, 8.41; N, 11.20. FTIR: $\nu_{\text{max}}(\text{solid})/\text{cm}^{-1}$: 3127br, 3094br, 2956br, 2928br, 2869br, 1734w, 1671m, 1582w, 1568w, 1520w, 1480sh, 1455sh, 1438s, 1411vs, 1358m, 1268br, 1229s, 1207m, 1173m, 1117w, 1087w, 1067w, 1047w, 1024w, 876w, 740s, 712m, 691m, 672m. ¹H NMR (CDCl₃, 300 MHz) δ: 0.93 (3H, t, ³J = 7.5 Hz, CH₃ butyl), 1.24 (3H, t, ³J = 7.5 Hz, SCH₂CH₃), 1.36 (2H, m, NCH₂CH₂CH₂CH₃), 1.73 (2H, m, NCH₂CH₂CH₂CH₃), 2.54 (2H, q, ³J = 7.5 Hz, SCH₂CH₃), 2.91 (2H, t, ³J = 6.9 Hz, NCH₂CH₂S), 4.01 (2H, t, ³J = 7.5 Hz, NCH₂CH₂CH₂CH₃), 4.20 (2H, t, ³J = 7.2 Hz, NCH₂CH₂S), 6.66 and 6.75 (2H, AB spin system, ³J = 2.4 Hz, CH=CH). ¹³C{¹H} NMR (CDCl₃, 75.5 MHz) δ: 13.70 (CH₃ butyl), 14.86 (SCH₂CH₃), 19.80 (NCH₂CH₂CH₂CH₃), 26.19 (SCH₂CH₃), 30.02 (NCH₂CH₂S), 30.96 (NCH₂CH₂CH₂CH₃), 47.63 (NCH₂CH₂CH₂CH₃), 47.92 (NCH₂CH₂S), 116.44, 117.44 (CH=CH), 161.56 (NCN). MS (ESI): *m/z* 251.1[M + Li]⁺.

3·S: R = methyl ; R' = phenyl.

The same procedure was used with KHMDS (0.235 g, 1.18 mmol), **3·HCl** (0.300 g, 1.18 mmol) and S₈ (0.151 g, 0.59 mmol). The product was isolated as an orange solid. Yield: 78%. Anal. Calc. for C₁₂H₁₄N₂S₂ (250.38): C, 57.56; H, 5.64; N, 11.19. Found: C, 57.22; H, 5.87; N, 10.71. FTIR: $\nu_{\text{max}}(\text{solid})/\text{cm}^{-1}$: 3307br, 3162br, 2963br, 2924br, 2869br, 2178m, 1732w, 1625w, 1534m, 1439m, 1401s, 1333w, 1225m, 1186w, 1111vs, 1048w, 1017vs, 874w, 713w, 670sh, 654m. ¹H NMR (CDCl₃, 300 MHz) δ: 3.38 (2H, t, ³J = 6.6 Hz, NCH₂CH₂S), 3.57 (3H, s, NCH₃), 4.22 (2H, t, ³J = 6.6 Hz, NCH₂CH₂S), 6.59 and 6.65 (2H, AB spin system, ³J = 2.4 Hz, CH=CH), 7.19-7.40 (5H, m, H arom). ¹³C{¹H} NMR (CDCl₃, 75.5 MHz) δ: 31.63 (NCH₂CH₂S), 35.06 (NCH₃), 47.53 (NCH₂CH₂S), 117.51, 117.72 (CH=CH), 126.40 (*C para*-phenyl), 129.10 (*C meta*-phenyl), 129.21 (*C ortho*-phenyl), 134.69 (*C ipso*-phenyl), 161.95 (NCN). MS (ESI): *m/z* 290.1 [M + K]⁺.

4·S: R = *n*-butyl ; R' = phenyl.

The same procedure was used with KHMDS (0.202 g, 1.01 mmol), **4·HCl** (0.300 g, 1.01 mmol) and S₈ (0.130 g, 0.51 mmol). The product was isolated as an orange solid. Yield: 80%. Anal. Calc. for C₁₅H₂₀N₂S₂ (292.46): C, 61.60; H, 6.89; N, 9.58. Found: C, 61.36; H, 6.42; N, 10.01. FTIR: $\nu_{\text{max}}(\text{solid})/\text{cm}^{-1}$: 3133br, 3053br, 2957br, 2930br, 2871br, 1667w, 1582w, 1517w, 1480sh, 1439m, 1412s, 1380w, 1358w, 1327w, 1264w, 1230m, 1114m, 1087w,

1021m, 942w, 876w, 732vs, 690s, 674m. ^1H NMR (CDCl_3 , 300 MHz) δ : 0.94 (3H, t, $^3J = 7.5$ Hz, CH_3 butyl), 1.35 (2H, m, CH_2CH_3), 1.71 (2H, m, $\text{CH}_2\text{CH}_2\text{CH}_3$), 3.37 (2H, t, $^3J = 6.6$ Hz, $\text{NCH}_2\text{CH}_2\text{S}$), 3.98 (2H, t, $^3J = 7.5$ Hz, $\text{NCH}_2\text{CH}_2\text{CH}_2$), 4.22 (2H, t, $^3J = 6.6$ Hz, $\text{NCH}_2\text{CH}_2\text{S}$), 6.59 and 6.65 (2H, AB spin system, $^3J = 2.4$ Hz, $\text{CH}=\text{CH}$), 7.15-7.39 (5H, m, H arom). $^{13}\text{C}\{\text{H}\}$ NMR (CDCl_3 , 75.5 MHz) δ : 13.72 (CH_3), 19.83 (CH_2CH_3), 30.95 ($\text{NCH}_2\text{CH}_2\text{S}$), 31.67 ($\text{NCH}_2\text{CH}_2\text{CH}_2$), 47.43 ($\text{NCH}_2\text{CH}_2\text{CH}_2$), 47.62 ($\text{NCH}_2\text{CH}_2\text{S}$), 116.33, 117.75 ($\text{CH}=\text{CH}$), 125.52 (*C para*-phenyl), 129.11 (*C meta*-phenyl), 129.14 (*C ortho*-phenyl), 134.83 (*C ipso*-phenyl), 161.60 (NCN). MS (ESI): m/z 332.2 [$\text{M} + \text{K}$] $^+$.

Synthesis of the Silver Complexes **5·AgI - 8·AgI**

5·AgI: R = 2,4,6-trimethylphenyl ; R' = ethyl.

The imidazolium iodide **5·HI** (0.080 g, 0.199 mmol) was dissolved in dry CH_2Cl_2 and solid Ag_2O (0.046 g, 0.199 mmol) was added under nitrogen. The reaction mixture was stirred for 2 h in the dark at room temperature. Then the suspension was filtered through a Celite pad, and the solvent was evaporated under reduced pressure to give the product as a light-sensitive white solid. Yield: 88%. Anal. Calc. for $\text{C}_{16}\text{H}_{22}\text{AgIN}_2\text{S}$ (509.20): C, 37.74; H, 4.35; N, 5.50. Found: C, 37.55; H, 4.52; N, 5.31. FTIR: $\nu_{\text{max}}(\text{solid})/\text{cm}^{-1}$: 3116br, 3086br, 2962m, 2914m, 2862br, 2733br, 1607w, 1558w, 1545w, 1486m, 1444m, 1408m, 1375w, 1352w, 1300sh, 1259s, 1223m, 1200w, 1152w, 1088s, 1065s, 1015vs, 968sh, 934w, 851m, 797vs, 733vs, 684m, 667m. ^1H NMR (CDCl_3 , 300 MHz) δ : 1.19 (3H, t, $^3J = 7.4$ Hz, SCH_2CH_3), 1.87 (6H, s, 2 CH_3 *ortho*-Mes), 2.33 (3H, s, CH_3 *para*-Mes), 2.46 (2H, q, $^3J = 7.4$ Hz, SCH_2CH_3), 2.95 (2H, t, $^3J = 6.6$ Hz, $\text{NCH}_2\text{CH}_2\text{S}$), 4.43 (2H, t, $^3J = 6.3$ Hz, $\text{NCH}_2\text{CH}_2\text{S}$), 6.88 and 7.42 (2H, AB spin system, $^3J = 1.7$ Hz, $\text{CH}=\text{CHNCH}_2$ and $\text{MesNCH}=\text{CH}$), 6.90 (2H, s, 2H *meta*-Mes). $^{13}\text{C}\{\text{H}\}$ NMR (CDCl_3 , 75.5 MHz) δ : 14.89 (SCH_2CH_3), 17.77 (2 CH_3 *ortho*-Mes), 21.16 (CH_3 *para*-Mes), 26.68 (SCH_2CH_3), 33.43 ($\text{NCH}_2\text{CH}_2\text{S}$), 51.61 ($\text{NCH}_2\text{CH}_2\text{S}$), 122.04, 122.33 ($\text{CH}=\text{CH}$), 129.22 (2 CH *meta*-Mes), 134.90 (2 *C ortho*-Mes), 135.58 (*C ipso*-Mes), 139.16 (*C para*-Mes), 183.26 (NCN). MS (ESI): m/z 381.1 [$\text{M} - \text{I}$] $^+$.

The silver cluster $[\mathbf{5}\cdot(\text{AgI})_2]_2$ was synthesized using the same procedure, with further addition of AgI (0.047 g, 0.199 mmol). This compound is poorly soluble in organic solvents, the ^1H NMR spectrum recorded shows the same pattern as that of **5·AgI**. The ESI-MS spectrum shows a signal corresponding to $[(\mathbf{5}\cdot(\text{AgI})_2)_2 - \text{I}]^+$ in accordance with a structure being partially retained in solution.

MS (ESI): m/z 1487.5 [$\text{M} - \text{I}$] $^+$. Far FT-IR $\nu_{\text{max}}(\text{crystals})/\text{cm}^{-1}$: 236vs ($\mu_2\text{-I}$), 154vs ($\mu_3\text{-I}$).

6·AgI: R = 2,6-diisopropylphenyl ; R' = ethyl.

The same procedure was used with **6·HI** (0.110 g, 0.25 mmol) and Ag₂O (0.057 g, 0.25 mmol). The product was isolated as a light-sensitive white solid. Yield: 84%. Anal. Calc. for C₁₉H₂₈AgIN₂S (551.28): C, 41.40; H, 5.12; N, 5.08. Found: C, 41.08; H, 5.26; N, 4.88. FTIR: $\nu_{\text{max}}(\text{solid})/\text{cm}^{-1}$: 2963m, 2928m, 2870br, 1460m, 1416w, 1386w, 1364w, 1305w, 1261m, 1219w, 1191w, 1105m, 1072m, 1059m, 1024m, 938w, 874sh, 853vs, 806s, 762m, 741m, 691w, 670w. ¹H NMR (CDCl₃, 300 MHz) δ : 0.92 and 1.06 (2 x 6H, 2 d, ³J = 6.6 Hz, 2 CH(CH₃)₂), 1.18 (3H, t, ³J = 7.3 Hz, SCH₂CH₃), 2.26 (2H, sept, ³J = 6.8 Hz, 2 CH(CH₃)₂), 2.49 (2H, q, ³J = 7.2 Hz, SCH₂CH₃), 2.96 (2H, br, NCH₂CH₂S), 4.31 (2H, br, NCH₂CH₂S), 6.95 and 7.43 (2H, AB spin system, ³J = 1.5 Hz, CH=CHNCH₂ and DiipNCH=CH), 7.17 (2H, d, ³J = 7.8 Hz, 2H meta-Diip), 7.41 (1H, t, ³J = 7.8 Hz, H para-Diip)., ¹³C{¹H} NMR (CDCl₃, 75.5 MHz) δ : 14.84 (SCH₂CH₃), 24.04, 24.20 (2 CHCH₃), 24.57 (SCH₂CH₃), 28.08 (2 CHCH₃), 33.49 (NCH₂CH₂S), 51.38 (NCH₂CH₂S), 124.16, 124.61 (CH=CH), 129.28 (C ipso-Diip), 130.41 (CH meta-Diip), 134.68 (CH para-Diip), 145.82 (C ortho-Diip), 181.48 (NCN). MS (ESI): *m/z* 423.1 [M - I]⁺.

7·AgI: R = 2,4,6-trimethylphenyl ; R' = phenyl.

The same procedure was used with **7·HI** (0.120 g, 0.27 mmol) and Ag₂O (0.062 g, 0.27 mmol). The product was isolated as a light-sensitive white solid. Yield: 91%. Anal. Calc. for C₂₀H₂₂AgIN₂S (557.24): C, 43.11; H, 3.98; N, 5.03. Found: C, 42.73; H, 4.10; N, 4.88. FTIR: $\nu_{\text{max}}(\text{solid})/\text{cm}^{-1}$: 3150br, 2965m, 2929br, 2871br, 1583w, 1564w, 1549w, 1459m, 1440m, 1415w, 1387w, 1366w, 1309w, 1264w, 1217w, 1188m, 1105m, 1088w, 1072m, 1059m, 1025w, 937w, 875sh, 828vs, 737vs, 692s, 671s. ¹H NMR (CDCl₃, 300 MHz) δ : 1.79 (6H, s, 2 CH₃ ortho-Mes), 2.30 (3H, s, CH₃ para-Mes), 3.32 (2H, t, ³J = 6.0 Hz, NCH₂CH₂S), 4.43 (2H, t, ³J = 6.0 Hz, NCH₂CH₂S), 6.80 and 7.36 (2H, AB spin system, ³J = 1.6 Hz, CH=CHNCH₂ and MesNCH=CH), 6.84 (2H, s, 2H meta-Mes), 7.24 – 7.26 (5H, m, H aromatics). ¹³C{¹H} NMR (CDCl₃, 75.5 MHz) δ : 17.87 (2 CH₃ ortho-Mes), 21.21 (CH₃ para-Mes), 35.62 (NCH₂CH₂S), 50.94 (NCH₂CH₂S), 122.19, 122.53 (CH=CH), 126.60 (CH para-Ph), 129.16 (2 CH meta-Ph), 129.32 (2 CH meta-Mes), 129.42 (2 CH ortho-Ph), 134.91 (C ipso-Mes), 134.98 (2 C ortho-Mes), 135.64 (C ipso-Ph), 139.01 (C para-Mes), 183.10 (NCN). MS (ESI): *m/z* 431.1 [M - I]⁺.

8·AgI: R = 2,6-diisopropylphenyl ; R' = phenyl.

The same procedure was used with **8·HI** (0.100 g, 0.20 mmol) and Ag₂O (0.047 g, 0.20 mmol). The product was isolated as a light-sensitive white solid.

Yield: 68%. Anal. Calc. for C₂₃H₂₈AgIN₂S (599.32): C, 46.09; H, 4.71; N, 4.67. Found: C, 45.62; H, 4.33; N, 5.04. FTIR: $\nu_{\text{max}}(\text{solid})/\text{cm}^{-1}$: 3143br, 2962s, 2927m, 2869m, 1591w, 1563w, 1549w, 1458s, 1414s, 1363m, 1261m, 1218w, 1182w, 1105m, 1072m, 1059s, 960w, 938w, 876m, 833vs, 761w, 737m, 687w. ¹H NMR (CDCl₃, 300 MHz) δ : 0.86 and 1.07 (2 x 6H, 2 d, ³J = 6.9 Hz, 2 CH(CH₃)₂), 2.33 (2H, sept, ³J = 6.9 Hz, 2 CH(CH₃)₂), 3.04 (2H, br, NCH₂CH₂S), 4.28 (2H, br, NCH₂CH₂S), 7.02 and 7.54 (2H, AB spin system, ³J = 1.8 Hz, CH=CHNCH₂ and DiipNCH=CH), 7.13 (2H, d, ³J = 7.5 Hz, 2H meta-Diip), 7.21 – 7.28 (5H, m, H aromatics), 7.43 (1H, t, ³J = 7.5 Hz, H para-Diip). MS (ESI): *m/z* 473.1 [M - I]⁺.

Synthesis of the Mono-NHC Chelated Palladium Dichloride Complexes 10 – 12:

The low solubility of these compounds in organic solvents prevented recording of their ¹³C{¹H} NMR spectra. Two synthetic methods, routes A and B, are detailed below.

Route A: the Transmetalation Reaction. The imidazolium chloride was dissolved in dry CH₂Cl₂ and solid Ag₂O was added under nitrogen. The reaction mixture was stirred for 2 h in the dark at room temperature. Then the suspension was filtered through a Celite pad under nitrogen, and the resulting clear solution was slowly added to a suspension of the desired palladium precursor. A white solid precipitated rapidly. The suspension was then filtered through Celite and the solvent was evaporated under reduced pressure. The resulting solid was then washed with pentane (2 x 25 mL) and crystallized from a dichloromethane/pentane solution.

Route B: *In Situ* Deprotonation of a Zwitterionic Intermediate. The zwitterionic precursor (see below complexes **13 – 16**) and Cs₂CO₃ were placed in a Schlenk tube under nitrogen and MeCN was added. The reaction mixture was heated at 60 °C for 3 h and then allowed to cool to room temperature. After filtration through a Celite pad, the solvent was evaporated under reduced pressure. The resulting solid was washed with pentane (2 x 20 mL) and recrystallized from a dichloromethane/pentane solution.

Synthesis of **9**: R = methyl ; R' = ethyl.

Route A: see ref. 18e

Route B: Zwitterion **13** (0.070 g, 0.18 mmol) and Cs₂CO₃ (0.059 g, 0.18 mmol). The product was isolated as a yellow solid. Yield: 76%.

Synthesis of **10**: R = *n*-butyl ; R' = ethyl.

Route **A**: **2**·HCl (0.250 g, 1.00 mmol), Ag₂O (0.233 g, 1.00 mmol) and [PdCl₂(cod)] (0.287 g, 1.00 mmol). The product was isolated as a yellow solid. Yield: 80%. Anal. Calc. for C₁₁H₂₀Cl₂N₂PdS (389.68): C, 33.90; H, 5.17; N, 7.19. Found: C, 33.32; H, 5.44; N, 6.87. FTIR: $\nu_{\text{max}}(\text{solid})/\text{cm}^{-1}$: 3162w, 3124w, 3097w, 3047w, 2958m, 2940m, 2930m, 2869w, 1581w, 1572w, 1550w, 1479w, 1460m, 1438m, 1420s, 1381w, 1354w, 1275m, 1231s, 1202w, 1158w, 1129w, 1107w, 1107w, 1087w, 1074w, 1022m, 960w, 895w, 869w, 833w, 826w, 799w, 758m, 735vs, 726vs, 704vs, 688vs, 669s, 312vs ($\nu_{\text{Pd-Cl}}$), 296vs ($\nu_{\text{Pd-Cl}}$). ¹H NMR (CD₂Cl₂, 300 MHz) δ : 0.98 (3H, t, ³J = 7.5 Hz, CH₃ butyl), 1.40 (5H, m, SCH₂CH₃ and NCH₂CH₂CH₂CH₃), 1.91 (2H, m, NCH₂CH₂CH₂CH₃), 2.55 (2H, br, SCH₂CH₃), 2.89 (2H, br, NCH₂CH₂S), 4.52 (4H, br, NCH₂CH₂S and NCH₂CH₂CH₂CH₃), 7.01 and 7.20 (2H, AB spin system, ³J = 1.8 Hz, CH=CH). MS (ESI): *m/z* 355.0 [M - Cl]⁺.

Route **B**: Zwitterion **14** (0.100 g, 0.23 mmol) and Cs₂CO₃ (0.076 g, 0.23 mmol). Yield: 74%.

Synthesis of **11**: R = methyl ; R' = phenyl.

Route **A**: **3**·HCl (0.250 g, 0.98 mmol), Ag₂O (0.227 g, 0.98 mmol) and [PdCl₂(cod)] (0.280 g, 0.98 mmol). The product was isolated as a yellow solid. Yield: 77%. Anal. Calc. for C₁₂H₁₄Cl₂N₂PdS (395.64): C, 36.43; H, 3.57; N, 7.08. Found: C, 35.78; H, 3.22; N, 7.42. FTIR: $\nu_{\text{max}}(\text{solid})/\text{cm}^{-1}$: 3162w, 3124w, 3055w, 2946br, 1582w, 1572w, 1479w, 1466m, 1438s, 1405m, 1356w, 1337w, 1279w, 1230s, 1185sh, 1161w, 1120sh, 1087m, 1023m, 977w, 893w, 835w, 765sh, 742s, 727vs, 700s, 686vs, 672s, 311vs ($\nu_{\text{Pd-Cl}}$), 296vs ($\nu_{\text{Pd-Cl}}$). ¹H NMR (CD₂Cl₂, 300 MHz) δ : 3.06 (2H, br, NCH₂CH₂S), 3.91 (3H, br s, CH₃), 4.63 (2H, br, NCH₂CH₂S), 6.88 (1H, br s, CH=CH), 7.04 (1H, br s, CH=CH), 7.37-7.45 (5H, m, H phenyl). MS (ESI): *m/z* 361.0 [M - Cl]⁺.

Route **B**: Zwitterion **15** (0.100 g, 0.23 mmol) and Cs₂CO₃ (0.75 g, 0.23 mmol). Yield: 71%.

Synthesis of **12**: R = *n*-butyl ; R' = phenyl.

Route **A**: **4**·HCl (0.250 g, 0.84 mmol), Ag₂O (0.195 g, 0.84 mmol) and [PdCl₂(cod)] (0.240 g, 0.84 mmol). The product was isolated as a yellow solid. Yield: 84%. Anal. Calc. for C₁₅H₂₀Cl₂N₂PdS (437.72): C, 41.16; H, 4.61; N, 6.40. Found: C, 41.48; H, 4.39; N, 6.09. FTIR: $\nu_{\text{max}}(\text{solid})/\text{cm}^{-1}$: 3158w, 3128w, 3099w, 3058w, 2956m, 2929m, 2870w, 1734w, 1719w, 1580w, 1563w, 1472m, 1457m, 1441s, 1425s, 1414m, 1377w, 1356w, 1336w, 1283w, 1240m, 1218w, 1197w, 1159w, 1134w, 1109w, 1059w, 1024w, 999w, 955w, 870w, 739vs, 708w, 686vs, 295vs ($\nu_{\text{Pd-Cl}}$). ¹H NMR (CD₂Cl₂, 300 MHz) δ : 0.88 (3H, t, ³J = 7.3 Hz,

CH_3), 1.29 (2H, m, CH_2CH_3), 1.65 (2H, br m, $\text{CH}_2\text{CH}_2\text{CH}_3$), 3.17 (2H, br, $\text{NCH}_2\text{CH}_2\text{S}$), 4.44 (2H, br, $\text{NCH}_2\text{CH}_2\text{CH}_2$), 4.65 (2H, br, $\text{NCH}_2\text{CH}_2\text{S}$), 7.00 (1H, br s, $\text{CH}=\text{CH}$), 7.18 (H, br s, $\text{CH}=\text{CH}$), 7.37-7.45 (5H, m, H phenyl). MS (ESI): m/z 403.0 [M - Cl]⁺.

Route **B**: Zwitterion **16** (0.120 g, 0.25 mmol) and Cs_2CO_3 (0.082 g, 0.25 mmol). Yield: 69%.

Synthesis of the Zwitterionic Palladium Complexes **13 – 16**:

Because of their low solubility in organic solvents, recording of the $^{13}\text{C}\{\text{H}\}$ NMR spectra of complexes **13 – 15** was prevented.

13: R = methyl ; R' = ethyl.

Solid [PdCl₂(cod)] (0.276 g, 0.97 mmol) was added to a solution of **1**·HCl (0.200 g, 0.97 mmol) in dichloromethane. The reaction mixture was stirred for 2 h at room temperature, until a yellow precipitate appeared. The solvent was removed *via* canula, and the solid washed with pentane (2 x 20 mL) and dried under vacuum. The product was isolated as a yellow solid. Yield: 87%. Anal. Calc. for C₈H₁₅Cl₃N₂PdS (384.06): C, 25.02; H, 3.94; N, 7.29. Found: C, 25.30; H, 3.64; N, 7.44. FTIR: $\nu_{\text{max}}(\text{solid})/\text{cm}^{-1}$: 3160w, 3090s, 3071s, 3007w, 2958w, 2924sh, 2942w, 2866w, 1639w, 1574m, 1558s, 1450s, 1427s, 1375m, 1330w, 1314w, 1285w, 1272w, 1250w, 1225m, 1165vs, 1122m, 1090sh, 1061m, 1046w, 1016m, 991w, 970w, 856vs, 798m, 767vs, 752s, 711w, 347vs ($\nu_{\text{Pd-Cl}}$), 306vs ($\nu_{\text{Pd-Cl}}$), 286vs ($\nu_{\text{Pd-Cl}}$). ^1H NMR (d_6 -DMSO, 300 MHz) δ : 1.19 (3H, t, $^3J = 7.5$ Hz, SCH_2CH_3), 2.57 (overlapped with solvent peak, SCH_2CH_3), 2.99 (2H, t, $^3J = 6.6$ Hz, $\text{NCH}_2\text{CH}_2\text{S}$), 3.89 (3H, s, NCH_3), 4.37 (2H, t, $^3J = 6.6$ Hz, $\text{NCH}_2\text{CH}_2\text{S}$), 7.73 (1H, br s, $\text{CH}=\text{CH}$), 7.82 (1H, br s, $\text{CH}=\text{CH}$), 9.22 (1H, br s, NCHN). MS (ESI): m/z 407.9 [M + Na]⁺, 348.9 [M - Cl]⁺.

14: R = *n*-butyl ; R' = ethyl.

The same procedure was used with [PdCl₂(cod)] (0.229 g, 0.80 mmol) and **2**·HCl (0.200 g, 0.80 mmol). The product was isolated as a yellow solid. Yield: 89%. Anal. Calc. for C₁₁H₂₁Cl₃N₂PdS (426.14): C, 31.00; H, 4.97; N, 6.57. Found: C, 30.31; H, 5.17; N, 6.09. FTIR: $\nu_{\text{max}}(\text{solid})/\text{cm}^{-1}$: 3136br, 3103s, 3078m, 2964m, 2930m, 2875br, 2861br, 1620w, 1564vs, 1451s, 1414s; 1405m, 1371m, 1355m, 1338w, 1308m, 1299w, 1268m, 1245w, 1226w, 1205w, 1178vs, 1157vs, 1122w, 1111w, 1069w, 1041w, 1005w, 956w, 891w, 838vs, 825s, 780m, 756vs, 749s, 344vs ($\nu_{\text{Pd-Cl}}$), 312vs ($\nu_{\text{Pd-Cl}}$), 286vs ($\nu_{\text{Pd-Cl}}$). ^1H NMR (d_6 -DMSO, 300 MHz) δ : 0.90 (3H, t, $^3J = 7.5$ Hz, CH_3 butyl), 1.17 (3H, t, $^3J = 7.5$ Hz, SCH_2CH_3), 1.26 (2H, m, $\text{NCH}_2\text{CH}_2\text{CH}_2\text{CH}_3$), 1.78 (2H, m, $\text{NCH}_2\text{CH}_2\text{CH}_2\text{CH}_3$), 2.54 (overlapped with solvent peak, SCH_2CH_3), 2.90 (2H, t, $^3J = 6.0$ Hz, $\text{NCH}_2\text{CH}_2\text{S}$), 4.20 (2H, t, $^3J = 7.2$ Hz,

$\text{NCH}_2\text{CH}_2\text{CH}_2\text{CH}_3$), 4.36 (2H, t, $^3J = 6.3$ Hz, $\text{NCH}_2\text{CH}_2\text{S}$), 7.81 (2H, br s, $\text{CH}=\text{CH}$), 9.23 (1H, br s, NCHN). MS (ESI): m/z 450.0 [M + Na]⁺, 392.0 [M - Cl]⁺.

15: R = methyl ; R' = phenyl.

The same procedure was used with [PdCl₂(cod)] (0.224 g, 0.79 mmol) and **3**·HCl (0.200 g, 0.79 mmol). The product was isolated as a yellow solid. Yield: 84%. Anal. Calc. for C₁₂H₁₅Cl₃N₂PdS (432.10): C, 33.35; H, 3.50; N, 6.48. Found: C, 32.94; H, 3.39; N, 7.01. FTIR: $\nu_{\text{max}}(\text{solid})/\text{cm}^{-1}$: 3155br, 3123w, 3111m, 3075m, 2982m, 2935w, 1618w, 1572m, 1479w, 1450w, 1443m, 1432m, 1423sh, 1404w, 1352m, 1313m, 1299m, 1275w, 1248w, 1176vs, 1170vs, 1110m, 1072w, 1047w, 1020w, 1000w, 954w, 924w, 890w, 838s, 753vs, 690vs, 668w, 335vs ($\nu_{\text{Pd-Cl}}$), 306vs ($\nu_{\text{Pd-Cl}}$), 287vs ($\nu_{\text{Pd-Cl}}$). ¹H NMR (*d*₆-DMSO, 300 MHz) δ : 3.49 (2H, t, $^3J = 6.6$ Hz, $\text{NCH}_2\text{CH}_2\text{S}$), 3.81 (3H, s, NCH_3), 4.38 (2H, t, $^3J = 6.6$ Hz, $\text{NCH}_2\text{CH}_2\text{S}$), 7.23-7.40 (5H, m, H phenyl), 7.62 (1H, br s, $\text{CH}=\text{CH}$), 7.74 (1H, br s, $\text{CH}=\text{CH}$), 9.10 (1H, br s, NCHN). MS (ESI): m/z 455.9 [M + Na]⁺, 397.9 [M - Cl]⁺.

16: R = *n*-butyl ; R' = phenyl.

The same procedure was used with [PdCl₂(cod)] (0.192 g, 0.67 mmol) and **4**·HCl (0.200 g, 0.67 mmol). The product was isolated as a yellow solid. Yield: 81%. Anal. Calc. for C₁₅H₂₁Cl₃N₂PdS (474.18): C, 37.99; H, 4.46; N, 5.91. Found: C, 37.48; H, 4.23; N, 5.70. FTIR: $\nu_{\text{max}}(\text{solid})/\text{cm}^{-1}$: 3130w, 3100m, 3056m, 2984sh, 2954sh, 2934w, 2859br, 1619w, 1577w, 1562s, 1468w, 1453m, 1440s, 1411w, 1382w, 1367w, 1346w, 1333w, 1311w, 1300w, 1249w, 1215w, 1207w, 1169s, 1151s, 1113w, 1101w, 1071w, 1041sh, 1022w, 1001w, 967w, 949w, 917w, 895sh, 882w, 855m, 826sh, 806sh, 743vs, 688s, 332vs ($\nu_{\text{Pd-Cl}}$), 305vs ($\nu_{\text{Pd-Cl}}$), 287vs ($\nu_{\text{Pd-Cl}}$). ¹H NMR (*d*₆-DMSO, 300 MHz) δ : 0.90 (3H, t, $^3J = 7.5$ Hz, CH₃ butyl), 1.25 (2H, m, CH_2CH_3), 1.73 (2H, m, $\text{CH}_2\text{CH}_2\text{CH}_3$), 3.50 (2H, t, $^3J = 6.3$ Hz, $\text{NCH}_2\text{CH}_2\text{S}$), 4.13 (2H, t, $^3J = 7.2$ Hz, $\text{NCH}_2\text{CH}_2\text{CH}_2$), 4.38 (2H, t, $^3J = 6.3$ Hz, $\text{NCH}_2\text{CH}_2\text{S}$), 7.22-7.39 (5H, m, H phenyl), 7.74 (1H, pseudo t, $^3J = ^4J = 1.5$ Hz, $\text{CH}=\text{CH}$), 7.79 (1H, pseudo t, $^3J = ^4J = 1.5$ Hz, $\text{CH}=\text{CH}$), 9.18 (1H, br s, NCHN). ¹³C{¹H} NMR (*d*₆-DMSO, 75.5 MHz) δ : 13.75 (CH₃), 19.20 (NCH₂CH₂CH₂CH₃), 31.75 (NCH₂CH₂S), 32.69 (NCH₂CH₂CH₂CH₃), 48.33 (NCH₂CH₂CH₂CH₃), 49.02 (NCH₂CH₂S), 122.84, 123.11 (CH=CH), 126.99 (*C para*-phenyl), 129.32 (*C meta*-phenyl), 129.70 (*C ortho*-phenyl), 136.86 (*C ipso*-phenyl), NCN resonance not observed. MS (ESI): m/z 498.0 [M + Na]⁺, 440.0 [M - Cl]⁺.

Synthesis of the Bis-NHC Palladium Dichloride Complexes 18 – 20.

The transmetalation reaction procedure described above (Route A) was followed for these complexes.

18: R = *n*-butyl ; R' = ethyl.

2·HCl (0.200 g, 0.80 mmol), Ag₂O (0.186 g, 0.80 mmol) and [PdCl₂(cod)] (0.115 g, 0.40 mmol). The product was isolated as a yellow solid. Yield: 74%. Anal. Calc. for C₂₂H₄₀Cl₂N₄PdS₂ (602.03): C, 43.89; H, 6.70; N, 9.31. Found: C, 43.48; H, 6.44; N, 9.62. FTIR: ν_{max} (solid)/cm⁻¹: 3163br, 3126br, 3048br, 2959br, 2940br, 2872br, 2360w, 2162w, 2050w, 1582w, 1479m, 1461m, 1439m, 1421s, 1381m, 1355m, 1276m, 1232m, 1203w, 1159w, 1130w, 1107w, 1088w, 1024m, 935w, 896w, 871w, 833w, 800w, 759m, 736vs, 728vs, 705vs, 689vs, 669m, 340vs ($\nu_{\text{Pd-Cl}}$). ¹H NMR (CD₂Cl₂, 300 MHz) δ : 1.05 (3H, t, ³J = 7.5 Hz, CH₃ butyl), 1.23 (3H, t, ³J = 7.5 Hz, SCH₂CH₃), 1.51 (2H, m, NCH₂CH₂CH₂CH₃), 2.01 (2H, m, NCH₂CH₂CH₂CH₃), 2.69 (2H, q, ³J = 7.5 Hz, SCH₂CH₃), 3.53 (2H, br, NCH₂CH₂S), 4.51 (2H, q, ³J = 7.2 Hz, NCH₂CH₂CH₂CH₃), 4.66 (2H, br, NCH₂CH₂S), 6.91 and 7.09 (2H, AB spin system, ³J = 1.8 Hz, CH=CH). ¹³C{¹H} NMR (CD₂Cl₂, 300 MHz) δ : 13.73 (CH₃ butyl), 14.75 (SCH₂CH₃), 20.04 (NCH₂CH₂CH₂CH₃), 26.18 (SCH₂CH₃), 31.08 (NCH₂CH₂S), 32.07 (NCH₂CH₂CH₂CH₃), 50.72 (NCH₂CH₂CH₂CH₃), 51.00 (NCH₂CH₂S), 118.93, 121.51 (CH=CH), NCN resonance not observed. MS (ESI): *m/z* 568.2 [M - Cl]⁺.

19: R = methyl ; R' = phenyl.

3·HCl (0.200 g, 0.79 mmol), Ag₂O (0.182 g, 0.79 mmol) and [PdCl₂(cod)] (0.112 g, 0.39 mmol). The product was isolated as a yellow solid. Yield: 72%. Anal. Calc. for C₂₄H₂₈Cl₂N₄PdS₂ (613.96): C, 46.95; H, 4.60; N, 9.13. Found: C, 50.24; H, 4.58; N, 9.41. FTIR: ν_{max} (solid)/cm⁻¹: 3161br, 3124br, 3098br, 3055br, 2947br, 1582w, 1572w, 1535w, 1479w, 1467m, 1439m, 1406m, 1356w, 1338w, 1279w, 1260w, 1230m, 1162w, 1087s, 1022s, 953w, 893w, 875w, 834w, 798m, 742s, 727vs, 698s, 687vs, 657w, 337vs ($\nu_{\text{Pd-Cl}}$). ¹H NMR (CD₂Cl₂, 300 MHz) δ : 3.72 (2H, t, ³J = 6.9 Hz, NCH₂CH₂S), 4.08 (3H, s, NCH₃), 4.65 (2H, t, ³J = 6.9 Hz, NCH₂CH₂S), 6.82 and 6.88 (2H, AB spin system, ³J = 1.8 Hz, CH=CH), 7.18-7.46 (5H, m, H phenyl). MS (ESI): *m/z* 580.1 [M - Cl]⁺.

20: R = *n*-butyl ; R' = phenyl.

4·HCl (0.200 g, 0.67 mmol), Ag₂O (0.156 g, 0.67 mmol) and [PdCl₂(cod)] (0.096 g, 0.34 mmol). The product was isolated as a yellow solid. Yield: 76%. Anal. Calc. for C₃₀H₄₀Cl₂N₄PdS₂ (698.12): C, 51.61; H, 5.78; N, 8.03. Found: C, 52.02; H, 5.39; N, 7.66.

FTIR: $\nu_{\text{max}}(\text{solid})/\text{cm}^{-1}$: 3158br, 3123br, 3096br, 3055br, 2957s, 2929s, 2871m, 1582m, 1480m, 1464m, 1439m, 1423m, 1378w, 1356w, 1278w, 1232m, 1202w, 1158w, 1132w, 1088w, 1041w, 1024w, 736vs, 703s, 691vs, 668w, 347vs ($\nu_{\text{Pd-Cl}}$). ^1H NMR (CD₂Cl₂, 300 MHz) δ : 0.99 (3H, t, $^3J = 7.2$ Hz, CH₃ butyl), 1.45 (2H, m, NCH₂CH₂CH₂CH₃), 2.05 (2H, m, NCH₂CH₂CH₂CH₃), 3.72 (2H, q, $^3J = 6.9$ Hz, NCH₂CH₂S), 4.46 (2H, q, $^3J = 7.5$ Hz, NCH₂CH₂CH₂CH₃), 4.68 (2H, q, $^3J = 6.9$ Hz, NCH₂CH₂S), 6.82 and 6.88 (2H, AB spin system, $^3J = 1.8$ Hz, CH=CH), 7.16-7.42 (5H, m, H phenyl). $^{13}\text{C}\{\text{H}\}$ NMR (CD₂Cl₂, 75 MHz) δ : 13.60 (CH₃), 20.07 (NCH₂CH₂CH₂CH₃), 33.04 (NCH₂CH₂S), 34.33 (NCH₂CH₂CH₂CH₃), 49.91 (NCH₂CH₂CH₂CH₃), 50.58 (NCH₂CH₂S), 120.37, 121.41 (CH=CH), 126.24 (C *para*-phenyl), 129.09 (C *meta*-phenyl), 129.23 (C *ortho*-phenyl), 135.13 (C *ipso*-phenyl), 170.10 (NCN). MS (ESI): *m/z* 664.2 [M – Cl]⁺.

Synthesis of the Bis-NHC Dicationic Palladium Complexes 21 – 24.

The transmetalation reaction procedure described above (Route A) was followed for these complexes.

21: R = methyl ; R' = ethyl.

1·HCl (0.200 g, 0.97 mmol), Ag₂O (0.224 g, 0.97 mmol) and [Pd(NCMe)₄][BF₄]₂ (0.215 g, 0.48 mmol). The product was isolated as a light brown solid. Yield: 68%. Anal. Calc. for C₁₆H₂₈B₂F₈N₄PdS₂ (620.58): C, 30.97; H, 4.55; N, 9.03. Found: C, 30.39; H, 5.04; N, 8.76. FTIR: $\nu_{\text{max}}(\text{solid})/\text{cm}^{-1}$: 3166br, 3140br, 2966br, 2933br, 1628br, 1568w, 1543w, 1527w, 1474m, 1453m, 1411m, 1381w, 1363w, 1337w, 1286w, 1268w, 1244w, 1214w, 1172w, 1030vs, 877w, 848w, 752s, 688m, 679m, 659w. ^1H NMR (CD₃CN, 300 MHz) δ : 1.23 (3H, t, $^3J = 6.9$ Hz, SCH₂CH₃), 2.67 (2H, br, SCH₂CH₃), 2.96 (2H, br, NCH₂CH₂S), 3.86 (3H, s, NCH₃), 4.45 (2H, br, NCH₂CH₂S), 7.18 (1H, br s, CH=CH), 7.32 (1H, br s, CH=CH). $^{13}\text{C}\{\text{H}\}$ NMR (CD₃CN, 75 MHz) δ : 13.38 (SCH₂CH₃), 32.36 (SCH₂CH₃), 32.25 (NCH₂CH₂S), 38.20 (NCH₃), 50.59 (NCH₂CH₂S), 124.33, 125.86 (CH=CH), 157.82 (NCN).

22: R = *n*-butyl ; R' = ethyl.

2·HCl (0.200 g, 0.80 mmol), Ag₂O (0.186 g, 0.80 mmol) and [Pd(NCMe)₄][BF₄]₂ (0.179 g, 0.40 mmol). The product was isolated as a light brown solid. Yield: 67%. Anal. Calc. for C₂₂H₄₀B₂F₈N₄PdS₂ (704.74): C, 37.49; H, 5.72; N, 7.95. Found: C, 37.01; H, 5.30; N, 8.34. FTIR: $\nu_{\text{max}}(\text{solid})/\text{cm}^{-1}$: 3144br, 3112sh, 2961m, 2933m, 2874w, 1623br, 1565w, 1533w, 1457m, 1427m, 1379w, 1354w, 1241w, 1201w, 1162m, 1047vs, 1033vs, 875w, 849w, 750s, 691m. ^1H NMR (CD₂Cl₂, 300 MHz) δ : 0.85 (3H, t, $^3J = 7.5$ Hz, CH₃ butyl), 1.20 (3H, t, $^3J =$

7.5 Hz, SCH_2CH_3), 1.35 (2H, m, $\text{NCH}_2\text{CH}_2\text{CH}_2\text{CH}_3$), 1.84 (2H, m, $\text{NCH}_2\text{CH}_2\text{CH}_2\text{CH}_3$), 2.53 (2H, br q, SCH_2CH_3), 2.95 (2H, br t, $\text{NCH}_2\text{CH}_2\text{S}$), 4.17 (2H, br t, $\text{NCH}_2\text{CH}_2\text{CH}_2\text{CH}_3$), 4.37 (2H, br t, $\text{NCH}_2\text{CH}_2\text{S}$), 7.15 (2H, br s, $\text{CH}=\text{CH}$). $^{13}\text{C}\{\text{H}\}$ NMR (CD_2Cl_2 , 75 MHz) δ : 13.30 (CH_3 butyl), 14.19 (SCH_2CH_3), 19.79 ($\text{NCH}_2\text{CH}_2\text{CH}_2\text{CH}_3$), 25.62 (SCH_2CH_3), 31.35 ($\text{NCH}_2\text{CH}_2\text{S}$), 32.44 ($\text{NCH}_2\text{CH}_2\text{CH}_2\text{CH}_3$), 49.83 ($\text{NCH}_2\text{CH}_2\text{CH}_2\text{CH}_3$), 50.90 ($\text{NCH}_2\text{CH}_2\text{S}$), 122.64, 122.72 ($\text{CH}=\text{CH}$), 157.06 (NCN).

23: R = methyl ; R' = phenyl.

3·HCl (0.200 g, 0.79 mmol), Ag_2O (0.182 g, 0.79 mmol) and $[\text{Pd}(\text{NCMe})_4]\text{[BF}_4\text{]}_2$ (0.174 g, 0.39 mmol). The product was isolated as a light brown solid. Yield: 64%. Anal. Calc. for $\text{C}_{24}\text{H}_{28}\text{B}_2\text{F}_8\text{N}_4\text{PdS}_2$ (716.66): C, 40.22; H, 3.94; N, 7.82. Found: C, 40.68; H, 3.69; N, 8.16. FTIR: $\nu_{\text{max}}(\text{solid})/\text{cm}^{-1}$: 3168w, 3141w, 2956w, 2922w, 2851w, 1577w, 1544w, 1473m, 1442m, 1408m, 1359w, 1337w, 1284w, 1241w, 1206w, 1171w, 1031vs, 999vs, 887m, 847w, 742s, 686s. ^1H NMR (CD_2Cl_2 , 300 MHz) δ : 3.37 (2H, br t, $\text{NCH}_2\text{CH}_2\text{S}$), 4.33 (2H, br, $\text{NCH}_2\text{CH}_2\text{S}$), 4.84 (3H, br s, CH_3), 7.02-7.42 (7H, m, $\text{CH}=\text{CH}$ and H phenyl). $^{13}\text{C}\{\text{H}\}$ NMR (CD_2Cl_2 , 75 MHz) δ : 33.75 ($\text{NCH}_2\text{CH}_2\text{S}$), 37.54 (NCH_3), 51.38 ($\text{NCH}_2\text{CH}_2\text{S}$), 123.42, 123.54 ($\text{CH}=\text{CH}$), 127.21 (*C para*-phenyl), 129.38 (*C meta*-phenyl), 130.18 (*C ortho*-phenyl), 132.90 (*C ipso*-phenyl), 155.20 (NCN).

24: R = *n*-butyl ; R' = phenyl.

4·HCl (0.200 g, 0.67 mmol), Ag_2O (0.156 g, 0.67 mmol) and $[\text{Pd}(\text{NCMe})_4]\text{[BF}_4\text{]}_2$ (0.150 g, 0.34 mmol). The product was isolated as a light brown solid. Yield: 71%. Anal. Calc. for $\text{C}_{30}\text{H}_{40}\text{B}_2\text{F}_8\text{N}_4\text{PdS}_2$ (800.82): C, 44.99; H, 5.03; N, 7.00. Found: C, 45.39; H, 5.14; N, 6.67. FTIR: $\nu_{\text{max}}(\text{solid})/\text{cm}^{-1}$: 3149br, 3112sh, 2960w, 2932w, 2873w, 2113w, 1724w, 1564w, 1473m, 1458sh, 1442m, 1430w, 1381w, 1356w, 1338w, 1285w, 1242w, 1163w, 1049vs, 1034vs, 1000s, 846w, 745s, 688m. ^1H NMR (CD_2Cl_2 , 300 MHz) δ : 0.91 (3H, t, $^3J = 7.3$ Hz, CH_3), 1.30 (2H, m, CH_2CH_3), 1.78 (2H, br m, $\text{CH}_2\text{CH}_2\text{CH}_3$), 3.66 (2H, br, $\text{NCH}_2\text{CH}_2\text{S}$), 4.45 (2H, br, $\text{NCH}_2\text{CH}_2\text{CH}_2$), 4.78 (2H, br, $\text{NCH}_2\text{CH}_2\text{S}$), 7.23-7.45 (7H, m, $\text{CH}=\text{CH}$ and H phenyl). $^{13}\text{C}\{\text{H}\}$ NMR (CD_2Cl_2 , 75 MHz) δ : 15.08 (CH_3), 21.26 ($\text{NCH}_2\text{CH}_2\text{CH}_2\text{CH}_3$), 33.67 ($\text{NCH}_2\text{CH}_2\text{S}$), 34.95 ($\text{NCH}_2\text{CH}_2\text{CH}_2\text{CH}_3$), 51.82 ($\text{NCH}_2\text{CH}_2\text{CH}_2\text{CH}_3$), 52.76 ($\text{NCH}_2\text{CH}_2\text{S}$), 124.27, 125.38 ($\text{CH}=\text{CH}$), 130.96 (*C para*-phenyl), 131.70 (*C meta*-phenyl), 132.18 (*C ortho*-phenyl), 132.41 (*C ipso*-phenyl), NCN resonance not observed.

General Procedure for the Suzuki-Miyaura Cross-Coupling Reaction.

The catalyst precursor (0.02 mmol), phenyl boronic acid (146.3 mg, 1.20 mmol), and Cs₂CO₃ (651.6 mg, 2.00 mmol) were placed in a Schlenk tube, and DMSO (3 mL) was added under nitrogen. Then 4-bromotoluene (123.1 µL, 171.0 mg, 1.00 mmol) was added, and the reaction mixture was heated for 2 h at 60 °C. The reaction was then quenched by rapid cooling to room temperature, and the suspension was filtered through a Celite pad. The resulting solution was then analyzed by gas chromatography. All runs were repeated two times, and the value reported is an average of the two yields measured. The corresponding yields in 4-methyl-biphenyl are reported in Tables 1 and 3.

The same procedure was used with different solvents (3 mL) or different bases (2.00 mmol), and the corresponding yields in 4-methyl-biphenyl are reported in Table 2.

The same procedure was used with catalyst (0.01 mmol) or 4-chlorotoluene (118.3 µL, 126.6 mg, 1.00 mmol) as reagent instead of 4-bromotoluene, and the corresponding yields in 4-methyl-biphenyl are reported in Table 4.

X-ray Data Collection, Structure Solution and Refinement for All Compounds.

Suitable crystals for the X-ray analysis of all compounds were obtained as described above. The intensity data were collected on a Kappa CCD diffractometer³² (graphite monochromated MoK_α radiation, $\lambda = 0.71073 \text{ \AA}$) at 173(2) K. Crystallographic and experimental details for the structures are summarized in Table 5. The structures were solved by direct methods (SHELXS-97) and refined by full-matrix least-squares procedures (based on F^2 , SHELXL-97)³³ with anisotropic thermal parameters for all the non-hydrogen atoms. The hydrogen atoms were introduced into the geometrically calculated positions (SHELXS-97 procedures) and refined *riding* on the corresponding parent atoms, except for the H1 atom in the structure of **8·HPF₆**. For **8·HPF₆**, the PF₆ anion was found disordered in two positions with equal occupancy factors and with a F-P-F axis in common. The disorder could be refined unrestrained. For [5·(AgI)₂]₂, the mesityl group was disordered with very close images. It was not possible to define the atomic coordinates for the two images of this disorder. Instead, this group was refined with restrained anisotropic parameters. A MULTISCAN correction was applied.³⁴ CCDC 778208-778212 contain the supplementary crystallographic data for this paper that can be obtained free of charge from the Cambridge Crystallographic Data Center via www.ccdc.cam.ac.uk/data_request/cif.

Table 5. Crystallographic data for compounds **8·HPF₆**, **[5·(AgI)₂]₂**, **10**, **12** and **18**.

Compound	8·HPF₆	[5·(AgI)₂]₂	10	12	18
Formula	C ₂₃ H ₂₉ F ₆ N ₂ PS	C ₃₂ H ₄₄ Ag ₄ I ₄ N ₄ S ₂	C ₁₁ H ₂₀ Cl ₂ N ₂ PdS	C ₁₅ H ₂₀ Cl ₂ N ₂ PdS	C ₂₂ H ₄₀ Cl ₂ N ₄ PdS ₂
Formula weight	510.51	1487.92	389.65	437.69	602.00
Crystal system	Monoclinic	Triclinic	Triclinic	Triclinic	Triclinic
<i>a</i> /Å	11.1279(6)	9.535(7)	7.8280(3)	8.1019(6)	7.9669(5)
<i>b</i> /Å	19.1377(6)	9.860(5)	9.1978(5)	9.1229(6)	12.5972(6)
<i>c</i> /Å	15.6504(6)	11.870(8)	10.9310(6)	12.9251(8)	15.1836(6)
α°	90.00	91.40(3)	83.665(2)	91.079(4)	109.441(3)
β°	130.591(3)	104.55(3)	85.152(3)	101.680(4)	90.829(3)
γ°	90.00	95.90(4)	71.768(3)	112.159(4)	98.612(3)
V/Å ³	2530.95(22)	1073.0(12)	741.92(6)	861.66(10)	1417.37(12)
T/K	173(2)	173(2)	173(2)	173(2)	173(2)
Space group	<i>P</i> 2 ₁ / <i>c</i>	<i>P</i> -1	<i>P</i> -1	<i>P</i> -1	<i>P</i> -1
<i>Z</i>	4	1	2	2	2
μ/mm^{-1}	0.249	4.800	1.732	1.502	1.007
Meas. refl.	9812	5742	6134	5387	9715
Indep. refl	5211	3977	4310	3789	6457
R_{int}	0.0352	0.0228	0.0268	0.0256	0.0256
R_I ($I > 2\sigma(I)$)	0.0541	0.0451	0.0476	0.0394	0.0451
$wR(F^2)$	0.1353	0.0994	0.1223	0.0948	0.1089
($I > 2\sigma(I)$)					
R_I (all data)	0.0994	0.0757	0.0724	0.0641	0.0869
$wR(F^2)$	0.1554	0.1104	0.1448	0.1233	0.1387
(all data)					
S on F^2	1.052	1.072	1.090	1.140	1.060

References

- (1) (a) Lappert, M. F. *J. Organomet. Chem.* **1988**, *358*, 185; (b) Lappert, M. F. *J. Organomet. Chem.* **2005**, *690*, 5467.
- (2) Arduengo III, A. J.; Harlow, R. L.; Kline, M. *J. Am. Chem. Soc.* **1991**, *113*, 361.
- (3) (a) Lin, J. C. Y.; Huang, R. T. W.; Lee, C. S.; Bhattacharyya, A.; Hwang, W. S.; Lin, I. J. B. *Chem. Rev.* **2009**, *109*, 3561; (b) Hahn, F. E.; Jahnke, M. C. *Angew. Chem. Int. Ed.* **2008**, *47*, 3122; (c) Arduengo III, A. J.; Dias, H. V. R.; Calabrese, J. C.; Davidson, F. *Organometallics* **1993**, *12*, 3405.
- (4) Wang, H. M. J.; Lin, I. J. B. *Organometallics* **1998**, *17*, 972.
- (5) (a) de Frémont, P.; Marion, N.; Nolan, S. P. *Coord. Chem. Rev.* **2009**, *253*, 862; (b) Hahn, F. E.; Jahnke, M. C. *Angew. Chem. Int. Ed.* **2008**, *47*, 3122; (c) Hahn, F. E. *Angew. Chem. Int. Ed.* **2006**, *45*, 1348; (d) Scott, N. M.; Nolan, S. P. *Eur. J. Inorg. Chem.* **2005**, *1815*; (e) César, V.; Bellemin-Laponnaz, S.; Gade, L. H. *Chem. Soc. Rev.* **2004**, *619*; (f) Herrmann, W. A. *Angew. Chem. Int. Ed.* **2002**, *41*, 1290; (g) Bourissou, D.; Guerret, O.; Gabbaï, F. P.; Bertrand, G. *Chem. Rev.* **2000**, *100*, 39.
- (6) Jafarpour, L.; Nolan, S. P. *Adv. Organomet. Chem.* **2000**, *46*, 181.
- (7) (a) Miura, M. *Angew. Chem. Int. Ed.* **2004**, *43*, 2201; (b) Gillespie, J. A.; Dodds, D. L.; Kamer, P. C. J. *Dalton Trans.* **2010**, *39*, 2751.
- (8) (a) Kantchev, E. A. B.; O'Brien, C. J.; Organ, M. G. *Angew. Chem., Int. Ed.* **2007**, *46*, 2768; (b) Díez-González, S.; Nolan, S. P. *Top. Organomet. Chem.* **2007**, *21*, 47.
- (9) See e.g.: Fliedel, C.; Maisse-François, A.; Bellemin-Laponnaz, S. *Inorg. Chim. Acta* **2007**, *360*, 143.
- (10) Marion, N.; Nolan, S. P. *Acc. Chem. Res.* **2008**, *41*, 1440.
- (11) (a) Flores-Figueroa, A.; Pape, T.; Feldmann, K.-O.; Hahn, F. E. *Chem. Commun.* **2010**, *46*, 324; (b) Kaufhold, O.; Stasch, A.; Pape, T.; Hepp, A.; Edwards, P. G.; Newman, P. D.; Hahn, F. E. *J. Am. Chem. Soc.* **2009**, *131*, 306; (c) Flores-Figueroa, A.; Kaufhold, O.; Hepp, A.; Fröhlich, R.; Hahn, F. E. *Organometallics* **2009**, *28*, 6362; (d) Mata, J. A.; Poyatos, M.; Peris, E. *Coord. Chem. Rev.* **2007**, *251*, 841; (e) Pugh, D.; Danopoulos, A. A. *Coord. Chem. Rev.* **2007**, *251*, 610; (f) Kaufhold, O.; Stasch, A.; Edwards, P. G.; Hahn, F. E. *Chem. Commun.* **2007**, 1822.
- (12) (a) Huynh, H. V.; Jothibasu, R. *Eur. J. Inorg. Chem.* **2009**, *1926*; (b) Hahn, F. E.; Jahnke, M. C.; Pape, T. *Organometallics* **2007**, *26*, 150; (c) Nielsen, D. J.; Cavell, K. J.; Skelton, B. W.; White, A. H. *Inorg. Chim. Acta* **2006**, *359*, 1855; (d) Pugh, D.; Wright, J. A.; Freeman, S.; Danopoulos,

- A. A. *Dalton Trans.* **2006**, 775; (e) Danopoulos, A. A.; Wright, J. A.; Motherwell, W. B.; Ellwood, S. *Organometallics* **2004**, 23, 4807; (f) Hahn, F. E.; Jahnke, M. C.; Gomez-Benitez, V.; Morales-Morales, D.; Pape, T. *Organometallics* **2005**, 24, 6458; (g) McGuinness, D. S.; Gibson, V. C.; Steed, J. W. *Organometallics* **2004**, 23, 6288; (h) Danopoulos, A. A.; Tulloch, A. A. D.; Winston, S.; Eastham, G.; Hursthouse, M. B. *Dalton Trans.* **2003**, 1009; (i) Miecznikowski, J. R.; Gründemann, S.; Albrecht, M.; Megret, C.; Clot, E.; Faller, J. W.; Eisenstein, O.; Crabtree, R. H. *Dalton Trans.* **2003**, 831; (j) Poyatos, M.; Mata, J. A.; Falomir, E.; Crabtree, R. H.; Peris, E. *Organometallics* **2003**, 22, 1110; (k) Simons, R. S.; Custer, P.; Tessier, C. A.; Youngs, W. J. *Organometallics* **2003**, 22, 1979; (l) Loch, J. A.; Albrecht, M.; Peris, E.; Mata, J.; Faller, J. W.; Crabtree, R. H. *Organometallics* **2002**, 21, 700; (m) Nielsen, D. J.; Cavell, K. J.; Skelton, B. W.; White, A. H. *Inorg. Chim. Acta* **2002**, 327, 116; (n) Peris, E.; Loch, J. A.; Mata, J.; Crabtree, R. H. *Chem. Commun.* **2001**, 201; (o) Tulloch, A. A. D.; Danopoulos, A. A.; Tizzard, G. J.; Coles, S. J.; Hursthouse, M. B.; Hay-Motherwell, R. S.; Motherwell, W. B. *Chem. Commun.* **2001**, 1270; (p) Gründemann, S.; Albrecht, M.; Loch, J. A.; Faller, J. W.; Crabtree, R. H. *Organometallics* **2001**, 20, 5485; (q) Hahn, F. E.; Foth, M. J. *Organomet. Chem.* **1999**, 585, 241; (r) Herrmann, W. A.; Elison, M.; Fischer, J.; Köcher, C.; Artus, G. R. J. *Angew. Chem. Int. Ed.* **1995**, 34, 2371.
- (13) (a) Jahnke, M. C.; Pape, T.; Hahn, F. E. *Eur. J. Inorg. Chem.* **2009**, 1960; (b) Jiménez, M. V.; Pérez-Torrente J. J.; Bartolomé, M. I.; Gierz, V.; Lahoz, F. J.; Oro, L. A. *Organometallics* **2008**, 27, 224; (c) Danopoulos, A. A.; Tsoureas, N.; Macgregor, S. A.; Smith, C. *Organometallics* **2007**, 26, 253; (d) Stylianides, N.; Danopoulos A. A.; Tsoureas, N. J. *Organomet. Chem.* **2005**, 690, 5948; (e) Gade, L. H.; César, V.; Bellemin-Laponnaz, S. *Angew. Chem. Int. Ed.* **2004**, 43, 1014; (f) César, V.; Bellemin-Laponnaz, S.; Gade, L. H. *Organometallics* **2002**, 21, 5204; (g) McGuinness, D. S.; Cavell, K. J. *Organometallics* **2000**, 19, 741.
- (14) (a) Jones, N. A.; Liddle, S. T.; Wilson, C.; Arnold, P. L. *Organometallics* **2007**, 26, 755; (b) Arnold, P. L.; Rodden, M.; Wilson, C. *Chem. Commun.* **2005**, 1743; (c) Clavier, H.; Coutable, L.; Toupet, L.; Guillemin, J. C.; Mauduit, M. J. *Organomet. Chem.* **2005**, 690, 5237; (d) Arnold, P. L.; Blake, A. J.; Wilson, C. *Chem. Eur. J.* **2005**, 11, 6095; (e) Arnold, P. L.; Rodden, M.; Davis, K. M.; Scarisbrick, A. C.; Blake, A. J. *Chem. Commun.* **2004**, 1612; (f) Waltman, A. W.; Grubbs, R. H. *Organometallics* **2004**, 23, 3105; (g) Arnold, P. L.; Scarisbrick, A. C.; Blake, A. J.; Wilson, C. *Chem. Commun.* **2001**, 2340.
- (15) (a) Danopoulos, A. A.; Tsoureas, N.; Macgregor, S. A.; Smith, C. *Organometallics* **2007**, 26, 253; (b) Lee, C. C.; Ke, W. C.; Chan, K. T.; Lai, C. L.; Hu, C. H.; Lee, H. M. *Chem. Eur. J.* **2007**, 13, 582; (c) Wolf, J.; Labande, A.; Daran, J.-C.; Poli, R. J. *Organomet. Chem.* **2006**, 691, 433; (d)

- Hahn, F. E.; Jahnke, M. C.; Pape, T. *Organometallics* **2006**, *25*, 5927; (e) Zeng, J. Y.; Hsieh, M.-H.; Lee, H. M. *J. Organomet. Chem.* **2005**, *690*, 5662; (f) Field, L. D.; Messerle, B. A.; Vuong, K. Q.; Turner, P. *Organometallics* **2005**, *24*, 4241; (g) Chiu, P. L.; Lee, H. M. *Organometallics* **2005**, *24*, 1692; (h) Lee, H. M.; Zeng, J. Y.; Hu, C.-H.; Lee, M.-T. *Inorg. Chem.* **2004**, *43*, 6822; (i) Yang, C.; Lee, H.M.; Nolan, S. P. *Org. Lett.* **2001**, *3*, 1511; (j) Tsoureas, N.; Danopoulos, A. A.; Tulloch, A. A. D.; Light, M. E. *Organometallics* **2003**, *22*, 4750.
- (16) Normand, A. T.; Cavell, K. J. *Eur. J. Inorg. Chem.* **2008**, 2781.
- (17) (a) Braunstein, P.; Naud, F. *Angew. Chem. Int. Ed.* **2001**, *40*, 680; (b) Braunstein, P. *J. Organomet. Chem.* **2004**, 689, 3953.
- (18) (a) Huynh, H.V.; Chew, Y. X. *Inorg. Chim.Acta* **2010**, *363*, 1979; (b) Liu, S. T.; Lee, C.-I.; Fu, C.-F.; Chen, C.-H.; Liu, Y.-H.; Elsevier, C. J.; Peng, S.-M.; Chen, J.-T. *Organometallics* **2009**, *28*, 6957; (c) Huynh, H. V.; Yuan, D.; Han, Y. *Dalton Trans.* **2009**, 7262; (d) Gandolfi, C.; Heckenroth, M.; Neels, A.; Laurenczy, G.; Albrecht, M. *Organometallics* **2009**, *28*, 5112; (e) Fliedel, C.; Schnee, G.; Braunstein, P. *Dalton Trans.* **2009**, 2474; (f) McGuinness, D. S.; Suttil, J. A.; Gardiner, M. G.; Davies, N. W. *Organometallics* **2008**, *27*, 4238; (g) Roseblade S. J.; Ros A.; Monge D.; Alcarazo M.; Alvarez E.; Lassaletta J. M.; Fernandez, R. *Organometallics* **2007**, *26*, 2570; (h) Wolf J.; Labande A.; Daran J.-C.; Poli, R. *Eur. J. Inorg. Chem.* **2007**, 5069; (i) Huynh H. V.; Yeo C. H.; Tan, G. K. *Chem. Commun.* **2006**, 3833 ; (j) Ros A.; Monge D.; Alcarazo M.; Alvarez E.; Lassaletta J. M.; Fernandez, R. *Organometallics* **2006**, *25*, 6039 ; (k) Seo H.; Park H. J.; Kim B. Y.; Lee J. H.; Son S. U.; Chung, Y. K. *Organometallics* **2003**, *22*, 618 ; (l) Matsumura, N.; Kawano, J.-I.; Fukunishi, N.; Inoue, H.; Yasui, M.; Iwasaki, F. *J. Am. Chem. Soc.* **1995**, *117*, 3623; (m) Sellmann D.; Prechtel W.; Knoch F.; Moll, M. *Organometallics* **1992**, *11*, 2346.
- (19) (a) Fliedel, C.; Sabbatini, A.; Braunstein, P. *Dalton Trans.*, **2010**, *39*, 8820; (b) Iglesias-Sigüenza, J.; Ros, A.; Diez, E.; Magriz, A.; Vazquez, A.; Alvarez, E.; Fernandez, R.; Lassaletta, J. M. *Dalton Trans.* **2009**, 8485.
- (20) (a) Cabeza, J. A.; Silva, I. D.; del Rio, I.; Sanchez-Vega, M. G. *Dalton Trans.* **2006**, 3966 ; (b) Cabeza, J. A.; del Rio, I.; Sanchez-Vega, M. G.; Suarez, M. *Organometallics* **2006**, *25*, 1831.
- (21) Wolf, J.; Labande, A.; Natella, M.; Daran, J.-C.; Poli, R. *J. Mol. Catal. A* **2009**, *259*, 205.
- (22) (a) Lin, I. J. B.; Vasam, C. S. *Coord. Chem. Rev.*, **2007**, *251*, 642; (b) Garrison, J. C.; Youngs, W. *J. Chem. Rev.*, **2005**, *105*, 3978.
- (23) (a) Teo, B.-K.; Calabrese, J. C. *Inorg. Chem.* **1976**, *15*, 2474; (b) Teo, B.-K.; Calabrese, J. C. *J. Am. Chem. Soc.* **1975**, *97*, 1256.
- (24) see e.g. (for poly-NHCs): (a) Rit, A.; Pape, T.; Hahn, F. E. *J. Am. Chem. Soc.* **2010**, *132*, 4572; (b) Hahn, F. E.; Radloff, C.; Pape, T.; Hepp, A. *Chem.-Eur. J.* **2008**, *14*, 10900; (for N-) (c) Li, F.; Bai, S.; Hor, T. S. A. *Organometallics* **2008**, *27*, 672; (d) Tulloch, A. A. D.;

- Danopoulos, A. A.; Winston, S.; Kleinhenz, S.; Eastham, G. *J. Chem. Soc., Dalton Trans.* **2000**, 4499; (for P-) (e) Raynal, M.; Liu, X.; Pattacini, R.; Vallée, C.; Olivier-Bourbigou, H.; Braunstein, P. *Dalton Trans.* **2009**, 7288.
- (25) (a) Bencze, É.; Pápai, I.; Mink, J.; Goggin, P. L. *J. Organomet. Chem.* **1999**, 584, 118; (b) Clark, R. J. H.; Williams, C. S. *Inorg. Chem.* **1965**, 4, 350.
- (26) Pfeffer, M.; Braunstein, P.; Dehand, J. *Spectrochim. Acta* **1974**, 30A, 341.
- (27) (a) Zhang, X.; Xia, Q.; Chen, W. *Dalton Trans.* **2009**, 7045; (b) Zhang, X.; Xi, Z.; Liu, A.; Chen, W. *Organometallics* **2008**, 27, 4401; (d) Ye, J.; Chen, W.; Wang, D. *Dalton Trans.* **2008**, 4015; (d) Chiu, P. L.; Lai, C.-L.; Chang, C.-F.; Hu, C.-H.; Lee, H. M. *Organometallics* **2005**, 24, 6169 ; (e) McGuinness, D. S.; Cavell, K. J. *Organometallics* **2000**, 19, 741.
- (28) Nishikata, T.; Abela, A. R.; Huang, S.; Lipshutz, B. H. *J. Am. Chem. Soc.* **2010**, 132, 4978 and references therein.
- (29) (a) Diebolt, O.; Braunstein, P.; Nolan, S. P.; Cazin, C. S. J. *Chem. Commun.* **2008**, 3190; (b) Bedford, R. B.; Cazin, C. S. J.; Holder, D. *Coord. Chem. Rev.* **2004**, 248, 2283; (c) Littke, A. F.; Fu, G. C. *Angew. Chem. Int. Ed.* **2002**, 41, 4176; (d) Grushin, V. V.; Alper, H. *Chem. Rev.* **1994**, 94, 1047.
- (30) Drew, D.; Doyle, J. R. *Inorg. Synth.* **1972**, 13, 47.
- (31) Wayland, B. B.; Schrammz, R. F. *Inorg. Chem.* **1969**, 8, 971.
- (32) Bruker-Nonius, *Kappa CCD Reference Manual*, Nonius BV, The Netherlands, **1998**.
- (33) Sheldrick, G. M. *Acta Crystallogr.* **2008**, A64, 112-122.
- (34) (a) Spek, L.; *J. Appl. Cryst.* **2003**, 36, 7; (b) Blessing, B.; *Acta Cryst.*, **1995**, A51, 33.

Chapitre 4

Thioether-functionalized
Bis(diphenylphosphino)amine Ligands:
Synthesis, Coordination Chemistry and
Applications

Résumé du chapitre 4

Nous avons synthétisé des ligands de type bis(diphenylphosphino)amine substitués sur l'atome d'azote par une fonction alkyl- ou aryl-thioéther. La nature de l'espaceur entre l'azote et le soufre a été variée, une chaîne propyle dans le cas du ligand **1** et un phényle dans le cas de **2**. Nous avons ensuite formé des complexes de nickel et de chrome avec ces ligands, que nous avons évalués en réaction catalytique d'oligomérisation d'éthylène. Ces ligands bifonctionnels, par réaction avec des sels de fer ou de cobalt, nous ont permis d'isoler des complexes avec des structures très originales et inattendues. Finalement, nous avons synthétisé des complexes de palladium, de cuivre et un cluster moléculaire de cobalt portant deux ligands. Les groupements soufrés dans ces complexes sont dirigés dans des directions opposées, ce qui permettra de les utiliser par la suite comme métallo-ligands pour connecter entre elles des sphères microscopiques partiellement recouvertes d'or.

Abstract of Chapter 4

We synthesized thioether N-functionalized bis(diphenylphosphino)amine type ligands. We varied the spacer between the two chemically different functions, a propyl chain in the case of ligand **1** and a phenyl ring in the case of **2**. We then formed nickel and chromium complexes with these ligands, which were evaluated in catalytic ethylene oligomerization. By reaction of these ligands with iron or cobalt salts, we were able to isolate complexes with unpredictable structures. Finally, we synthesized palladium and copper complexes and a tetracobalt cluster bearing two ligands. In these complexes, the sulfur atoms are oriented in opposite directions which will allow their use as metallo-ligands to connect partially gold covered microscopic spheres.

Introduction

Short-bite ligands, in which the spacer between the donor atoms contains a single atom, are very attractive in fundamental coordination chemistry and for the potential application of their organometallic complexes.¹ These ligands offer various coordination modes, they can act as monodentate, bidentate chelating or bridging ligands towards metal centers. The most common bidentate ligands of this type are diphosphines, in particular dppm [bis(diphenylphosphino)methane = Ph₂PCH₂PPh₂] and dppa [bis(diphenylphosphino)amine = Ph₂PNHPPPh₂], in which the two phosphorous atoms are separated by a methylene and an amine group, respectively. Their functionalization could offer the opportunity to enlarge their scope of applications by modification of their physical, electronic and/or steric properties. Whereas the NH proton of dppa is more “acidic” than the CH₂ protons of dppm, ligand functionalization by deprotonation and subsequent reaction with an organic electrophile only works in few cases and/or gives low yields. Otherwise, the reaction of functionalized primary amines with chlorophosphines to afford *N*-functionalized dppa-type ligands works well under mild conditions² and offers a large choice of ligands. During the last decade, numerous alkyl³ or aryl-dppa derivatives⁴ were reported. Examples of multi-bis(diphenylphosphino)amine systems linked through a central aryl moiety have been reported.⁵

The introduction of a functional chain on the *N*-substituent attracted also much attention. Thus, introduction of alkoxy silyl groups⁶ allowed the grafting of metal clusters into inorganic matrices and the subsequent preparation of highly dispersed metal-containing particles.⁷ Few examples of structurally characterized clusters coordinated by *N*-substituted dppa have been reported in the literature, and these include homometallic Ru₃,⁸ Ru₄,⁹ Co₄^{6b,10} and bimetallic Co₂Pt¹¹ and CoPd₂¹² clusters. The presence of a coordinating function on the *N*-substituent can allow the stepwise formation of multinuclear species,¹⁰ or of potentially hemilabile systems for catalytic applications. Interesting results were obtained in olefin oligomerization/polymerization with such functionalized dppa type ligands.¹³ We recently reported the grafting of a molecular cluster on gold surfaces *via* a thiol functionalized monophosphine ligand.¹⁴ The limited stability of this mono-substituted cluster and the rapidly oxidized thiol group encouraged us to use a more stabilizing ligand, a thioether functionalized diphosphine ligand.

Here, we report the synthesis of *N*-thioether-functionalized bis(diphenylphosphino)amine type ligands, Ph₂P*N*(*n*-PrSMe)PPh₂ (**1**) and Ph₂P*N*(*Php*-SMe)PPh₂ (**2**), and the applications of their metal complexes in various field of chemistry and physical-chemistry. To allow better comparisons, we choose to modify only the linker between the two chemically different donor functions. We will thus compare the reactivity of an alkyl- and an aryl- substituted PNP ligand and examine how this affects the steric and electronic properties of the resulting ligands.

Selective oligomerization of ethylene for the formation of linear α -olefins attracts considerable interest due to their increasing industrial demand. *N*-functionalized bis(diphenylphosphino)amines Ni(II) complexes have shown high activity for ethylene oligomerization with a high selectivity for linear α -olefins.¹⁵ Diphosphine-containing Ni complexes also showed great activity in Suzuki-Miyaura cross-coupling reaction.¹⁶ More recently, Cr(III) catalysts supported by dppa-type ligands were established as the most efficient catalysts for selective ethylene tetramerization.¹⁷ The nickel dichloride complexes of **1** and **2**, NiCl₂(**1**) (**3**) and NiCl₂(**2**) (**4**), respectively, were synthesized and used as well defined pre-catalysts for ethylene oligomerization. Herein we also report the synthesis of different chromium trichloride complexes bearing ligands **1** and **2**, complexes **5a** and **6a**, respectively, as thf (thf = tetrahydrofuran) adducts of general formula [CrCl₃(P,P)(thf)]. The complexes **5b** and **6b** are the dmap (dmap = *p*-dimethylaminopyridine) adducts of the chromium complexes of **1** and **2**, respectively, of general formula [CrCl₃(P,P)(dmap)]. The nickel complexes **3** and **4**, and the chromium complexes **5a** and **5b**, were unambiguously structurally characterized by single crystal X-ray diffraction. All these complexes were then used as well-defined precatalyst for evaluation in catalytic ethylene oligomerization reaction with MAO (MAO = methyl aluminoxane) or EADC (EADC = ethyl aluminium dichloride) as co-catalysts.

The versatile coordination geometries and intrinsic properties of 3d metal ions oriented part of our work toward the study of Fe(II) and Co(II) ions towards ligands **1** and **2**. The resulting complexes could lead to original and interesting candidates for EPR and magnetism investigations. Reaction of anhydrous dichloride salts of iron and cobalt with ligands **1** and **2** in a 1:1 stoichiometry resulted in unexpected structures corresponding to the formula [MCl₂(P,P)]. Collaborations with different groups of the Université de Strasbourg and Universität des Saarlandes (Germany) were developed to evaluate the properties of these compounds.

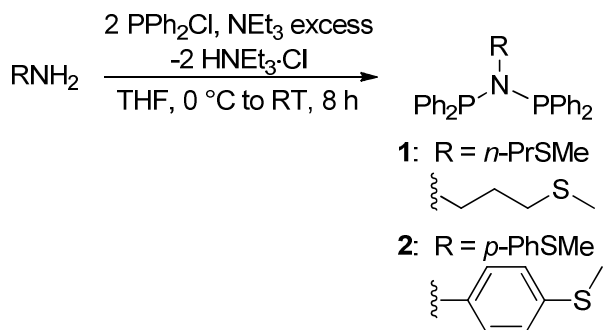
In view of the affinity of sulfur-based functions for gold surfaces, we explored the potential of our ligands and their metal complexes towards such substrates. The specific aim was to link two micrometer size, partly gold covered spheres *via* well defined organometallic species. We developed a series of compounds, in which, two ligands are coordinated around a central metal *core* and their sulfur moieties oriented in two opposite directions. Ligands **1** and **2** were reacted with mono- or polynuclear precursors, $[\text{Pd}(\text{NCMe})_4]\text{[BF}_4\text{]}_2$, $[\text{Cu}(\text{NCMe})_4]\text{[PF}_6\text{]}$ or a Co_4 *core* carbonyl cluster to form the corresponding bis-chelated or doubly-bridged species.

Results and Discussion

Ligands Synthesis

Bis(phosphino)amine ligands bearing a third donor function on the nitrogen offer more coordination possibilities to stabilize metal centers through intra- or intermolecular interactions. The synthesis of *N*-substituted dppa-type ligands is readily achieved by reaction of chlorodiphenylphosphine with the corresponding primary amine in the presence of triethylamine as HCl scavenger (Scheme 1). In course of this work, the synthesis and structure of ligand **1** was published by Hor *et al.*^{13a} and we provide here additional $^{13}\text{C}\{^1\text{H}\}$ NMR characterization of this compound. The ligands are obtained in 94 and 86% yields for **1** and **2**, respectively, and could be characterized by multinuclear NMR, FT-IR spectroscopy techniques, ESI-MS and elemental analysis. Ligand **2** showed a typical resonance at 70.6 ppm in the $^{31}\text{P}\{^1\text{H}\}$ NMR spectrum, characteristic for aryl substituted dppa-type ligands.¹⁰

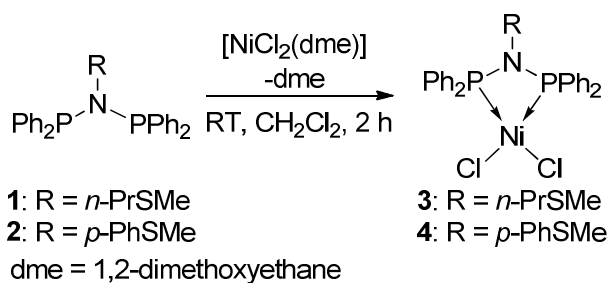
Scheme 1. Synthesis of the ligands **1** and **2**.



Nickel(II) and Chromium(III) Complexes

Nickel(II) complexes. Addition of $[\text{NiCl}_2(\text{dme})]$ to a dichloromethane solution of ligand **1** or **2** afforded complexes **3** and **4**, respectively, as red crystalline solids in good yield (Scheme 2). The red color of these compounds is characteristic of a square planar coordination geometry around the Ni center. This was confirmed by single crystal X-ray diffraction analysis of complexes **3** and **4**· $2\text{CH}_2\text{Cl}_2$ (Fig. 1 and Fig. 2).

Scheme 2. Synthesis of the Ni(II) complexes **3** and **4**.



In each case, a distorted square planar geometry is observed, due to the constrained bite angle of the PNP moiety [$\text{P1-Ni1-P2} = 73.69(3)$ Å (**3**) and $74.20(6)$ Å (**4**· $2\text{CH}_2\text{Cl}_2$)] and to the strong *trans* influence exerted by the phosphorous donors, with P-Ni bond lengths between 2.1099(15) and 2.1278(8) Å and Ni-Cl bond lengths between 2.1833(15) and 2.2017(15) Å. In the case of complex **4**, the thioether-phenyl ring is almost coplanar with the Ni coordination plane, with a (C1-C6)-(P1Ni1P2) angle of 9.80°.

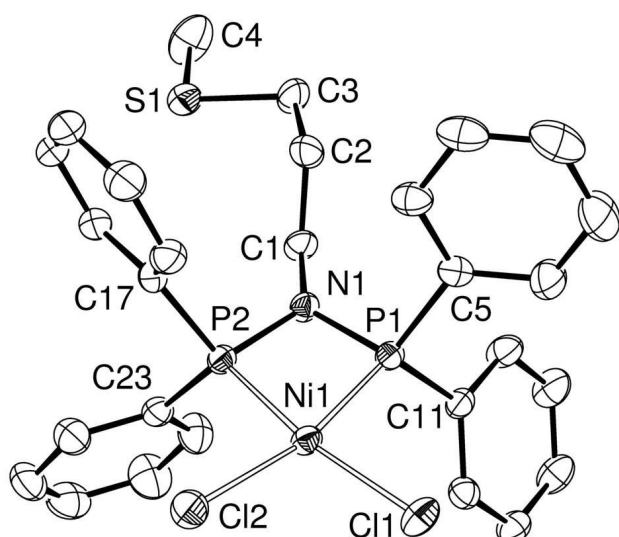


Fig. 1 View of the molecular structure of **3**. Hydrogen atoms omitted for clarity. Ellipsoids are represented at 50% probability level.

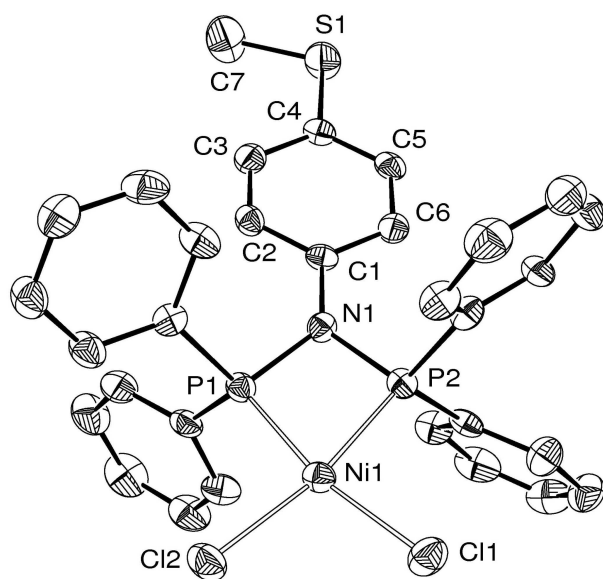


Fig. 2 View of the molecular structure of **4**·2CH₂Cl₂. Hydrogen atoms omitted for clarity. Ellipsoids are represented at 50% probability level.

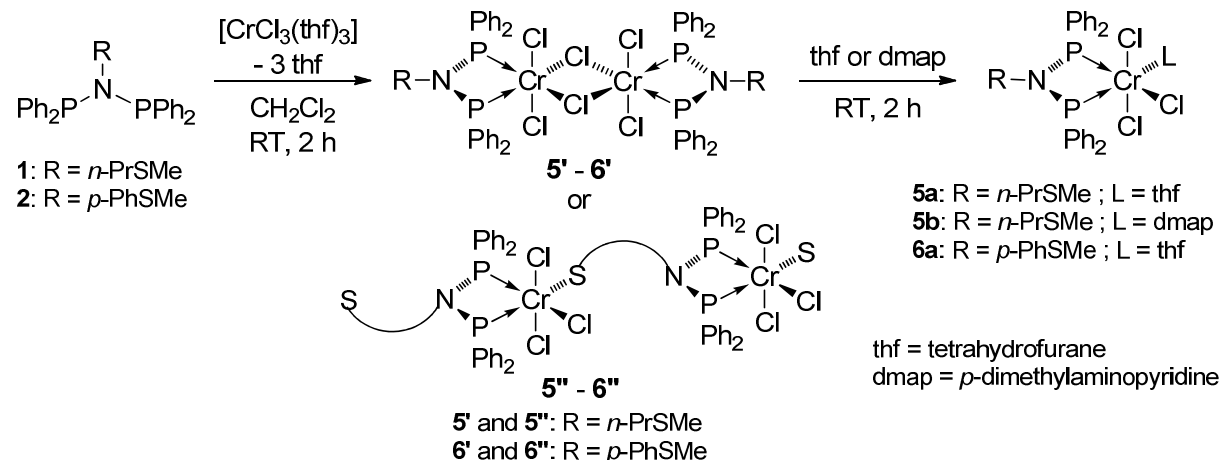
The diamagnetic square planar geometry of the complexes is retained in solution and allows to record their ³¹P{¹H} NMR spectra. They exhibit a sharp singlet for the two equivalent phosphorous atoms at 43.8 and 46.6 ppm for **3** and **4**, respectively. The ¹H NMR chemical shift of the singlet observed for the CH₃ group linked to the S atom at 1.84 and 2.32 ppm for **3** and **4**, respectively, is not much displaced compared to the free ligands, 1.82 (**1**) and 2.36 ppm (**2**), which suggests no interaction between the thioether function and the Ni center in solution.

Table 1. Selected bond lengths (Å) and angles (deg) for **3**, **4**, **5a** and **5b**.

	3	4 ·2CH ₂ Cl ₂	5a	5b
Bond lengths, Å	M = Ni	M = Ni	M = Cr	M = Cr
M1-P1	2.1278(8)	2.1099(15)	2.4759(13)	2.4925(8)
M1-P2	2.1164(8)	2.1275(15)	2.5302(13)	2.5015(8)
M1-Cl1	2.1901(8)	2.1833(15)	2.2923(13)	2.3093(9)
M1-Cl2	2.1990(8)	2.2017(15)	2.2840(13)	2.2995(8)
M1-Cl3			2.3105(13)	2.3084(8)
M1-O1			2.059(3)	
M1-N2				2.070(2)
Bond angles, deg				
P1-M1-P2	73.69(3)	74.20(6)	66.39(4)	66.76(3)
Cl1-M1-Cl2	99.77(3)	99.26(6)	91.13(5)	92.90(3)
P1-N1-P2	97.59(11)	96.7(2)	107.39(19)	108.16(12)
O1-M1-Cl2			98.30(10)	
N2-M1-Cl2				96.46(7)

Chromium(III) complexes. Reaction of $[\text{CrCl}_3(\text{thf})_3]$ with ligands **1** or **2** in a 1:1 metal/ligand ratio in dichloromethane afforded insoluble blue powders (Scheme 3). The structure of these compounds could be of the doubly-bridged dinuclear species **5'** – **6'** or polymeric type **5''** – **6''** in which the sulfur atom from the thioether function interacts with an adjacent Cr center. An example of doubly-bridged dinuclear complex bearing an ether-functionalized dppa-type ligand was recently reported.^{17a,c} These bridges and the coordination polymers could easily be broken in the presence of a donor solvent/ligand such as thf or dmap to afford the corresponding complexes **5a**, **5b** and **6a**. Nitriles solvents are also suitable donors.^{13a} Single crystal X-ray diffraction studies on complexes **5a** and **5b** revealed a mononuclear structure (Fig. 3 and Fig. 4).

Scheme 3. Synthesis of the Cr(III) complexes.



The molecular structures of **5a** and **5b** are very similar and the complexes adopt a distorted octahedral *mer*- $[\text{CrCl}_3]$ structure with the PNP ligand chelating the chromium center and the labile ligand, thf (**5a**) or dmap (**5b**), occupying a position *trans* to P1. In the case of the nitriles adducts of such compounds described by Hor *and coll.* only the *fac*- $[\text{CrCl}_3]$ isomer was formed.^{13a} The chelating ligand forms a four-membered metallocycle, with a P-Cr-P angle of $66.39(4)^\circ$ (**5a**) and $66.76(3)^\circ$ (**5b**), much smaller than those observed in the square planar complexes **3** and **4**, but in the range of those observed in dinuclear complexes [$66.837(18)^\circ$ ($\text{R} = (\text{CH}_2)_2\text{OCH}_3$)^{17a} and $66.62(7)^\circ$ ($\text{R} = \text{Ph}$)^{17c}] and nitriles adducts [$66.37(9)^\circ$ ($\text{L} = \text{MeCN}$) and $66.01(5)^\circ$ ($\text{L} = \text{EtCN}$)].^{13a}

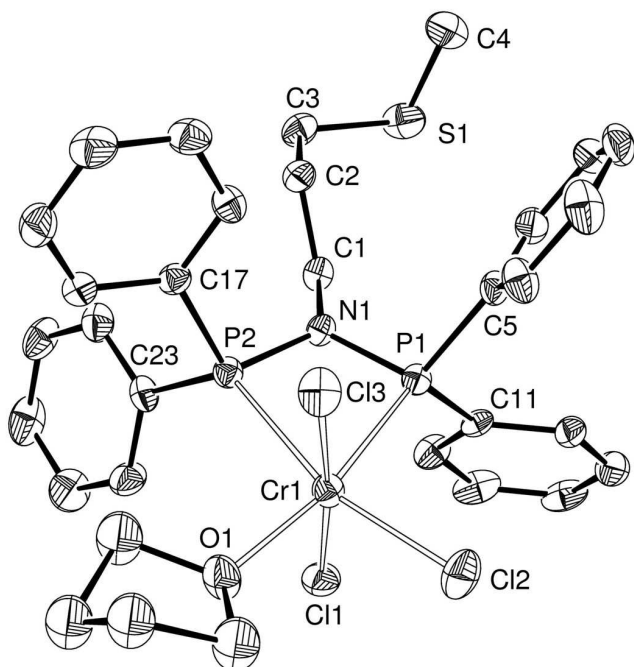


Fig. 3 View of the molecular structure of **5a**. Hydrogen atoms omitted for clarity. Ellipsoids are represented at 50% probability level.

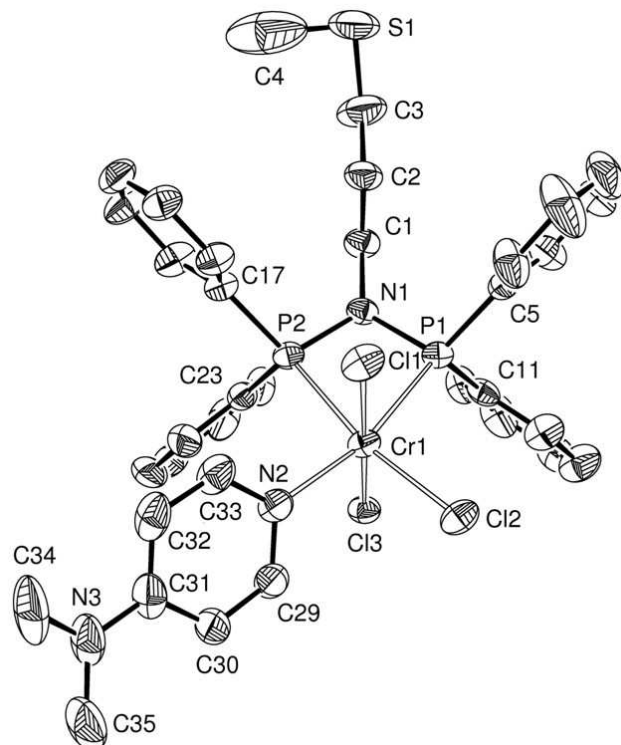


Fig. 4 View of the molecular structure of **5b**. Hydrogen atoms omitted for clarity. Ellipsoids are represented at 50% probability level.

Table 2. Catalytic oligomerization of ethylene studies

Entry	Complex	Time (min)	Cocatalyst (eq.)	[Cata] (10^5 g/mol ⁻¹)	Pressure (bar)	T (°C)	Activity ^a	Productivity ^b	TOF ^y	Selectivity %				Alpha %		
										C4	C6	C8	C10+			
1	3	35	EADC (10) EADC (3)	4 4	10 10	25 1800	10500 3100	18000 6500	38000 67.1	77 30.1	21.1 2.8	1.8 0	0.07 17.2	15.4 5.0	2.7 5.0	
2	3	35	EADC (3)	1	10	25	200	300	600	98.3	2.1	0	0	80.1	84.6	0
3	3	35	EADC (10)	1	10	25	23500	40200	84400	76.6	21.6	1.8	0	20.3	3.3	1.2
4	3	35	MAO (200)	4	10	25	850	1427	3000	83.7	15.2	1.1	0	64.6	43.8	32.2
6	4	35	EADC (10) EADC (3)	4 4	10 10	25 2600	14000 4500	24000 9400	50400 78.3	68.3	28.7	2.4	0.5	2.7	0.3	18.2
7	4	35	EADC (10)	1	10	25	14100	24200	50700	79.1	19.5	1.4	0	24.4	4.5	20
9	4	35	EADC (10)	1	10	25	9200	15800	33000	78.9	19.5	1.6	0	28.3	5.3	0
10	4	35	MAO (200)	4	30	25	850	1450	3000	92	8	0	0	48.3	32.4	0
11	5a	35	EADC (10) MAO (400)	4 4	10 30	25 80	650	1100	2100	0.3	0.05	PE: 5.7g				
12	5a	180												63.6	68.7	70.7
13	6a	35	EADC (10) MAO (200)	4 4	10 10	25 25	900 -90	1500 -153	2832	0.4	0.3	0	PE: 8g			
14	6a	35												5.8	PE: 6g	
15	6a	180	MAO (400)	4	30	80	9200	3100	29259	12.1	16.6	13.1	9.5	87.7	88.4	90.1

^a(g oligomers/g Metal); ^b(g C₂H₄(g Metal x h)); ^y(mol C₂H₄/(mol Metal x h))

The ESI-MS analysis suggests a similar arrangement for the complexes formed with ligand **2**. The formation of these thf or dmap adducts, complexes **5a – 6b**, was investigated for their higher solubility, which could be beneficial for their use in catalysis.

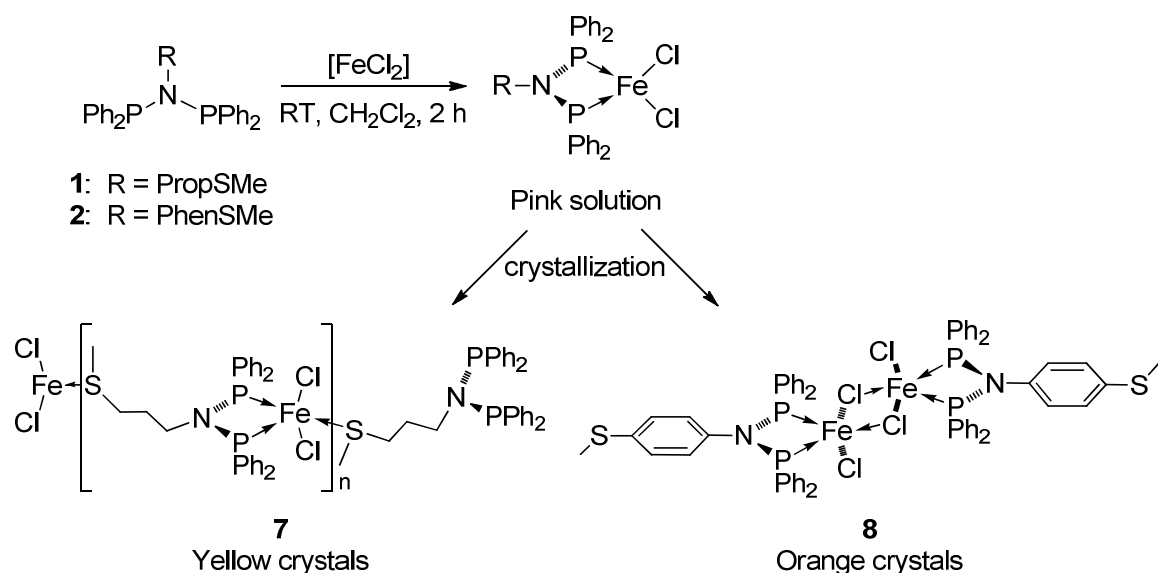
Preliminary Catalytic Ethylene Oligomerization Studies

The Ni complexes generally show a greater activity, productivity and a better TOF than the chromium complexes. The best TOF observed for the Cr complexes is around a third of that observed for the best Ni catalyst, see entries 14 and 4, respectively. Two very different catalytic systems, entries 3 and 10, afford very high selectivities for short chain oligomers (C4 and C6). Entry 3, the Ni complex **3** with a small amount of cocatalyst (3 eq.) gives rise to more than 98% selectivity for butenes. This complex shows also more than 80% selectivity for α -olefins. The Cr/MAO systems (with 400 eq. cocatalyst) exhibit interesting activities but moderate selectivity for specific chain lengths. These systems are remarkable for the high selectivity in α -olefins of the products (Entries 12 and 15).

The nickel complexes will now be evaluated in cross-coupling reactions to see if the additional donor function can increase their activity compared to existing systems.¹⁶ In the case of the chromium complexes, we have to repeat some experiments and to evaluate the dmap adducts (**5b** and **6b**). We will further attempt to crystallize the poorly soluble blue species and the different adducts formed with ligand **2**.

Iron(II) and Cobalt(II) Complexes

Iron(II) complexes. Addition of anhydrous FeCl₂ to a dichloromethane solution of ligand **1** or **2**, in a 1:1 metal/ligand ratio, leads to slow color change to light pink. After filtration and crystallization by slow diffusion of pentane in this solution, quantitative transformation into yellow or orange crystals for **7** and **8**, respectively, was observed (Scheme 4). The process affording the iron complex FeCl₂(**1**) (**7**) is irreversible because the yellow crystals could not be redissolved in dichloromethane. The polymeric structure of **7** could be unambiguously established by single crystal X-ray diffraction studies (Fig. 5). In the case of **8**, formation of a chloride bridged dinuclear complex instead of a polymer is due to a less accessible sulfur atom in **2** than in ligand **1** (Fig. 7). This emphasizes the importance of the nature of the spacer between the two donors functions, the (P,P) and the S moieties. Selected bond lengths and angles in the two iron(II) structures are given in Table 3.

Scheme 4. Synthesis of Fe(II) complexes

The molecular structure of complex **7** shows a distorted trigonal bipyramidal coordination geometry around the iron center, in which the trigonal plane is formed by P3-Cl1-Cl2 with a longer P3-Fe bond [2.4570(16) Å] compared to the Cl-Fe bonds [2.2524(17) and 2.2581(17) Å]. The longest bonds in the structure are between the iron center and the apical ligands, P4 and S1 with 2.7980(18) and 2.5803(19) Å, respectively. The P4-Fe1 distance is unusually long and there is no obvious steric or electronic reason that could explain it, i.e. there is no bulky group linked to the metal or strong donor in *trans* position to P4. The distance between P4 and Fe1 is situated between a dative bond (2.10 – 2.52 Å) and a Fe···P short contact (3.0 – 5.0 Å). The most significant distortion in the structure is imposed by the chelation angle of the ligand [P3-Fe1-P4 64.55(5)°]. Important parameters for further magnetic studies are the distance between the iron centers, Fe1···Fe2 = 10.352(1) Å, and the Fe-Fe-Fe angle of 109.37(1)°. A related iron(II) coordination polymer with a zig-zag chain structure assembled by nitrogen-containing ligands revealed an interesting spin-crossover (HS \leftrightarrow LS transition) as a function of temperature.¹⁸

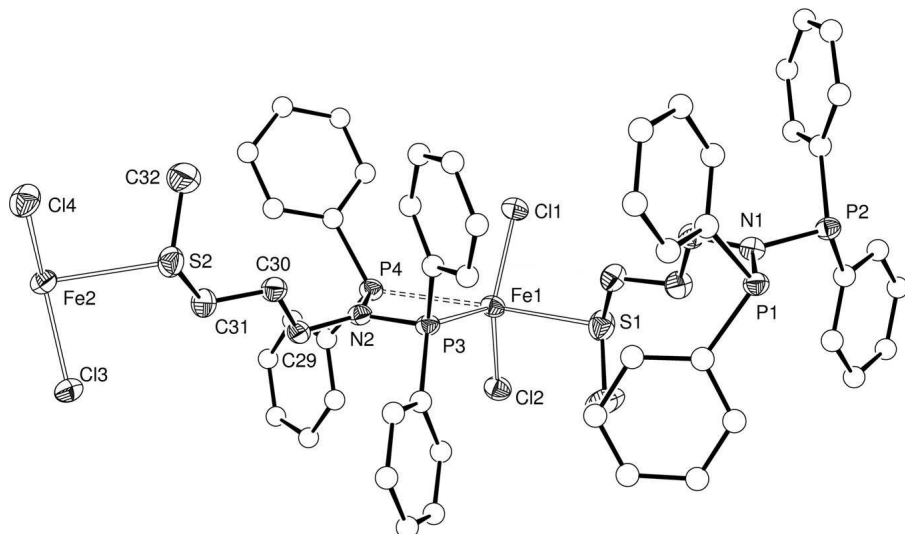


Fig. 5 View of the molecular structure of the asymmetric unit of **7**. Hydrogen atoms omitted for clarity. Ellipsoids are represented at 50% probability level.

Figure 6 shows a simplified view of the solid state arrangement of complex **7** and highlights the zig-zag topology of the coordination polymer formed by assembling the iron centers through ligand **1**, which is P,P-chelating Fe1 and Fe2 *via* the sulfur atom from the thioether function. The polymer was grown along the b axis.

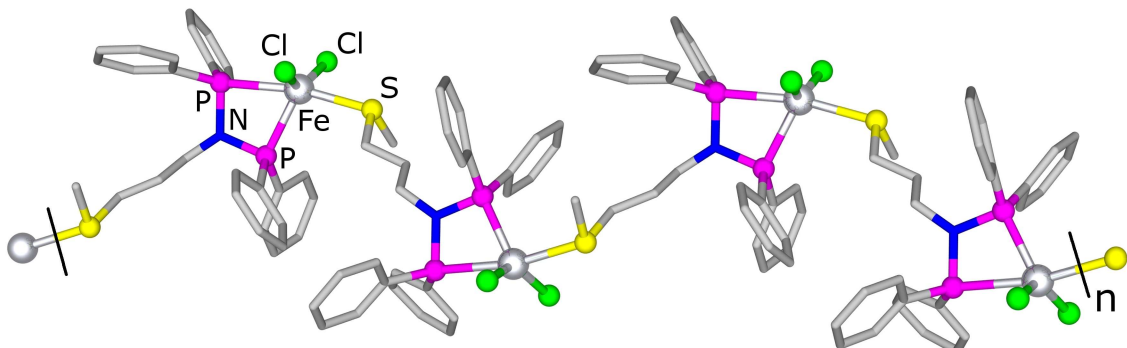


Fig. 6. Simplified view of **7** illustrating the zig-zag conformation. The H atoms are omitted for clarity and only the ipso carbons of the phenyl rings are represented.

The coordination geometry around the iron center in the centrosymmetric solid state molecular structure of **8** is also trigonal bipyramidal distorted. The trigonal plane is formed by P2-Cl1-Cl2 with P2-Fe1 [2.4654(9) Å] being significantly longer than the iron chloride bonds [2.3386(9) (Cl1) and 2.2208(10) Å (Cl2)]. The apical positions of the bipyramid are occupied by P1 and Cl1ⁱ. The Fe-Cl1ⁱ bond length [2.5150(9) Å] is typical for an iron chloride-bridge dimer. The P1···Fe1 distance is shorter than in the case of complex **7** [2.7616(10) Å], but its length is also between a coordination bond and a short contact. The more similar structural parameters between complexes **7** and **8** are those involving the ligand, see e.g. the Fe-P, Fe-Cl

bonds and the P-N-P, P-Fe-P angles. In contrast, the most affected by the change in the spacer group are those involving the bridging ligands, with an average gap around 8° between the P-Fe-S and P-Fe-Cl 1‡ angles, and significant differences between the Fe-S and Fe-Cl 1‡ bonds. Owing to the nature of the bridging ligand, the Fe $1\cdots$ Fe 1^{\ddagger} [3.5397(7) Å] distance in complex **8**, is much shorter than the Fe $1\cdots$ Fe 2 [10.352(1) Å] distance in complex **7**.

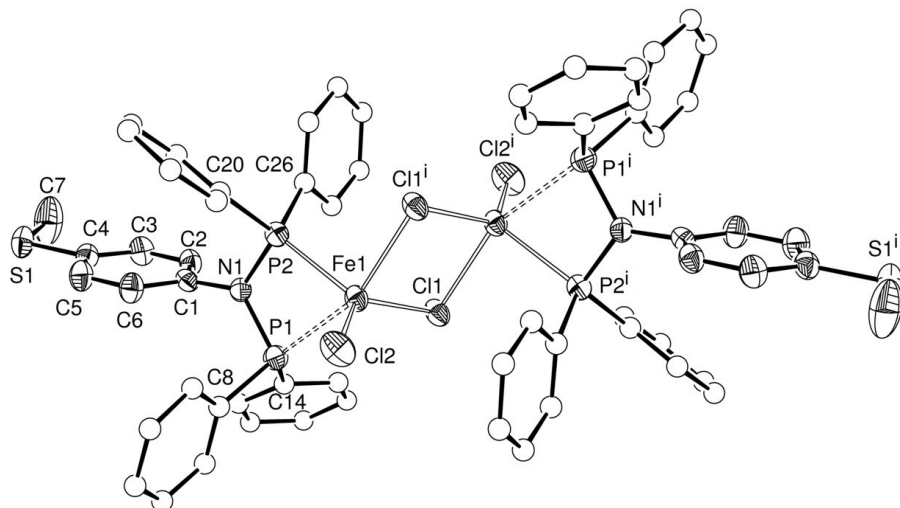


Fig. 7. View of the molecular structure of **8**. Hydrogen atoms omitted for clarity. Ellipsoids are represented at 50% probability level.

Table 3. Selected bond lengths (Å) and angles (deg) for **7** and **8**.

	7	8	7	8
Bond lengths, Å			Bond angles, deg	
Fe1-P3	2.4570(16)		P3(2)-Fe1-Cl1	110.87(7)
Fe1-P2		2.4654(9)	P3(2)-Fe1-Cl2	109.76(6)
Fe1-Cl1	2.2524(17)	2.3386(9)	P3(2)-Fe1-P4(1)	64.55(5)
Fe1-Cl2	2.2581(17)	2.2208(10)	P3-Fe1-S1	104.29(6)
Fe1-S1	2.5803(19)		P4-Fe1-S1	168.78(6)
Fe1-Cl1 ‡		2.5150(9)	P2-Fe1-Cl1 ‡	92.89(3)
Fe1-P4	2.7980(18)		P1-Fe1-Cl1 ‡	156.47(3)
Fe1-P1		2.7616(10)	P3(2)-N2-P4(1)	111.7(3)
				110.96(13)

The comparison between **7** and **8** illustrated the dramatic influence of the nature of spacer between the two donor set in these polyfunctionnal ligands. Under similar reaction conditions, a flexible aliphatic spacer leads to a polymeric assembly involving coordination of the second donor function whereas with a rigid aromatic spacer, a chloride bridged dinuclear complex was formed and no interaction was observed with the thioether function. We are now interested to evaluate the impact of these structural differences on the magnetic properties of these complexes in collaboration with other groups.

Co(II) complexes. Reaction of anhydrous CoCl₂ with ligands **1** and **2**, in a 1:1 metal/ligand ratio, in dichloromethane, led to dark brown solutions, which after crystallization afforded dichroic green/red crystals of complex **9** and green crystals of complex **10**, respectively (Scheme 5). The structure of complex **9**·2CH₂Cl₂ was established by single crystal X-ray diffraction studies (Fig. 8). The two chemically different Co centers exhibit different coordination geometries. Co1 is pentacoordinated in a slightly distorted trigonal bipyramidal geometry, with P1, P4 and Cl1 being coplanar and the apical positions being occupied by P2 and P3. The longest basal P-Co bond is P1-Co1 [2.2830(17) Å] and the Co1-P4 [2.2212(18) Å] and Co1-Cl [2.2321(18) Å] bonds are similar. The bond lengths between the metal center and the apical ligands are similar [Co1-P2 (2.2499(19) Å) and Co1-P3 (2.2328(19) Å)]. The strongest distortion away from a regular trigonal bipyramid is induced by the PNP chelate, with P1-Co1-P2 and P3-Co1-P4 angles of 71.69(6)° and 71.33(7)°, respectively. The second Co center (Co2) is in a distorted tetrahedral coordination geometry. The three Co-Cl bond lengths are very similar, in the range 2.236(2) - 2.246(2) Å, whereas the Co2-S2 [2.3964(18) Å] bond is longer. The angles involving S2 are in a broader range [between Cl3-Co2-S2 97.74(7) and Cl4-Co2-S2 108.49(8)°] than those involving only chlorides and the cobalt center [between Cl4-Co2-Cl2 112.79(9) and Cl3-Co2-Cl2 117.92(8)°].

Two structures for complex **10** could be reasonably proposed: a structure similar to that of complex **9** with a CoCl moiety bis-chelated by two ligands **2** and a CoCl₃ fragment stabilized by a sulfur ligand or, in view of the different structures obtained in the case of the Fe(II) complexes **7** and **8**, an ionic form with a dicationic tetrahedral bis-chelated Co center associated with a CoCl₄ dianion. This situation was observed in the case of a Ni(II) complex, bis-chelated by a (P,N) ligand with a NiCl₄ counter ion.¹⁹ EPR studies are in progress on these systems to define the fundamental spin state and the e⁻/nuclei interaction. We hope, by comparison, to be able to determine the chemical environment of the metal centers, and in the case of the zwitterionic complex **9**, the oxidation state of the two chemically different cobalt centers and a possible communication between them.

Scheme 5. Synthesis of Co(II) complexes

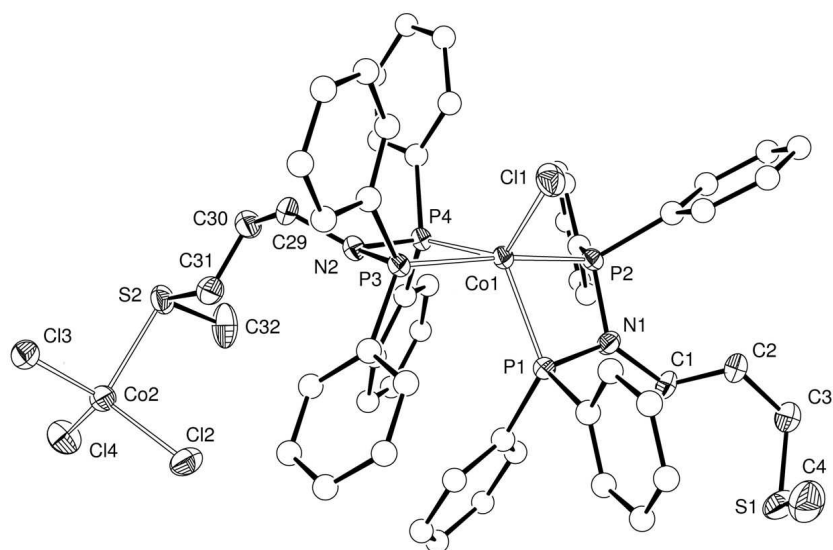
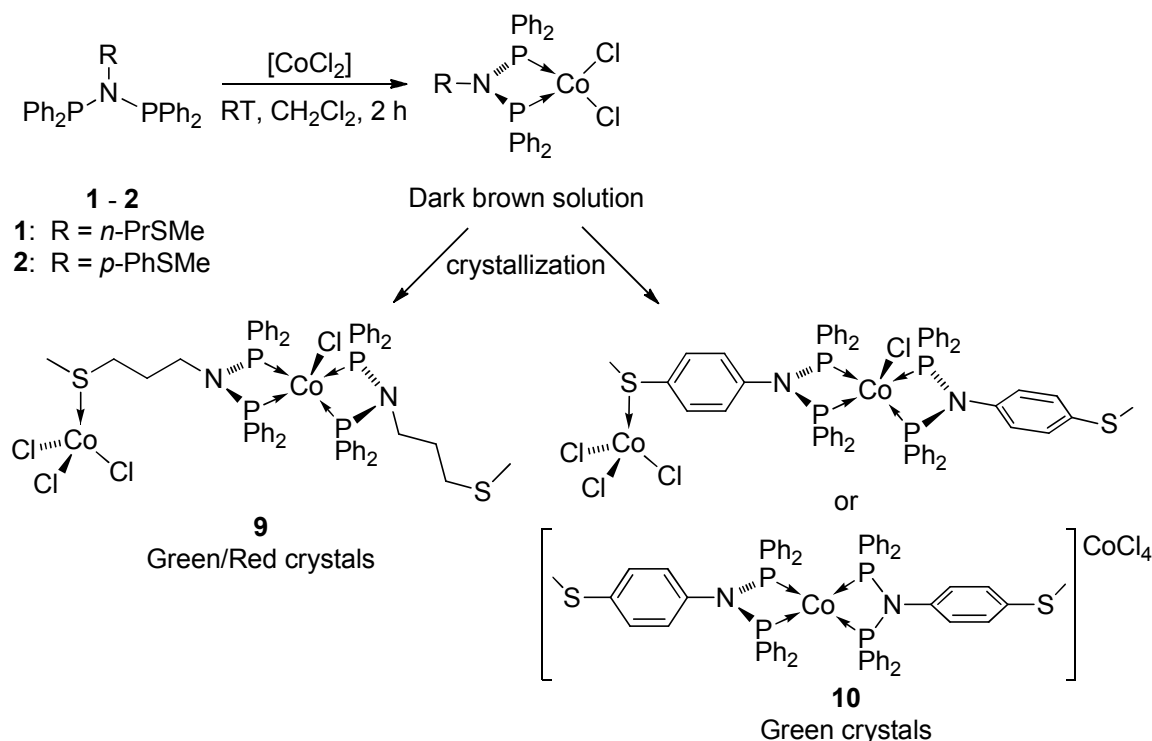
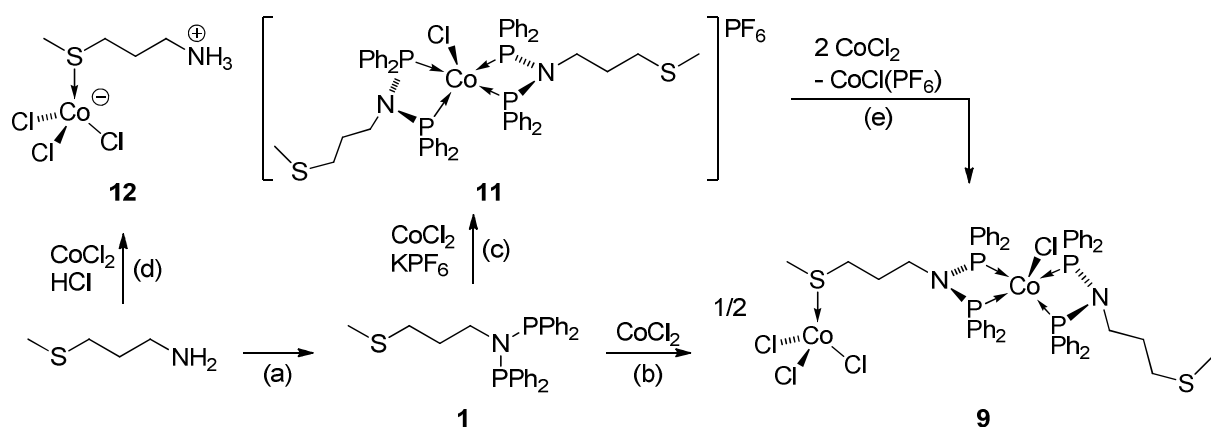


Fig. 8. View of the molecular structure of $9\cdot2\text{CH}_2\text{Cl}_2$. Solvent molecules and hydrogen atoms were omitted for clarity. Ellipsoids are represented at 50% probability level.

For comparison and to facilitate the interpretation of EPR data on complexes **9**·2CH₂Cl₂ and **10**, we wished to isolate separate fragments of these compounds. It would be desirable with each ligand (**1** and **2**), to obtain a bis-chelated, cationic (P,P)₂CoCl fragment, and obtain its EPR and FarIR signature (see Co1 in **9**·2CH₂Cl₂). We also tried to synthesize the SCoCl₃ fragment observed in the molecular structure of **9**·2CH₂Cl₂, or hypothesized for **10** (Scheme 5).

Scheme 6. Synthesis of the fragments of complex **9**

(a) See Scheme 1, (b) see Scheme 5, (c) CH_2Cl_2 , room temp. 2 h, (d) CH_2Cl_2 , room temp. 2 h, (e) CH_2Cl_2 , room temp. 2 h.

Complex **11** was formed by reaction of anhydrous CoCl_2 with ligand **1** in a 1:2 ratio, in the presence of excess KPF_6 (Scheme 6, (c)). Its structure was determined by X-ray analysis and is depicted in Fig. 9. The coordination geometry around the Co center and the arrangement of the ligands are very similar to those in complex **9** \cdot $2\text{CH}_2\text{Cl}_2$. Comparison of the characteristic bond lengths and angles are reported in Table 4.

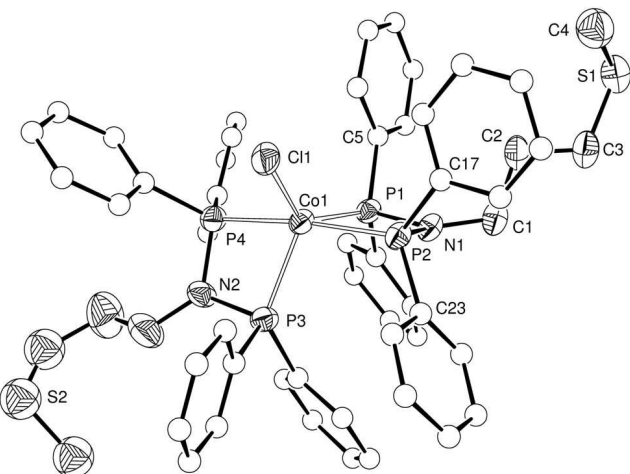


Fig. 9. View of the molecular structure of **11** \cdot CH_2Cl_2 . Counter ion, solvent molecule and hydrogen atoms omitted for clarity. Ellipsoids are represented at 50% probability level.

Complex **12**, analogous to the S-supported CoCl_3 fragment of **9**, was obtained by addition of HCl to a mixture of CoCl_2 and ligand **1**. This complex could be characterized by single crystal X-ray diffraction studies and showed a very similar arrangement to that of $\text{Co}2$ in complex **9** \cdot $2\text{CH}_2\text{Cl}_2$ (Fig. 10). We can observe a non-classical intra-molecular H-bond between a methyl-hydrogen and a chloride from the CoCl_3 fragment, with a $\text{H9}\cdots\text{Cl3}$ distance

of 3.181(4) Å. Another inter-molecular H-bond can be observed between the same Cl3 atom and the N1 from the ammonium part of a second molecule [Cl3···N1 = 3.220(3) Å]. Table 4 allows a comparison of selected bond lengths and angles.

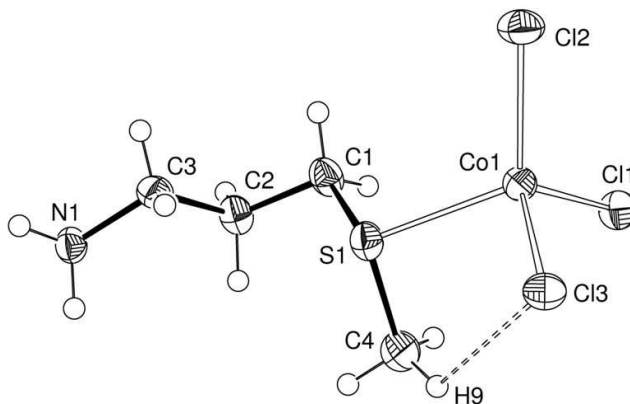


Fig. 10. View of the molecular structure of **12**. Ellipsoids are represented at 50% probability level.

Finally, by reaction of complex **11** with two equivalents CoCl_2 afforded the zwitterionic complex **9** in good yield (Scheme 6).

Table 4. Selected bond lengths (Å) and angles (deg) for **9**· $2\text{CH}_2\text{Cl}_2$, **11**· CH_2Cl_2 and **12**.

	9 · $2\text{CH}_2\text{Cl}_2$	11 · CH_2Cl_2	12
Bond lengths, Å			Bond lengths, Å
Co1-P1	2.2830(17)	2.2395(14)	
Co1-P2	2.2477(19)	2.2391(15)	
Co1-P3	2.2328(19)	2.2644(14)	
Co1-P4	2.2212(18)	2.2414(15)	
Co1-Cl1	2.2321(18)	2.2267(13)	
Co2-S2	2.3964(18)		Co1-S1 2.3650(9)
Co2-Cl2	2.246(2)		Co1-Cl1 2.2510(8)
Co2- Cl3	2.236(2)		Co1- Cl2 2.2331(8)
Co2- Cl4	2.242(2)		Co1- Cl3 2.2636(8)
Bond angles, deg			Bond angles, deg
P1-Co1-P2	71.69(6)	71.65(5)	S1-Co1-Cl1 108.33(3)
P3-Co1-P4	71.33(7)	71.32(5)	S1-Co1-Cl2 114.05(3)
P1-Co1-Cl1	119.45(7)	134.78(6)	S1-Co1-Cl3 96.56(3)
P3-Co1-Cl1	94.63(7)	118.80(6)	Cl1- Co1-Cl2 113.51(3)
S2-Co2-Cl2	100.40(7)		Cl1- Co1-Cl3 112.99(3)
Cl2- Co2-Cl3	117.92(8)		Cl2- Co1-Cl3 110.28(3)
P1-N1-P2	102.6(3)	101.7(2)	C1-S1-C4 101.18(19)
P3-N2-P4	99.0(3)	101.7(2)	

Similar experiments were performed with ligand **2** to try to isolate the different fragments constituting complex **10** (Scheme 7). Only complex **14**, obtained by reaction of CoCl_2 in the

presence of HCl with the amine corresponding to ligand **2** could be characterized by X-ray diffraction and its molecular structure is reported in Fig. 11. Complex **14** is a salt, composed by a CoCl_4 dianion and two ammonium cations. The 1:1:1 ($\text{CoCl}_2/\text{amine}/\text{HCl}$) stoichiometry of the reaction is respected. In this structure, like in the case of the Fe complexes, there is no sulfur-metal interaction. In view of this observation, we believe that the ionic form of complex **10** could be more favored than a zwitterionic (Scheme 5), similar to that observed in the case of complex **9**.

Scheme 7. Synthesis of the fragments of complex **10**

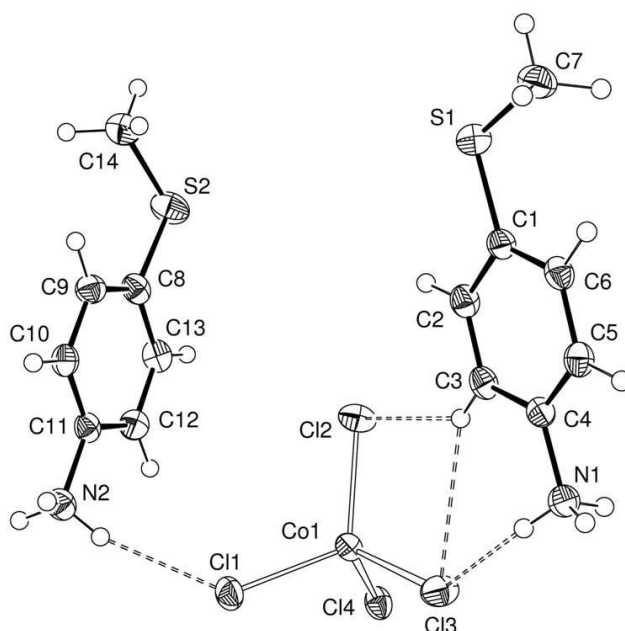
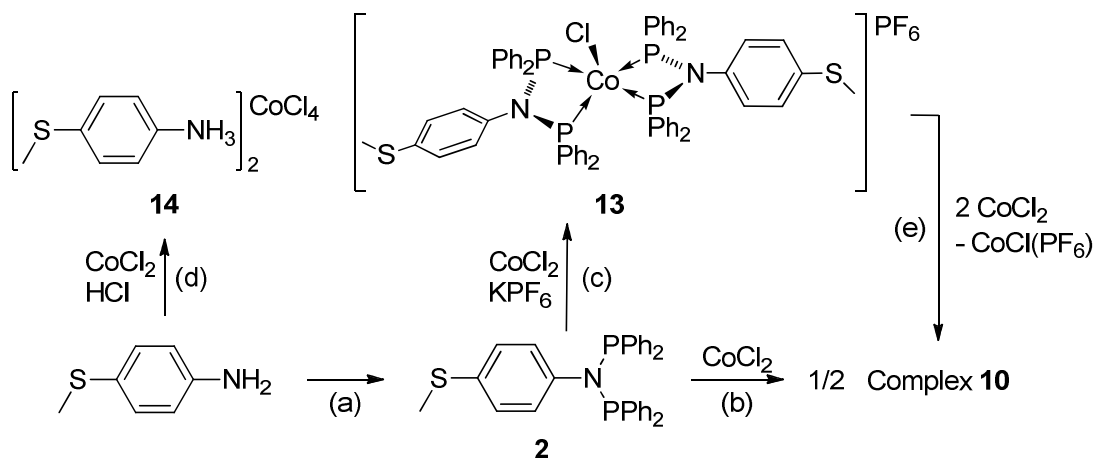


Fig. 11. View of the molecular structure of **14**. Ellipsoids are represented at 50% probability level. Selected bond lengths (\AA) and angles (deg): Co1-Cl1 2.2712(5), N1-C4 1.471(3), S1-C1 1.755(2), Cl2-Co1-Cl1 115.27(2), C1-S1-C7 103.04(11).

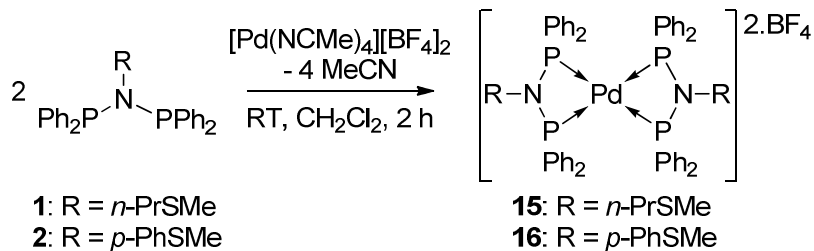
We showed in this section the stepwise formation of the zwitterionic complex **9** from isolated and structurally characterized building blocks. Similar attempts were made with ligand **2**, but unfortunately, all the complexes could not yet be fully characterized. Compounds **9 – 14** are now under EPR investigations with the group of Prof. Turek, but these results will be discussed elsewhere.

Palladium(II) and Copper(I) Complexes and Co₄ Cluster

Organometallic complexes bearing two ligands (**1** or **2**), with opposite orientations of the sulfur groups, should be interesting as assembling metallo-ligands for deposition on partially gold covered nano/macrosopic entities. Three candidates were selected for this study, Pd(II), Cu(I) and a Co₄(0) *core* cluster for their different coordination geometries. Whereas a square planar coordination geometry is anticipated for the Pd(II) complexes, Cu(I) should give rise to a tetrahedral complex.

Palladium(II) complexes. Reaction of [Pd(NCMe)₄][BF₄]₂ with ligands **1** or **2** in a 1:2 metal/ligand ratio afforded the corresponding bis-chelated dicationic complex (Scheme 8). The ³¹P{¹H} NMR spectra of complexes **15** and **16** showed an upfield shift of the signal corresponding to the two equivalent phosphorous atoms with a singlet at 48.40 and 55.46 ppm for **15** and **16**, respectively, whereas the free ligands resonate at 64.06 (**1**) and 70.60 ppm (**2**). As in the case of the Ni complexes, no significant shift of the resonance of the protons adjacent to the sulfur could be observed, which suggest that there is no S···metal interaction. The bis-chelated dicationic structures were confirmed by X-ray diffraction studies. The molecular structures of complexes **15** and **16** are depicted in Fig. 12 and Fig. 13, respectively.

Scheme 8. Synthesis of bis-chelated Pd (II) complexes



The complexes **15** and **16**·2(CH₂Cl₂) crystallize in a centrosymmetric space group with the inversion center located on the Pd center. Their solid state structures are very similar, with the Pd center in a distorted square planar coordination geometry, constrained by the angle imposed by the chelating PNP groups [P1-Pd1-P2 = 69.802(18) (**15**) and 70.77(4)° (**16**)]. The

sulfur atoms are, as wanted, oriented in opposite directions along the S1-Pd1-S1ⁱ axe. In the structure of **16·2(CH₂Cl₂)** the angle between the two planes, (P1-Pd1-P2) and (C1-C6) is 67.70(1)^o. The *p*-substituted phenyls is not perpendicular to the Pd coordination plane, which could be the most sterically preferred orientation, and not quasi coplanar like in the case of the Ni complex **4·2(CH₂Cl₂)**. This angle is comparable to that in a recently reported PdCl₂ complex bearing a *p*-bromobiphenyl substituted dppa type ligand [angle between P1,N1,P2 and C1-C6: 66.4(8)^o].¹⁰ The characteristic bond lengths and angles of complexes **15** and **16·2(CH₂Cl₂)** are reported in Table 5.

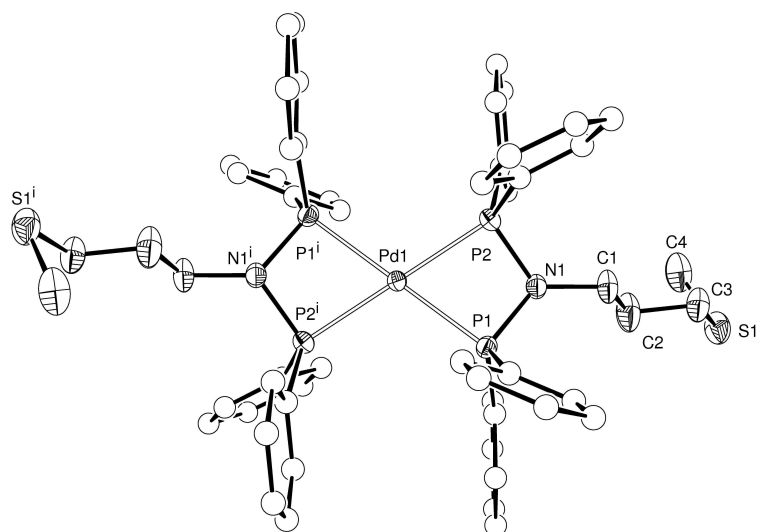


Fig. 12. View of the molecular structure of **15**. Ellipsoids are represented at 50% probability level. Hydrogen atoms and BF₄ anions omitted for clarity.

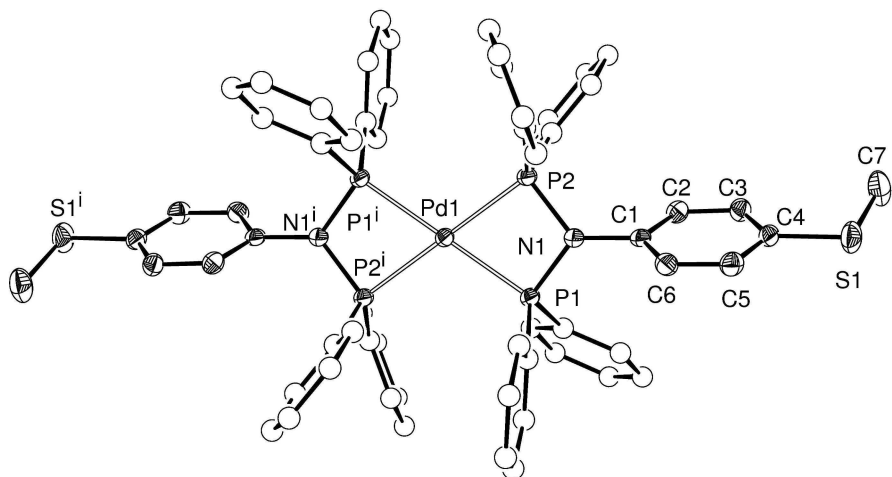
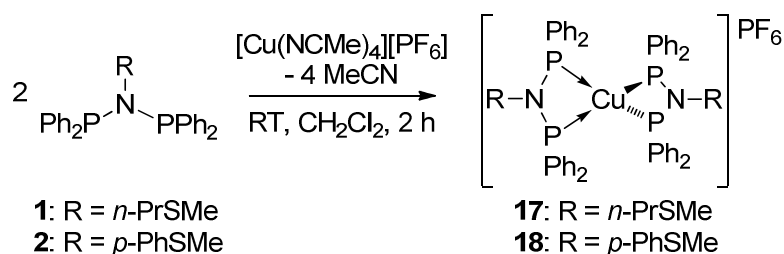


Fig. 13. View of the molecular structure of **16·2(CH₂Cl₂)**. Ellipsoids are represented at 50% probability level. Hydrogen atoms, solvent molecules and BF₄ anions omitted for clarity.

Table 5. Selected bond lengths (Å) and angles (deg) for **15**, **16·2(CH₂Cl₂)** and **17**.

	15	16·2(CH₂Cl₂)	17
Bond lengths, Å	M = Pd	M = Pd	M = Cu
M1-P1	2.3047(5)	2.3016(11)	2.2873(10)
M1-P2	2.3037(5)	2.2961(11)	2.2921(10)
M1-P3			2.2920(11)
M1-P4			2.2827(10)
Bond angles, deg			
P1-M1-P2	69.802(18)	70.77(4)	72.92(4)
P3-M1-P4			73.37(4)
P1-N1-P2	101.48(9)	102.2(2)	105.99(15)
P3-N2-P4			105.80(17)

Copper (I) complexes. The reaction of ligand **1** or **2** with [Cu(NCMe)₄]PF₆ was performed in a 2:1 ratio, in order to form the bis-chelated tetrahedral complex. Decoordination of MeCN was readily observed in the ¹H NMR spectrum, while the ³¹P{¹H} NMR resonance for the four equivalent phosphorous nuclei was downfield shifted to 85.6 and 90.1 ppm, for **17** and **18**, respectively, compared to the resonance of the free ligands at 64.06 (**1**) and 70.60 ppm (**2**) (Scheme 9).

Scheme 9. Synthesis of Cu(I) bis-chelated complexes

The bis-chelated, distorted tetrahedral coordination geometry around the copper center was confirmed by single crystal X-ray diffraction analysis on **17** (Fig. 14). In this structure all the Cu-P bond lengths are in the same range (\approx 2.29 Å) and similar to those observed for the bis-chelated palladium complexes (\approx 2.30 Å). The P-Cu-P chelate angles are also equivalent but wider than those observed in the structures of **15** and **16**, probably because of the higher atomic radii of Cu(I) compared to Pd(II). The characteristic bond lengths and angles of complex **17** are reported in Table 5.

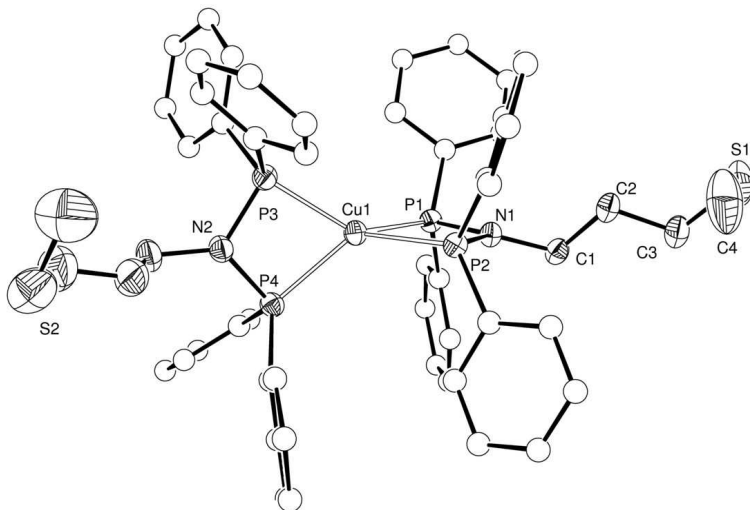


Fig. 14. View of the molecular structure of **17**. Ellipsoids are represented at 50% probability level. Hydrogen atoms and PF_6^- anion omitted for clarity.

Co₄ core cluster. We study only ligand **2** in this section, because the presence of the aromatic spacer seems to be more interesting for the desired application of this cluster. A doubly bridged cobalt carbonyl cluster was obtained by stepwise coordination of one then another diphosphine ligand. Reaction of one equivalent ligand **2** with the tetrahedral $[\text{Co}_4(\text{CO})_{12}]$ precursor afforded after purification by column chromatography the corresponding mono-bridged cluster **19'**, which was immediately engaged in the reaction with a second equivalent of ligand **2** to form cluster **19**, in a global yield of 50% after recrystallization (Scheme 10). Its $^{31}\text{P}\{\text{H}\}$ NMR spectrum contains three broad signals at 93.8, 97.2 and 112.5 ppm. The most upfield signal corresponds to the two P atoms of the diphosphine ligand linked to two basal Co atoms (their inequivalence may be masked by the broadness of the signal). The signal at 97.2 ppm corresponds to the P atom, of the second ligand, linked to the third basal Co, and finally the resonance of the P atom linked to the apical Co is the most downfield shifted. The structure of cluster **19** could be unambiguously confirmed by single crystal X-ray diffraction analysis (Fig. 15) and showed the tetrahedral arrangement of the four cobalt centers in a tetrahedral geometry. The two ligands bridge each two cobalt centers. Since P1 and P2, from one diphosphine, bridge the two basal Co₄ and Co₂ atoms, respectively, P4 and P3, from the second diphosphine, bridge Co₁, the third basal Co, and Co₃, the apical cobalt center, respectively. The orientation of the sulfur atoms, pointing away from each other, is most appropriate for further anchoring studies.

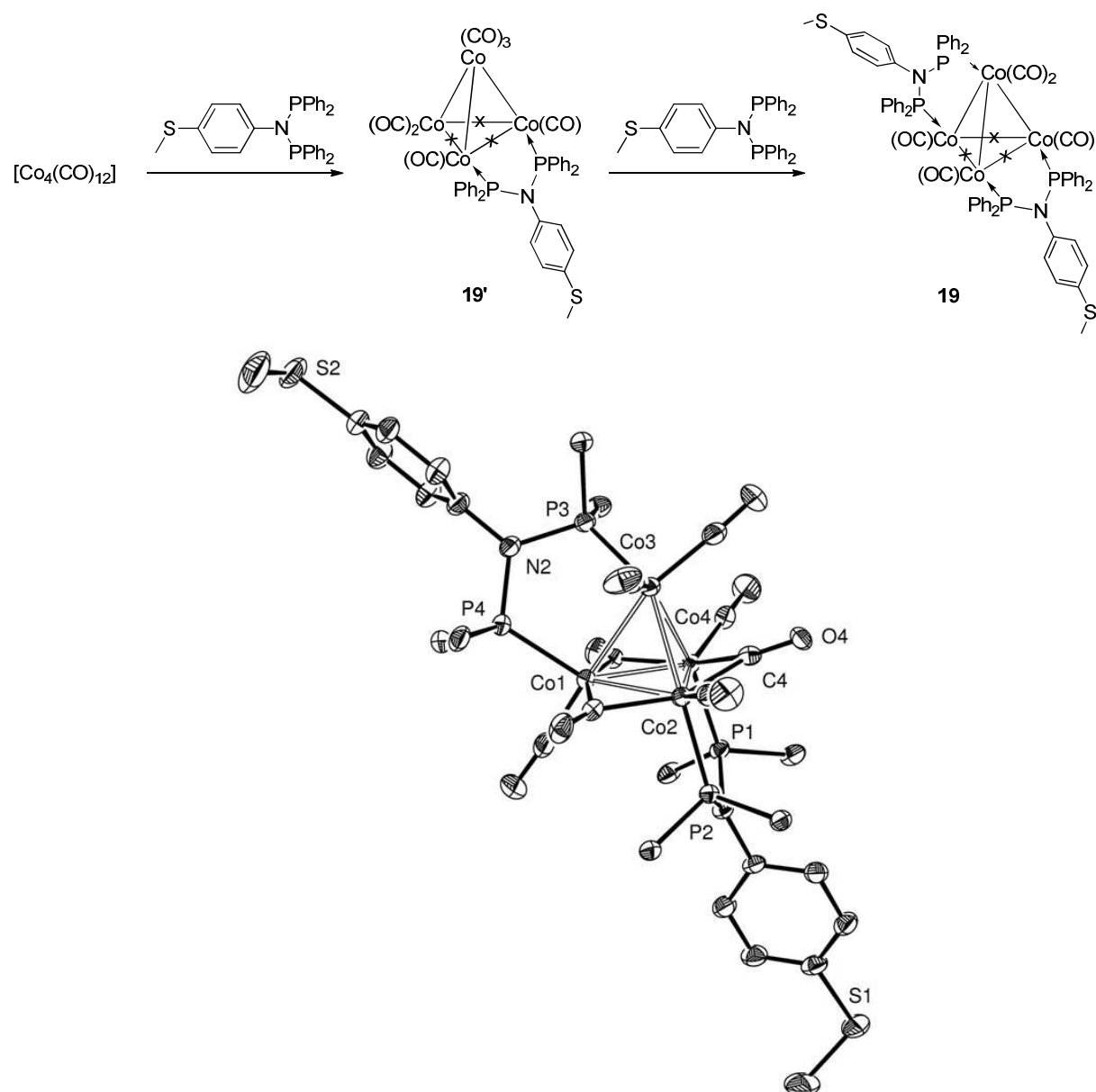
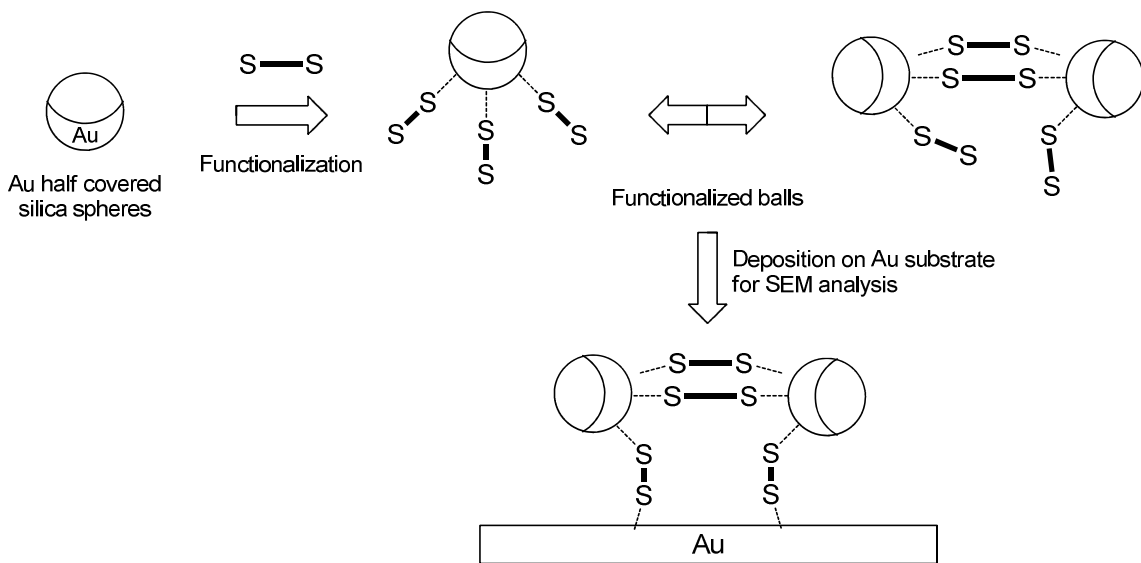
Scheme 10. Synthesis of the doubly bridged Co_4 core cluster.

Fig. 15. View of the molecular structure of $\mathbf{19}$. Ellipsoids are represented at 50% probability level. Hydrogen atoms omitted for clarity. Only the ipso carbons of the phenyl rings are represented. Selected distances (\AA) and angles ($^\circ$): Co1–Co2 2.5096(5), Co1–Co3 2.5535(5), Co1–Co4 2.4901(5), Co2–Co3 2.5200(5), Co2–Co4 2.4026(5), Co3–Co4 2.5349(5), P1–Co4 2.1825(7), P2–Co2 2.1823(7), P3–Co3 2.1979(8), P4–Co1 2.1884(7), Co2–Co1–Co4 57.442(14), Co2–Co1–Co3 59.691(14), Co3–Co1–Co4 60.328(13), Co1–Co2–Co3 61.021(14), Co1–Co2–Co4 60.871(14), Co3–Co2–Co4 61.934(14), Co1–Co3–Co2 59.288(14), Co1–Co3–Co4 58.596(13), Co2–Co3–Co4 56.757(13), Co1–Co4–Co2 61.687(14), Co1–Co4–Co3 61.076(13), Co2–Co4–Co3 61.309(14), P1–N1–P2 117.70(12), P3–C31–P4 114.73(12).

Preliminary Anchoring Studies.

Solutions of the palladium complexes **15** or **16** at different concentrations (0.1 and 0.01 mmol.L⁻¹) were mixed with partially gold-covered silica spheres, prepared by Vina Faramarzi in the IPCMS (Strasbourg), with the objective to link these spheres through the two thioether functions of the organometallic complexes (Scheme 11). After filtration and washing, the spheres were deposited on a gold substrate and analyzed by SEM (Scanning Electron Microscopy). When spheres (without complexes) were deposited on this gold substrate, and the latter washed, no sphere remained on the surface. However, when spheres which have been contacted with the complexes were deposited on the gold substrates, and the latter washed, they stayed on the gold substrate owing to interactions between the thioether groups of the complexes attached to the gold layer covering the spheres and the gold substrate (Scheme 11).

Scheme 11. Protocol for partially gold covered spheres functionalization and analysis.



SEM images of the high concentrated batch (0.1 mmol.L⁻¹) showed pollution of excess complexes around the spheres. We could not conclude of the nature of the link between spheres and between the spheres and the gold substrate (Fig. 16). At lower concentration (0.01 mmol.L⁻¹), no aggregates were observed, but only well-defined arrangements of spheres (Fig. 17). We conclude that the complexes were chemisorbed on the gold surfaces and connected the spheres to each other.

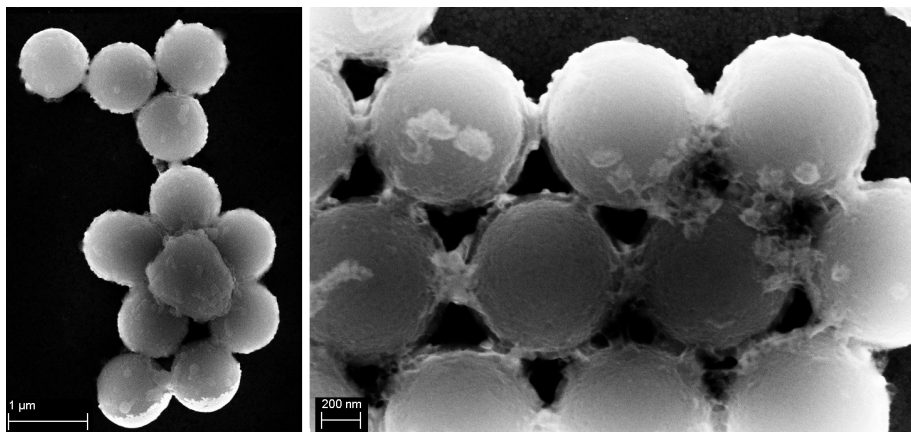


Fig. 16. SEM images of functionalized microspheres partially covered with Au, treated with a solution of complex **16** at 0.1 mmol.L^{-1} .

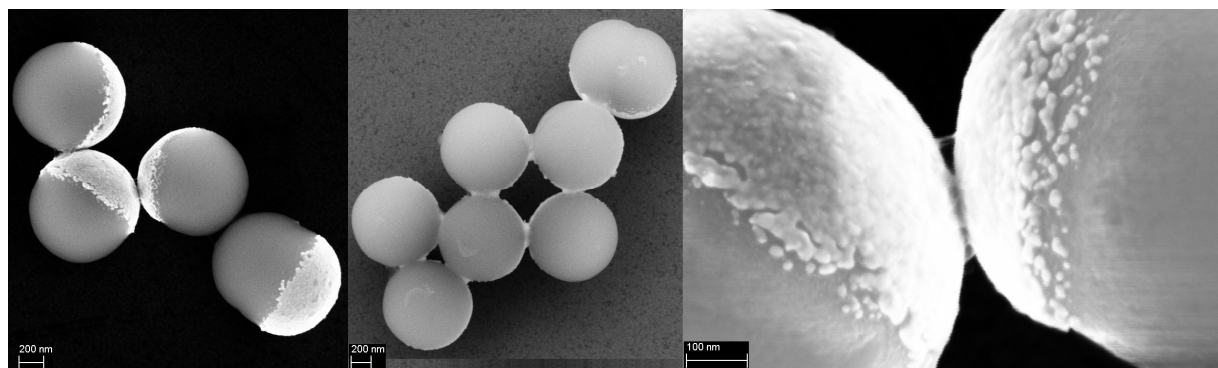
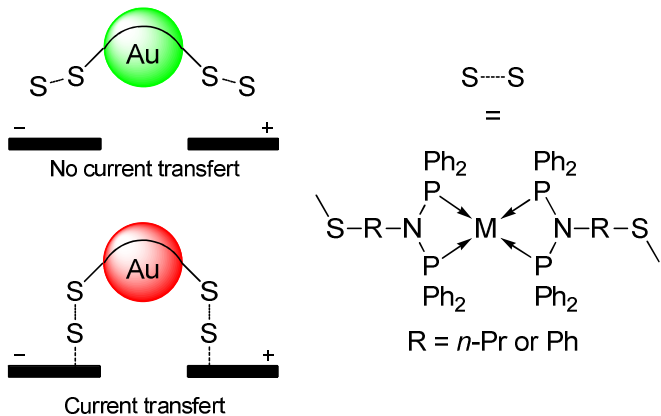


Fig. 17. SEM images of functionalized microspheres partially covered with Au, treated with a solution of complex **16** at 0.01 mmol.L^{-1} .

These experiments are done in collaboration with the group of Prof. B. Doudin in the IPCMS (Strasbourg) and will now be investigated in more details. These preliminary results showed the affinity of our thioether-functionalized organometallic compounds for gold surfaces and showed that they are able to “stick” macroscopic entities through their functional group. We are also interested to see in the future if these systems could be used for electronic transport, as illustrated in Scheme 12.

Scheme 12. Application of the bis-chelated or doubly-bridged compounds in electronic transport studies.



Conclusion

In this chapter we reported the synthesis and characterization of thioether functionalized bis(diphenylphosphino)amine ligands, ligand **1** with an aliphatic chain linking the PNP moiety and the thioether function, and ligand **2** with a *para*-SMe substitution on a phenyl ring.

We succeeded in the formation of Ni(II) and Cr(III) complexes bearing ligands **1** and **2** and we evaluated them for the catalytic oligomerization of ethylene. The Ni(II) complexes showed generally a higher activity and selectivity for C4 oligomers, while the Cr(III) complexes produced mainly α -olefins.

We formed unpredicted assemblies when we reacted ligand **1** or **2** with Fe(II) or Co(II) salts, which are interesting compounds for further EPR and magnetism studies.

Finally, we were able to produce bis-functionalized complexes with different metallic *core*, which could be deposited on partially gold covered spheres and were able to connect them together.

This work open many collaborations, and will be continued after the end of this thesis work.

Experimental Section

General Procedures. All operations were carried out using standard Schlenk techniques under inert atmosphere. Solvents were purified and dried under nitrogen by conventional methods. CD_2Cl_2 and CDCl_3 were dried over 4 Å molecular sieves, degassed by freeze-pump-thaw cycles and stored under argon. NMR spectra were recorded at room temperature on a Bruker AVANCE 300 spectrometer (^1H , 300 MHz; ^{13}C , 75.47 MHz; ^{31}P , 121.49 MHz and ^{19}F , 282.38 MHz) and referenced using the residual proton solvent (^1H) or solvent (^{13}C) resonance. Assignments are based on ^1H , ^1H -COSY, ^1H , ^{13}C -HMQC and ^1H , ^{13}C -HMBC experiments. Chemical shifts (δ) are given in ppm. IR spectra were recorded in the region 4000-100 cm^{-1} on a Nicolet 6700 FT-IR spectrometer (ATR mode, SMART ORBIT accessory, Diamond crystal). Elemental analyses were performed by the “Service de microanalyses”, Université de Strasbourg and by the “Service Central d’Analyse”, USR-59/CNRS, Solaize. Electrospray mass spectra (ESI-MS) were recorded on a microTOF (Bruker Daltonics, Bremen, Germany) instrument using nitrogen as drying agent and nebulising gas and Maldi-TOF analyses were carried out on a Bruker AutiflexII TOF/TOF (Bruker Daltonics, Bremen, Germany), using dithranol (1.8.9 trihydroxyanthracene) as a matrix. The complexe $[\text{Pd}(\text{NCMe})_4][\text{BF}_4]_2$,²⁰ was prepared according to literature method. All other reagents were used as received from commercial suppliers.

The synthesis of the Ni(II), Cr(III), Fe(II) and Co(II) complexes and the ethylene oligomerization catalytic studies were done in collaboration with Dr. Vitor Rosa, a post-doctoral researcher.

Some results being very recent, all the characterization could not yet be reported in this manuscript.

Synthesis of ligands **1** and **2** ($\text{Ph}_2\text{PNRPPPh}_2$).

Ligand **1**, R = *n*-PrSMe

Chlorodiphenylphosphine in excess (4.07 mL, 5.00 g, 22.65 mmol) was added dropwise to a solution of 3-(methylthio)propylamine (1.27 mL, 1.19 g, 11.32 mmol) and triethylamine (3.95 mL, 2.86 g, 28.31 mmol) in THF at 0 °C under inert atmosphere. The reaction mixture was stirred for 2 h at 0 °C and then at room temperature for 6 h. After filtration, the volatiles were removed under reduced pressure and the residue was washed twice with pentane to give **1** as colourless solid. Yield: 68%. Anal. Calcd. for $\text{C}_{28}\text{H}_{29}\text{NP}_2\text{S}$ (473.55): C, 71.02; H, 6.17; N, 2.96. Found: C, 71.33; H, 6.32; N, 2.71. ^1H NMR (CDCl_3) δ: 1.39 (2H, m, CH_2SCH_3), 1.82 (3H, s, CH_2SCH_3), 2.08 (2H, m, $\text{CH}_2\text{CH}_2\text{SCH}_3$), 3.35 (2H, m, NCH_2CH_2), 7.31–7.42 (20H, m, H-phenyl); $^{13}\text{C}\{\text{H}\}$ NMR (CDCl_3) δ: 15.38 (CH_3), 30.43 (CH_2SCH_3), 31.41 ($\text{CH}_2\text{CH}_2\text{SCH}_3$), 52.11 (NCH_2CH_2), 128.13 (m-Ph), 128.82 (p-Ph), 132.72 (o-Ph), 139.37 (ipso-Ph); $^{31}\text{P}\{\text{H}\}$ (CDCl_3) δ: 64.06 (s).

Ligand **2**, R = *p*-PhSMe

The same procedure was used with chlorodiphenylphosphine (5.15 mL, 6.34 g, 28.73 mmol), 4-(methylthio)aniline (1.79 mL, 2.00 g, 14.37 mmol) and triethylamine (5.01 mL, 3.63 g, 35.91 mmol). Yield: 71%. Anal. Calcd. for $\text{C}_{31}\text{H}_{27}\text{NP}_2\text{S}$ (507.57): C, 73.36; H, 5.36; N, 2.76. Found: C, 72.98; H, 5.48; N, 2.51. ^1H NMR (CDCl_3) δ: 2.32 (3H, s, CH_3), 6.55 [2H, d, $^3J_{\text{HH}} = 8.7$ Hz, N($\text{C}_6\text{H}_4\text{S}$), $\text{H}_{\text{ortho/N}}$], 6.85 [2H, d, $^3J_{\text{HH}} = 8.7$ Hz, N($\text{C}_6\text{H}_4\text{S}$), $\text{H}_{\text{meta/N}}$], 7.26–7.40 (20H, m, H-phenyl); $^{31}\text{P}\{\text{H}\}$ (CDCl_3) δ: 70.60 (s).

Synthesis of Ni(II) complexes **3** and **4**.

Complex **3**, [$\text{NiCl}_2(\mathbf{1})$]

To a suspension of [$\text{NiCl}_2(\text{dme})$] (0.093 g, 0.42 mmol) in CH_2Cl_2 (10 mL) was added a solution of ligand **1** (0.200 g, 0.42 mmol) in CH_2Cl_2 (20 mL). The solution quickly turned to orange/red and was stirred at room temperature for 12 h. The solvent was removed under reduced pressure and the red/orange solid was washed with diethyl ether and pentane yielding 0.220 g (86%) of complex **3**. Red crystals suitable for single crystal X-ray diffraction were grown from a mixture of CH_2Cl_2 /pentane. Anal. Calcd. for $\text{C}_{28}\text{H}_{29}\text{Cl}_2\text{NNiP}_2\text{S}$ (603.15): C, 55.76; H, 4.85; N, 2.32. Found: *waiting for results.* ^1H NMR (CD_2Cl_2) δ: 8.02–7.95 (m, 8H, Ar), 7.75–7.70 (m, 4H, Ar), 7.63–7.58 (m, 8H, Ar), 2.90 (m, 2H, NCH_2), 2.06 (m, 2H, CH_2S),

1.84 (s, 3H, SCH_3), 1.28-1.19 (m, 2H, $\text{CH}_2\text{CH}_2\text{CH}_2$). $^{31}\text{P}\{\text{H}\}$ (CD_2Cl_2) δ : 42.9 (s). FTIR: $\nu_{\text{max}}(\text{solid})/\text{cm}^{-1}$ 1478w, 1433m, 1307w, 1223w, 1182w, 1145m, 1098s, 1067sh, 996w, 853m, 817w, 748s, 717m, 693vs. MS (ESI): m/z 566.1 [M-Cl] $^+$.

Complex 4, $[\text{NiCl}_2(2)]$

To a suspension of $[\text{NiCl}_2(\text{dme})]$ (0.130 g, 0.59 mmol) in CH_2Cl_2 (10 mL) was added a solution of ligand **2** (0.300 g, 0.59 mmol) in CH_2Cl_2 (20 mL). The solution quickly turned to orange/red and was stirred at room temperature for 12 h. The solvent was removed under reduced pressure and the red solid was washed with diethyl ether and pentane yielding 0.312 g (83%) of complex **4**. Red crystals suitable for single crystal X-ray diffraction were grown from a mixture of CH_2Cl_2 /pentane. Anal. Calcd. for $\text{C}_{31}\text{H}_{27}\text{Cl}_2\text{NNiP}_2\text{S}$ (637.16): C, 58.44; H, 4.27; N, 2.20. Found: *waiting for results*. ^1H NMR (CD_2Cl_2) δ : 8.05-7.98 (m, 8H, Ar), 7.73-7.68 (m, 4H, Ar), 7.59-7.54 (m, 8H, Ar), 6.86-6.83 (m, 2H, Ar), 6.39-6.36 (m, 2H, Ar), 2.32 (s, 3H, CH_3). $^{31}\text{P}\{\text{H}\}$ (CD_2Cl_2) δ : 46.6 (s). FTIR: $\nu_{\text{max}}(\text{solid})/\text{cm}^{-1}$ 1589w, 1492m, 1480m, 1433m, 1309w, 1254s, 1182w, 1104s, 1096s, 997w, 951m, 906s, 823w, 749m, 737m, 720m, 687vs. MS (ESI): m/z 600.0 [M-Cl] $^+$.

Synthesis of Cr(III) complexes **5a**, **5b** and **6a**.

Complex **5a**, $[\text{CrCl}_3(1)(\text{thf})]$

To a solution of $[\text{CrCl}_3(\text{thf})_3]$ (0.230 g, 0.63 mmol) in CH_2Cl_2 (20 mL) was added a solution of ligand **1** (0.300 g, 0.63 mmol) in CH_2Cl_2 (20 mL). The violet solution turned to blue/violet after 1 h and was stirred at room temperature for 12 h. The solvent was removed under reduced pressure and the blue/violet solid was washed with diethyl ether and pentane yielding 0.270 g (61%) of complex **5**. Anal. Calcd. for $\text{C}_{32}\text{H}_{37}\text{Cl}_3\text{CrNOP}_2\text{S}$ (704.01): C, 54.91; H, 4.75; N, 2.00. Found: *waiting for results*. Violet crystals suitable for single crystal X-ray diffraction were grown from a mixture of THF/pentane. MS (ESI): m/z 663.1 [M-Cl] $^+$.

Complex **6a**, $[\text{CrCl}_3(2)(\text{thf})]$

To a solution of $[\text{CrCl}_3(\text{THF})_3]$ (0.221 g, 0.59 mmol) in CH_2Cl_2 (20 mL) was added a solution of ligand **2** (0.300 g, 0.59 mmol) in CH_2Cl_2 (20 mL). The violet solution was stirred at room temperature for 12 h. The solvent was removed under reduced pressure and the violet solid was washed with diethyl ether and pentane yielding 0.280 g (65%) of complex **6a**. Anal. Calcd. for $\text{C}_{35}\text{H}_{35}\text{Cl}_3\text{CrNOP}_2\text{S}$ (738.03): C, 57.27; H, 4.26; N, 1.91. Found: *waiting for*

results. MS (ESI): m/z 697.0 [M-Cl]⁺.

Complex **5b**, [CrCl₃(**1**)(dmap)]

To a solution of **5a** (0.100 g, 0.16 mmol) in CH₂Cl₂ (10 mL) was added a solution of dmap (0.020 g, 0.16 mmol) in THF (20 mL). The violet solution quickly turned to blue and was stirred at room temperature for 12 h. The solvent was removed under reduced pressure, and the blue solid was washed with diethyl ether and pentane yielding 0.092 g (77%) of complex **5b**. Blue crystals suitable for single crystal X-ray diffraction were grown from a mixture of CH₂Cl₂/pentane. Anal. Calcd. for C₃₅H₃₉Cl₃CrN₃P₂S (754.07): C, 55.75; H, 5.21; N, 5.57. Found: *waiting for results.* MS (ESI): m/z 754.1 [M-Cl]⁺.

Synthesis of Fe(II) and Co(II) complexes **7 - 14**.

Complex **7**, [FeCl₂(**1**)_n

To a suspension of anhydrous FeCl₂ (0.127 g, 1.06 mmol) in CH₂Cl₂ (10 mL) was added a solution of ligand **1** (0.500 g, 1.06 mmol) in CH₂Cl₂ (20 mL). The solution quickly turned to pink and was stirred at room temperature for 12 h. The solution was concentrated to a third of its original volume and crystallization by slow diffusion of pentane afforded yellow crystals of complex **7**. Yield: 0.545 g (86%). Anal. Calcd. for C₂₈H₂₉Cl₂FeNP₂S (600.30): C, 56.02; H, 4.87; N, 2.33. Found: C, 55.71; H, 4.66; N, 2.57. Yellow crystals suitable for single crystal X-ray diffraction were grown from a mixture of CH₂Cl₂/pentane.

Complex **8**, [FeCl₂(**2**)₂

The same procedure was used with anhydrous FeCl₂ (0.075 g, 0.59 mmol) and ligand **1** (0.300 g, 0.59 mmol) affording orange crystals of complex **8**. Yield: 0.320 g (85%). Anal. Calcd. for C₆₂H₅₄Cl₄Fe₂N₂P₄S₂ (1268.63): C, 58.70; H, 4.29; N, 2.21. Found: C, 58.36; H, 4.04; N, 1.97.

Complex **9**, [Co₂Cl₄(**1**)₂]

To a suspension of anhydrous CoCl₂ (0.082 g, 0.63 mmol) in CH₂Cl₂ (10 mL) was added a solution of ligand **1** (0.300 g, 0.63 mmol) in CH₂Cl₂ (20 mL). The solution quickly turned to green and was stirred at room temperature for 12 h. The solution was filtered through a Celite pad and the solvent was removed under reduced pressure and the dark green solid was washed with diethyl ether and pentane yielding 0.210 g (83%) of complex **9**. Red/green crystals suitable for single crystal X-ray diffraction were grown from a mixture of CH₂Cl₂/pentane.

Anal. Calcd. for $C_{56}H_{58}Cl_4Co_2N_2P_4S_2$ (1206.78): C, 55.74; H, 4.84; N, 2.32. Found: *waiting for results*. FTIR: $\nu_{\text{max}}(\text{solid})/\text{cm}^{-1}$ 1770w, 1480w, 1433s, 1310w, 1184w, 1091s, 1069sh, 1037sh, 997m, 879m, 734s, 694vs. FarFTIR: $\nu_{\text{max}}(\text{solid})/\text{cm}^{-1}$ 531s, 511s, 502s, 490s, 482s, 319vs. MS (ESI): m/z 1171.1 [M-Cl]⁺.

Complex **10**, $[\text{CoCl}_2(\mathbf{2})]_2$

The same procedure was used with anhydrous CoCl_2 (0.051 g, 0.39 mmol) and ligand **2** (0.200 g, 0.39 mmol) affording complex **10** as green crystalline solid. Yield: 0.312 g (83%). Anal. Calcd. for $C_{62}H_{54}Cl_4Co_2N_2P_4S_2$ (1274.81): C, 58.41; H, 4.27; N, 2.20. Found: *waiting for results*. FTIR: $\nu_{\text{max}}(\text{solid})/\text{cm}^{-1}$ 1586w, 1491m, 1433s, 1299w, 1271w, 1217m, 1158w, 1093s, 1026w, 1010w, 998w, 934m, 894s, 811w, 736s, 691vs. MS (ESI): m/z 1005.2 [M- CoCl_4]⁺.

Complex **11**, $[\text{CoCl}(\mathbf{1})_2]\text{PF}_6$

The same procedure was used with anhydrous CoCl_2 (0.069 g, 0.53 mmol), KPF_6 (0.098 g, 0.53 mmol) and ligand **1** (0.500 g, 1.06 mmol) affording green crystals of complex **11**. Yield: 0.590 g (94%). Anal. Calcd. for $C_{56}H_{58}\text{ClCoF}_6N_2P_5S_2$ (1186.45): C, 56.69; H, 4.93; N, 2.36. Found: *waiting for results*. FTIR: $\nu_{\text{max}}(\text{solid})/\text{cm}^{-1}$ 1434m, 1312w, 1187w, 1091s, 999w, 834vs, 734s, 693s. FarFTIR: $\nu_{\text{max}}(\text{solid})/\text{cm}^{-1}$ 556vs, 529vs, 511vs, 500vs, 490vs, 481m. MS (ESI): m/z 1040.2 [M- PF_6]⁺.

Complex **13**, $[\text{CoCl}(\mathbf{2})_2]\text{PF}_6$

The same procedure was used with anhydrous CoCl_2 (0.064 g, 0.49 mmol), KPF_6 (0.090 g, 0.49 mmol) and ligand **2** (0.500 g, 0.98 mmol) affording green crystals of complex **13**. Yield: 0.580 g (94%). Anal. Calcd. for $C_{62}H_{54}\text{ClCoF}_6N_2P_5S_2$ (1254.48): C, 59.36; H, 4.34; N, 2.23. Found: *waiting for results*. FTIR: $\nu_{\text{max}}(\text{solid})/\text{cm}^{-1}$ 1490m, 1434m, 1217m, 1094m, 937m, 898m, 836vs, 736m, 694s. MS (ESI): m/z 1108.2 [M- PF_6]⁺.

Complex **12**, $[\text{CoCl}_3(\text{MeSn-PropNH}_3)]$

A HCl (37%) solution (0.39 mL, 0.173 g, 4.75 mmol) was added to a solution 3-(methylthio)propylamine (0.53 mL, 0.500 g, 4.75 mmol) in CH_2Cl_2 . A white precipitate was instantaneously formed. Anhydrous CoCl_2 (0.617 g, 4.75 mmol) was then added to the suspension, which turned blue, and the mixture was stirred for 2 h. The volatiles were then removed under reduced pressure and the solid washed with diethyl ether (2 x 20 mL).

Complex **12** was isolated as a blue powder. Yield: 1.11 g (86%). Anal. Calcd. for C₄H₁₂Cl₃CoNS (271.50): C, 17.70; H, 4.45; N, 5.16. Found: *waiting for results*. FarFTIR: $\nu_{\text{max}}(\text{solid})/\text{cm}^{-1}$ 318sh, 305sh, 287vs, 275sh. MS (ESI): *m/z* 234.9 [M-Cl]⁺.

Complex **14**, [CoCl₄(H₃Np-PhenSMe)₂]

The same procedure was used with anhydrous CoCl₂ (0.466 g, 3.59 mmol), HCl (0.29 mL, 0.131 g, 3.59 mmol) and 4-(methylthio)aniline (0.45 mL, 0.500 g, 3.59 mmol) affording complex **14** as a blue powder. Yield: 0.760 g (44%). Anal. Calcd. for C₁₄H₂₀Cl₄CoN₂S₂ (481.20): C, 34.94; H, 4.19; N, 5.82. Found: *waiting for results*. FarFTIR: $\nu_{\text{max}}(\text{solid})/\text{cm}^{-1}$ 320s, 294vs, 271vs, 125vs, 117vs. MS (ESI): *m/z* 140.1 [CH₃S(C₆H₄)NH₃]⁺.

Synthesis of Pd(II) complexes **15 – 16**.

Complex **15**, [Pd(**1**)₂][BF₄]₂

A solution of [Pd(NCMe)₄][BF₄]₂ (0.094 g, 0.21 mmol) in CH₂Cl₂ was added to a solution of ligand **1** (0.200 g, 0.42 mmol) in CH₂Cl₂ and stirred at room temperature for 2 h. the reaction mixture was filtered through a Celite pad and the volatiles were removed under reduced pressure. The residue was washed with diethyl ether (2 x 20 mL) and dried, affording complex **15** as a yellow solid. Yield: 0.240 g (93%). Anal. Calcd. for C₅₆H₅₈B₂F₈N₂P₄PdS₂ (1227.13): C, 54.81; H, 4.76; N, 2.28. Found: *waiting for results*. ¹H NMR (CDCl₃) δ : 2.03 (4H, m, CH₂S), 1.84 (6H, s, CH₃S), 2.98 (4H, m, CH₂CH₂S), 3.41 (4H, m, NCH₂), 7.09-7.65 (40H, m, H arom). ³¹P{¹H} NMR (CDCl₃) δ : 48.4 (s).

Complex **16**, [Pd(**2**)₂][BF₄]₂

The same procedure was used with [Pd(NCMe)₄][BF₄]₂ (0.088 g, 0.20 mmol) and ligand **2** (0.200 g, 0.39 mmol) affording complex **16** as a yellow solid. Yield: 0.232 g (91%). Anal. Calcd. for C₆₂H₅₄B₂F₈N₂P₄PdS₂ (1295.16): C, 57.50; H, 4.20; N, 2.16. Found: *waiting for results*. ¹H NMR (CDCl₃) δ : 2.41 (6H, s, CH₃S), 6.44 (4H, d, ³J_{HH} = 8.6 Hz, H arom), 6.70 (4H, d, ³J_{HH} = 8.6 Hz, H arom), 7.05-7.70 (40H, m, H arom). ³¹P{¹H} NMR (CDCl₃) δ : 55.5 (s).

Synthesis of Cu(I) complex **17 -18**.

Complex **17**, [Cu(**1**)₂][PF₆].

The same procedure was used with [Cu(NCMe)₄][PF₆] (0.039 g, 0.11 mmol) and ligand **1**

(0.100 g, 0.21 mmol) affording complex **17** as a colorless solid. Yield: 0.106 g (87%). Anal. Calcd. for $C_{56}H_{58}CuF_6N_2P_5S_2$ (1155.61): C, 58.20; H, 5.06; N, 2.42. Found: *waiting for results*. 1H NMR ($CDCl_3$) δ : 1.92 (4H, m, CH_2S), 1.73 (6H, s, CH_3S), 3.05 (4H, m, CH_2CH_2S), 3.30 (4H, m, NCH_2), 6.92-7.75 (40H, m, H arom). $^{31}P\{^1H\}$ NMR ($CDCl_3$) δ : 85.6 (s), -143.0 (sept., $^1J_{P,F} = 712$ Hz, PF_6).

Complex **18**, $[Cu(2)_2][PF_6]$.

The same procedure was used with $[Cu(NCMe)_4][PF_6]$ (0.037 g, 0.10 mmol) and ligand **2** (0.100 g, 0.20 mmol) affording complex **18** as a colorless solid. Yield: 0.109 g (90%). Anal. Calcd. for $C_{62}H_{54}CuF_6N_2P_5S_2$ (1223.64): C, 60.86; H, 4.45; N, 2.29. Found: *waiting for results*. 1H NMR ($CDCl_3$) δ : 2.32 (6H, s, CH_3S), 6.20 (4H, d, $^3J_{HH} = 8.6$ Hz, H arom), 6.75 (4H, d, $^3J_{HH} = 8.6$ Hz, H arom), 7.02-7.60 (40m, H arom). $^{31}P\{^1H\}$ NMR ($CDCl_3$) δ : 90.1 (s), -143.0 (sept., $^1J_{P,F} = 712$ Hz, PF_6).

Synthesis of Co₄ cluster **19**.

A solution of ligand **2** (0.300 g, 0.59 mmol) in CH_2Cl_2 (20 mL) was slowly added to a solution of $[Co_4(CO)_{12}]$ (0.338 g, 0.59 mmol) in CH_2Cl_2 (20 mL). The reaction mixture was stirred at room temperature under argon atmosphere and gas evolution occurred through an oil bubbler. The reaction was followed by TLC, stopped after 6 h and the solvent was evaporated under reduced pressure. Cluster **19'** was purified by column chromatography (CH_2Cl_2 /pentane 50:50). $R_f = 0.57$ (CH_2Cl_2 /pentane 50:50). Red solid, yield: 0.375 g, 62%.

A solution of ligand **2** (0.186 g, 0.37 mmol) in CH_2Cl_2 (20 mL) was slowly added to a solution of **19'** (0.375 g, 0.37 mmol) in CH_2Cl_2 (20 mL). The reaction mixture was stirred at room temperature under argon atmosphere and gas evolution occurred through an oil bubbler. The reaction was followed by TLC, stopped after 6 h and the solvent was evaporated under reduced pressure. Cluster **19** was purified by column chromatography (CH_2Cl_2 /pentane 50:50). $R_f = 0.36$ (CH_2Cl_2 /pentane 50:50). Green solid, yield: 0.448 g, 83%. Anal. Calc. for $C_{70}H_{54}Co_4N_2O_8P_4S_2$ (1474.94): C, 57.00; H, 3.69; N, 1.90. Found: *waiting for results*. $^{31}P\{^1H\}$ NMR ($CDCl_3$) δ : 93.8 (br s, P_{basal}), 97.2 (br s, P_{basal}), 112.5 (br s, P_{apical}). MS (ESI): m/z 1474.0 [M]⁺.

X-ray data collection, structure solution and refinement for all compounds

Suitable crystals for the X-ray analysis of all compounds were obtained as described above. The intensity data were collected on a Kappa CCD diffractometer²¹ (graphite monochromated MoK α radiation, $\lambda = 0.71073 \text{ \AA}$) at 173(2) K. Crystallographic and experimental details for the structures are summarized in Table 1. The structures were solved by direct methods (SHELXS-97) and refined by full-matrix least-squares procedures (based on F^2 , SHELXL-97)²² with anisotropic thermal parameters for all the non-hydrogen atoms. The hydrogen atoms were introduced into the geometrically calculated positions (SHELXS-97 procedures) and refined *riding* on the corresponding parent atoms. For some compounds a MULTISCAN correction was applied.²³

Table 6. Crystallographic data for compounds **3**, **4·2(CH₂Cl₂)**, **5a** and **5b**.

Compound	3	4·2(CH₂Cl₂)	5a	5b
Chemical formula	C ₂₈ H ₂₉ Cl ₂ NNiP ₂ S	C ₃₃ H ₃₁ Cl ₆ NNiP ₂ S	C ₃₂ H ₃₇ Cl ₃ CrNOP ₂ S	C ₃₅ H ₃₉ Cl ₃ CrN ₃ P ₂ S
Formula Mass	603.13	807.00	703.98	754.04
Crystal system	Orthorhombic	Monoclinic	Monoclinic	Monoclinic
<i>a</i> /Å	9.2439(2)	9.8740(3)	13.1440(5)	11.1734(5)
<i>b</i> /Å	14.7453(3)	15.0213(7)	14.2278(5)	9.2708(3)
<i>c</i> /Å	20.8360(5)	24.2524(10)	17.3758(7)	35.8179(15)
$\alpha/^\circ$	90.00	90.00	90.00	90.00
$\beta/^\circ$	90.00	90.662(3)	96.877(2)	101.061(2)
$\gamma/^\circ$	90.00	90.00	90.00	90.00
V/Å ³	2840.03(11)	3596.9(2)	3226.1(2)	3641.3(3)
T/K	173(2)	173(2)	173(2)	173(2)
Space group	<i>P</i> 2 ₁ 2 ₁ 2 ₁	<i>C</i> c	<i>P</i> 2 ₁ /c	<i>P</i> 2 ₁ /c
<i>Z</i>	4	4	4	4
μ/mm^{-1}	1.076	1.157	0.795	0.709
No. of reflections measured	21228	6923	18277	12738
No. of independent reflections	6472	6922	7346	8240
R_{int}	0.0486	0.0258	0.0777	0.0325
Final R_I values ($I > 2\sigma(I)$)	0.0336	0.0515	0.0760	0.0499
Final $wR(F^2)$ values ($I > 2\sigma(I)$)	0.0755	0.1164	0.1311	0.1374
Final R_I values (all data)	0.0450	0.0900	0.1352	0.0841
Final $wR(F^2)$ values (all data)	0.0923	0.1415	0.1578	0.1603
Goodness of fit on F^2	1.131	1.078	1.096	0.986

Table 7. Crystallographic data for compounds **7** and **8**.

Compound	7	8
Chemical formula	C ₅₆ H ₅₈ Cl ₄ Fe ₂ N ₂ P ₄ S ₂	C ₆₂ H ₅₄ Cl ₄ Fe ₂ N ₂ P ₄ S ₂
Formula Mass	1200.54	1268.57
Crystal system	Triclinic	Triclinic
a/Å	9.1061(3)	10.6991(5)
b/Å	17.0094(7)	11.8203(6)
c/Å	18.7819(8)	12.0953(4)
α/°	91.446(2)	92.167(3)
β/°	92.284(2)	101.448(2)
γ/°	90.945(2)	94.786(2)
V/Å ³	2905.4(2)	1491.67(11)
T/K	173(2)	173(2)
Space group	P-1	P-1
Z	2	1
μ/mm ⁻¹	0.903	0.884
No. of reflections measured	31430	9480
No. of independent reflections	13006	6539
R _{int}	0.1148	0.0263
Final R _I values (I > 2σ(I))	0.0772	0.0491
Final wR(F ²) values (I > 2σ(I))	0.2112	0.1177
Final R _I values (all data)	0.1201	0.0906
Final wR(F ²) values (all data)	0.2373	0.1369
Goodness of fit on F ²	1.113	1.095

Table 8. Crystallographic data for compounds **9·2(CH₂Cl₂)**, **11**, **12** and **14**.

Compound	9·2(CH₂Cl₂)	11	12	14
Chemical formula	C ₅₈ H ₆₂ Cl ₈ Co ₂ N ₂ P ₄ S ₂	C ₅₇ H ₆₀ Cl ₃ CoF ₆ N ₂ P ₅ S ₂	C ₄ H ₁₂ Cl ₃ CoNS	C ₁₄ H ₂₀ N ₂ S ₂ Cl ₄ Co
Formula Mass	1376.56	1271.32	271.49	481.03
Crystal system	Triclinic	Monoclinic	Orthorhombic	Triclinic
a/Å	11.7798(5)	44.4062(17)	10.5383(4)	6.9440(3)
b/Å	15.9919(9)	13.0561(6)	11.1199(5)	12.4765(5)
c/Å	16.8204(9)	22.6438(5)	18.1015(9)	12.7558(4)
α/°	93.135(2)	90.00	90.00	69.658(2)
β/°	95.456(3)	106.959(2)	90.00	82.329(2)
γ/°	98.989(3)	90.00	90.00	86.360(2)
V/Å ³	3107.8(3)	12557.3(8)	2121.22(16)	1026.75(7)
T/K	173(2)	173(2)	173(2)	173(2)
Space group	P-1	C2/c	Pbca	P-1
Z	2	8	8	2
μ/mm ⁻¹	1.087	0.650	2.508	1.558
No. reflections measured	32917	18810	4030	8420
No. independent reflections	14090	11109	2165	5971
R _{int}	0.1680	0.0372	0.0413	0.0219
Final R _I values (I > 2σ(I))	0.0873	0.0772	0.0369	0.0365
Final wR(F ²) values (I > 2σ(I))	0.1827	0.2224	0.0687	0.0864
Final R _I values (all data)	0.1805	0.1141	0.0604	0.0544
Final wR(F ²) values (all data)	0.2396	0.2436	0.0746	0.0960
Goodness of fit on F ²	1.045	1.069	1.036	1.054

Table 9. Crystallographic data for compounds **15**, **16·2(CH₂Cl₂)**, **17** and **19**.

Compound	15	16·2(CH₂Cl₂)	17	19
Chemical formula	C ₅₆ H ₅₈ B ₂ F ₈ N ₂ P ₄ PdS ₂	C ₆₆ H ₆₂ B ₂ Cl ₈ F ₈ N ₂ P ₄ PdS ₂	C ₅₆ H ₅₈ CuF ₆ N ₂ P ₅ S ₂	C ₇₀ H ₅₄ Co ₄ N ₂ O ₈ P ₄ S ₂
Formula Mass	1227.06	1634.80	1155.55	1474.87
Crystal system	Orthorhombic	Triclinic	Monoclinic	Triclinic
a/Å	17.6285(2)	11.9008(4)	17.6838(6)	13.4668(4)
b/Å	16.7144(3)	11.9643(3)	16.9367(3)	15.7054(3)
c/Å	19.2078(3)	12.8949(3)	20.6900(6)	18.5623(5)
α/°	90.00	81.067(2)	90.00	75.876(2)
β/°	90.00	85.747(2)	115.810(2)	79.6230(10)
γ/°	90.00	82.589(2)	90.00	89.398(2)
V/Å ³	5659.57(15)	1795.87(9)	5578.6(3)	3742.70(17)
T/K	173(2)	173(2)	173(2)	173(2)
Space group	<i>Pbca</i>	<i>P-1</i>	<i>P2₁/c</i>	<i>P-1</i>
Z	4	1	4	2
μ/mm ⁻¹	0.580	0.766	0.668	1.062
No. reflections measured	47103	20718	21597	24731
No. independent reflections	6480	8220	11548	17006
R _{int}	0.0540	0.0611	0.0492	0.0267
Final R _I values (I > 2σ(I))	0.0342	0.0737	0.0578	0.0433
Final wR(F ²) values (I > 2σ(I))	0.0923	0.2055	0.1547	0.1143
Final R _I values (all data)	0.0488	0.0907	0.1061	0.0644
Final wR(F ²) values (all data)	0.1053	0.2266	0.1832	0.1229
Goodness of fit on F ²	1.132	1.057	0.996	1.004

References

- (1) Selected review articles: (a) T. Appleby and J. D. Woollins, *Coord. Chem. Rev.*, 2002, **235**, 121; (b) P. Braunstein, M. Knorr and C. Stern, *Coord. Chem. Rev.*, 1998, **178–180**, 903; (c) P. Bhattacharyya and J. D. Woollins, *Polyhedron*, 1995, **14**, 3367; (d) M. Witt and H. W. Roesky, *Chem. Rev.*, 1994, **94**, 1163; (e) M. S. Balakrishna, Y. Sreenivasa Reddy, S. S. Krishnamurthy, J. F. Nixon and J. C. T. R. Burckett St. Laurent, *Coord. Chem. Rev.*, 1994, **129**, 1; (f) J. T. Mague, *J. Cluster Sci.*, 1995, **6**, 217; (g) R. J. Puddephatt, *Chem. Soc. Rev.*, 1983, **12**, 99.
- (2) See e.g.: I. Bachert, P. Braunstein and R. Hasselbring, *New J. Chem.*, 1996, **20**, 993.
- (3) See e.g.: (a) B. Lin, Z. Liu, M. Liu, C. Pan, J. Ding, H. Wu and J. Cheng, *Catal. Commun.*, 2007, **8**, 2150; (b) T. Posset, F. Rominger and J. Bluemel, *Chem. Mater.*, 2005, **17**, 586; (c) Q. Zhang, G. Hua, P. Bhattacharyya, A. M. Z. Slawin and J. D. Woollins, *Dalton Trans.*, 2003, 3250; (d) I. M. Aladzheva, D. I. Lobanov, O. V. Bykhovskaya, P. V. Petrovskii, K. A. Lyssenko and T. A. Mastryukova, *Heteroat. Chem.*, 2003, **14**, 596; (e) I. Bachert, I. Bartusseck, P. Braunstein, E. Guillon, J. Rose and G. Kickelbick, *J. Organomet. Chem.*, 1999, **580**, 257; (f) H. G. Fick and W.

- Beck, *J. Organomet. Chem.*, 1983, **252**, 83; (g) J. Blin, P. Braunstein, J. Fischer, G. Kickelbick, M. Knorr, X. Morise and T. Wirth, *J. Chem. Soc., Dalton Trans.*, 1999, 2159; (h) B. Guemguem, O. Akba, F. Durap, L. T. Yildirim, D. Uelkue and S. Oezkar, *Polyhedron*, 2006, **25**, 3133; (i) G. Singh, S. Bali and A. K. Singh, *Polyhedron*, 2007, **26**, 897; (j) K. Issleib and H. Oehme, *Z. Anorg. Allg. Chem.*, 1977, **428**, 16.
- (4) See e.g.: (a) E. Killian, K. Blann, A. Bollmann, J. T. Dixon, S. Kuhlmann, M. C. Maumela, H. Maumela, D. H. Morgan, P. Nongodlwana, M. J. Overett, M. Pretorius, K. Hoefener and P. Wasserscheid, *J. Mol. Catal. A: Chem.*, 2007, **270**, 214; (b) M. Alajarín, C. Lopez-Leonardo and J. Berna, *Sci. Synth.*, 2007, **31b**, 1873; (c) S.-K. Yip, W. H. Lam, N. Zhu and V. W.-W. Yam, *Inorg. Chim. Acta*, 2006, **359**, 3639; (d) Z. Sun, F. Zhu, Q. Wu and S.-a. Lin, *Appl. Organomet. Chem.*, 2006, **20**, 175; (e) Z. Fei, W. H. Ang, D. Zhao, R. Scopelliti and P. J. Dyson, *Inorg. Chim. Acta*, 2006, **359**, 2635; (f) F. Majoumo, P. Loennecke, O. Kuehl and E. Hey-Hawkins, *Z. Anorg. Allg. Chem.*, 2004, **630**, 305; (g) Z. Fei, N. Biricik, D. Zhao, R. Scopelliti and P. J. Dyson, *Inorg. Chem.*, 2004, **43**, 2228; (h) N. Biricik, Z. Fei, R. Scopelliti and P. J. Dyson, *Eur. J. Inorg. Chem.*, 2004, 4232; (i) Z. Fei, R. Scopelliti and P. J. Dyson, *Dalton Trans.*, 2003, 2772; (j) N. Biricik, Z. Fei, R. Scopelliti and P. J. Dyson, *Helv. Chim. Acta*, 2003, **86**, 3281; (k) K. G. Gaw, M. B. Smith and A. M. Z. Slawin, *New J. Chem.*, 2000, **24**, 429; (l) V. W. Seidel and M. Alexiev, *Z. Anorg. Allg. Chem.*, 1978, **438**, 68; (m) G. Gotsmann and M. Schwarzmann, *Justus Liebigs Ann. Chem.*, 1969, **729**, 106.
- (5) (a) M. Rodriguez-Zubiri, V. Gallo, J. Rosé, R. Welter and P. Braunstein, *Chem. Commun.*, 2008, 64; (b) F. Majoumo-Mbe, P. Loennecke, E. V. Novikova, G. P. Belov and E. Hey-Hawkins, *Dalton Trans.*, 2005, 3326; (c) K. G. Gaw, M. B. Smith and J. W. Steed, *J. Organomet. Chem.*, 2002, **664**, 294.
- (6) (a) P. Braunstein, *J. Organomet. Chem.*, 2004, **689**, 3953; (b) A. Choualeb, P. Braunstein, J. Rosé, S.-E. Bouaoud and R. Welter, *Organometallics*, 2003, **22**, 4405; (c) F. Schweyer-Tihay, P. Braunstein, C. Estournès, J. L. Guille, B. Lebeau, J.-L. Paillaud, M. Richard-Plouet and J. Rosé, *Chem. Mater.*, 2003, **15**, 57.
- (7) P. Braunstein, H.-P. Kormann, W. Meyer-Zaika, R. Pugin and G. Schmid, *Chem. Eur. J.*, 2000, **6**, 4637.
- (8) (a) K. Raghuraman, S. S. Krishnamurthy and M. Nethaji, *J. Organomet. Chem.*, 2003, **669**, 79; (b) D. W. Engel, K. G. Moodley, L. Subramony and R. J. Haines, *J. Organomet. Chem.*, 1988, **349**, 393; (c) L. Subramony, D. W. Engel and K. G. Moodley, *Acta Crystallogr., Sect.A: Found Crystallogr.*, 1984, **40**, C297.
- (9) T. S. Venkatakrishnan, S. S. Krishnamurthy and M. Nethaji, *J. Organomet. Chem.*, 2005, **690**, 4001.
- (10) C. Fliedel, R. Pattacini and P. Braunstein, *J. Clust. Sci.*, 2010, DOI 10.1007/s10876-010-0315-9.

- (11) V. Gallo, P. Mastrorilli, C. F. Nobile, P. Braunstein and U. Englert, *Dalton Trans.*, 2006, 2342.
- (12) I. Bachert, P. Braunstein, M. K. McCart, F. Fabrizi de Biani, F. Laschi, P. Zanello, G. Kickelbick and U. Schubert, *J. Organomet. Chem.*, 1999, **573**, 47.
- (13) See e.g.: (a) Z. Weng, S. Teo and T. S. A. Hor, *Dalton Trans.*, 2007, 3493; (b) C. Wang, Z. Ma, X.-L. Sun, Y. Gao, Y.-H. Guo, Y. Tang and L.-P. Shi, *Organometallics*, 2006, **25**, 3259; (c) D. J. Jones, V. C. Gibson, S. M. Green, P. J. Maddox, A. J. P. White and D. J. Williams, *J. Am. Chem. Soc.*, 2005, **127**, 11037; (d) E. Y. Tshuva, S. Groysman, I. Goldberg, M. Kol and Z. Goldschmidt, *Organometallics*, 2002, **21**, 662.
- (14) A. Naitabdi, O. Toulemonde, J. P. Bucher, J. Rosé, P. Braunstein, R. Welter and M. Drillon, *Chem. Eur. J.*, 2008, **14**, 2355.
- (15) K. Song, H. Gao, F. Liu, J. Pan, L. Guo, S. Zai and Q. Wu, *Eur. J. Inorg. Chem.*, 2009, 3016.
- (16) See e.g. Y.-L. Zhao, Y. Li, Y. Li, L.-X. Gao and F.-S. Han, *Chem. Eur. J.*, 2010, **16**, 4991.
- (17) (a) P. R. Elowe, C. McCann, P. G. Pringle, S. K. Spitzmesser and J. E. Bercaw, *Organometallics*, 2006, **25**, 5255; (b) M. J. Overett, K. Blann, A. Bollmann, J. T. Dixon, D. Haasbroek, E. Killian, H. Maumela, D. S. McGuinness and D. H. Morgan, *J. Am. Chem. Soc.*, 2005, **127**, 10723; (c) A. Bollmann, K. Blann, J. T. Dixon, F. M. Hess, E. Killian, H. Maumela, D. S. McGuinness, D. H. Morgan, A. Neveling, S. Otto, M. Overett, A. M. Z. Slawin, P. Wasserscheid and S. Kuhlmann, *J. Am. Chem. Soc.*, 2004, **126**, 14712.
- (18) G. S. Matouzenko, G. Molnar, N. Bréfuel, M. Perrin, A. Bousseksou and S. A. Borshch, *Chem. Mater.*, 2003, **15**, 550.
- (19) M. O'Reilly, R. Pattacini and P. Braunstein, *Dalton Trans.*, 2009, 6092.
- (20) Wayland, B. B.; Schrammz, R. F. *Inorg. Chem.* **1969**, 8, 971.
- (21) Bruker-Nonius, *Kappa CCD Reference Manual*, Nonius BV, The Netherlands, **1998**.
- (22) Sheldrick, G. M. *Acta Cryst.* **2008**, *A64*, 112-122.
- (23) (a) Spek, L.; *J. Appl. Cryst.* **2003**, *36*, 7; (b) Blessing, B.; *Acta Cryst.*, **1995**, *A51*, 33.

Chapitre 5

Mono- and Dinuclear Complexes
and Tetranuclear Clusters
with Bromine-functionalized
Bis(diphenylphosphino)amine Ligands

Résumé du chapitre 5

Nous avons reporté la préparation de ligands bis(diphenylphosphino) amine fonctionalisés par un groupement bromo-aryl, de type $\text{Ph}_2\text{PNArPPh}_2$ (**1**, Ar = *p*-BrC₆H₄; **2**, Ar = *p*-BrC₆H₄–C₆H₄) et leur propriétés en chimie de coordination. Des complexes mono- et dinucléaires de Cu(I), Au(I), Pd(II), Pt(II) ont été formés et des clusters tétranucléaires de cobalt ont également été obtenus. Les structures cristallines de [PdCl₂(**1**)] (**3**), [PdCl₂(**2**)] (**4**), [(AuCl)(μ-**1**)] (**6**), [Co₄(CO)₅(μ-CO)₃(μ-dppa)(μ-**1**)] (dppa = Ph₂PNH₂PPh₂) (**8**) et [Co₄(CO)₅(μ-CO)₃(μ-dppm)(μ-**1**)] (dppm = Ph₂PCH₂PPh₂) (**9**) ont été obtenues par diffraction de rayons Xy. Alors que les ligands diphosphines chélatent le centre métallique **3** et **4**, et dans le complexe de Pt(II) **5** qui est analogue à **3**, le ligand **1** est pontant dans **6** avec une séparation entre les deux centres d’Au(I) de 3.0402(5) Å. Dans les clusters tétranucléaires **8** et **9**, et dans le cluster **10** analogue de **9** avec **2** comme ligand pontant, deux arêtes orthogonales Co–Co sont pontées par un ligand diphosphine et chaque cobalt est coordonné à un atome de phosphore. Le complexe **3** a montré une réactivité avec un complexe de Pd(0), [Pd(db_a)₂] (db_a = dibenzylideneacetone) pour donner un complexe tétranucléaire résultant de l’insertion de Pd(0) dans la liaison C–Br du ligand et à une réaction de comproportionation Pd(II)/Pd(0) pour donner un corps Pd(I)–Pd(I) doublement ponté.

Référence du chapitre 5

Christophe Fliedel • Roberto Pattacini • Pierre Braunstein

Journal of Cluster Science, 2010, **21**, 397-415.

Mots clés : Assembling ligands · Cobalt · Diphosphines · Clusters · Functionalized-dppa · Gold · Metal insertion · Mononuclear complexes · Palladium · Platinum

Abstract of Chapter 5

We report the preparation of bromo-aryl functionalized bis(diphenylphosphino) amine ligands of the type $\text{Ph}_2\text{PNArPPh}_2$ (**1**, Ar = *p*-BrC₆H₄; **2**, Ar = *p*-BrC₆H₄–C₆H₄) and their coordination properties. Mono- and dinuclear complexes were formed with Cu(I), Au(I), Pd(II), Pt(II) and tetranuclear cobalt carbonyl clusters were obtained. The crystal structures of [PdCl₂(**1**)] (**3**), [PdCl₂(**2**)] (**4**), [(AuCl)(μ-**1**)] (**6**), [Co₄(CO)₅(μ-CO)₃(μ-dppa)(μ-**1**)] (dppa = Ph₂PNH₂PPh₂) (**8**) and [Co₄(CO)₅(μ-CO)₃(μ-dppm)(μ-**1**)] (dppm = Ph₂PCH₂PPh₂) (**9**) have been determined by X-ray diffraction. Whereas the diphosphine ligands chelate the metal center in **3** and **4**, and in the Pt(II) complex **5** which is analogous to **3**, ligand **1** acts as a bridge in **6** where the separation between the two Au(I) centers is 3.0402(5) Å. In the tetranuclear clusters **8** and **9**, and in the cluster **10** analogous to **9** with **2** as bridging ligand, two orthogonal Co–Co edges are bridged by a diphosphine ligand and each cobalt center is thus coordinated by one P donor. Complex **3** was shown to react with the Pd(0) complex [Pd(db_a)₂] (db_a = dibenzylideneacetone) to afford a tetranuclear complex resulting from both the insertion of Pd(0) into the ligand C–Br bond and Pd(II)/Pd(0) comproportionation to form a doubly ligand-bridged Pd(I)–Pd(I) core.

Reference of Chapter 5

Christophe Fliedel • Roberto Pattacini • Pierre Braunstein

Journal of Cluster Science, 2010, **21**, 397-415.

Keywords: Assembling ligands · Cobalt · Diphosphines · Clusters · Functionalized-dppa · Gold · Metal insertion · Mononuclear complexes · Palladium · Platinum

Introduction

N-Functionalization of bis(diphenylphosphino)amine ($\text{Ph}_2\text{PNHPPH}_2$, dppa) ligands offers the opportunity to broaden the scope of applications of such bidentate diphosphines for metal coordination and to fine-tune their stereoelectronic features. Whereas the NH proton of dppa is more acidic than the CH_2 protons of the related ligand $\text{Ph}_2\text{PCH}_2\text{PPh}_2$ (dppm), which facilitates subsequent *N*-functionalization, the corresponding anions, $(\text{Ph}_2\text{PNPPh}_2)^-$ and $(\text{Ph}_2\text{PCHPPH}_2)^-$, respectively, often possess significantly different reactivities, as clearly shown e.g. when they are exposed to oxidizing conditions, such as iodine [1, 2]. It may be advantageous to coordinate the dppa ligand to one (chelating mode) or two (bridging mode) metal centers prior to *N*-deprotonation and functionalization [3, 4]. Nevertheless, functionalization of free or coordinated dppa by deprotonation of the NH function followed by reaction with an organic electrophile only works in few cases and/or gives low yields. In contrast, pre-functionalization of the nitrogen atom of primary amines followed by reaction with chlorophosphines to afford a *N*-functionalized dppa-type ligand is more readily achieved [5] and this can result in a broader choice of ligands. Their metal complexes can be exploited in catalysis (e.g. in the catalytic oligomerization of ethylene) [6–18] or grafted to inorganic matrices through a suitable *N*-bound function, such as an alkoxyisilyl group [19–22], allowing for the subsequent preparation of highly dispersed metal-containing particles [21]. Few examples of structurally characterized clusters coordinated by *N*-substituted dppa have been reported in the literature, and these include homometallic Ru_3 [23–25], Ru_4 [26], Co_4 [19] and bimetallic Co_2Pt [27] and CoPd_2 [3] clusters. Two unique Co_{12} and Co_{16} “clusters of clusters” have been also reported, which contain four separated Co_3 and Co_4 cores, respectively, branched through thioether chains to a central aryl group [28]. However, to the best of our knowledge, only very few examples of complexes or clusters containing a halogen-functionalized dppa ligand have been reported, all limited to systems containing fluorinated aryls [29, 30]. Herein we report the preparation and the coordination properties of bromo-aryl diphosphines of this type. This bromo function is well known in organic chemistry to facilitate further functionalization, via e.g. Heck or Suzuki cross-coupling reactions [31] or nucleophilic substitutions. Furthermore, bromo-aryl groups can readily react with zerovalent Pd precursors by oxidative addition [31]. This should offer the possibility to exploit such functionalized complexes as precursors to di- or multinuclear complexes.

Experimental Section

General Procedures

All operations were carried out using standard Schlenk techniques under inert atmosphere. Solvents were purified and dried under nitrogen by conventional methods. CDCl_3 was dried over 4 Å molecular sieves, degassed by freeze–pump–thaw cycles and stored under argon. NMR spectra were recorded at room temperature on a Bruker AVANCE 300 spectrometer (^1H , 300 MHz; $^{13}\text{C}\{^1\text{H}\}$, 75.47 MHz and $^{31}\text{P}\{^1\text{H}\}$, 121.49 MHz) and referenced using the residual solvent signals (^1H and ^{13}C) or 85% H_3PO_4 for $^{31}\text{P}\{^1\text{H}\}$. Assignments are based on ^1H , $^{13}\text{C}\{^1\text{H}\}$, ^1H -COSY, ^1H , ^{13}C -HMQC and ^1H , ^{13}C -HMBC experiments. Chemical shifts are given in ppm. FTIR spectra were recorded in the region 4000–100 cm^{-1} on a Nicolet 6700 FT-IR spectrometer (ATR mode, SMART ORBIT accessory, diamond or germanium crystals). Elemental analyses were performed by the “Service de microanalyses”, Université de Strasbourg and by the “Service Central d’Analyse”, USR-59/CNRS, Solaize. Electrospray mass spectra (ESI-MS) were recorded on a microTOF (Bruker Daltonics, Bremen, Germany) instrument using nitrogen as drying agent and nebulising gas and Maldi-TOF analyses were carried out on a Bruker AutiflexII TOF/TOF (Bruker Daltonics, Bremen, Germany), using dithranol (1.8.9 trihydroxyanthracene) as a matrix. The complexes $[\text{PdCl}_2(\text{cod})]$ [32], $[\text{PtCl}_2(\text{cod})]$ [33], $[\text{AuCl}(\text{tht})]$ [34], $[\text{Co}_4(\text{CO})_{10}(\mu\text{-dppm})]$ [19], $[\text{Co}_4(\text{CO})_{10}(\mu\text{-dppa})]$ [35] and $[\text{Pd}(\text{dba})_2]$ [36] were prepared according to literature methods. All other reagents were used as received from commercial suppliers.

Synthesis of Ligands **1** and **2**

Ligand $\text{Ph}_2\text{PNArPPh}_2$ (**1**, Ar = *p*-BrC₆H₄)

Chlorodiphenylphosphine in excess (6.00 mL, 7.37 g, 33.43 mmol) was added dropwise to a solution of 4-bromoaniline (2.30 g, 13.37 mmol) and triethylamine (5.12 mL, 3.72 g, 36.77 mmol) in THF (120 mL) at 0 °C under inert atmosphere. The reaction mixture was stirred for 2 h at 0 °C and then at room temperature for 6 h. After filtration, the volatiles were removed under reduced pressure and the residue was washed twice with pentane to give **1** as a colourless solid. Yield: 1.59 g, 64%. Anal. Calc. for C₃₀H₂₄BrNP₂ (540.37): C, 66.68; H, 4.48; N, 2.59. Found: C, 66.78; H, 4.32; N, 2.71. FTIR: (pure, diamond, cm^{-1}): 3036br, 2979w, 2920br, 2604br, 2497w, 1583w, 1475s, 1430s, 1397w, 1280w, 1235w, 1211m, 197m, 1173m, 1120w, 1091m, 1069m, 1037w, 1010m, 959m, 937w, 896s, 851w, 834w, 818w, 802m, 738s,

711sh, 692vs. ^1H NMR (CDCl_3) δ : 6.74 [2H, d, $^3J_{\text{HH}} = 8.7$ Hz, N($\text{C}_6\text{H}_4\text{Br}$), H_{ortho/N}], 7.04 [2H, d, $^3J_{\text{HH}} = 8.7$ Hz, N($\text{C}_6\text{H}_4\text{Br}$), H_{meta/N}], 7.28–7.38 (20H, m, Ph); $^{13}\text{C}\{^1\text{H}\}$ NMR (CDCl_3) d: 118.6 (C–Br), 128.2 (*m*-Ph), 129.2 [N($\text{C}_6\text{H}_4\text{Br}$), C_{meta/N}], 130.7 (*p*-Ph), 131.2 [t, $^3J_{\text{C,P}} = 9.2$ Hz, N($\text{C}_6\text{H}_4\text{Br}$), C_{ortho/N}], 133.2 (*o*-Ph), 138.8 (*ipso*-Ph), 146.3 (C–N); $^{31}\text{P}\{^1\text{H}\}$ (CDCl_3) δ : 70.8 (s).

Ligand $\text{Ph}_2\text{PNArPPh}_2$ (**2**, Ar = *p*-BrC₆H₄–C₆H₄)

The same procedure was used with chlorodiphenylphosphine (1.81 mL, 2.22 g, 10.08 mmol), 4'-bromo-[1,1'-biphenyl]-4-amine (1.00 g, 4.03 mmol) and triethylamine (1.54 mL, 1.12 g, 11.08 mmol). Yield: 4.05 g, 56%. Anal. Calc. for C₃₆H₂₈BrNP₂ (616.47): C, 70.14; H, 4.58; N, 2.27. Found: C, 70.20; H, 4.69; N, 2.13. ^1H NMR (CDCl_3) δ : 6.72 [2H, d, $^3J_{\text{HH}} = 8.7$ Hz, N($\text{C}_{12}\text{H}_8\text{Br}$), H_{ortho/N}], 7.15 [2H, d, $^3J_{\text{HH}} = 8.7$ Hz, N($\text{C}_{12}\text{H}_8\text{Br}$), H_{meta/N}], 7.28–7.33 [12H, m, Ph and N($\text{C}_{12}\text{H}_8\text{Br}$), H_{meta/Br}], 7.36–7.42 [12H, m, Ph and N($\text{C}_{12}\text{H}_8\text{Br}$), H_{ortho/Br}]; $^{13}\text{C}\{^1\text{H}\}$ NMR (CDCl_3) δ : 116.3 (C–Br), 127.8 (C_{biphenyl}), 128.02 (*m*-Ph), 128.60 [t, $^3J_{\text{C,P}} = 10.6$ Hz, N($\text{C}_{12}\text{H}_8\text{Br}$), C_{ortho/N}], 129.6 (C_{biphenyl}), 130.8 (*p*-Ph), 131.1 (C_{biphenyl}), 131.4 (C_{biphenyl}), 131.7 (C_{biphenyl}), 133.3 (*o*-Ph), 139.92 (*ipso*-Ph), 146.45 (C–N); $^{31}\text{P}\{^1\text{H}\}$ NMR (CDCl_3) δ : 69.8 (s).

Synthesis of Metal Complexes **3** – **7**

The low solubility of these compounds in common organic solvents prevented recording of $^{13}\text{C}\{^1\text{H}\}$ NMR spectra.

Complex 3: A solution of ligand **1** (0.212 g, 0.392 mmol) in CH_2Cl_2 (10 mL) was slowly added to a suspension of [PdCl₂(cod)] (0.112 g, 0.392 mmol) in CH_2Cl_2 (10 mL) at room temperature under argon. The reaction mixture was stirred for 2 h and then filtered through a Celite pad. The volume of the solvent was reduced to one-third and the product was precipitated by addition of pentane (30 mL). The resulting yellow solid was then washed twice with pentane and dried under vacuum. Complex **3** was isolated as a pale yellow solid. Yield: 0.236 g, 84%. Anal. Calc. for C₃₀H₂₄BrCl₂NP₂Pd (717.70): C, 50.21; H, 3.37; N, 1.95. Found: C, 50.72; H, 2.98; N, 2.23. FTIR: ν_{max} (pure, diamond)/cm⁻¹: 3055br, 2962br, 1582w, 1484s, 1433s, 1311w, 1243s, 1182w, 1163w, 1124w, 1105s, 1096s, 1080m, 1022m, 1001m, 997m, 944s, 924sh, 903s, 855w, 821s, 758sh, 743s, 720s, 698vs, 685vs. ^1H NMR (CDCl_3) δ : 6.38 [2H, d, $^3J_{\text{HH}} = 8.9$ Hz, N($\text{C}_6\text{H}_4\text{Br}$), H_{ortho/N}], 7.20 [2H, d, $^3J_{\text{HH}} = 8.8$ Hz, N($\text{C}_6\text{H}_4\text{Br}$), H_{meta/N}], 7.52 (8H, m, Ph), 7.66 (4H, m, *p*-Ph), 7.88 (8H, m, Ph); $^{31}\text{P}\{^1\text{H}\}$ NMR (CDCl_3) δ : 35.8 (s). MS (Maldi-TOF): m/z 681.9 [M–Cl]⁺.

Complex **4** was prepared following the same procedure as for **3**, by addition of ligand **2** (0.300 g, 0.487 mmol) to [PdCl₂(cod)] (0.139 g, 0.487 mmol), which afforded a pale yellow solid. Yield: 0.313 g, 81%. Anal. Calc. for C₃₆H₂₈BrCl₂NP₂Pd (793.79): C, 54.47; H, 3.56; N, 1.76. Found: C, 54.20; H, 3.75; N, 1.78. ¹H NMR (CDCl₃) δ: 6.60 [2H, d, ³J_{HH} = 8.4 Hz, N(C₁₂H₈Br), H_{ortho/N}], 7.29 [4H, m, N(C₁₂H₈Br), H_{meta/N} and H_{meta/Br}], 7.52 [10H, m, Ph and N(C₁₂H₈Br), H_{ortho/Br}], 7.65 (4H, m, *p*-Ph), 7.94 (8H, m, Ph); ³¹P{¹H} NMR (CDCl₃) δ: 36.3 (s). MS (Maldi-TOF): m/z 757.9 [M–Cl]⁺.

Complex **5** was prepared following the same procedure as for **3** and **4**, by addition of **1** (0.199 g, 0.369 mmol) to [PtCl₂(cod)] (0.138 g, 0.369 mmol), which gave a colourless solid. Yield: 0.229 g, 77%. Anal. Calc. for C₃₀H₂₄BrCl₂NP₂Pt (806.36): C, 44.68; H, 3.00; N, 1.74. Found: C, 44.72; H, 3.18; N, 1.85. FTIR: ν_{max}(pure, diamond)/cm⁻¹: 3054br, 2604br, 2498br, 1584w, 1485m, 1434m, 1397w, 1310w, 1245m, 1181w, 1099s, 1003m, 945m, 893s, 822m, 745s, 720sh, 689vs. ¹H NMR (CDCl₃) δ: 6.31 [2H, d, ³J_{HH} = 8.7 Hz, N(C₆H₄Br), H_{ortho/N}], 7.20 [2H, d, ³J_{HH} = 8.7 Hz, N(C₆H₄Br), H_{meta/N}], 7.50 (8H, m, Ph), 7.63 (4H, m, *p*-Ph), 7.84 (8H, m, Ph); ³¹P{¹H} NMR (CDCl₃) δ: 23.0 (s, ¹J_{P,Pt} = 3337 Hz). MS (ESI): m/z 766.1 [M–Cl]⁺, 824.0 [M+Na]⁺.

Complex **6** was prepared following the same procedure as for **3–5**, using ligand **1** (0.421 g, 0.780 mmol) and [AuCl(tht)] (0.500 g, 1.56 mmol), which gave a colourless solid. Yield: 0.572 g, 73%. Anal. Calc. for C₃₀H₂₄Au₂BrCl₂NP₂ (1005.21): C, 35.85; H, 2.41; N, 1.39. Found: C, 35.69; H, 2.32; N, 1.15. FTIR: ν_{max}(pure, diamond)/cm⁻¹: 3063br, 3039br, 3013br, 1585w, 1473m, 1434m, 1391w, 1308w, 1196m, 1159w, 1099s, 1072m, 1026w, 1004m, 996sh, 958s, 922m, 909s, 840w, 809w, 751m, 740m, 718m, 700vs, 688vs. ¹H NMR (CDCl₃) δ: 6.13 [2H, d, ³J_{HH} = 8.4 Hz, N(C₆H₄Br), H_{ortho/N}], 6.91 [2H, d, ³J_{HH} = 8.7 Hz, N(C₆H₄Br), H_{meta/N}], 7.42–7.47 (8H, m, Ph), 7.54–7.66 (12H, m, Ph); ³¹P{¹H} NMR (CDCl₃) δ: 89.4 (s). MS (ESI): m/z 970.0 [M–Cl]⁺, 1027.9 [M+Na]⁺.

Complex **7** was prepared following a procedure similar to that giving **3–6**. A solution of ligand **1** (0.870 g, 1.61 mmol) in CH₂Cl₂ (10 mL) was slowly added to a slurry of [Cu(NCMe)₄]PF₆ (0.300 g, 0.805 mmol) in CH₂Cl₂ (10 mL) at room temperature under argon. The reaction mixture was stirred for 2 h and then filtered through a Celite pad. The volume of the solvent was reduced to one-third and the product was precipitated by addition of Et₂O (30 mL), giving a colourless solid which was washed with Et₂O (10 mL) and dried under vacuum. Complex **7** was isolated as a colourless solid. Yield: 0.830 g, 80%. Anal. Calc. for C₆₀H₄₈Br₂

$\text{CuF}_6\text{N}_2\text{P}_5$ (1289.25): C, 55.90; H, 3.75; N, 2.17. Found: C, 56.04; H, 3.56; N, 1.96. FTIR: ν_{max} (pure, diamond)/cm⁻¹: 3201br, 3053br, 3005br, 1588w, 1479s, 1437s, 1395w, 1291w, 1265sh, 1194m, 1177m, 1160w, 1132m, 1099s, 1072m, 1027sh, 1009m, 998sh, 955m, 916m, 891m, 832vs, 740vs, 709sh, 691vs. ¹H NMR (CDCl_3) δ : 6.60 [2H, d, ³ $J_{\text{HH}} = 8.7$ Hz, N($\text{C}_6\text{H}_4\text{Br}$), H_{ortho/N}], 6.95–7.00 [14H, m, Ph and N($\text{C}_6\text{H}_4\text{Br}$), H_{meta/N}], 7.25–7.27 (8H, m, Ph); ³¹P{¹H} NMR (CDCl_3) δ : 60.9 (s, P–Cu), -143.0 (sept., ¹ $J_{\text{P},\text{F}} = 712$ Hz, PF_6). MS (ESI): m/z 1143.1 [$\text{M}-\text{PF}_6$]⁺.

Synthesis of Clusters **8 – 10**

Cluster 8: A solution of ligand **1** (0.118 g, 0.222 mmol) in CH_2Cl_2 (20 mL) was slowly added to a solution of $[\text{Co}_4(\text{CO})_{10}(\mu\text{-dppa})]$ (0.200 g, 0.222 mmol) in CH_2Cl_2 (20 mL). The reaction mixture was stirred at room temperature under argon atmosphere and gas evolution occurred through an oil bubbler. The reaction was followed by TLC, stopped after 6 h and the solvent was evaporated under reduced pressure. Cluster **8** was purified by column chromatography ($\text{CH}_2\text{Cl}_2/\text{pentane}$ 50:50). The unreacted cluster precursor could be recycled. $R_f = 0.36$ ($\text{CH}_2\text{Cl}_2/\text{pentane}$ 50:50). Yield: 0.203 g, 66%. Anal. Calc. for $\text{C}_{62}\text{H}_{45}\text{BrCo}_4\text{N}_2\text{O}_8\text{P}_4$ (1383.86): C, 53.74; H, 3.27; N, 2.02. Found: C, 53.53; H, 2.97; N, 2.17. FTIR: ν_{max} (pure, Ge)/cm⁻¹: (ν_{CO}) 2013s, 1978vs, 1964vs, 1953s, 1823w, 1787m, 1774m. ¹H NMR (CDCl_3) δ : 3.41 (1H, br, NH), 6.08 (2H, br, N($\text{C}_6\text{H}_4\text{Br}$), H_{ortho/N}), 6.69 (2H, br, N($\text{C}_6\text{H}_4\text{Br}$), H_{meta/N}), 7.20–7.53 (40H, br m, Ph); ³¹P{¹H} NMR (CDCl_3) δ : 74.0 (br s, 2P_{dppa}), 97.1 (br s, P_{basal/1}), 116.6 (br s, P_{apical/1}). MS (ESI): m/z 1385.9 [M]⁺.

Cluster 9 was obtained as a dark green solid, following the same procedure as used for **8**, by reaction of ligand **1** (0.120 g, 0.222 mmol) with $[\text{Co}_4(\text{CO})_{10}(\mu\text{-dppm})]$ (0.200 g, 0.222 mmol). $R_f = 0.44$ ($\text{CH}_2\text{Cl}_2/\text{pentane}$ 50:50). Yield: 0.221 g, 72%. Anal. Calc. for $\text{C}_{63}\text{H}_{46}\text{BrCo}_4\text{NO}_8\text{P}_4$ (1384.57): C, 54.65; H, 3.35; N, 1.01. Found: C, 54.33; H, 3.18; N, 1.09. FTIR: ν_{max} (pure, Ge)/cm⁻¹: (ν_{CO}) 2005s, 1970vs, 1938s, 1836w, 1791m, 1767m. ¹H NMR (CDCl_3) δ : 3.65 (2H, br, CH_2), 6.11 [2H, br, N($\text{C}_6\text{H}_4\text{Br}$), H_{ortho/N}], 6.70 [2H, br, N($\text{C}_6\text{H}_4\text{Br}$), H_{meta/N}], 7.25–7.44 (40H, br m, Ph); ³¹P{¹H} NMR (CDCl_3) δ : 25.2 (br s, P_{dppm}), 28.8 (br s, P_{dppm}), 97.4 (br s, P_{basal/1}), 112.0 (br s, P_{apical/1}). MS (ESI): m/z 1384.9 [M]⁺.

Cluster 10 was obtained as a dark green solid, following the same procedure as used for **8** and **9**, by reaction of **2** (0.300 g, 0.333 mmol) with $[\text{Co}_4(\text{CO})_{10}(\mu\text{-dppm})]$ (0.205 g, 0.333 mmol). $R_f = 0.41$ ($\text{CH}_2\text{Cl}_2/\text{pentane}$ 50:50). Yield: 0.287 g, 59%. Anal. Calc. for $\text{C}_{69}\text{H}_{50}\text{BrCo}_4\text{NO}_8\text{P}_4$ (1460.67): C, 56.74; H, 3.45; N, 0.96. Found: C, 57.06; H, 3.18; N, 0.88. FTIR: ν_{max} (pure,

Ge)/cm⁻¹: (ν_{CO}) 2031m, 2001s, 1967vs, 1821w, 1781m, 1762m. ¹H NMR (CDCl₃) δ: 3.56 (2H, br, CH₂), 6.03 [2H, br, N(C₁₂H₈Br), H_{ortho/N}], 6.63 [4H, br, N(C₁₂H₈Br), H_{meta/N} and H_{meta/Br}], 7.18–7.36 [42H, br m, Ph and N(C₁₂H₈Br), H_{ortho/Br}]; ³¹P{¹H} NMR (CDCl₃) δ: 24.8 (br s, P_{dppm}), 28.5 (br s, P_{dppm}), 96.7 (br s, P_{basal/2}), 112.2 (br s, P_{apical/2}).

Synthesis of the Tetranuclear Complex **11** Solid [Pd(db_a)₂] (0.016 g, 0.028 mmol) and 1,2-bis(diphenylphosphine)ethane (dppe) (0.008 g, 0.019 mmol) were placed in a Schlenk tube equipped with a magnetic stirrer and toluene (10 mL) was added. Then complex **3** (0.013 g, 0.019 mmol) was added to the red solution under argon. The reaction mixture turned brown-orange and was stirred for 2 h at 60 °C. After cooling down to room temperature, the mixture was filtered through a Celite pad to eliminate the PdCl₂ formed. The volume of the solvent was reduced to one-third and the product was precipitated by addition of diethyl ether (30 mL). The resulting orange-brown solid was then washed twice with diethyl ether and dried under vacuum. Complex **11** was isolated as an orange solid. Yield: 0.017 g, 75%. FTIR: ν_{max} (pure, diamond)/cm⁻¹: 3070br, 2961br, 2922br, 2852br, 2162w, 1979w, 1586w, 1572sh, 1490m, 1480m, 1433s, 1312w, 1245s, 1184w, 1160w, 1096s, 1024m, 997m, 948s, 910s, 799m, 761s, 742s, 721s, 686vs, 312s (Pd–Br) [37, 38], 293s (Pd–Cl). ¹H NMR (CDCl₃) δ: 2.36 [8H, br, 4 CH₂], 7.07–7.91 (80H, m, Ph); ³¹P{¹H} NMR (CDCl₃) δ: 39.0 [d, ³J_{P,P} = 26.0 Hz, P (dppe)], 63.7 [s, P (**1**)], 67.6 [d, ³J_{P,P} = 26.0 Hz, P (dppe)].

X-ray Data Collection and Structure Refinement

Suitable crystals for the X-ray analysis were obtained as described in the experimental section. The intensity data were collected at 173(2) K on a Kappa CCD diffractometer [39] (graphite monochromated MoK_α radiation, λ = 0.71073 Å). Crystallographic and experimental details for the structure are summarized in Table 1. The structures were solved by direct methods (SHELXS-97) and refined by full-matrix least-squares procedures (based on F^2 , SHELXL-97) [40] with anisotropic thermal parameters for all the non-hydrogen atoms. The hydrogen atoms were introduced into the geometrically calculated positions (SHELXS-97 procedures) and refined *riding* on the corresponding parent atoms, except the N-bound nitrogen in **8** which was found in the density maps and refined isotropically. A severe disorder involved the solvent in **8**. Since any attempt to identify the atomic positions failed, a PLATON-SQUEEZE procedure was applied. [41] The residue electron density corresponding to the voids (997 Å³) was 366 e, consistent with four couples of CH₂Cl₂/pentane [(42e + 48e) × Z]. This data treatment resulted in an improved quality of the model. The crystals of **4** were

of poor quality. The refinement parameters improved significantly by applying the twin matrix: -1 0 -1 0 -1 0 0 0 1 (180° rotation around -1 0 2), relating two components [refined mutual contribution: 0.35/0.65]. A MULTISCAN absorption correction [42] was applied for **6**.

Complexes of bromo-aryl functionalized dppa-type ligands

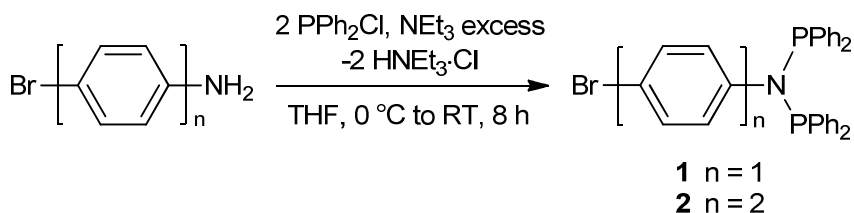
Compound	3 · 2(CH ₂ Cl ₂)	4 · 2(CH ₂ Cl ₂)	6	8	9
Formula	C ₃₀ H ₂₄ BrCl ₂ NP ₂ Pd·2(CH ₂ Cl ₂)	C ₃₀ H ₂₈ BrCl ₂ NP ₂ Pd·2(CH ₂ Cl ₂)	C ₃₀ H ₂₄ Au ₂ BrCl ₂ NP ₂	C ₆₂ H ₄₅ BrCo ₄ N ₂ O ₈ P ₄	C ₆₃ H ₄₆ BrCo ₄ NO ₈ P ₄
Formula weight	887.50	963.60	1005.18	1385.14	1384.52
Crystal system	Monoclinic	Monoclinic	Tetragonal	Monoclinic	Monoclinic
<i>a</i> (Å)	20.1238(4)	16.7198(11)	9.9250(2)	11.4816(2)	17.1901(7)
<i>b</i> (Å)	14.9514(4)	17.9855(9)	9.9250(2)	26.8268(7)	18.7227(9)
<i>c</i> (Å)	30.4835(6)	14.4177(11)	31.0540(6)	23.1501(3)	20.2031(7)
α (°)	90.00	90.00	90.00	90.00	90.00
β (°)	129.106(1)	114.588(5)	90.00	117.457(1)	117.041(2)
γ (°)	90.00	90.00	90.00	90.00	90.00
<i>V</i> (Å ³)	7117.2(3)	3942.5(4)	3058.99(11)	6327.4(2)	5791.4(4)
<i>T</i> (K)	173(2)	173(2)	173(2)	173(2)	173(2)
Space group	<i>P</i> 2 ₁ / <i>c</i>	<i>P</i> 4 ₃ 2 ₁ <i>c</i>	<i>P</i> 4 ₃ 2 ₁ <i>c</i>	<i>P</i> 2 ₁ / <i>c</i>	<i>P</i> 2 ₁ / <i>c</i>
<i>Z</i>	8	4	4	4	4
μ (mm ⁻¹)	2.209	2.001	11.187	1.816	1.983
Meas. refl.	57909	18656	18242	26424	33793
Indep. refl.	14764	6805	4460	14992	11999
<i>R</i> _{int}	0.0906	0.1118	0.0836	0.0484	0.0931
<i>R</i> ₁ (<i>I</i> > 2 <i>σ</i> (<i>I</i>))	0.0459	0.0875	0.0397	0.0455	0.0505
<i>wR</i> (<i>F</i> ²) (<i>I</i> > 2 <i>σ</i> (<i>I</i>))	0.0723	0.2153	0.0697	0.0929	0.0810
<i>R</i> ₁ (all data)	0.1320	0.1387	0.0640	0.0942	0.1388
<i>wR</i> (<i>F</i> ²) (all data)	0.0841	0.2476	0.0774	0.1043	0.0935
S on <i>F</i> ²	0.947	1.165	1.010	0.920	0.945
Flack parameter			-0.023(11)		

Table 1 X-ray data collection and refinement for all structures

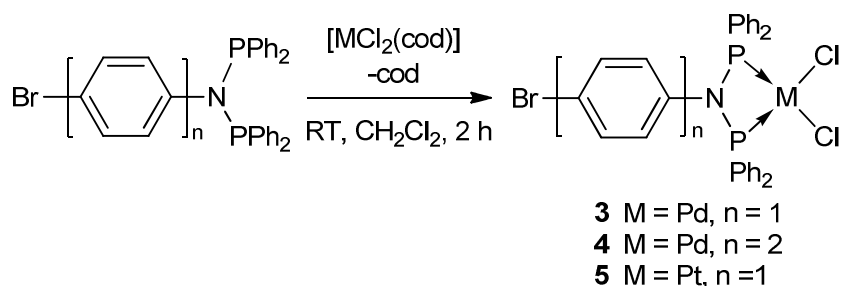
Results and Discussion

Mono- and Dinuclear Complexes

The new diphosphines **1** and **2** were obtained by reaction of 2.5 equivalents of chlorodiphenylphosphine with the corresponding amines, in the presence of triethylamine as HCl scavenger (Scheme 1). The $^{31}\text{P}\{\text{H}\}$ NMR spectra show typical signals for aromatic substituted bis(diphenylphosphino)amine (dppa) derivatives [27] at 70.8 and 69.8 ppm for **1** and **2**, respectively.



Scheme 1 Synthesis of the diphosphine ligands



Scheme 2 Synthesis of Pd (II) and Pt (II) complexes

These diphosphines were reacted with $[\text{PdCl}_2(\text{cod})]$ and $[\text{PtCl}_2(\text{cod})]$ (cod : 1,5-cyclooctadiene), as shown in Scheme 2. Phosphorus coordination resulted in an upfield shift of the $^{31}\text{P}\{\text{H}\}$ signals, from ca. 70 ppm for the free ligands to 35.8 and 36.3 ppm for the Pd(II) complexes $[\text{PdCl}_2(\mathbf{1})]$ (**3**) and $[\text{PdCl}_2(\mathbf{2})]$ (**4**), respectively. An even larger upfield shift to 23.0 ppm was observed for **5**. The value of the $^1J_{\text{P},\text{Pt}}$ coupling constant (3337 Hz) for this complex is consistent with the *trans* influence exerted by the terminal chlorides [43]. The molecular structures of **3** and **4**, determined by single crystal X-ray diffraction are reported in Figs. 1 and 2, respectively. In the molecular structure of **3**, the metal center is chelated by ligand **1** through the P donors, forming a four-membered metallocycle. The slightly distorted squareplanar coordination is completed by two terminal chlorides. The ligand adopts a different conformation when compared to that in **6**, **8** and **9** (see below). The *p*-BrPh group is

almost parallel to the coordination plane [angle of $173.4(1)^\circ$ between the C1–C6,Br1 and Pd1,Cl1,Cl2 mean planes], whereas it is almost orthogonal to the P1,P2,M1,M2 plane in the three aforementioned structures (see below, e.g., for **6**), in which the ligand shows a bridging coordination mode. This reflects the significantly smaller P–N–P angle in **3** [$99.0(2)^\circ$] compared to e.g., **6** [$118.4(3)^\circ$], which reduces the steric repulsion between the phenyl and the bromo-aryl groups. In reported examples of aryl-N-substituted dppa complexes of the type [PdCl₂(ar-dppa)], the aryl group is parallel to the metal coordination plane when no substituent is present in ortho or meta position of the phenyl, while it is orthogonal in the other cases. [29, 44–47] The P–N bond lengths are not significantly influenced by this feature.

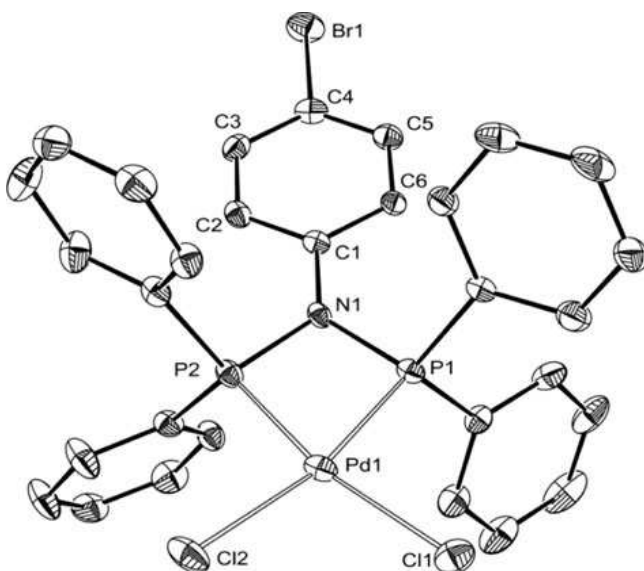


Fig. 1 ORTEP of the molecular structure of **3** (ellipsoids at 40% probability level). Hydrogen atoms omitted for clarity. Only one of the two analogous crystallographically independent molecules is depicted. Selected distances (\AA) and angles (deg): Pd1–P1 2.209(2), Pd1–P2 2.197(1), Pd1–Cl1 2.3605(9), Pd1–Cl2 2.360(2), P1–N1 1.712(3), P2–N1 1.720(4), N1–C1 1.435(7), Br1–C4 1.898(7); P1–Pd1–P2 72.66(5), P1–Pd1–Cl1 94.69(5), Cl1–Pd1–Cl2 98.05(5), Cl2–Pd1–P2 94.58(5), P1–Pd1–Cl2 166.97(5), P2–Pd1–Cl1 167.35(5), P1–N1–P2 99.0(2), P1–N1–C1 131.8(3), P2–N1–C1 129.2(3)

The structure of **4** is analogous to that of **3**, with **2** replacing **1**, respectively. The aryl ring on the nitrogen in **4** is not coplanar with the phosphorus and the palladium atoms (angle between the mean planes P1,N1,P2 and C1–C6: $66.4(8)^\circ$) as in the case of **3**, which induces a different orientation of the phenyl groups. This is probably due to a packing effect, since no bulky group substitute the aryl moieties. We then wished to evaluate the coordination properties of the *p*-bromo-aryl substituted dppa ligands towards d¹⁰ metal ions. Ligand **1** was

reacted with d¹⁰ group 11 metal complexes, namely [AuCl(tht)] (tht = tetrahydrothiophene) and [Cu(NCMe)₄]PF₆ (Scheme 3). The reaction of **1** with the gold derivative, in a 1:2 ratio, afforded [(AuCl)₂(μ-**1**)] (**6**) in good yields. The ligand acts as a bridge, with a characteristic downfield shift of 89.4 ppm. Its molecular structure is reported in Fig. 3.

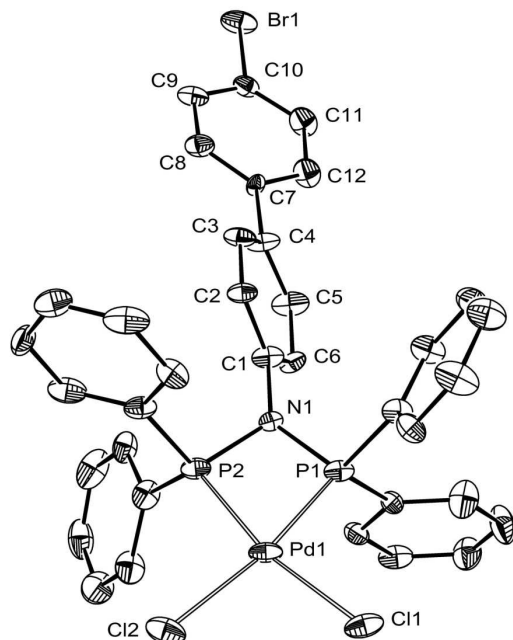
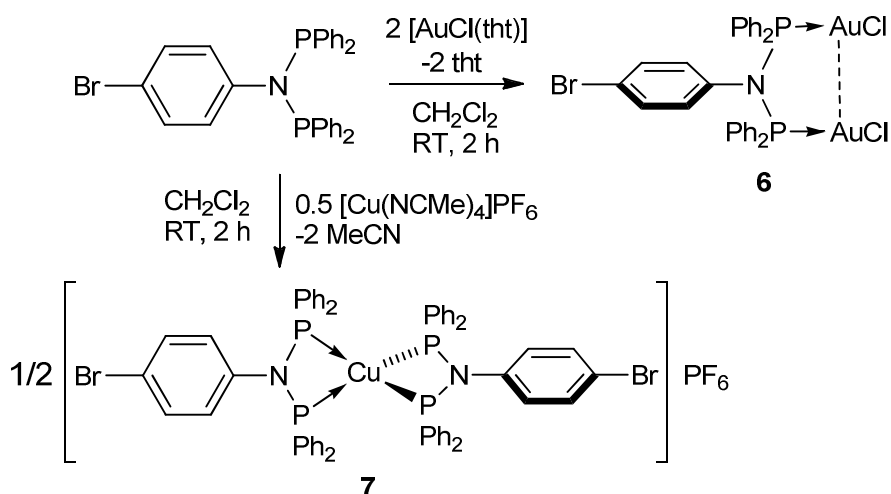


Fig. 2 ORTEP of the molecular structure of **4** (ellipsoids at 40% probability level). Hydrogen atoms omitted for clarity. Selected distances (Å) and angles (deg): Pd1-P1 2.210(3), Pd1-P2 2.215(3), Pd1-Cl1 2.340(4), Pd1-Cl2 2.352(4), P1-N1 1.68(1), P2-N1 1.72(1), N1-C1 1.46(1), C4-C7 1.49(1), C10-Br1 1.91(1), P1-Pd1-P2 72.5(1), Cl1-Pd1-Cl2 95.7(1), P1-Pd1-Cl2 169.2(1), P2-Pd1-Cl1 167.3(1), P1-Pd1-Cl1 95.0(1), P2-Pd1-Cl2 96.9(1), P1-N1-P2 100.6(5), P1-N1-C1 132.5(8), P2-N1-C1 126.9(8).



Scheme 3 Synthesis of d¹⁰ metal complexes from ligand **1**

In the crystal structure of **6**, which has a crystallographically imposed C_2 symmetry, the two Au(I) centers are bridged by ligand **1** through the two P donors. Each metal center is further coordinated by a chlorine, giving rise to a slightly distorted linear coordination for the Au atoms. The intermetallic Au···Au distance is 3.0402(5) Å, suggesting a d¹⁰–d¹⁰ aurophilic interaction, although only a slight deviation from linearity is observed on the P1–Au1–Cl1 angle. The two P–Au lines are not parallel, forming an angle of 51.4(4) [P1–Au1···Au1ⁱ–P1ⁱ torsion: 50.79(6) $^\circ$]. The *p*-BrPh group is orthogonal to the P–N–P plane angle between the two mean planes: 89.5(4) $^\circ$. This is probably due to the wider P–N–P angle [118.4(3) $^\circ$] compared to e.g. **3** [99.0(2) $^\circ$], which results in an enhanced steric hindrance between the phenyls and the *p*-bromo aryl.

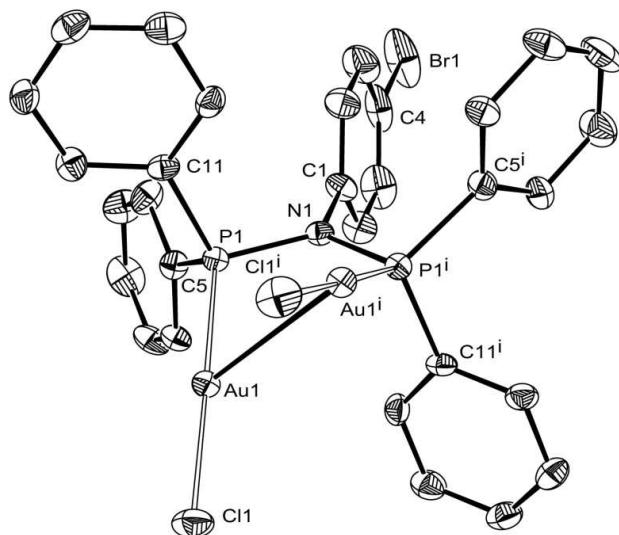


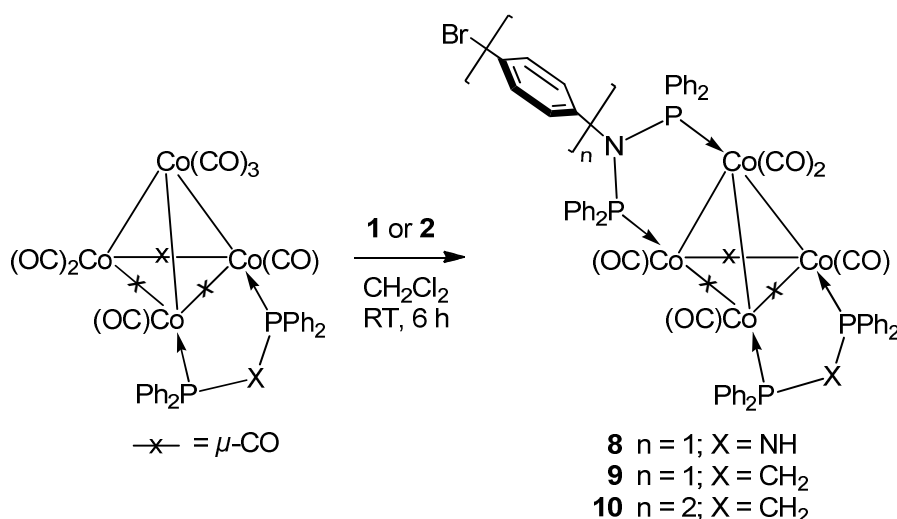
Fig. 3 ORTEP of the molecular structure of **6** (ellipsoids at 40% probability level). Hydrogen atoms omitted for clarity. Selected distances (Å) and angles (deg): Au1-Au1ⁱ 3.0402(5), Au1-Cl1 2.281(2), Au1-P1 2.233(2), C4-Br1 1.912(8), P1-N1 1.717(3), P1-Au1-Cl1 177.99(7), Au1ⁱ-Au1-Cl1 101.95(5), Au1ⁱ-Au1-P1 80.04(4), P1-N1-P1ⁱ 118.4(3). Symmetry transformation generating equivalent atoms (ⁱ): y, x, -z.

Complex **6** belongs to the family of diphosphine-bridged $[(\text{AuCl})_2(\mu-\text{L})]$ complexes. Dppa-[48, 49] and dppm-type [50–54] diphosphines (functionalized or not) are known to support efficiently the Au^I···Au^I interaction. In $[(\text{AuCl})_2(\text{l-dppa})]$ [49], the reported interatomic Au···Au distance is 3.121 Å, slightly longer than that found in **6**. This probably stems from the influence (likely steric) of the *p*-bromo phenyl group, which results in a smaller P–N–P angle in **6** [118.4(3) $^\circ$] than in $[(\text{AuCl})_2(\mu\text{-dppa})]$ [122.4 $^\circ$]. The complex crystallized in the tetragonal chiral space group P4₃2₁2 and gave rise to a spontaneous resolution of one of the two possible helicoidal enantiomers.

We have then reacted ligand **1** with $[\text{Cu}(\text{NCMe})_4]\text{PF}_6$ in a 2:1 ratio, in order to favour the formation of a bischelated tetrahedral complex, which was expectedly stable. Decoordination of MeCN was readily observed in the ^1H NMR spectrum, while the slight upfield shift of the $^{31}\text{P}\{\text{H}\}$ NMR resonance (to 60.9 ppm), together with its value, confirmed the formation of the P,P-bischelated tetrahedral complex $[\text{Cu}(\mathbf{1})_2]\text{PF}_6$ (7, Scheme 3).

Tetranuclear Cobalt Clusters

We wished to study the bridging coordination properties of ligands **1** and **2** on carbonyl clusters and these diphosphines were reacted with the Co_4 core clusters $[\text{Co}_4(\text{CO})_{10}(\mu\text{-dppm})]$ and $[\text{Co}_4(\text{CO})_{10}(\mu\text{-dppa})]$. The choice stems from: (a) the stabilizing effect of the dppa and dppm ligands, which bridge two of the basal Co atoms and (b) their diagnostic $^{31}\text{P}\{\text{H}\}$ NMR signals, which are far enough from those expected for coordinated **1** and **2** to permit a clear assignment. The reactions of **1** with $[\text{Co}_4(\text{CO})_{10}(\mu\text{-dppa})]$ and $[\text{Co}_4(\text{CO})_{10}(\mu\text{-dppm})]$ afforded clusters $[\text{Co}_4(\mu\text{-CO})_3(\text{CO})_5(\mu\text{-dppa})(\mu\text{-1})]$ (**8**) and $[\text{Co}_4(\mu\text{-CO})_3(\text{CO})_5(\mu\text{-dppm})(\mu\text{-1})]$ (**9**), respectively (Scheme 4). The reaction of **2** with $[\text{Co}_4(\text{CO})_{10}(\mu\text{-dppm})]$ afforded the cluster $[\text{Co}_4(\mu\text{-CO})_3(\text{CO})_5(\mu\text{-dppm})(\text{l-2})]$ (**10**). Clusters **8** and **9** were unambiguously characterized by single crystal X-ray diffraction (Figs. 4 and 5, respectively).



Scheme 4 Synthesis of Co₄ carbonyl clusters

The molecular structure of the 60 electron cluster **8** shows a tetrahedral Co_4 *core* and follows the 6 SEP (skeletal electron pairs) count required by the Wade–Mingos rules for a *nido*-trigonal bipyramidal structure [55, 56]. Three cobalt atoms (Co_2 , Co_3 and Co_4) form a triangle whose edges are each supported by a bridging CO. There is no bridging carbonyl between the apical Co_1 and the three basal cobalt atoms. The cluster *core* forms a distorted

tetrahedron, the Co–Co bond lengths ranging from 2.4230(6) (Co3–Co4) to 2.5409(7) Å (Co1–Co3). The longest ones correspond to the non CO-supported metal–metal bonds (see below, Table 2). This feature has also been observed in the three previously reported structures of $\text{Co}_4(\mu\text{-P,P})_2$ -type clusters ($\mu\text{-P,P}$ = diphosphine), which share with **1** the same ligand arrangement [19, 57, 58]. Each of the two bidentate diphosphines (dppa and **1**) bridges an edge of the tetrahedron, in such a way that each cobalt atom is coordinated by one P donor. Whereas P2 occupies an equatorial site, P3 and P4 are in axial positions. The coordination over the metal cluster is completed by five terminal carbonyls, two at Co1 and one at each of the three basal metal centers. Overall, the structure retains a carbonyl arrangement similar to that of $[\text{Co}_4(\text{CO})_{12}]$ [59].

The molecular structure of **9** is analogous to that of **8**, with the dppm ligand replacing dppa, on the same positions. Only slight changes in the arrangement of the ligands are observed. A comparison between selected metal–metal bond distances is reported in Table 2.

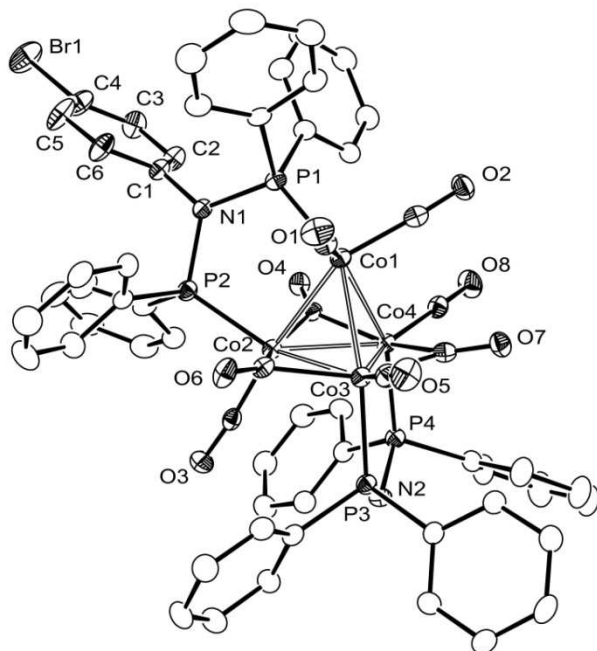


Fig. 4 ORTEP of the molecular structure of **8** (ellipsoids at 40% probability level). Hydrogen atoms omitted for clarity. Selected distances (Å) and angles (deg): Co1-Co2 2.5074(7), Co1-Co3 2.5409(7), Co1-Co4 2.5357(5), Co2-Co3 2.4828(6), Co2-Co4 2.4744(7), Co3-Co4 2.4230(6), Co1-C55 1.781(3), Co1-C56 1.784(4), Co2-C57 1.774(4), Co2-C58 1.926(4), Co2-C60 1.889(3), Co3-C59 1.756(3), Co3-C60 1.990(3), Co3-C61 1.922(4), Co4-C58 1.910(3), Co4-C61 1.922(3), Co4-C62 1.754(4), Co1-P1 2.212(1), Co2-P2 2.1642(9), Co3-P3 2.186(1), Co4-P4 2.174(1), P1-N1 1.722(3), P2-N1 1.736(3), P3-N2 1.700(2), P4-N2 1.689(4); Co2-

Co1–Co3 58.91(2), Co2–Co1–Co4 58.76(2), Co3–Co1–Co4 57.02(2), Co1–Co2–Co3 61.22(2), Co1–Co2–Co4 61.19(2), Co3–Co2–Co4 58.52(2), Co1–Co3–Co2 59.87(2), Co1–Co3–Co4 61.38(2), Co2–Co3–Co4 60.57(2), Co1–Co4–Co2 60.05(2), Co1–Co4–Co3 61.60(2), Co2–Co4–Co3 60.91(2), Co2–C58–Co4 80.3(1), Co2–C60–Co3 79.6(1), Co3–C61–Co4 78.1(1), P1–N1–P2 117.7(1), P3–N2–P4 122.5(2).

The Co–Co bond length showing the most significant difference between **8** and **9** is Co1–Co2. This is rather surprising since this bond is supported, in the two clusters, by the same diphosphine, whereas the Co3–Co4 edges, bridged by different ligands have very similar bond lengths. That this Co–Co bond is the shortest in both clusters can be related to the fact that it is bridged by a CO and a diphosphine ligand. The variations involving the aforementioned Co1–Co2 and (to a lesser extent) Co1–Co3, Co1–Co4 and Co2–Co3 bonds are difficult to rationalize and may be the result of a variation in the arrangement of the ligands, sterically triggered by the significantly different orientation of the phenyl rings between dppa and dppm in **8** and **9**, respectively (Fig. 6).

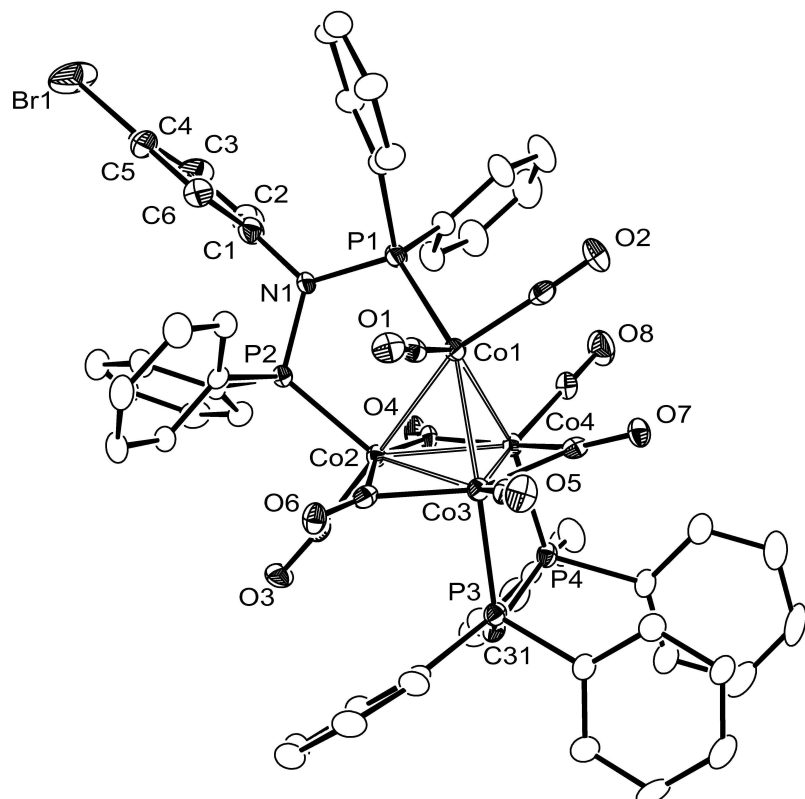


Fig. 5 ORTEP of the molecular structure of **9** (ellipsoids at 40% probability level). Hydrogen atoms omitted for clarity. Selected distances (\AA) and angles (deg): Co1–Co2 2.5632(7), Co1–Co3 2.499(1), Co1–Co4 2.5634(8), Co2–Co3 2.512(1), Co2–Co4 2.4724(8), Co3–Co4

2.4330(9), P1-Co1 2.198(2), P2-Co2 2.174(2), P3-Co3 2.188(1), P4-Co4 2.211(1), Co1-C56 1.788(6), Co1-C57 1.804(4), Co2-C58 1.755(3), Co2-C61 1.943(5), Co2-C59 1.945(4), Co3-C60 1.769(6), Co3-C61 1.937(4), Co3-C62 1.920(3), Co4-C63 1.755(4), Co4-C62 1.915(5), Co4-C59 1.890(5), P1-N1 1.731(3), P2-N1 1.726(3), P3-C31 1.836(4), P4-C31 1.837(4); Co2-Co1-Co3 59.49(2), Co2-Co1-Co4 57.67(2), Co3-Co1-Co4 57.43(2), Co1-Co2-Co3 58.99(2), Co1-Co2-Co4 61.17(2), Co3-Co2-Co4 58.43(2), Co1-Co3-Co2 61.52(2), Co1-Co3-Co4 62.61(3), Co2-Co3-Co4 59.97(2), Co1-Co4-Co2 61.16(2), Co1-Co4-Co3 59.96(2), Co2-Co4-Co3 61.60(3), Co2-C61-Co3 80.7(2), Co2-C59-Co4 80.3(2), Co3-C62-Co4 78.7(2), P1-N1-P2 115.2(2), P3-C31-P4 108.4(2).

Table 2. Comparison of the Co-Co bond lengths (\AA) in **8** and **9**.

	8	9
Co1-Co2	2.5074(7)	2.5632(7)
Co1-Co3	2.5409(7)	2.499(1)
Co1-Co4	2.5357(5)	2.5634(8)
Co2-Co3	2.4828(6)	2.512(1)
Co2-Co4	2.4744(7)	2.4724(8)
Co3-Co4	2.4230(6)	2.4330(9)

The spectroscopic data of **8** and **9** are consistent with their solid state structures. In the $^{31}\text{P}\{\text{H}\}$ spectrum of **9**, the dppm P nuclei resonate at 25.2 and 28.8 ppm, giving rise to two broad signals. The non-equivalence of the two phosphorus atoms is due to the different chemical environment of the basal Co3 and Co4 metal centers (see Fig. 7). Thus, considering the direction of the P1–Co1 vector, the transoid P1–Co1–Co3–P3 arrangement differs from P1–Co1–Co4–P4. The non-equivalence between P3 and P4 suggests a rather rigid situation in solution. Diphosphine **1** gives rise to two broad resonances at significantly different chemical shifts of 97.4 (P2) and 112.0 (P1) ppm, as expected since non-equivalent P1 and P2 coordinate to the apical and one of the basal metal centers, respectively. Cluster **10** shows a very similar $^{31}\text{P}\{\text{H}\}$ spectrum, with signals at 24.8 and 28.5 ppm for dppm, while P2 and P1 from **2** resonate at 96.7 and 112.2 ppm.

In the $^{31}\text{P}\{\text{H}\}$ spectrum of **8**, non-equivalent P nuclei were observed for **1** (97.1 and 116.6 ppm), while the ancillary dppa ligand gave rise to a broad signal at 74.0 ppm. The non-equivalence of P3 and P4 is possibly masked by the broadness of their signals when compared to those in **9** and **10**.

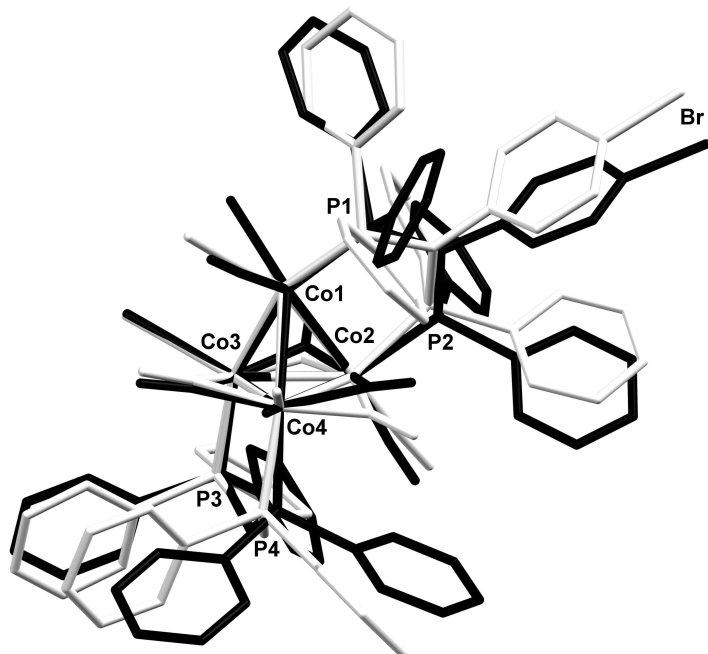


Fig. 6 Superimposed structural diagrams of **8** (black) and **9** (white), highlighting the different orientation of the phenyl rings (see e.g. P4) and its consequence on the carbonyl arrangement (e.g.: μ -CO on Co2-Co4) and thus on the geometrical features of ligand **1**. The structures are represented to give the best overlap between the Co2, Co3 and Co4 atoms of the two structures.

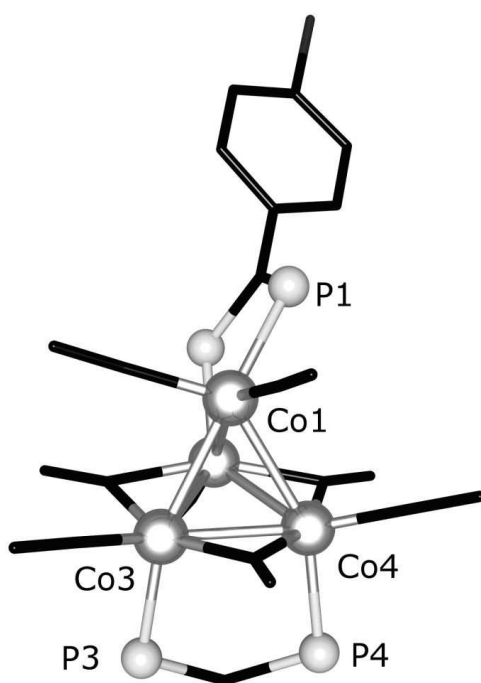
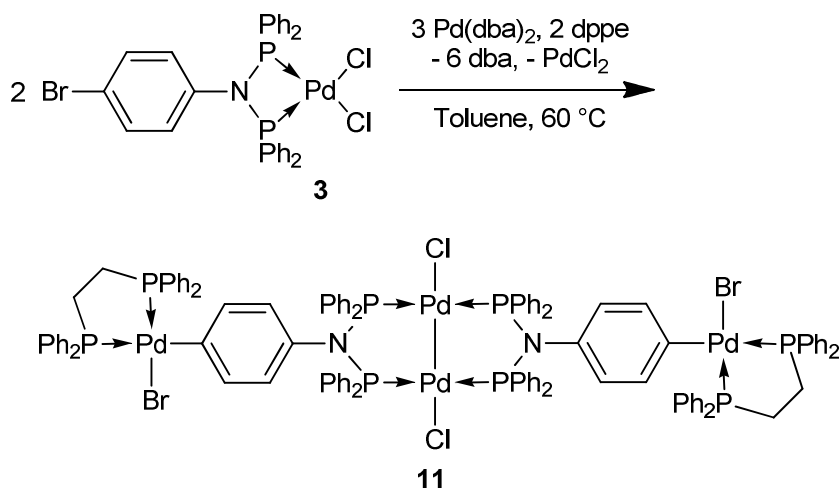


Figure 7. Simplified structural diagram of **9**, highlighting the non-equivalent environment of the Co3 and Co4 centers.

Palladium(0) Insertion into the C–Br and Pd–P Bonds

To evaluate the reactivity of the C–Br function and its potential for subsequent cross-coupling reactions, we reacted the Pd(II) complex **3** with 1.5 equivalents of the Pd(0) complex $[\text{Pd}(\text{dba})_2]$ (dba = dibenzylideneacetone) in the presence of one equivalent of dppe (dppe = 1,2-bis(diphenylphosphino)ethane) as a stabilizing diphosphine ligand in toluene at 60 °C for 2 h. This reaction should mimic the first step of a coupling reaction, namely the oxidative addition of Pd(0) by insertion into the carbon-bromine bond [60]. Interestingly, we observed a competition between this insertion reaction and the reduction of the Pd(II) center by Pd(0)–Pd(II) disproportionation to form a doubly bridged Pd(I)–Pd(I) dinuclear complex. For this reason, we repeated the reaction with 1.5 equivalents of the Pd(0) complex to allow both reactions to be complete (Scheme 5). Unfortunately, this complex slowly decomposes in solution to give complex **3** and degradation products (NMR evidence).



Scheme 5 Pd(0) insertion reactions leading to a tetranuclear, mixed-valent complex

Reduction of the Pd(II) center with formation of the metal–metal bonded dinuclear Pd(I) unit was indicated by the downfield shift of the $^{31}\text{P}\{^1\text{H}\}$ resonance of the equivalent PNP phosphorous nuclei from 35.8 to 63.7 ppm. This value is in the range of those observed in the dppa-bridged Pd(I) dimer (59.7 ppm) and the phenyl-functionalized dppa Pd(I) dimer (78.3 ppm). The difference in shift is probably due to the influence of the $\text{PdBr}(\text{dppe})$ unit in the *para* position of the metalloligand. The $^{31}\text{P}\{^1\text{H}\}$ spectrum of complex **11** also contains two doublets at 39.0 and 67.6 ppm ($^3J_{\text{P},\text{P}} = 26.0$ Hz) for the AX pattern corresponding to the P atoms of the dppe ligand which chelates the $\text{PdBrC}_{\text{ipso}}$ unit (Table 3). These values are consistent with those reported for a dppe ligand chelating a Pd center inserted into a C–Br bond [60]. An absorption band at 292 cm⁻¹ in the far-infrared spectrum of **11** is consistent

with the formation of a linear Cl–Pd–Pd–Cl unit by comparison with the $\nu(\text{Pd–Cl})$ value found for the dppa-bridged dinuclear complex $[\text{PdCl}(\mu\text{-dppa})]_2$ (293 cm^{-1}) [62].

Table 3. Comparison of the $^{31}\text{P}\{\text{H}\}$ chemical shifts of the PNP nuclei in the free ligands, and the chelating ligand in $[\text{PdCl}_2(\text{PNP})]$ and the bridging ligand in $[\text{PdCl}_2(\mu\text{-PNP})]_2$ (PNP: bidentate P,P ligand).^a

	Ligand (PNP)	$\text{PdCl}_2(\text{PNP})$	$[\text{PdCl}(\mu\text{-PNP})]_2$
dppm	- 21.2	- 53.7 ^b	- 2.5 ^b
dppa	44.2	7.1 ^d	59.7 ^c
<i>Ph</i> -dppa	67.9 ^e	34.7 ^e	78.3 ^c
1	70.8	35.8	63.7

^a In CDCl_3 solution. ^b Taken from reference [61]. ^c Synthesized following the procedure described in reference [62]. ^d In d_6 -DMSO. ^e Synthesized following the same procedure as for **1** and **3**, respectively.

Conclusion

We have reported the synthesis and structural characterization of mononuclear, dinuclear and cluster compounds bearing new bromo-functionalized dppa-type ligands containing an aryl spacer between the N atom of the bidentate ligand and the bromine atom. This functionality should allow further reactions on these complexes, as demonstrated with preliminary experiments involving Pd(0) insertion into the C–Br bond. Future work will involve the use of such function via coupling or oxidative-addition reactions, for the formation of multi-*core* clusters or heterometallic complexes.

Supplementary Materials

Crystallographic data for the structural analyses have been deposited with the Cambridge Crystallographic Data Center, CCDC Nos. 769343, 769344, 769345, 769346 and 769347 for compounds **3**, **4**, **6**, **8** and **9**, respectively. Copies of this information may be obtained free of charge from The Director, CCDC, 12 Union Road, Cambridge CB2 1EZ, UK. Fax: (int.code) +44(1223)336-033 or e-mail: deposit@ccdc.cam.ac.uk or the website <http://www.ccdc.cam.ac.uk>.

Acknowledgements We are grateful to the CNRS, the Ministère de l'Enseignement Supérieur et de la Recherche (Paris), the Deutsch-Französische Hochschule/Université franco-allemande (International Research Training Group 532-GRK532 of the Deutsche Forschungsgemeinschaft) and the Erasmus Program for funding. We also thank Nadine Bachmann (Sarrebrücken, Germany) and Anna Vidal-Zaragoza (Valencia, Spain) for their contributions to this work during their stay in Strasbourg and Dr. Jacky Rosé for fruitful discussions.

References

- (1) P. Braunstein, R. Hasselbring, A. Tiripicchio, and F. Uguzzoli (1995). *J. Chem. Soc. Chem. Commun.* **37**.
- (2) P. Braunstein, R. Hasselbring, A. DeCian, and J. Fischer (1995). *Bull. Soc. Chim. Fr.* **132**, 691.
- (3) I. Bachert, P. Braunstein, M. K. McCart, F. Fabrizi de Biani, F. Laschi, P. Zanello, G. Kickelbick, and U. Schubert (1999). *J. Organomet. Chem.* **573**, 47.
- (4) I. Bachert, I. Bartusseck, P. Braunstein, E. Guillon, J. Rosé, and G. Kickelbick (1999). *J. Organomet. Chem.* **588**, 143.
- (5) I. Bachert, P. Braunstein, and R. Hasselbring (1996). *New J. Chem.* **20**, 993.
- (6) A. Dulai, H. de Bod, M. J. Hanton, D. M. Smith, S. Downing, S. M. Mansell, and D. F. Wass (2009). *Organometallics* **28**, 4613.
- (7) L. Lavanant, A.-S. Rodrigues, E. Kirillov, J.-F. Carpentier, and R. F. Jordan (2008). *Organometallics* **27**, 2107.
- (8) Z. Weng, S. Teo, and T. S. A. Hor (2007). *Dalton Trans.* 3493.
- (9) K. Blann, A. Bollmann, H. De Bod, J. T. Dixon, E. Killian, P. Nongodlwana, M. C. Maumela, H. Maumela, A. E. McConnell, D. H. Morgan, M. J. Overett, M. Pretorius, S. Kuhlmann, and P. Wasserscheid (2007). *J. Catal.* **249**, 244.
- (10) A. J. Rucklidge, D. S. McGuinness, R. P. Tooze, A. M. Z. Slawin, J. D. A. Pelletier, M. J. Hanton, and P. B. Webb (2007). *Organometallics* **26**, 2782.
- (11) D. S. McGuinness, M. Overett, R. P. Tooze, K. Blann, J. T. Dixon, and A. M. Z. Slawin (2007). *Organometallics* **26**, 1108.
- (12) P. R. Elowe, C. McCann, P. G. Pringle, S. K. Spitzmesser, and J. E. Bercaw (2006). *Organometallics* **25**, 5255.
- (13) S. J. Schofer, M. W. Day, L. M. Henling, J. A. Labinger, and J. E. Bercaw (2006). *Organometallics* **25**, 2743.
- (14) T. Agapie, M. W. Day, L. M. Henling, J. A. Labinger, and J. E. Bercaw (2006). *Organometallics* **25**, 2733.
- (15) A. Jabri, P. Crewdson, S. Gambarotta, I. Korobkov, and R. Duchateau (2006). *Organometallics* **25**, 715.
- (16) A. Bollmann, K. Blann, J. T. Dixon, F. M. Hess, E. Killian, H. Maumela, D. S. McGuinness, D. H. Morgan, A. Neveling, S. Otto, M. Overett, A. M. Z. Slawin, P. Wasserscheid, and S. Kuhlmann (2004). *J. Am. Chem. Soc.* **126**, 14712.
- (17) T. Agapie, S. J. Schofer, J. A. Labinger, and J. E. Bercaw (2004). *J. Am. Chem. Soc.* **126**, 1304.
- (18) N. A. Cooley, S. M. Green, D. F. Wass, K. Heslop, A. G. Orpen, and P. G. Pringle (2001). *Organometallics* **20**, 4769.
- (19) A. Choualeb, P. Braunstein, J. Rosé, S.-E. Bouaoud, and R. Welter (2003). *Organometallics* **22**,

- 4405.
- (20) F. Schweyer-Tihay, P. Braunstein, C. Estournes, J. L. Guille, B. Lebeau, J. L. Paillaud, M. Richard-Plouet, and J. Rosé (2003). *Chem. Mater.* **15**, 57.
- (21) P. Braunstein, H.-P. Kormann, W. Meyer-Zaika, R. Pugin, and G. Schmid (2000). *Chem. Eur. J.* **6**, 4637.
- (22) P. Braunstein (2004). *J. Organomet. Chem.* **689**, 3953.
- (23) K. Raghuraman, S. S. Krishnamurthy, and M. Nethaji (2003). *J. Organomet. Chem.* **669**, 79.
- (24) D. W. Engel, K. G. Moodley, L. Subramony, and R. J. Haines (1988). *J. Organomet. Chem.* **349**, 393.
- (25) L. Subramony, D. W. Engel, and K. G. Moodley (1984). *Acta Crystallogr. Sect. A* **40**, C297.
- (26) T. S. Venkatakrishnan, S. S. Krishnamurthy, and M. Nethaji (2005). *J. Organomet. Chem.* **690**, 4001.
- (27) V. Gallo, P. Mastrorilli, C. F. Nobile, P. Braunstein, and U. Englert (2006). *Dalton Trans.* 2342.
- (28) M. Rodriguez-Zubiri, V. Gallo, J. Rosé, R. Welter, and P. Braunstein (2008). *Chem. Commun.* 64.
- (29) Z. Fei, W. H. Ang, D. Zhao, R. Scopelliti, and P. J. Dyson (2006). *Inorg. Chim. Acta* **359**, 2635.
- (30) V. W.-W. Yam, W. K.-M. Fung, and M.-T. Wong (1997). *Organometallics* **16**, 1772.
- (31) C. Elschenbroich *Organometallchemie*, 6th ed (Teubner, Wiesbaden, 2008), pp. 600–606.
- (32) D. Drew and J. R. Doyle (1972). *Inorg. Synth.* **13**, 47.
- (33) H. C. Clark and L. E. Manzer (1973). *J. Organomet. Chem.* **59**, 411.
- (34) R. Uson, A. Laguna, and M. Laguna (1989). *Inorg. Synth.* **26**, 85.
- (35) C. Moreno, M. J. Macazaga, M. L. Marcos, J. González-Velasco, and S. Delgado (1993). *J. Organomet. Chem.* **452**, 185.
- (36) T. Ukai, H. Kawazura, Y. Ishii, J. J. Bonnet, and J. A. Ibers (1974). *J. Organomet. Chem.* **65**, 253.
- (37) M. Pfeffer, P. Braunstein, and J. Dehand (1974). *Spectrochim. Acta A* **30**, 341.
- (38) R. J. Goodfellow, J. G. Evans, P. L. Goggin, and D. A. Duddell (1968). *J. Chem. Soc. A*, 1604.
- (39) Bruker-Nonius *Kappa CCD Reference Manual* (Nonius BV, The Netherlands, 1998).
- (40) G. M. Sheldrick *SHELXL-97, Program for crystal structure refinement* (University of Göttingen, Germany, 1997).
- (41) A. L. Spek (2003). *J. Appl. Crystallogr.* **36**, 7.
- (42) R. H. Blessing (1995). *Acta Crystallogr.* **51**, 33.
- (43) A. Pidcock, R. E. Richards, and L. M. Venanzi (1966). *J. Chem. Soc. A*, 1707.
- (44) F. Durap, N. Biricik, B. Gumgum, S. Ozkar, W. H. Ang, Z. Fei, and R. Scopelliti (2008). *Polyhedron* **27**, 196.
- (45) B. Gumgum, N. Biricik, F. Durap, I. Ozdemir, N. Gurbuz, W. H. Ang, and P. J. Dyson (2007). *Appl. Organomet. Chem.* **21**, 711.
- (46) Z. Fei, R. Scopelliti, and P. J. Dyson (2004). *Eur. J. Inorg. Chem.*, 530.
- (47) K. G. Gaw, M. B. Smith, and A. M. Z. Slawin (2000). *New J. Chem.* **24**, 429.

- (48) C. Ganesamoorthy, M. S. Balakrishna, J. T. Mague, and H. M. Tuononen (2008). *Inorg. Chem.* **47**, 2764.
- (49) P. Lange, A. Schier, and H. Schmidbaur (1997). *Z. Naturforsch. B* **52**, 769.
- (50) M. Freytag, S. Ito, and M. Yoshifuji (2006). *Chem. Asian J.* **1**, 693.
- (51) M. Bardaji, P. G. Jones, A. Laguna, M. D. Villacampa, and N. Villaverde (2003). *Dalton Trans.* 4529.
- (52) P. G. Jones and E. Bembeneck (1996). *Acta Crystallogr. Sect. C* **52**, 2396.
- (53) H. Schmidbaur, W. Graf, and G. Muller (1988). *Angew. Chem. Int. Ed.* **27**, 417.
- (54) H. Schmidbaur, A. Wohlleben, F. Wagner, O. Obama, and G. Huttner (1977). *Chem. Ber.* **110**, 1748.
- (55) K. Wade (1976). *Adv. Inorg. Chem. Radiochem.* **18**, 1.
- (56) D. M. P. Mingos (1984). *Acc. Chem. Res.* **17**, 311.
- (57) M. I. Bruce, A. J. Carty, B. G. Ellis, P. J. Low, B. W. Skelton, A. H. White, K. A. Udachin, and N. N. Zaitseva (2001). *Aust. J. Chem.* **54**, 277.
- (58) H. A. Mirza, J. J. Vittal, R. J. Puddephatt, C. S. Frampton, L. Manojlovic-Muir, W. Xia, and R. H. Hill (1993). *Organometallics* **12**, 2767.
- (59) L. J. Farrugia, D. Braga, and F. Grepioni (1999). *J. Organomet. Chem.* **573**, 60.
- (60) H. Weissman, E. Shirman, T. Ben-Moshe, R. Cohen, G. Leitus, L. J. W. Shimon, and B. Rybtchinski (2007). *Inorg. Chem.* **46**, 4790.
- (61) C. T. Hunt and A. L. Balch (1981). *Inorg. Chem.* **20**, 2267.
- (62) R. Uson, J. Fornies, R. Navarro, M. Tomas, C. Fortuno, J. I. Cebollada, and A. J. Welch (1989). *Polyhedron* **8**, 1045.

Conclusion Générale

Bilan

Lors de ces travaux de thèse, nous avons réussi notre pari, qui été la formation de ligands bifonctionnels, de type carbènes N-hétérocycliques/thioéther (S,C_{NHC}), de type bis(diphenylphosphino)amine/thioéther (S,P,P) et bis(diphenylphosphino)amine/brome (Br,P,P). Ces différentes familles de ligands ont permis la formation de complexes organométalliques et leur application en catalyse.

Ligands Carbènes N-hétérocycliques

Dans un premier temps, nous avons développé une nouvelle famille de précurseurs de ligands carbènes N-hétérocycliques (NHCs), portant un groupement alkyle sur un atome d'azote et un groupement thioéther sur le second. Cette synthèse a été réalisée en une seule étape, sans solvant et nous avons obtenu de très bons rendements.

Par extension et adaption de cette synthèse, nous avons pu créer une autre série de sels d'imidazoliums où le groupement alkyle a été remplacé par un groupement aryle.

Enfin, nous avons étendu cette stratégie de synthèse à la formation de précurseurs de ligands NHCs portant un groupement thioéther sur chacun des atomes d'azote.

Nous avons étudié la chimie de coordination de ces ligands vis-à-vis de complexes d' $Ag(I)$ et de $Pd(II)$. La structure moléculaire de l'un des complexes d'argent révéla une structure unique avec un corps métallique plan composé de 4 atomes d'argent. En fonction du ratio métal/ligand utilisé, les complexes de palladium formés ont montré la diversité des modes de coordination de ces ligands. Dans le cas de complexes de palladium bis-NHC, nous avons observé la formation sélective des isomères *trans* dans le cas du précurseur de type $[PdCl_2(cod)]$ et *cis* dans le cas de l'utilisation du précurseur dicationique de type $[Pd(NCMe)_4][BF_4]_2$.

Les complexes de palladium formés ont montré une bonne activité en réaction catalytique de couplage croisé de Suzuki-Myiaura vis-à-vis de substrats bromés.

Ligands Diphosphines

Nous avons développé deux types de ligands bifonctionnels portant le squelette bis(diphenylphosphino)amine (dppa), l'un portant un groupement thioéther et l'autre un aryl-bromé, potentiellement attractifs pour la chimie de coordination et/ou la catalyse.

Nous avons par la suite étudié leur chimie de coordination vis-à-vis des métaux de transition et nous avons eu la chance de pouvoir en caractériser une grande partie par diffraction de rayons X, ce qui nous a permis de mettre en évidence des arrangements originaux inattendus à l'état solide.

Une partie de ces complexes été dédiée à des applications en catalyse homogène et a montré des activités non négligeable en oligomérisation d'éthylene.

Certains de ces complexes se sont révélés être de très bons candidats pour des études poussées en RPE ou pour des applications dans le domaine des nanomatériaux ou de l'électronique moléculaire.

Perspectives

En perspectives, nous envisageons d'étudier la chimie de coordination des ligands de type (S,C_{NHC}) avec d'autres métaux de transition, en visant des applications dans d'autres types de réactions catalytiques.

En ce qui concerne les ligands de type (S,P,P), c'est l'étude des propriétés magnétiques de certains de leurs complexes organométalliques qui nous intéressent.

Et pour finir, il serait intéressant de mettre à profit les propriétés de « ligand assebleur » du ligand (Br,P,P) pour la formation de complexes de haute nucléarité.

